

Judul Artikel : Design and Synthesis of Conducting Polymer Bio-Based Polyurethane Produced from Palm Kernel Oil  
Nama Jurnal : International Journal of Polymer Science  
ISSN : 1687-9430  
Tahun Terbit : 2022  
Penerbit : Hindawi  
No. Halaman : 1-13  
Url Cek Plagiasi : [http://elibrary.almaata.ac.id/2470/30/P7\\_turnitin.pdf](http://elibrary.almaata.ac.id/2470/30/P7_turnitin.pdf)  
Url Index : <https://www.scopus.com/sourceid/21100228096>  
Url Jurnal : <https://doi.org/10.1155/2022/6815187>

[← BACK](#) [DASHBOARD / ARTICLE DETAILS](#)

Updated on 2021-06-18

Version 1 ▾

# Design and Synthesis of Conducting Polymer Based on Polyurethane produced from Palm Kernel Oil

VIEWING AN OLDER VERSION

ID 6815187

Muhammad Abdurrahman Munir <sup>SA</sup><sup>1</sup>,  
Khairiah Haji Badri <sup>CA</sup><sup>1</sup>, Lee Yook Heng<sup>1</sup>  
[+ Show Affiliations](#)

## Article Type

Research Article

## Journal

International Journal of  
Polymer Science

Rydz Joanna

Submitted on 2021-06-14 (2 years ago)

[> Abstract](#)[> Author Declaration](#)[> Files](#) 2

## — Editorial Comments

**Peter Foot**

18.06.2021

**Decision**

Revision requested

**Message for Author**

The topic of this manuscript is suitable for Int. J. Polym. Sci. but it must be revised before it can be sent for peer-review. The grammar and typing are very poor, and there are many incorrectly-used words. Reviewers would not properly understand the authors' meaning in many parts of the text. The authors should also emphasize the novel aspects of their research, since there is an abundance of published work on PUs made from vegetable oil derivatives.

---

[Hindawi](#) [Privacy Policy](#) [Terms of Service](#) Support: [help@hindawi.com](mailto:help@hindawi.com)

# Design and Synthesis of Conducting Polymer Based on Polyurethane produced from Palm Kernel Oil

Muhammad Abdurrahman Munir<sup>1</sup>, Khairiah Haji Badri<sup>1,2\*</sup>, Lee Yook Heng<sup>1</sup>

<sup>1</sup>Department of Chemical Sciences, Faculty of Science and Technology, Universiti Kebangsaan Malaysia, Bangi, Malaysia

<sup>2</sup>Polymer Research Center, Universiti Kebangsaan Malaysia, Bangi, Malaysia

\*Email: [kaybadri@ukm.edu.my](mailto:kaybadri@ukm.edu.my)

## Abstract

Polyurethane (PU) is a unique polymer that has versatile processing method and mechanical properties upon inclusion of selected additives. In this study, a freestanding bio-polyurethane film on screen – printed electrode (SPE) was prepared by solution casting technique, using acetone as solvent. It was a one-pot synthesis between major reactants namely, palm kernel oil-based polyol (PKOp) and 4,4-methylene diisocyanate. The PU undergone strong adhesion on SPE. The formation of urethane linkages (NHCO backbone) after polymerization was confirmed by the absence of N=C=O peak at 2241 cm<sup>-1</sup>. The glass transition temperature ( $T_g$ ) of the polyurethane was detected at 78.1°C. The conductivity of PU was determined using cyclic voltammetry (CV) and differential pulse voltammetry (DPV). The current of electrode was at 5.2 x 10<sup>-5</sup> A.

**Keywords:** Polyurethane, polymerization, screen – printed electrode, voltammetry

## 1. Introduction

Polymers are molecules composed of many repeated sub-units referred to as monomers (Sengodu & Deshmukh 2015). Conducting polymers (CPs) are polymers that exhibit electrical behaviour (Alqarni et al. 2020). The conductivity of CPs was first observed in polyacetylene,



27 nevertheless owing to its instability led to the discovery of other forms of CPs such as  
28 polyaniline (PANI), poly(o-toluidine) (PoT), polythiophene (PTh), polyfluorene (PF) and  
29 polyurethane (PU). Furthermore, natural CPs have low conductivity and are often semi-  
30 conductive. Therefore, it is essential to increase their conductivity mainly for use in  
31 electrochemical sensor programs (Dzulkipli et al. 2021; Wang et al. 2018). Conducting  
32 polymers (CPs) represent a sizeable range of useful organic substances. Their unique electrical,  
33 chemical and physical properties; reasonable price; simple preparation; small dimensions and  
34 large surface area have enabled researchers to discover a wide variety of uses such as sensors,  
35 biochemical applications, solar cells and electrochromic devices (Alqarni et al. 2020). There  
36 are many scientific documentations on the use of conductive polymers in various studies such  
37 as polyaniline (Pan & Yu 2016), polypyrrole (Ladan et al. 2017) and polyurethane (Tran et al.  
38 2020; Vieira et al. 2020; Guo et al. 2020; Fei et al. 2020).

39 The application of petroleum as polyol in order to produce polyurethane has been applied. The  
40 coal and crude oil used as raw materials to produce it. Nevertheless, these materials become  
41 very rare to find and the price is very expensive at the same time required sophisticated system  
42 to produce it. These reasons have been considered and finding utilizing plants that can be used  
43 as alternative polyols should be done immediately (Badri 2012). Furthermore, in order to avoid  
44 the application of petroleum as raw material for polyol, vegetable oils become a better choice  
45 as polyol in order to obtain a biodegradable polyol. Vegetable oils that generally used for  
46 synthesis polyurethane are soybean oil, corn oil, sunflower seed oil, coconut oil, nuts oil, rape  
47 seed, olive oil and palm oil (Badri 2012; Borowicz et al. 2019).

48 Biopolymer, a natural biodegradable polymer has attracted much attention in recent years.  
49 Global environmental awareness and fossil fuel depletion urged researchers to work in the  
50 biopolymer field (Priya et al. 2018). Polyurethane is one of the most common, versatile and  
51 researched materials in the world. These materials combine the durability and toughness of

52 metals with the elasticity of rubber, making them suitable to replace metals, plastics and rubber  
53 in several engineered products. They have been widely applied in biomedical applications,  
54 building and construction applications, automotive, textiles and in several other industries due  
55 to their superior properties in terms of hardness, elongation, strength and modulus (Zia et al.  
56 2014; Romaskevicius et al. 2006).

57 The urethane group is the major repeating unit in PU and is produced from the reaction between  
58 alcohol (-OH) and isocyanate (NCO); albeit polyurethanes also contain other groups such as  
59 ethers, esters, urea and some aromatic compounds. Due to the wide variety of sources from  
60 which PU can be synthesized, thus a wide range of specific applications can be generated.  
61 They are grouped into several different classes based on the desired properties: rigid, flexible,  
62 thermoplastic, waterborne, binders, coating, adhesives, sealants and elastomers (Akindoyo et  
63 al. 2016).

64 Although, PU has low conductivity but it is lighter than other materials such as metals. The  
65 hardness of PU also relies on the aromatic rings number in the polymer structure (Janpoung et  
66 al, 2020; Su'ait et al. 2014), majorly contributed by the isocyanate derivatives. PU has also a  
67 conjugate structure where electrons can move in the main chain that causing electricity  
68 produced even the conductivity is low. The electrical conductivity of conjugated linear ( $\pi$ ) can  
69 be explained by the distance between the highest energy level containing electrons (HOMO)  
70 called valence band and the lowest energy level not containing electrons (LUMO) called the  
71 conduction band (Wang et al. 2017; Kotal et al. 2011).

72 The purpose of this work was to study the conductivity of polyurethane using cyclic  
73 voltammetry (CV) and differential pulse voltammetry (DPV) attached onto screen printed  
74 electrode (SPE). To the best of our knowledge, this is the first attempt to use a modified  
75 polyurethane electrode. The electrochemistry of polyurethane mounted onto screen-printed

76 electrode (SPE) is discussed in detail. Polyurethane is possible to become an advanced frontier  
77 material in chemically modified electrodes for bio sensing application.

78

## 79 **2. Experimental**

### 80 **2.1 Chemicals**

81 *Synthesis of polyurethana film:* Palm kernel oil (PKOp) supplied by UKM Technology Sdn  
82 Bhd through MPOB/UKM station plant, Pekan Bangi Lama, Selangor and prepared using  
83 Badri et al. (2000) method. 4, 4-diphenylmethane diisocyanate (MDI) was acquired from  
84 Cosmopolyurethane (M) Sdn. Bhd., Klang, Malaysia. Solvents and analytical reagents were  
85 benzene ( $\geq 99.8\%$ ), toluene ( $\geq 99.8\%$ ), hexane ( $\geq 99\%$ ), acetone ( $\geq 99\%$ ), tetrahydrofuran  
86 (THF), dimethylformamide (DMF) ( $\geq 99.8\%$ ), dimethylsulfoxide (DMSO) ( $\geq 99.9\%$ ) and  
87 polyethylene glycol (PED) with a molecular weight of 400 Da obtained from Sigma Aldrich  
88 Sdn Bhd, Shah Alam.

89

### 90 **2.2 Apparatus**

91 Tensile testing was performed using a universal testing machine model Instron 5566 following  
92 ASTM 638 (Standard Test Method for Tensile Properties of Plastics). The tensile properties of  
93 the polyurethane film were measured at a velocity of 10 mm/min with a cell load of 5 kN.  
94 The thermal properties were performed using thermogravimetry analysis (TGA) and  
95 Differential Scanning Calorimetry (DSC) analysis. TGA was performed using a thermal  
96 analyzer of Perkin Elmer Pyris model with heating rate of 10 °C/minute at a temperature range  
97 of 30 to 800 °C under a nitrogen gas atmosphere. The DSC analysis was performed using a  
98 thermal analyzer of Perkin Elmer Pyris model with heating rate of 10 °C /minute at a  
99 temperature range of -100 to 200 °C under a nitrogen gas atmosphere. Approximately, 5-10  
100 mg of PU was weighed. Sample was heated from 25 to 150 °C for one minute, then cooled

101 immediately from 150 -100 °C for another one minute and finally, reheated to 200 °C at a rate  
102 of 10 °C /min. At this point, the polyurethane encounters changes from elastic properties to  
103 brittle due to changes in the movement of the polymer chains. Therefore, the temperature in  
104 the middle of the inclined regions is taken as the glass transition temperature ( $T_g$ ). The melting  
105 temperature ( $T_m$ ) is identified as the maximum endothermic peak by taking the area below the  
106 peak as the enthalpy point ( $\Delta H_m$ ).

107 The morphological analysis of PU film was performed by Field Emission Scanning Electron  
108 Microscope (FESEM) model Gemini SEM microscope model 500-70-22. Before the analysis  
109 was carried out, the polyurethane film was coated with a thin layer of gold to increase the  
110 conductivity of the film. The coating method was carried out using a sputter - coater. The  
111 observations were conducted at magnification of 200× and 5000 × with 10.00 kV (Electron  
112 high tension - EHT).

113 The crosslinking of PU was determined using soxhlet extraction method. About 0.60 g of PU  
114 sample was weighed and put in an extractor tube containing 250 ml of toluene, used as a  
115 solvent. This flow of toluene was let to run for 24 hours. Mass of the PU was weighed before  
116 and after the reflux process was carried out. Then, the sample was dried in the conventional  
117 oven at 100 °C for 24 hours in order to get a constant mass. The percentage of crosslinking  
118 content known as the gel content, can be calculated using Equation (1).

119

$$120 \quad \text{Gel content (\%)} = \frac{W_o - W}{W} \times 100 \% \quad (1)$$

121  $W_o$  is mass of PU before the reflux process (g) and  $W$  is mass of PU after the reflux process  
122 (g).

123

124 FTIR spectroscopic analysis was performed using a Perkin-Elmer Spectrum BX instrument  
125 using the Diamond Attenuation Total Reflectance (DATR) method to confirm the

126 polyurethane, PKOp and MDI functional group. FTIR spectroscopic analysis was performed  
127 at a wave number of 4000 to 600  $\text{cm}^{-1}$  to identify the peaks of the major functional groups in  
128 the formation of polymer such as amide group (-NH), urethane carbonyl group (-C = O) and  
129 carbamate group (-CN).

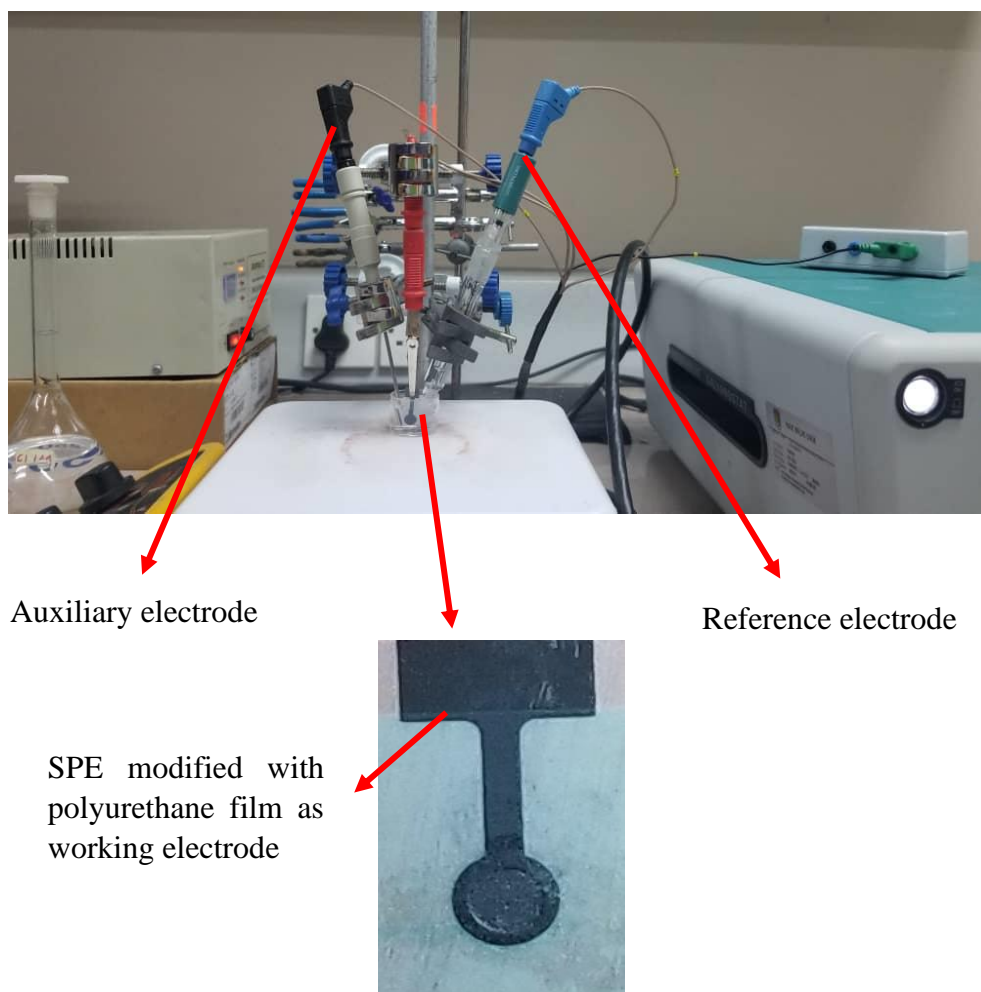
130

### 131 **2.3 Modification of Electrode**

132 Voltammetric tests were performed using Metrohm Autolab Software (**Figure 1**) analyzer  
133 using cyclic voltammetry (CV) method or known as amperometric mode and differential pulse  
134 voltammetry (DPV). All electrochemical experiments were carried out using screen printed  
135 electrode (diameter 3 mm) modified using polyurethane film as working electrode, platinum  
136 wire as auxiliary electrode and AG/AgCl electrode as reference electrode. All experiments  
137 were conducted at temperature of  $20 \pm 2^\circ\text{C}$ .

138 PU casted onto the screen – printed electrode (SPE + PU) was analyzed using a single  
139 voltammetric cycle between -1200 and +1500 mV (vs AG/AgCl) of ten cycles at a scanning rate  
140 of 100 mV/s in 5 ml of KCl in order to study the activity of SPE and polyurethane film.  
141 Approximately (0.1, 0.3 & 0.5) mg of palm – based prepolyurethane was dropped separately  
142 onto the surface of the SPE and dried at room temperature. The modified palm-based  
143 polyurethane electrodes were then rinsed with deionized water to remove physically adsorbed  
144 impurities and residues of unreacted material on the electrode surface. All electrochemical  
145 materials and calibration measurements were carried out in a 5 mL glass beaker with a  
146 configuration of three electrodes inside it. Platinum wire and AG/AgCl electrodes were used  
147 as auxiliary and reference electrodes, while screen printed electrode that had been modified  
148 with polyurethane was applied as a working electrode.

149



150 **Figure 1.** Potentiostat instrument to study the conductivity of SPE modified with  
 151 polyurethane film using cyclic voltametry (CV) and differential pulse voltammetry (DPV)

152

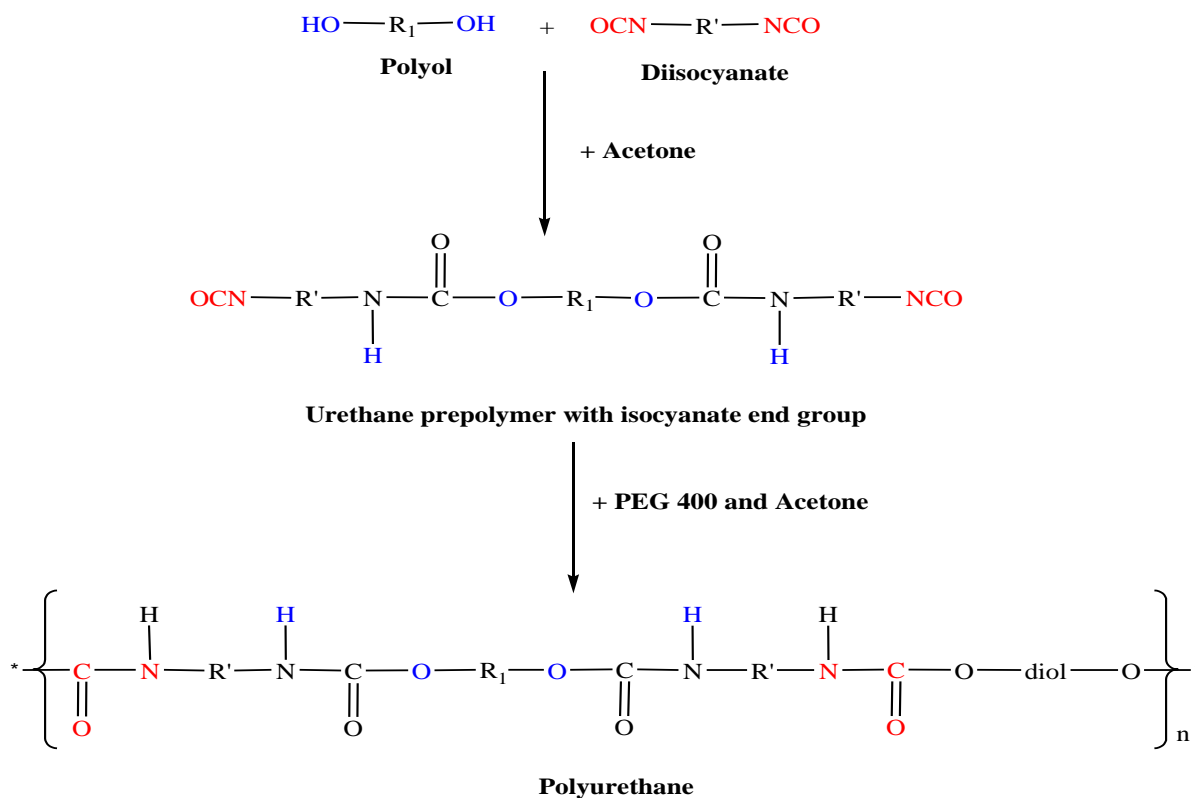
### 153 3. Results and Discussion

154 The synthesis of PU films was carried out using pre - polymerization method which involves  
 155 the formation of urethane polymer at an early stage. The reaction took place between palm  
 156 kernel oil – based polyol (PKOp) and diisocyanate (MDI). The structural chain was extended  
 157 with the aid of polyethylene glycol (PED) to form flexible and elastic polyurethane film. In  
 158 order to form the urethane prepolymer, one of the isocyanate groups (NCO) reacts with one  
 159 hydroxyl group (OH) of polyol while the other isocyanate group attacks another hydroxyl  
 160 group in the polyol (Wong & Badri 2012) as shown in **Figure 2.**

161

162 a. FTIR analysis

163 **Figure 3** shows the FTIR spectrum for polyurethane, exhibiting the important functional group  
164 peaks. According to study researched by Wong & Badri 2012, PKO-p reacts with MDI to form  
165 urethane prepolymers. The NCO group on MDI reacts with OH group on polyol whether  
166 PKOp or PEG. It can be seen there are no important peaks of MDI in the FTIR spectrums.  
167 This is further verified by the absence of peak at the  $2400\text{ cm}^{-1}$  belongs to MDI (-NCO groups).  
168 This could also confirm that the NCO group on MDI had completely reacted with PKO-p to  
169 form the urethane -NHC (O) backbone. The presence of amides (-NH), carbonyl urethane  
170 group (-C = O), carbamate group (C-NH) and -C-O-C confirmed the formation of urethane  
171 chains. In this study, the peak of carbonyl urethane (C = O) detected at  $1727\text{ cm}^{-1}$  indicated  
172 that the carbonyl urethane group was bonded without hydrogen owing to the hydrogen reacted  
173 with the carbonyl urethane group.



174

175 **Figure 2.** The chemical route of producing polyurethane via pre-polymerization method

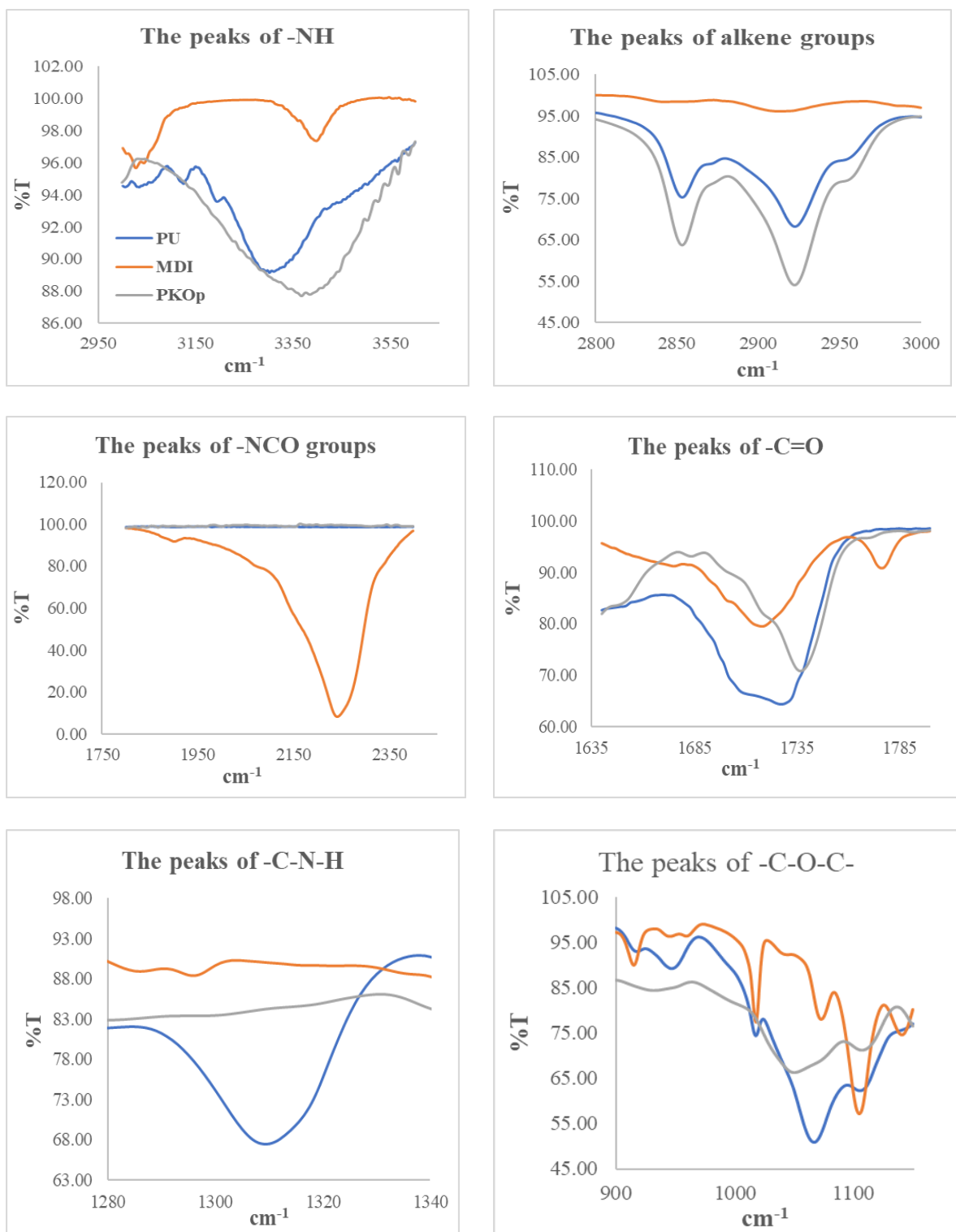
176

(Wong & Badri 2012).

177 The reaction of polyurethane has been studied by Hamuzan & Badri (2016) where the urethane  
178 carbonyl group was detected at  $1730 - 1735 \text{ cm}^{-1}$  while the MDI carbonyl was detected at  $2400$   
179  $\text{cm}^{-1}$ . The absence of peaks at  $2250 - 2270 \text{ cm}^{-1}$  indicates the absence of NCO groups. It shows  
180 that the polymerization reaction occurs entirely between NCO groups in MDI with hydroxyl  
181 groups on polyols and PEG (Mishra et al. 2012). The absence of peaks at  $1690 \text{ cm}^{-1}$   
182 representing urea (C = O) in this study indicated, there is no urea formation as a byproduct  
183 (Clemitson 2008) of the polymerization reaction that possibly occur due to the excessive water.  
184 For the amine (NH) group, hydrogen-bond to NH and oxygen to form ether and hydrogen bond  
185 to NH and oxygen to form carbonyl on urethane can be detected at the peak of  $3301 \text{ cm}^{-1}$  and  
186 in the wave number at range  $3326 - 3428 \text{ cm}^{-1}$ . This has also been studied and detected by  
187 Lampman et. al. (2010) and Mutsuhisa et al. (2007). In this study, the hydrogen bond formed  
188 by C = O acts as a proton acceptor whereas NH acts as a proton donor. The urethane group in  
189 the hard segment (MDI) has electrostatic forces on the oxygen, hydrogen and nitrogen atoms  
190 and these charged atoms form dipoles that attract other opposite atoms. These properties make  
191 isocyanates are highly reactive and having different properties (Leykin et al. 2016).

192 MDI was one of the isocyanate used in this study, has an aromatic group and more  
193 reactive compared to aliphatic group isocyanates such as hexamethylene diisocyanate (HDI)  
194 or isoporona diisocyanate (IPDI). Isocyanates have two groups of isocyanates on each  
195 molecule. Diphenylmethane diisocyanate is an exception owing to its structure consists of two,  
196 three, four or more isocyanate groups (Nohra et al. 2013). The use of PEG 400 in this study as  
197 a chain extender for polyurethane increases the chain mobility of polyurethane at an optimal  
198 amount. The properties of polyurethane are contributed by hard and soft copolymer segments  
199 of both polyol monomers and MDI. This makes the hard segment of urethane serves as a  
200 crosslinking site between the soft segments of the polyol (Leykin et al. 2016).





201 **Figure 3.** FTIR spectrums of several important peaks between polyurethane, PKO-p and MDI

202

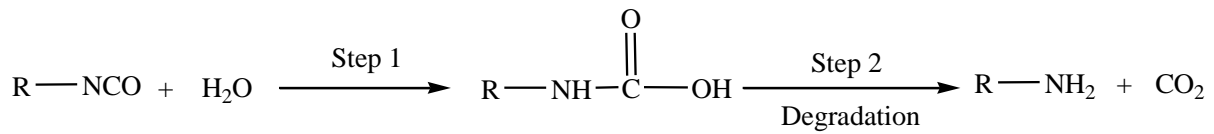
203 The mechanism of the pre – polymerization in urethane chains formation is a

204 nucleophilic substitution reaction as studied by Yong et al. (2009). However, this study found

205 amines as nucleophiles. Amine attacks carbonyl on isocyanate in MDI in order to form two  
206 resonance structures of intermediate complexes A and B. Intermediate complex B has a greater  
207 tendency to react with polyols due to stronger carbonyl (C = O) bonds than C = N bonds on  
208 intermediate complexes A. Thus, intermediate complex B is more stable than intermediate  
209 complex A, as suggested by previous researchers who have conducted by Wong and Badri  
210 (2012). Moreover, nitrogen was more electropositive than oxygen, therefore, -CN bonds were  
211 more attracted to cations (H<sup>+</sup>) than -CO. The combination between long polymer chain and  
212 low cross linking content gives the polymer an elastic properties whereas short chain and high  
213 cross linking producing hard and rigid polymers. Cross linking in polymers consist of three -  
214 dimensional networks with high molecular weight. In some aspects, polyurethane can be a  
215 macromolecule, a giant molecule. Polyurethanes are usually thermoset polymers (Petrovic  
216 2008).

217         Moreover, reaction between MDI and PEG as a chain extender where oxygen on the  
218 nucleophile PEG attacks the NCO group in the MDI to form two intermediate complexes A  
219 and B can occur. Nevertheless, nucleophilic substitution reactions have a greater tendency to  
220 occur in PKOp compared to PEG because the presence of nitrogen atoms is more  
221 electropositive than oxygen atoms in PEG. Amine has a higher probability of to react compared  
222 to hydroxyl (Herrington & Hock 1997). Amine with high alkalinity reacts with carbon atoms  
223 on MDI as proposed by Wong and Badri (2012). PKOp contains long carbon chains that can  
224 easily stabilize alkyl ions when intermediate complexes are formed. Therefore, polyol is more  
225 reactive than PEG to react with MDI. However, the addition of PEG will increase the length  
226 of the polyurethane chain and prevent side effects such as the formation of urea by -products  
227 of the NCO group reaction in urethane pre - polymer and water molecules from the  
228 environment. If the NCO group reacts with the excess water in the environment, the formation

229 of urea and carbon dioxide gas will also occur excessively (**Figure 4**). This reaction can cause  
230 a polyurethane foam not polyurethane film as we studied the film.



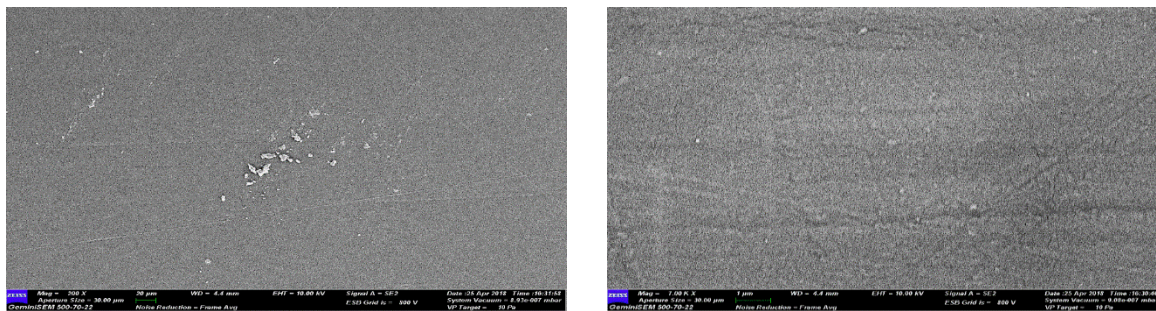
232 **Figure 4.** The reaction between NCO group and water producing carbon dioxide

233

#### 234 b. Morphological analysis

235 The Field Emission Scanning Electron Microscope (FESEM) micrograph in **Figure 5** shows  
236 the formation of a uniform polymer film contributed by the polymerization method applied.  
237 The magnification used for this surface analysis ranged from 200 to 5000 ×. The  
238 polymerization method can also avoid the failure of the reaction in PU polymerization.  
239 Furthermore, no trace of separation was detected by FESEM. This has also been justified by  
240 the wavelengths obtained by the FTIR spectrums above.

241



242 **Figure 5.** The micrograph of polyurethane films analysed by FESEM at (a) 200 × and (b)  
243 5000× magnifications.

244

#### 245 c. The crosslinking analysis

246 Soxhlet analysis was applied to determine the degree of crosslinking between the hard  
247 segments and the soft segments in the polyurethane. The urethane group on the hard segment  
248 along the polyurethane chain is polar (Cuve & Pascault 1991). Therefore, during the testing, it  
249 was very difficult to dissolve in toluene, as the testing reagent. The degree of the crosslinking

250 is determined by the percentage of the gel content. The analysis result obtained from the  
 251 Soxhlet testing indicating a 99.3 % gel content. This is significant in getting a stable polymer  
 252 at higher working temperature (Rogulska et al. 2007).

$$\text{Gel content (\%)} = \frac{(0.6 - 0.301) \text{ g}}{0.301 \text{ g}} \times 100\% = 99.33\%$$

253  
 254  
 255 d. The thermal analysis

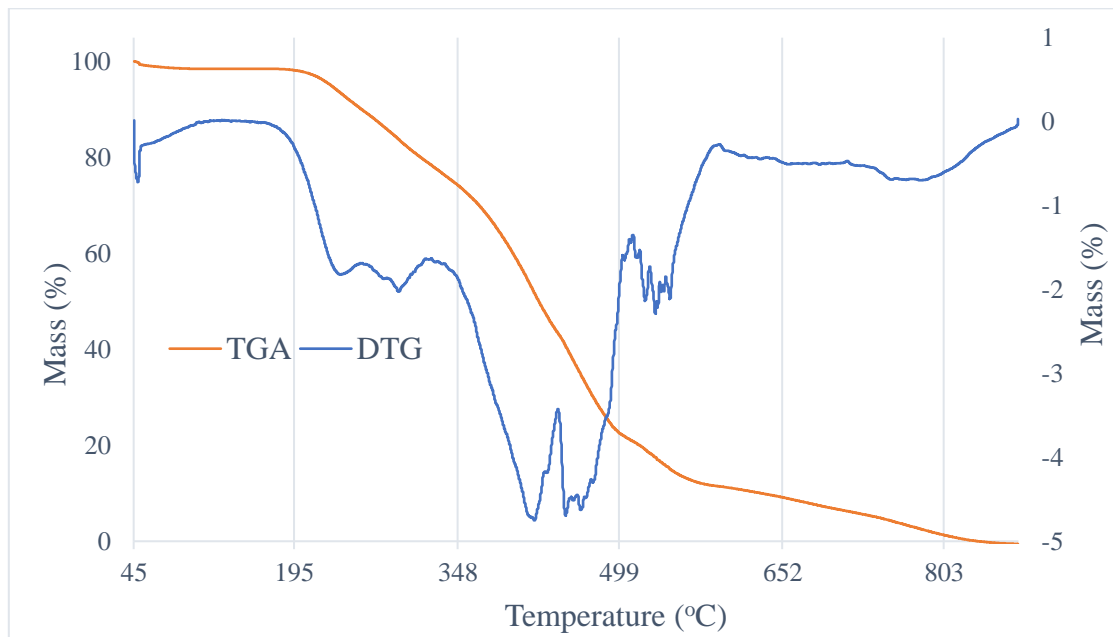
256 **Figure 6** shows the TGA and DTG thermograms of polyurethane. The percentage weight loss  
 257 (%) is listed in **Table 1**. Generally, only a small amount of weight was observed. It is shown  
 258 in **Figure 6** in the region of 45 – 180°C. This is due to the presence of condensation on moisture  
 259 and solvent residues.

260 **Table1** Weight loss percentage of (wt%) polyurethane film

Sample	% Weight loss (wt%)				Total of weight loss (%)	Residue after 550°C (%)
	T <sub>max</sub> , °C	T <sub>d1</sub> , 200 – 290°C	T <sub>d2</sub> , 350 – 500°C	T <sub>d3</sub> , 500 – 550°C		
Polyurethane	240	8.04	39.29	34.37	81.7	18.3

261  
 262 The bio polyurethane is thermally stable up to 240 °C before it undergone thermal degradation.  
 263 The first stage of thermal degradation (T<sub>d1</sub>) on polyurethane films was shown in the region of  
 264 200 – 290°C as shown in **Figure 6**. The T<sub>d1</sub> is associated with degradation of the hard segments  
 265 of the urethane bond, forming alcohol or degradation of the polyol chains and releasing of  
 266 isocyanates (Berta et al. 2006), primary and secondary amines as well as carbon dioxide  
 267 (Corcuera et al. 2011; Pan & Webster 2012). Meanwhile, the second thermal degradation stage  
 268 (T<sub>d2</sub>) of polyurethane films experienced a weight loss of 39.29 %. This endotherm of T<sub>d2</sub> is  
 269 related to dimerization of isocyanates to form carbodiimides and release CO<sub>2</sub>. The formed

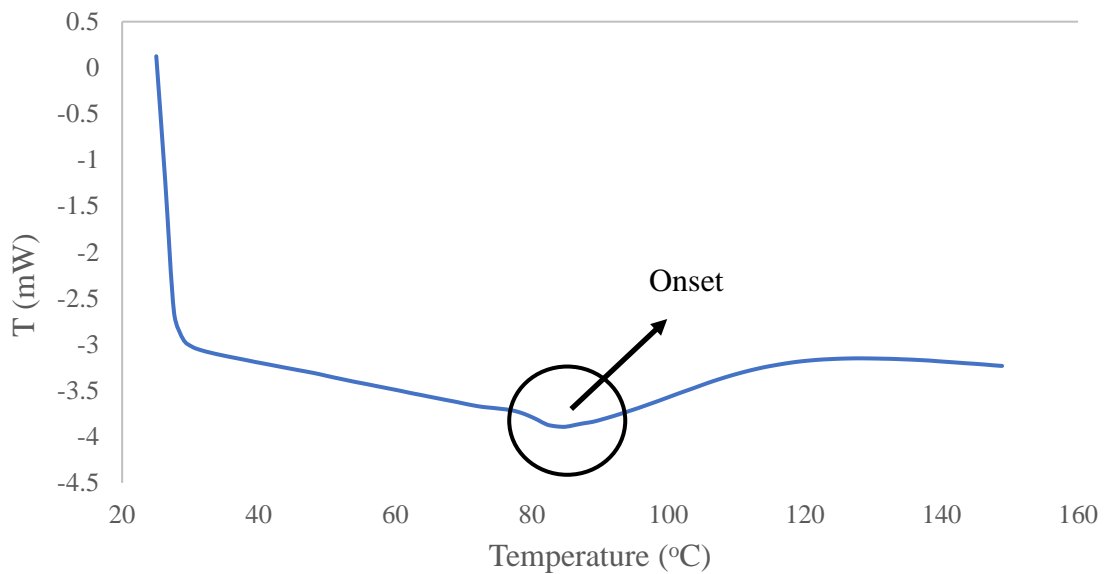
270 carbodiimide reacts with alcohol to form urea. For the third stage of thermal degradation ( $T_{d3}$ )  
271 is related to the degradation on urea (Berta et al. 2006) and the soft segment on polyurethane.



272  
273 **Figure 6.** DTG and TGA thermogram of polyurethane film  
274

275 Generally, DSC analysis exhibited thermal transitions as well as the initial  
276 crystallisation and melting temperatures of the polyurethane (Khairuddin et al. 2018). It serves  
277 to analyse changes in thermal behaviour due to changes occurring in the chemical chain  
278 structure based on the glass transition temperature ( $T_g$ ) of the sample obtained from the DSC  
279 thermogram (**Figure 7**). DSC analysis on polyurethane films was performed in the temperature  
280 at range 100 °C to 200 °C using nitrogen gas as blanket as proposed by Furtwengler et al.  
281 (2017). The glass transition temperature ( $T_g$ ) on polyurethane was above room temperature, at  
282 78.1 °C indicated the state of glass on polyurethane. The presence of MDI contributes to the  
283 formation of hard segments in polyurethanes. During polymerization, this hard segment  
284 restricts the mobility of the polymer chain (Ren et al. 2013) owing to steric effect on benzene  
285 ring in hard segment. The endothermic peak of acetone used as the solvent in this study was  
286 supposedly be at 56°C. However, it was detected in the DSC thermogram nor the TGA  
287 thermogram, which indicates that acetone was removed from the polyurethane during the

288 synthesis process, owing to its volatility nature. The presence of acetone in the synthesis was  
289 to lower the reaction kinetics.



290

291 **Figure 7.** DSC thermogram of polyurethane film

292

293

294

e. The solubility and mechanical properties of the polyurethane film

295

The chemical resistivity of a polymer will be the determinant in performing as conductor. Thus,

296

its solubility in various solvents was determined by dissolving the polymer in selected solvents

297

such as hexane, benzene, acetone, tetrahydrofuran (THF), dimethylformamide (DMF) and

298

dimethylformamide (DMSO). On the other hand, the mechanical properties of polyurethane

299

were determined based on the standard testing following ASTM D 638 (Standard Test Method

300

for Tensile Properties of Plastics) . The results from the polyurethane film solubility and tensile

301

test are shown in **Table 2**. Polyurethane films were insoluble with benzene, hexane and acetone

302

and are only slightly soluble in tetrahydrofuran (THF), dimethylformamide (DMF) and

303

dimethylformamide (DMSO) solutions. While the tensile strength of a PU film indicated how

304

much elongation load the film was capable of withstanding the material before breaking.

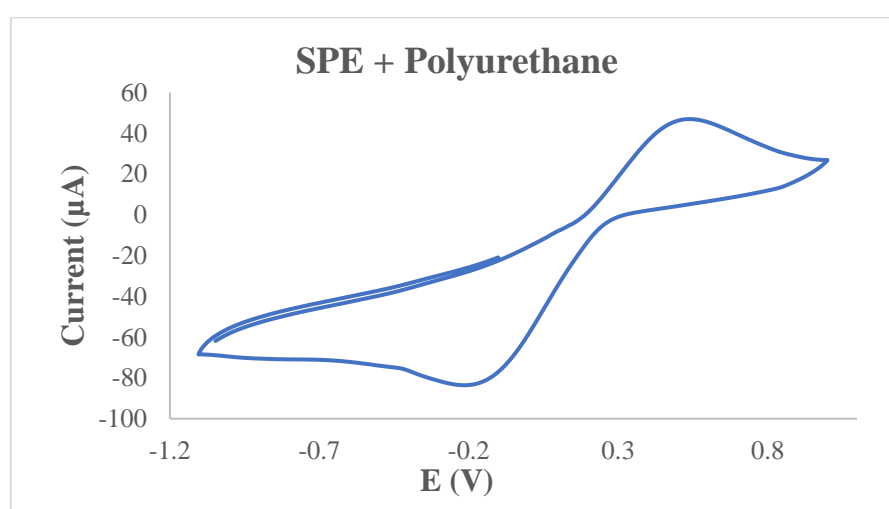
305 The tensile stress, strain and modulus of polyurethane film also indicated that polyurethane has  
 306 good mechanical properties that are capable of being a supporting substrate for the next stage  
 307 of study. In the production of polyurethane, the properties of polyurethane are easily influenced  
 308 by the content of MDI and polyol used. The length of the chain and its flexibility are contributed  
 309 by the polyol which makes it elastic. High crosslinking content can also produce hard and rigid  
 310 polymers. MDI is a major component in the formation of hard segments in polyurethane. It is  
 311 this hard segment that determines the rigidity of the PU. Therefore, high isocyanate content  
 312 results in higher rigidity on PU (Petrovic et al. 2002). Thus, the polymer has a higher resistance  
 313 to deformation and more stress can be applied to the PU.

314 **Table 2** The solubility and mechanical properties of the polyurethane film

Parameters		Polyurethane film
Solubility	Benzene	Insoluble
	Hexane	Insoluble
	Acetone	Insoluble
	THF	Less soluble
	DMF	Less soluble
	DMSO	Less soluble
Stress (MPa)		8.53
Elongation percentage (%)		43.34
Strain modulus (100) (MPa)		222.10

316  
 317 f. Conductivity of the polyurethane as polymeric film on SPE  
 318  
 319 Polyurethane film deposited onto the screen printed electrode by casting method as shown in  
 320 **Figure 1**. After that, the modified electrode was analysed using cyclic voltammetry (CV) and

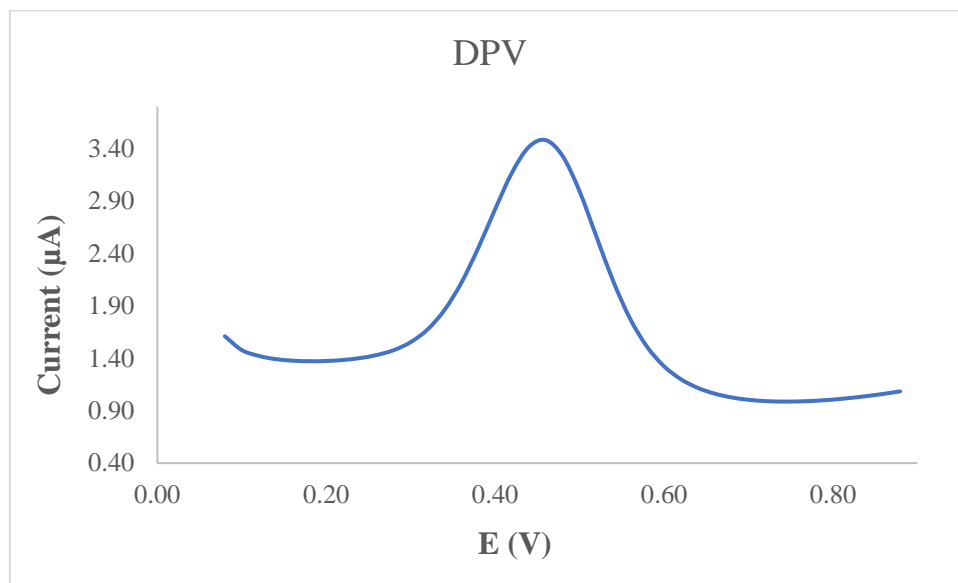
321 differential pulse voltammetry (DPV) in order to study the behaviour of modified electrode.  
322 The modified electrode was tested in a 0.1 mmol/L KCl solution containing 5 mmol/L ( $K_3Fe$   
323  $(CN)_6$ ). The use of potassium ferricyanide is intended to increase the sensitivity of the KCl  
324 solution. The conductivity of the modified electrode was studied. The electrode was analyzed  
325 by cyclic voltammetry method with a potential range of -1.00 to +1.00 with a scan rate of 0.05  
326 V/s. The voltamogram at electrode have shown a specific redox reactions. Furthermore, the  
327 conductivity of the modified electrode is lower due to the use of polyurethane. This occurs due  
328 to PU is a natural polymer produced from the polyol of palm kernel oil. The electrochemical  
329 signal at the electrode is low if there is a decrease in electrochemical conductivity (El - Raheem  
330 et al. 2020). It can be concluded that polyurethane is a bio – polymer with a low conductivity  
331 value. The current of modified electrode was found at  $5.3 \times 10^{-5}$  A or 53  $\mu$ A.  
332 According to **Figure 8**, it can be concluded that the anodic peak present in the modified  
333 electrode was at +0.5 V, it also represented the oxidation process of the modified electrode. The  
334 first oxidation scan on both electrodes ranged from -0.2 to +1.0 V, which showed a significant  
335 anodic peak at a potential of +0.5 V.



336  
337 **Figure 8.** The voltamogram of SPE – PU modified electrode after analysed using cyclic  
338 voltammetry (CV) technique  
339



340 **Figure 9** also presents the DPV voltammogram of modified electrode. DPV is a measurement  
 341 based on the difference in potential pulses that produce an electric current. Scanning the  
 342 capability pulses to the working electrode will produce different currents. Optimal peak  
 343 currents will be produced to the reduction capacity of the redox material. The peak current  
 344 produced is proportional to the concentration of the redox substance and can be detected up to  
 345 concentration below  $10^{-8}$  M. DPV conducted to obtain the current value that more accurate than  
 346 CV (Lee et al. 2018).



347  
 348 **Figure 9.** The voltammogram of SPE – PU modified electrode after analyzed using  
 349 differential pulse voltammetry (DPV) technique

350  
 351 This study used a redox pair ( $K_3Fe(CN)_6$ ) as a test device (probe). The currents generated by  
 352 SPE-PU and proved by CV and DPV have shown conductivity on polyurethane films. This  
 353 suggests that polyurethane films can conduct electron transfer. The electrochemical area on the  
 354 modified electrode can be calculated using the formula from Randles-Sevcik (Butwong et al.  
 355 2019), where the electrochemical area for SPE-PU is considered to be A, using Equation 2:

356  
 357 **Current of SPE-PU ,  $I_p = 2.65 \times 10^5 n^{3/2} A v^{1/2} CD^{1/2}$**  (2)

358 Where,  $n - 1$  is the amount of electron transfer involved, while  $C$  is the solvent concentration  
359 used (mmol/L) and the value of  $D$  is the diffusion constant of 5 mmol/L at  $(K_3Fe(CN)_6)$   
360 dissolved using 0.1 mmol/L KCl. The estimated surface area of the electrode (**Figure 1**) was  
361  $0.2 \text{ cm}^2$  where the length and width of the electrode used during the study was  $0.44 \text{ cm} \times 0.44$   
362  $\text{cm}$  while the surface area of the modified electrode was  $0.25 \text{ cm}^2$  with the length and width of  
363 the electrode estimated at  $0.5 \text{ cm} \times 0.5 \text{ cm}$ , and causing the modified electrode has a larger  
364 surface. The corresponding surface concentration ( $\tau$ ) ( $\text{mol}/\text{cm}^2$ ) is calculated using Equation 3.

$$365 \quad I_p = (n^2 F^2 / 4RT) A \tau v \quad (3)$$

366  $I_p$  is the peak current (A), while  $A$  is the surface area of the electrode ( $\text{cm}^2$ ), the value of  $v$  is  
367 the applied scan rate (mV/s) and  $F$  is the Faraday constant (96,584 C/mol),  $R$  is the constant  
368 ideal gas (8.314 J/mol K) and  $T$  is the temperature used during the experiment being conducted  
369 (298 K) (Koita et al. 2014).

370

#### 371 **4. Conclusion**

372 Polyurethane film was prepared by pre-polymerization between palm kernel oil-based polyol  
373 (PKO-p) with MDI. The presence of PEG 400 as the chain extender formed freestanding  
374 flexible film. Acetone was used as the solvent to lower the reaction kinetics since the pre-  
375 polymerization was carried out at room temperature. The formation of urethane links (NHCO  
376 – backbone) after polymerization was confirmed by the absence of  $N=C=O$  peak at  $2241 \text{ cm}^{-1}$   
377 and the presence of N-H peak at  $3300 \text{ cm}^{-1}$ , carbonyl (C=O) at  $1710 \text{ cm}^{-1}$ , carbamate (C-N) at  
378  $1600 \text{ cm}^{-1}$ , ether (C-O-C) at  $1065 \text{ cm}^{-1}$ , benzene ring (C = C) at  $1535 \text{ cm}^{-1}$  in the bio  
379 polyurethane chain structure. Soxhlet analysis for the determination of crosslinking on  
380 polyurethane films has yielded a high percentage of 99.33 %. This is contributed by the hard  
381 segments formed from the reaction between isocyanates and hydroxyl groups causing  
382 elongation of polymer chains. FESEM analysis exhibited absence of phase separation and

383 smooth surface. Meanwhile, the current of modified electrode was found at  $5.2 \times 10^{-5}$  A. This  
384 bio polyurethane film can be used as a conducting bio – polymer and it is very useful for other  
385 studies such as electrochemical sensor purpose.

386

## 387 **5. Patents**

388 There are no patents resulting from the work reported in this manuscript.

## 389 **6. Author contributions**

390 Munir. M.A. and Badri. K.H. performed the measurements, Badri. K.H. and Heng. L.Y. were  
391 involved in planning and supervised the work, Munir. M.A and Badri. K.H. processed the  
392 experimental data, performed the analysis, drafted the manuscript, designed the figures, and  
393 performed the calculations. Munir. M.A. and Badri. K.H. prepared and characterized the  
394 samples through FTIR spectroscopy, TGA and DSC analyses as well as the conductivity.  
395 Munir. M.A. and Badri. K.H. conducted the interpretation of results and write up of the  
396 manuscript. All authors discussed the results and commented on the manuscript.

397

## 398 **7. Funding**

399 This research was funded by Universiti Kebangsaan Malaysia, through its internal grant  
400 number GGP-2019-021. The APC was funded by Faculty of Science and Technology,  
401 Universiti Kebangsaan Malaysia.

402

## 403 **8. Acknowledgement**

404 The authors would like to thank Universiti Kebangsaan Malaysia for the partial sponsorship of  
405 the honorarium given to the first author through the research grant number GGP-2019-021. We  
406 would like to also, thank Department of Chemical Sciences, Universiti Kebangsaan Malaysia  
407 for the laboratory facilities and CRIM, UKM for the analysis infrastructure.

408

409 **9. Conflict of Interest**

410 The authors declare no conflict of interest.

411

412 **10. References**

413 Akindoyo, J. O., Beg, M.D.H., Ghazali, S., Islam, M.R., Jeyaratnam, N. & Yuvaraj, A.R.

414 (2016). Polyurethane types, synthesis and applications – a review. *RSC Advances*. **6**:

415 114453 – 114482.

416 Alqarni, S. A., Hussein, M. A., Ganash, A. A. & Khan, A. (2020). Composite material – based

417 conducting polymers for electrochemical sensor applications: a mini review.

418 *BioNanoScience*. **10**: 351 – 364.

419 Badri, K.H. (2012) Biobased polyurethane from palm kernel oil-based polyol. In Polyurethane;

420 Zafar, F., Sharmin, E., Eds. InTechOpen: Rijeka, Croatia. pp. 447–470.

421 Badri, K.H., Ahmad, S.H. & Zakaria, S. 2000. Production of a high-functionality RBD palm

422 kernel oil – based polyester polyol. *Journal of Applied Polymer Science* 81(2): 384 –

423 389.

424 Berta, M., Lindsay, C., Pans, G., & Camino, G. (2006). Effect of chemical structure on

425 combustion and thermal behaviour of polyurethane elastomer layered silicate

426 nanocomposites. *Polymer Degradation and Stability*. **91**: 1179-1191.

427 Borowicz, M., Sadowska, J. P., Lubczak, J. & Czuprynski, B. (2019). Biodegradable, flame –

428 retardant, and bio – based rigid polyurethane/polyisocyanurate foams for thermal

429 insulation application. *Polymers*. **11**: 1816 – 1839.

430 Butwong, N., Khajonklin, J., Thongbor, A. & Luong, J.H.T. (2019). Electrochemical sensing

431 of histamine using a glassy carbon electrode modified with multiwalled carbon nanotubes

432 decorated with Ag – Ag<sub>2</sub>O nanoparticles. *Microchimica Acta*. **186 (11)**: 1 – 10.

433 Clemitson, I. (2008). Castable Polyurethane Elastomers. Taylor & Francis Group, New York.  
434 doi:10.1201/9781420065770.

435 Corcuera, M.A., Rueda, L., Saralegui, A., Martin, M.D., Fernandez-d'Arlas, B., Mondragon,  
436 I. & Eceiza, A. (2011). Effect of diisocyanate structure on the properties and  
437 microstructure of polyurethanes based on polyols derived from renewable resources.  
438 *Journal of Applied Polymer Science*. **122**: 3677-3685.

439 Cuve, L. & Pascault, J.P. (1991). Synthesis and properties of polyurethanes based on  
440 polyolefine: Rigid polyurethanes and amorphous segmented polyurethanes prepared in  
441 polar solvents under homogeneous conditions. *Polymer*. **32** (2): 343- 352.

442 Dzulkipli, M. Z., Karim, J., Ahmad, A., DzulKurnain, N. A., Su'ait, M S., Fujita, M. Y., Khoon,  
443 L. T. & Hassan, N. H. (2021). The influences of 1-butyl-3-methylimidazolium  
444 tetrafluoroborate on electrochemical, thermal and structural studies as ionic liquid gel  
445 polymer electrolyte. *Polymers*. 13 (8): 1277 – 1294.

446 El-Raheem, H.A., Hassan, R.Y.A., Khaled, R., Farghali, A. & El-Sherbiny, I.M. (2020).  
447 Polyurethane – doped platinum nanoparticles modified carbon paste electrode for the  
448 sensitive and selective voltammetric determination of free copper ions in biological  
449 samples. *Microchemical Journal*. **155**: 104765.

450 Fei, T., Li, Y., Liu, B. & Xia, C. (2019). Flexible polyurethane/boron nitride composites with  
451 enhanced thermal conductivity. *High Performance Polymers*. **32** (3): 1 – 10.

452 Furtwengler, P., Perrin R., Redl, A. & Averous, L. (2017). Synthesis and characterization of  
453 polyurethane foams derived of fully renewable polyesters polyols from sorbitol.  
454 *European Polymer Journal*. **97**: 319 – 327.

455 Guo, S., Zhang, C., Yang, M., Zhou, Y., Bi, C., Lv, Q. & Ma, N. (2020). A facile and sensitive  
456 electrochemical sensor for non – enzymatic glucose detection based on three –

457 dimensional flexible polyurethane sponge decorated with nickel hydroxide. *Analytica*  
458 *Chimica Acta*. **1109**: 130 – 139.

459 Hamuzan, H.A. & Badri, K.H. (2016). The role of isocyanates in determining the viscoelastic  
460 properties of polyurethane. AIP Conference Proceedings. 1784, Issue 1.

461 Herrington, R. & Hock, K. (1997). Flexible polyurethane foams. 2nd Edition. Dow Chemical  
462 Company. Midlan.

463 Janpoung, P., Pattanauwat, P. & Potiyaraj, P. (2020). Improvement of electrical conductivity  
464 of polyurethane/polypyrrole blends by graphene. *Key Engineering Materials*. **831**: 122 –  
465 126.

466 Khairuddin, F.H., Yusof, N. I. M., Badri, K., Ceylan, H., Tawil, S. N. M. (2018). Thermal,  
467 chemical and imaging analysis of polyurethane/cecabase modified bitumen. *IOP Conf.*  
468 *Series: Materials Science and Engineering*. 512: 012032.

469 Koita, D., Tzedakis, T., Kane, C., Diaw, M., Sock, O. & Lavedan, P. (2014). Study of the  
470 histamine electrochemical oxidation catalyzed by nickel sulfate. *Electroanalysis*. **26 (10)**:  
471 2224 – 2236.

472 Kotal, M., Srivastava, S.K. & Paramanik, B. (2011). Enhancements in conductivity and thermal  
473 stabilities of polyurethane/polypyrrole nanoblends. *The Journal of Physical Chemistry*  
474 *C*. **115 (5)**: 1496 – 1505.

475 Ladan, M., Basirun, W.J., Kazi, S.N., Rahman, F.A. (2017). Corrosion protection of AISI 1018  
476 steel using Co – doped TiO<sub>2</sub>/polypyrrole nanocomposites in 3.5% NaCl solution.  
477 *Materials Chemistry and Physics*. **192**: 361 – 373.

478 Lampman, G.M., Pavia, D.L., Kriz, G.S. & Vyvyan, J.R. (2010). Spectroscopy. 4th Edition.  
479 Brooks/Cole Cengage Learning, Belmont, USA.

480 Lee, K.J., Elgrishi, N., Kandemir, B. & Dempsey, J.L. 2018. Electrochemical and spectroscopic  
481 methods for evaluating molecular electrocatalysts. *Nature Reviews Chemistry* 1(5): 1 -  
482 14.

483 Leykin, A., Shapovalov, L. & Figovsky, O. (2016). Non – isocyanate polyurethanes –  
484 Yesterday, today and tomorrow. *Alternative Energy and Ecology*. **191** (3 – 4): 95 – 108.

485 Mishra, K., Narayan, R., Raju, K.V.S.N. & Aminabhavi, T.M. (2012). Hyperbranched  
486 polyurethane (HBPU)-urea and HBPU-imide coatings: Effect of chain extender and  
487 NCO/OH ratio on their properties. *Progress in Organic Coatings*. **74**: 134 – 141.

488 Mutsuhisa F., Ken, K. & Shohei, N. (2007). Microphase separated structure and mechanical  
489 properties of norbornane diisocyanate – based polyurethane. *Polymer*. **48** (4): 997 – 1004.

490 Nohra, B., Candy, L., Blancos, J.F., Guerin, C., Raoul, Y. & Mouloungui, Z. (2013). From  
491 petrochemical polyurethanes to biobased polyhydroxyurethanes. *Macromolecules*. **46**  
492 (10): 3771 – 3792.

493 Pan, T. & Yu, Q. (2016). Anti – corrosion methods and materials comprehensive evaluation of  
494 anti – corrosion capacity of electroactive polyaniline for steels. *Anti – Corrosion Methods  
495 and Materials*. **63**: 360 – 368.

496 Pan, X. & Webster, D.C. (2012). New biobased high functionality polyols and their use in  
497 polyurethane coatings. *ChemSusChem*. **5**: 419-429.

498 Petrovic, Z.S. (2008). Polyurethanes from vegetable oils. *Polymer Reviews*. **48** (1): 109 – 155.

499 Priya, S. S., Karthika, M., Selvasekarapandian, S. & Manjuladevi, R. (2018). Preparation and  
500 characterization of polymer electrolyte based on biopolymer I-carrageenan with  
501 magnesium nitrate. *Solid State Ionics*. **327**: 136 – 149.

502 Ren, D. & Frazier, C.E. (2013). Structure–property behaviour of moisture-cure polyurethane  
503 wood adhesives: Influence of hard segment content. *Adhesion and Adhesives*. **45**: 118-  
504 124.

505 Rogulska, S.K., Kultys, A. & Podkoscielny, W. (2007). Studies on thermoplastic polyurethanes  
506 based on new diphenylethane – derivative diols. II. Synthesis and characterization of  
507 segmented polyurethanes from HDI and MDI. *European Polymer Journal*. **43**: 1402 –  
508 1414.

509 Romaskevicius, T., Budriene, S., Pielichowski, K. & Pielichowski, J. (2006). Application of  
510 polyurethane – based materials for immobilization of enzymes and cells: a review.  
511 *Chemija*. **17**: 74 – 89.

512 Sengodu, P. & Deshmukh, A. D. (2015). Conducting polymers and their inorganic composites  
513 for advanced Li-ion batteries: a review. *RSC Advances*. **5**: 42109 – 42130.

514 Su'ait, M. S., Ahmad, A., Badri, K. H., Mohamed, N. S., Rahman, M. Y. A., Ricardi, C. L. A.  
515 & Scardi, P. The potential of polyurethane bio – based solid polymer electrolyte for  
516 photoelectrochemical cell application. *International Journal of Hydrogen Energy*. **39** (6):  
517 3005 – 3017.

518 Tran, V.H., Kim, J.D., Kim, J.H., Kim, S.K., Lee, J.M. (2020). Influence of cellulose  
519 nanocrystal on the cryogenic mechanical behaviour and thermal conductivity of  
520 polyurethane composite. *Journal of Polymers and The Environment*. **28**: 1169 – 1179.

521 Viera, I.R.S., Costa, L.D.F.D.O., Miranda, G.D.S., Nardehcia, S., Monteiro, M.S.D. S.D.B.,  
522 Junior, E.R. & Delpech, M.C. (2020). Waterborne poly (urethane – urea)s  
523 nanocomposites reinforced with clay, reduced graphene oxide and respective hybrids:  
524 Synthesis, stability and structural characterization. *Journal of Polymers and The  
525 Environment*. **28**: 74 – 90.

526 Wang, B., Wang, L., Li, X., Liu, Y., Zhang, Z., Hedrick, E., Safe, S., Qiu, J., Lu, G. & Wang,  
527 S. (2018). Template – free fabrication of vertically – aligned polymer nanowire array on  
528 the flat – end tip for quantifying the single living cancer cells and nanosurface interaction.  
529 *a Manufacturing Letters*. **16**: 27 – 31.



- 530 Wang, J., Xiao, L., Du, X., Wang, J. & Ma, H. (2017). Polypyrrole composites with carbon  
531 materials for supercapacitors. *Chemical Papers*. **71** (2): 293 – 316.
- 532 Wong, C.S. & Badri, K.H. (2012). Chemical analyses of palm kernel oil – based polyurethane  
533 prepolymer. *Materials Sciences and Applications*. **3**: 78 – 86.
- 534 Yong, Z., Bo, Z.M., Bo, W., Lin, J.Z. & Jun, N. (2009). Synthesis and properties of novel  
535 polyurethane acrylate containing 3-(2-Hydroxyethyl) isocyanurate segment. *Progress in*  
536 *Organic Coatings*. **67**: 264 – 268
- 537 Zia, K. M., Anjum, S., Zuber, M., Mujahid, M. & Jamil, T. (2014). Synthesis and molecular  
538 characterization of chitosan based polyurethane elastomers using aromatic diisocyanate.  
539 *International of Journal of Biological Macromolecules*. **66**: 26 – 32.
- 540
- 541
- 542

[← BACK](#) [DASHBOARD / ARTICLE DETAILS](#)

Updated on 2021-09-02

Version 2

# Design and Synthesis of Conducting Polymer Based on Polyurethane produced from Palm Kernel Oil

VIEWING AN OLDER VERSION

ID 6815187

Muhammad Abdurrahman Munir <sup>SA CA</sup> <sup>1</sup>,  
Khairiah Haji Badri<sup>1</sup>, Lee Yook Heng<sup>1</sup>  
[+ Show Affiliations](#)

**Article Type**

Research Article



Hindawi

Muhammad Abdurrahman

Rydz Joanna

Submitted on 2021-06-14 (2 years ago)

[> Abstract](#)[> Author Declaration](#)[> Files](#) 2[- Editorial Comments](#)

**Peter Foot**

02.09.2021

**Decision**

Major Revision Requested

**Message for Author**

This manuscript is interesting and has sufficient merits to be considered further for publication after due amendments to address the reviewers' comments. The English is quite understandable, but it requires revision to improve the clarity sufficiently for publication.

**— Response to Revision Request****Muhammad Abdurrahman Munir**

22.07.2021

**Your Reply**

Dear Editor, Thank you for your comments to this manuscript. Here I attached the revised manuscript and I have highlighted several sentences as to response your comments before. Kind Regards.

**File**

Manuscript - Munir.docx 909 kB

**+ Reviewer Reports**

1           **Design and Synthesis of Conducting Polymer Based on Polyurethane**  
2   **produced from Palm Kernel Oil**

3           Muhammad Abdurrahman Munir<sup>1,2\*</sup>, Khairiah Haji Badri<sup>1,3</sup>, Lee Yook Heng<sup>1</sup>

4           <sup>1</sup>Department of Chemical Sciences, Faculty of Science and Technology, Universiti  
5   Kebangsaan Malaysia, Bangi, Malaysia

6           <sup>2</sup>Department of Pharmacy, Faculty of Health Science, Universitas Alma Ata, Daerah  
7   Istimewa Yogyakarta, Indonesia

8           <sup>3</sup>Polymer Research Center, Universiti Kebangsaan Malaysia, Bangi, Malaysia

9   \*Email: [muhammad@almaata.ac.id](mailto:muhammad@almaata.ac.id)

11   **Abstract**

12   Polyurethane (PU) is a unique polymer that has versatile processing method and mechanical  
13   properties upon inclusion of selected additives. In this study, a freestanding bio-polyurethane  
14   film on screen – printed electrode (SPE) was prepared by solution casting technique, using  
15   acetone as solvent. It was a one-pot synthesis between major reactants namely, palm kernel  
16   oil-based polyol (PKOp) and 4,4-methylene diisocyanate. The PU undergone strong adhesion  
17   on SPE. The formation of urethane linkages (NHCO backbone) after polymerization was  
18   confirmed by the absence of N=C=O peak at 2241 cm<sup>-1</sup>. The glass transition temperature (*T<sub>g</sub>*)  
19   of the polyurethane was detected at 78.1°C. The conductivity of PU was determined using  
20   cyclic voltammetry (CV) and differential pulse voltammetry (DPV). The current of electrode  
21   was at 5.2 x 10<sup>-5</sup> A.

22   **Keywords:** Polyurethane, polymerization, screen – printed electrode, voltammetry

## 26 **1. Introduction**

27 Polymers are molecules composed of many repeated sub-units referred to as monomers  
28 (Sengodu & Deshmukh 2015). Conducting polymers (CPs) are polymers that exhibit  
29 electrical behaviour (Alqarni et al. 2020). The conductivity of CPs was first observed in  
30 polyacetylene, nevertheless owing to its instability led to the discovery of other forms of CPs  
31 such as polyaniline (PANI), poly (o-toluidine) (PoT), polythiophene (PTh), polyfluorene (PF)  
32 and polyurethane (PU). Furthermore, natural CPs have low conductivity and are often semi-  
33 conductive. Therefore, it is essential to increase their conductivity mainly for use in  
34 electrochemical sensor programs (Dzulkipli et al. 2021; Wang et al. 2018). Conducting  
35 polymers (CPs) represent a sizeable range of useful organic substances. Their unique  
36 electrical, chemical and physical properties; reasonable price; simple preparation; small  
37 dimensions and large surface area have enabled researchers to discover a wide variety of uses  
38 such as sensors, biochemical applications, solar cells and electrochromic devices (Alqarni et  
39 al. 2020; Ghosh et al. 2018). There are scientific documentations on the use of conductive  
40 polymers in various studies such as polyaniline (Pan & Yu 2016), polypyrrole (Ladan et al.  
41 2017) and polyurethane (Tran et al. 2020; Vieira et al. 2020; Guo et al. 2020; Fei et al. 2020).  
42 The application of petroleum as polyol in order to produce polyurethane has been applied.  
43 The coal and crude oil used as raw materials to produce it. Nevertheless, these materials  
44 become very rare to find and the price is very expensive at the same time required  
45 sophisticated system to produce it. These reasons have been considered and finding utilizing  
46 plants that can be used as alternative polyols should be done immediately (Badri 2012).  
47 Furthermore, in order to avoid the application of petroleum as raw material for polyol,  
48 vegetable oils become a better choice as polyol in order to obtain a biodegradable polyol.  
49 Vegetable oils that generally used for synthesis polyurethane are soybean oil, corn oil,

50 sunflower seed oil, coconut oil, nuts oil, rape seed, olive oil and palm oil (Badri 2012;  
51 Borowicz et al. 2019).

52 It is very straightforward for vegetable oils to react with specific group in order to form PU  
53 such as epoxy, hydroxyl, carboxyl and acrylate owing to the existence of (-C=C-) in  
54 vegetable oils. Thus, it has provided appealing profits to vegetables oils compared to  
55 petroleum considered the toxicity, price and harm the environment (Mustapha et al. 2019;  
56 Mohd Noor et al. 2020). Palm oil becomes the chosen in this study to produce PU owing to it  
57 is largely cultivated in South Asia particularly in Malaysia and Indonesia. It has several  
58 profits compared to other vegetables oils such as the easiest materials obtained, the lowest  
59 cost of all the common vegetable oils and recognized as the plantation that has low  
60 environmental impact and removing CO<sub>2</sub> from atmosphere as netsequester (Tajau et al. 2021;  
61 Septevani et al. 2015).

62 Biopolymer, a natural biodegradable polymer has attracted much attention in recent years.  
63 Global environmental awareness and fossil fuel depletion urged researchers to work in the  
64 biopolymer field (Priya et al. 2018). Polyurethane is one of the most common, versatile and  
65 researched materials in the world. These materials combine the durability and toughness of  
66 metals with the elasticity of rubber, making them suitable to replace metals, plastics and  
67 rubber in several engineered products. They have been widely applied in biomedical  
68 applications, building and construction applications, automotive, textiles and in several other  
69 industries due to their superior properties in terms of hardness, elongation, strength and  
70 modulus (Zia et al. 2014; Romaskevicius et al. 2006). Polyurethanes also considered to be one  
71 of the most useful materials with many profits such as, possess low conductivity, low density,  
72 absorption capability and dimensional stability. They are clearly a great research subject  
73 owing to their mechanical, physical and chemical properties (Badan & Majka 2017).

74 The urethane group is the major repeating unit in PUs and is produced from the reaction  
75 between alcohol (-OH) and isocyanate (NCO); albeit polyurethanes also contain other groups  
76 such as ethers, esters, urea and some aromatic compounds. Due to the wide variety of sources  
77 from which PUs can be synthesized, thus a wide range of specific applications can be  
78 generated. They are grouped into several different classes based on the desired properties:  
79 rigid, flexible, thermoplastic, waterborne, binders, coating, adhesives, sealants and elastomers  
80 (Akindoyo et al. 2016).

81 Although, PU has low conductivity but it is lighter than other materials such as metals. The  
82 hardness of PU also relies on the aromatic rings number in the polymer structure (Janpoung  
83 et al, 2020; Su'ait et al. 2014), majorly contributed by the isocyanate derivatives. PU has also  
84 a conjugate structure where electrons can move in the main chain that causing electricity  
85 produced even the conductivity is low. The electrical conductivity of conjugated linear ( $\pi$ )  
86 can be explained by the distance between the highest energy level containing electrons  
87 (HOMO) called valence band and the lowest energy level not containing electrons (LUMO)  
88 called the conduction band (Wang et al. 2017; Kotal et al. 2011).

89 Nowadays, screen – printed electrodes (SPEs) modified with conducting polymer have been  
90 developed for various electrochemical sensing. SPE becomes the best solution owing to its  
91 frugal manufacture, tiny size, able to produce in large – scale and can be applied for on – site  
92 detection (Nakthong et al. 2020). Conducting polymers (CPs) become an alternative to  
93 modify the screen – printed electrodes due to their electrical conductivity, able to capture  
94 analyte by chemical/physical adsorption, large surface area and making CPs are very  
95 appealing material from electrochemical perspectives (Baig et al. 2019). Such advantages of  
96 SPE encourage us to construct a new electrode for electrochemical sensing, and no research  
97 reported on direct electrochemical oxidation of histamine using screen printed electrode

98 modified by polyurethane. Therefore, this research is the first to develop a new electrode  
99 using (screen printed polyurethane electrode) SPPE without any conducting materials.

100 The purpose of this work was to synthesis, characterize and study the conductivity of  
101 polyurethane using cyclic voltammetry (CV) and differential pulse voltammetry (DPV)  
102 attached onto screen printed electrode (SPE). To the best of our knowledge, this is the first  
103 attempt to use a modified polyurethane electrode. The electrochemistry of polyurethane  
104 mounted onto screen-printed electrode (SPE) is discussed in detail. Polyurethane is possible  
105 to become an advanced frontier material in chemically modified electrodes for bio sensing  
106 application.

107

## 108 **2. Experimental**

### 109 **2.1 Chemicals**

110 *Synthesis of polyurethana film:* Palm kernel oil (PKOp) supplied by UKM Technology Sdn  
111 Bhd through MPOB/UKM station plant, Pekan Bangi Lama, Selangor and prepared using  
112 Badri et al. (2000) method. 4, 4-diphenylmethane diisocyanate (MDI) was acquired from  
113 Cosmopolyurethane (M) Sdn. Bhd., Klang, Malaysia. Solvents and analytical reagents were  
114 benzene ( $\geq 99.8\%$ ), toluene ( $\geq 99.8\%$ ), hexane ( $\geq 99\%$ ), acetone ( $\geq 99\%$ ), tetrahydrofuran  
115 (THF), dimethylformamide (DMF) ( $\geq 99.8\%$ ), dimethylsulfoxide (DMSO) ( $\geq 99.9\%$ ) and  
116 polyethylene glycol (PED) with a molecular weight of 400 Da obtained from Sigma Aldrich  
117 Sdn Bhd, Shah Alam.

118

### 119 **2.2 Apparatus**

120 Tensile testing was performed using a universal testing machine model Instron 5566  
121 following ASTM 638 (Standard Test Method for Tensile Properties of Plastics). The tensile



122 properties of the polyurethane film were measured at a velocity of 10 mm/min with a cell  
123 load of 5 kN.

124 The thermal properties were performed using thermogravimetry analysis (TGA) and  
125 differential scanning calorimetry (DSC) analysis. TGA was performed using a thermal  
126 analyzer of Perkin Elmer Pyris model with heating rate of 10 °C/minute at a temperature  
127 range of 30 to 800 °C under a nitrogen gas atmosphere. The DSC analysis was performed  
128 using a thermal analyzer of Perkin Elmer Pyris model with heating rate of 10 °C /minute at a  
129 temperature range of -100 to 200 °C under a nitrogen gas atmosphere. Approximately, 5-10  
130 mg of PU was weighed. Sample was heated from 25 to 150 °C for one minute, then cooled  
131 immediately from 150 -100 °C for another one minute and finally, reheated to 200 °C at a  
132 rate of 10 °C /min. At this point, the polyurethane encounters changes from elastic properties  
133 to brittle due to changes in the movement of the polymer chains. Therefore, the temperature  
134 in the middle of the inclined regions is taken as the glass transition temperature ( $T_g$ ). The  
135 melting temperature ( $T_m$ ) is identified as the maximum endothermic peak by taking the area  
136 below the peak as the enthalpy point ( $\Delta H_m$ ).

137 The morphological analysis of PU film was performed by Field Emission Scanning Electron  
138 Microscope (FESEM) model Gemini SEM microscope model 500-70-22. Before the analysis  
139 was carried out, the polyurethane film was coated with a thin layer of gold to increase the  
140 conductivity of the film. The coating method was carried out using a sputter - coater. The  
141 observations were conducted at magnification of 200× and 5000 × with 10.00 kV (Electron  
142 high tension - EHT).

143 The crosslinking of PU was determined using soxhlet extraction method. About 0.60 g of PU  
144 sample was weighed and put in an extractor tube containing 250 ml of toluene, used as a  
145 solvent. This flow of toluene was let to run for 24 hours. Mass of the PU was weighed before  
146 and after the reflux process was carried out. Then, the sample was dried in the conventional

147 oven at 100 °C for 24 hours in order to get a constant mass. The percentage of crosslinking  
148 content known as the gel content, can be calculated using Equation (1).

$$149 \quad \text{Gel content (\%)} = \frac{W_0 - W}{W} \times 100 \% \quad (1)$$

150  $W_0$  is mass of PU before the reflux process (g) and  $W$  is mass of PU after the reflux process  
151 (g).

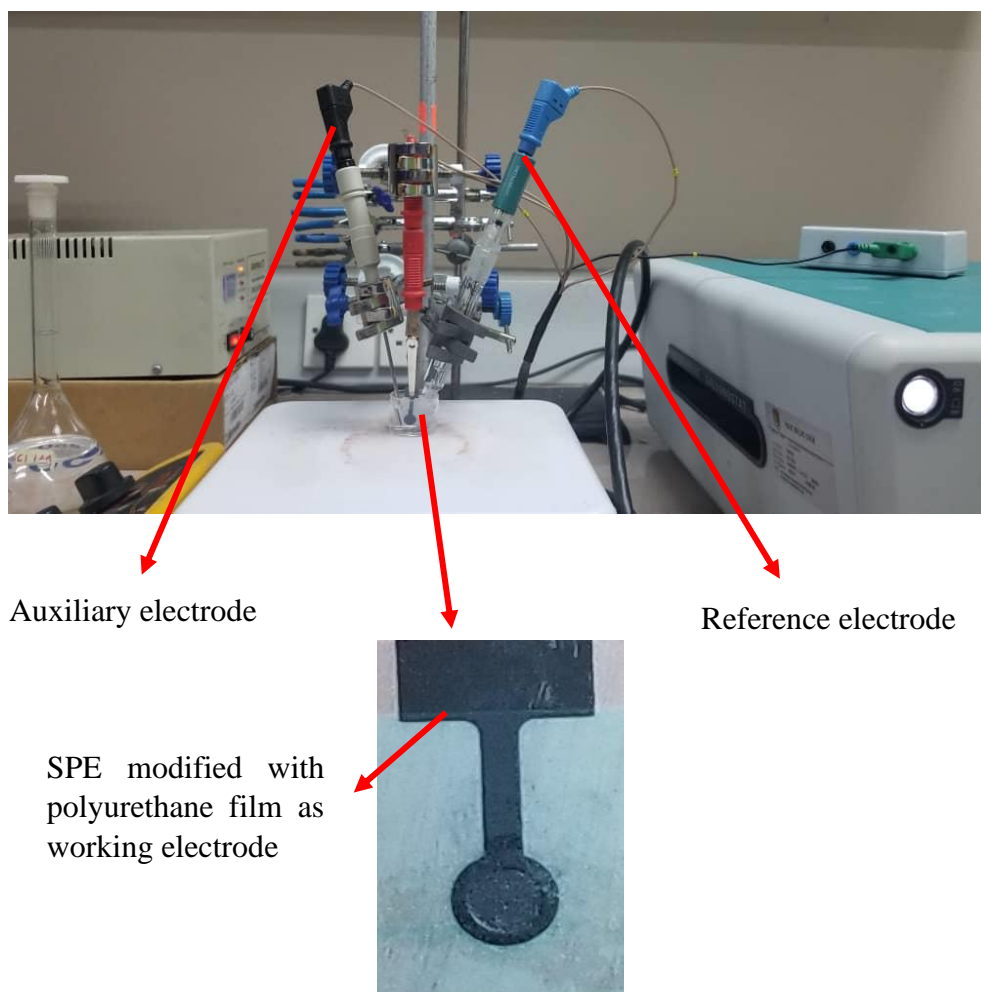
152

153 FTIR spectroscopic analysis was performed using a Perkin-Elmer Spectrum BX instrument  
154 using the Diamond Attenuation Total Reflectance (DATR) method to confirm the  
155 polyurethane, PKOp and MDI functional group. FTIR spectroscopic analysis was performed  
156 at a wave number of 4000 to 600  $\text{cm}^{-1}$  to identify the peaks of the major functional groups in  
157 the formation of polymer such as amide group (-NH), urethane carbonyl group (-C = O) and  
158 carbamate group (-CN).

159

### 160 **2.3 Modification of Electrode**

161 Voltammetric tests were performed using Metrohm Autolab Software (**Figure 1**) analyzer  
162 using cyclic voltammetry (CV) method or known as amperometric mode and differential  
163 pulse voltammetry (DPV). All electrochemical experiments were carried out using screen  
164 printed electrode (diameter 3 mm) modified using polyurethane film as working electrode,  
165 platinum wire as auxiliary electrode and Ag/AgCl electrode as reference electrode. All  
166 experiments were conducted at temperature of  $20 \pm 2^\circ\text{C}$ .



167 **Figure 1.** Potentiostat instrument to study the conductivity of SPE modified with  
 168 polyurethane film using cyclic voltametry (CV) and differential pulse voltammetry (DPV)  
 169  
 170 PU casted onto the screen – printed electrode (SPE + PU) was analyzed using a single  
 171 voltammetric cycle between -1200 and +1500 mV (vs Ag/AgCl) of ten cycles at a scanning  
 172 rate of 100 mV/s in 5 ml of KCl in order to study the activity of SPE and polyurethane film.  
 173 Approximately (0.1, 0.3 & 0.5) mg of palm – based prepolyurethane was dropped separately  
 174 onto the surface of the SPE and dried at room temperature. The modified palm-based  
 175 polyurethane electrodes were then rinsed with deionized water to remove physically adsorbed  
 176 impurities and residues of unreacted material on the electrode surface. All electrochemical  
 177 materials and calibration measurements were carried out in a 5 mL glass beaker with a  
 178 configuration of three electrodes inside it. Platinum wire and silver/silver chloride (Ag/AgCl)

179 electrodes were used as auxiliary and reference electrodes, while screen printed electrode that  
180 had been modified with polyurethane was applied as a working electrode.

181

### 182 **3. Results and Discussion**

183 The synthesis of PU films was carried out using pre - polymerization method which involves  
184 the formation of urethane polymer at an early stage. The reaction took place between palm  
185 kernel oil – based polyol (PKOp) and diisocyanate (MDI). **Table 1** presents the PKO-p  
186 properties used in this study. The structural chain was extended with the aid of polyethylene  
187 glycol (PEG) to form flexible and elastic polyurethane film. In order to form the urethane  
188 prepolymer, one of the isocyanate groups (NCO) reacts with one hydroxyl group (OH) of  
189 polyol while the other isocyanate group attacks another hydroxyl group in the polyol (Wong  
190 & Badri 2012) as shown in **Figure 2**.

191

192 **Table 1** Characteristics of PKO-p (Badri et al. (2000)).

Property	Values
Viscosity at 25°C (cps)	1313.3
Specific gravity (g/mL)	1.114
Moisture content (%)	0.09
pH value	10 – 11
The hydroxyl number mg KOH/g	450 - 470

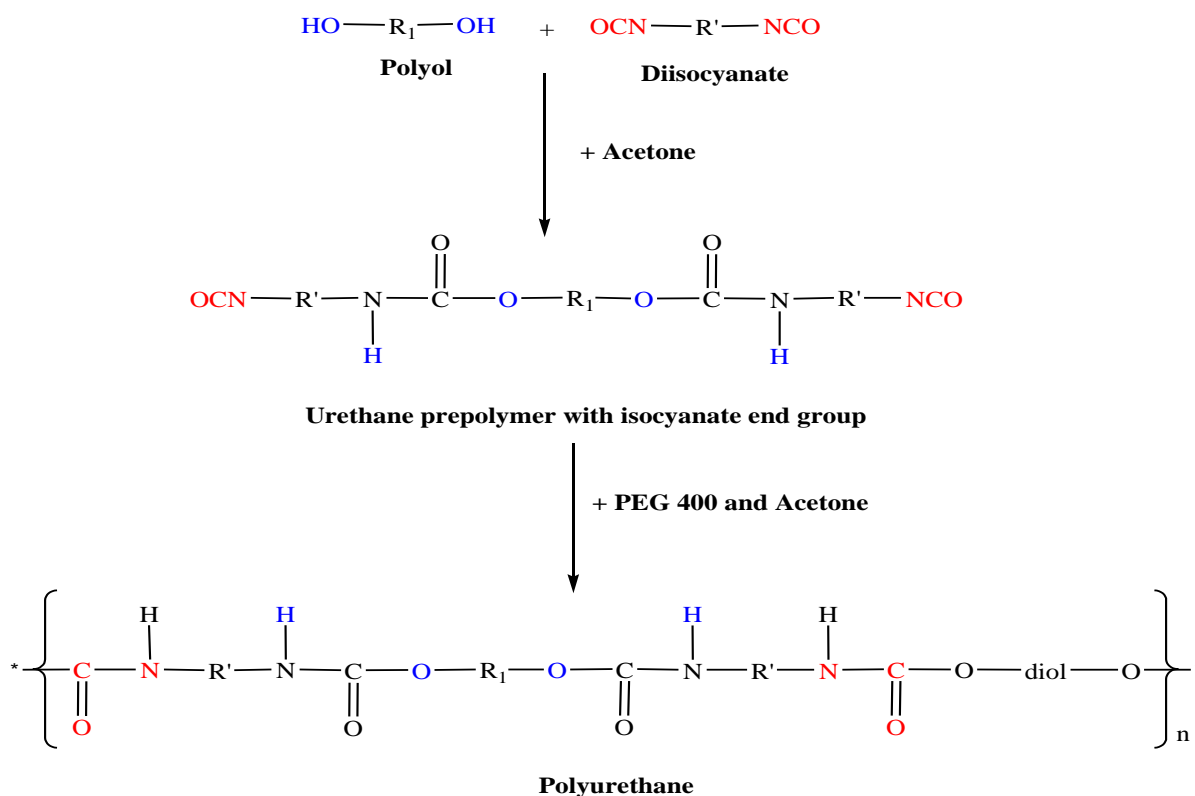
193

#### 194 a. FTIR analysis

195 **Figure 3** shows the FTIR spectrum for polyurethane, exhibiting the important functional  
196 group peaks. According to study researched by Wong & Badri 2012, PKO-p reacts with MDI  
197 to form urethane prepolymers. The NCO group on MDI reacts with OH group on polyol

198 whether PKOp or PEG. It can be seen there are no important peaks of MDI in the FTIR  
199 spectrums. This is further verified by the absence of peak at the  $2400\text{ cm}^{-1}$  belongs to MDI (-  
200 NCO groups). This could also confirm that the NCO group on MDI had completely reacted  
201 with PKO-p to form the urethane -NHC (O) backbone. The presence of amides (-NH),  
202 carbonyl urethane group (-C = O), carbamate group (C-NH) and -C-O-C confirmed the  
203 formation of urethane chains. In this study, the peak of carbonyl urethane (C = O) detected at  
204  $1727\text{ cm}^{-1}$  indicated that the carbonyl urethane group was bonded without hydrogen owing to  
205 the hydrogen reacted with the carbonyl urethane group.

206 The reaction of polyurethane has been studied by Hamuzan & Badri (2016) where the  
207 urethane carbonyl group was detected at  $1730 - 1735\text{ cm}^{-1}$  while the MDI carbonyl was  
208 detected at  $2400\text{ cm}^{-1}$ . The absence of peaks at  $2250 - 2270\text{ cm}^{-1}$  indicates the absence of  
209 NCO groups. It shows that the polymerization reaction occurs entirely between NCO groups  
210 in MDI with hydroxyl groups on polyols and PEG (Mishra et al. 2012). The absence of peaks  
211 at  $1690\text{ cm}^{-1}$  representing urea (C = O) in this study indicated, there is no urea formation as a  
212 byproduct (Clemitson 2008) of the polymerization reaction that possibly occur due to the  
213 excessive water. For the amine (NH) group, hydrogen-bond to NH and oxygen to form ether  
214 and hydrogen bond to NH and oxygen to form carbonyl on urethane can be detected at the  
215 peak of  $3301\text{ cm}^{-1}$  and in the wave number at range  $3326 - 3428\text{ cm}^{-1}$ . This has also been  
216 studied and detected by Lampman et. al. (2010) and Mutsuhisa et al. (2007). In this study, the  
217 hydrogen bond formed by C = O acts as a proton acceptor whereas NH acts as a proton  
218 donor. The urethane group in the hard segment (MDI) has electrostatic forces on the oxygen,  
219 hydrogen and nitrogen atoms and these charged atoms form dipoles that attract other opposite  
220 atoms. These properties make isocyanates are highly reactive and having different properties  
221 (Leykin et al. 2016).



222

223 **Figure 2.** The chemical route of producing polyurethane via pre-polymerization method

224 (Wong & Badri 2012).

225

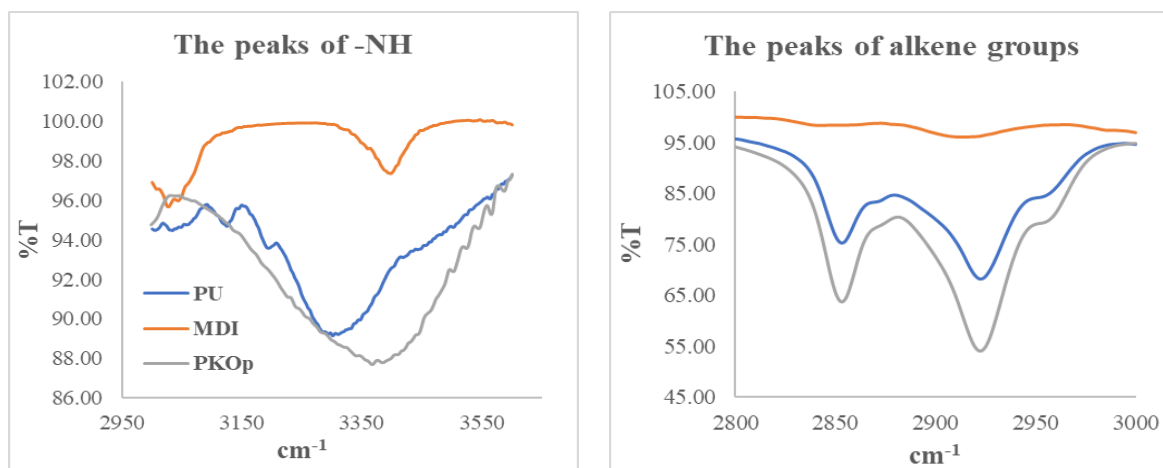
226 MDI was one of the isocyanate used in this study, has an aromatic group and more  
 227 reactive compared to aliphatic group isocyanates such as hexamethylene diisocyanate (HDI)  
 228 or isophorone diisocyanate (IPDI). Isocyanates have two groups of isocyanates on each  
 229 molecule. Diphenylmethane diisocyanate is an exception owing to its structure consists of two,  
 230 three, four or more isocyanate groups (Nohra et al. 2013). The use of PEG 400 in this study  
 231 as a chain extender for polyurethane increases the chain mobility of polyurethane at an  
 232 optimal amount. The properties of polyurethane are contributed by hard and soft copolymer  
 233 segments of both polyol monomers and MDI. This makes the hard segment of urethane  
 234 serves as a crosslinking site between the soft segments of the polyol (Leykin et al. 2016).

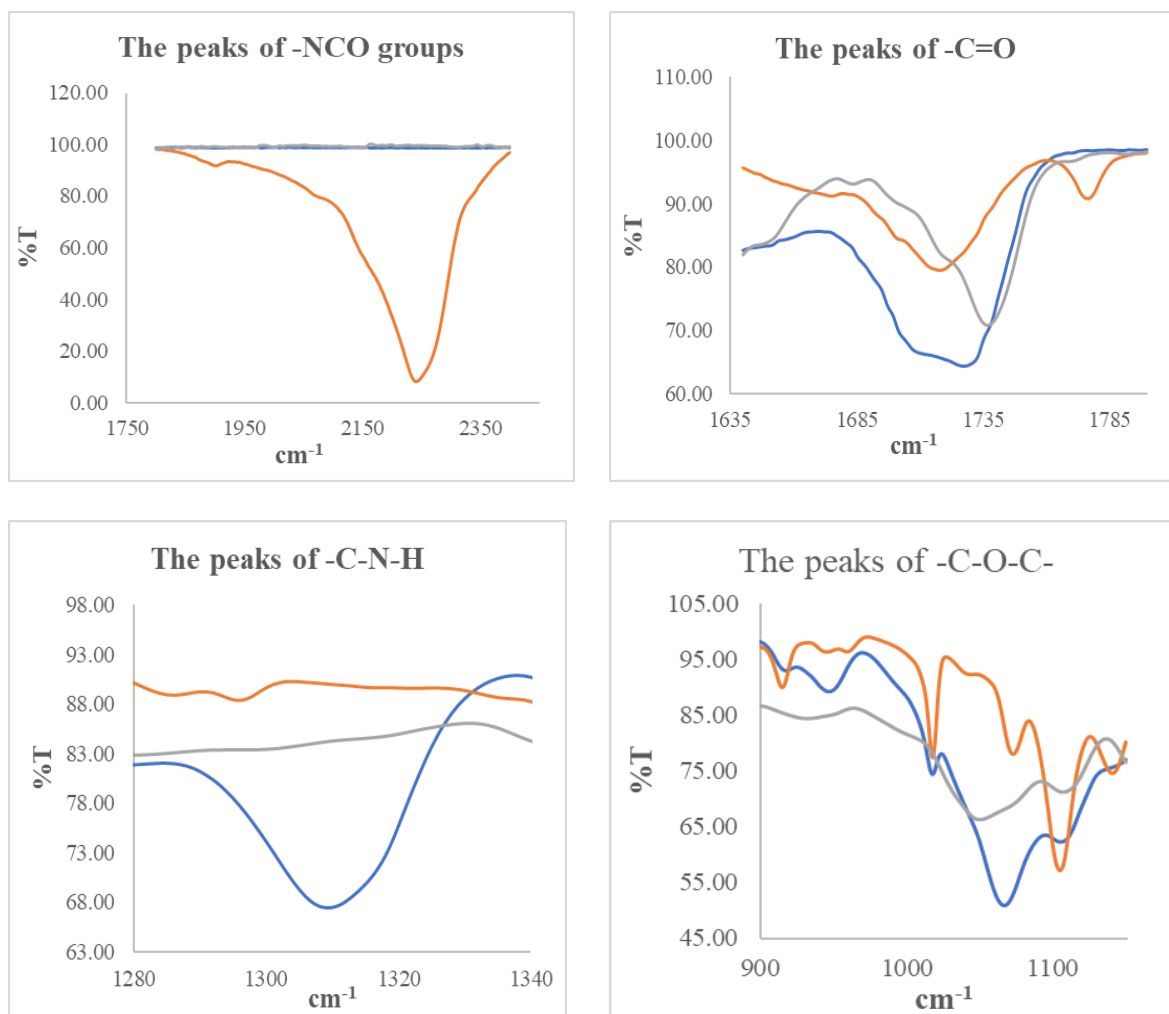
235 The mechanism of the pre – polymerization in urethane chains formation is a  
 236 nucleophilic substitution reaction as studied by Yong et al. (2009). However, this study found

237 amines as nucleophiles. Amine attacks carbonyl on isocyanate in MDI in order to form two  
238 resonance structures of intermediate complexes A and B. Intermediate complex B has a  
239 greater tendency to react with polyols due to stronger carbonyl (C = O) bonds than C = N  
240 bonds on intermediate complexes A. Thus, intermediate complex B is more stable than  
241 intermediate complex A, as suggested by previous researchers who have conducted by Wong  
242 and Badri (2012).

243 Moreover, nitrogen was more electropositive than oxygen, therefore, -CN bonds were  
244 more attracted to cations (H<sup>+</sup>) than -CO. The combination between long polymer chain and  
245 low cross linking content gives the polymer an elastic properties whereas short chain and  
246 high cross linking producing hard and rigid polymers. Cross linking in polymers consist of  
247 three - dimensional networks with high molecular weight. In some aspects, polyurethane can  
248 be a macromolecule, a giant molecule (Petrovic 2008).

249





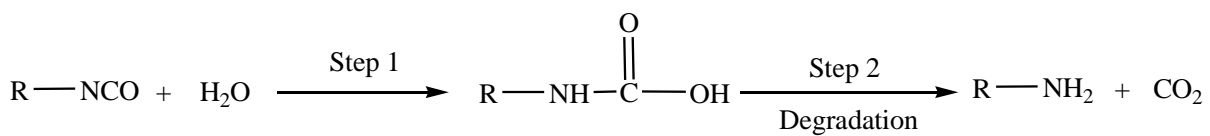
250 **Figure 3.** FTIR spectrums of several important peaks between polyurethane, PKO-p and  
 251 MDI

252

253 However, reaction between MDI and PEG as a chain extender where oxygen on the  
 254 nucleophile PEG attacks the NCO group in the MDI to form two intermediate complexes A  
 255 and B can occur. Nevertheless, nucleophilic substitution reactions have a greater tendency to  
 256 occur in PKOp compared to PEG because the presence of nitrogen atoms is more  
 257 electropositive than oxygen atoms in PEG. Amine has a higher probability of to react  
 258 compared to hydroxyl (Herrington & Hock 1997). Amine with high alkalinity reacts with  
 259 carbon atoms on MDI as proposed by Wong and Badri (2012). PKOp contains long carbon  
 260 chains that can easily stabilize alkyl ions when intermediate complexes are formed.



261 Therefore, polyol is more reactive than PEG to react with MDI. However, the addition of  
262 PEG will increase the length of the polyurethane chain and prevent side effects such as the  
263 formation of urea by -products of the NCO group reaction in urethane pre - polymer and  
264 water molecules from the environment. If the NCO group reacts with the excess water in the  
265 environment, the formation of urea and carbon dioxide gas will also occur excessively  
266 (**Figure 4**). This reaction can cause a polyurethane foam not polyurethane film as we studied  
267 the film.



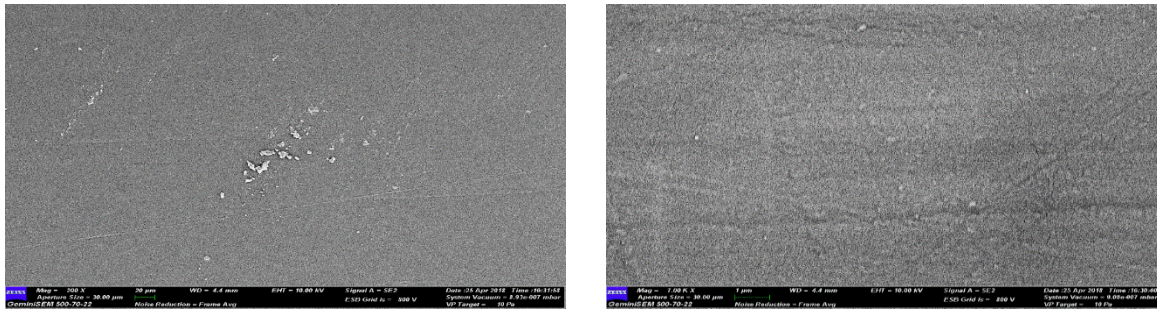
268  
269 **Figure 4.** The reaction between NCO group and water producing carbon dioxide

270  
271 Furthermore, the application of PEG can influence the conductivity of PU where  
272 Porcarelli et al. (2017) have reported the application of PEG using several molecular weights.  
273 PEG 1500 decreased the conductivity of PU in consequence of the semicrystalline phase of  
274 PEG 1500 that acted as a poor ion conducting phase for PU. It is also well known that PEG  
275 with molecular weight more than  $1000 \text{ g}\cdot\text{mol}^{-1}$  tends to crystallize with deleterious effects on  
276 room temperature ionic conductivity (Porcarelli et al. 2017).

#### 277 278 b. Morphological analysis

279 The Field Emission Scanning Electron Microscope (FESEM) micrograph in **Figure 5** shows  
280 the formation of a uniform polymer film contributed by the polymerization method applied.  
281 The magnification used for this surface analysis ranged from 200 to  $5000 \times$ . The  
282 polymerization method can also avoid the failure of the reaction in PU polymerization.  
283 Furthermore, no trace of separation was detected by FESEM. This has also been justified by  
284 the wavelengths obtained by the FTIR spectrums above.

285



286 **Figure 5.** The micrograph of polyurethane films analysed by FESEM at (a) 200 × and  
 287 5000× magnifications.

288  
 289 c. The crosslinking analysis

290 Soxhlet analysis was applied to determine the degree of crosslinking between the hard  
 291 segments and the soft segments in the polyurethane. The urethane group on the hard segment  
 292 along the polyurethane chain is polar (Cuve & Pascault 1991). Therefore, during the testing,  
 293 it was very difficult to dissolve in toluene, as the testing reagent. The degree of the  
 294 crosslinking is determined by the percentage of the gel content. The analysis result obtained  
 295 from the Soxhlet testing indicating a 99.3 % gel content. This is significant in getting a stable  
 296 polymer at higher working temperature (Rogulska et al. 2007).

297

$$\text{Gel content (\%)} = \frac{(0.6 - 0.301) \text{ g}}{0.301 \text{ g}} \times 100\% = 99.33\%$$

298  
 299 d. The thermal analysis

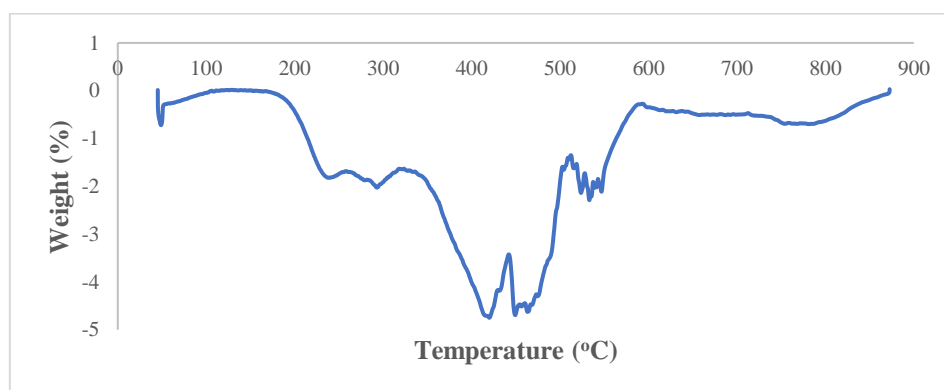
300 Thermogravimetric analysis (TGA) can be used to observe the material mass based on  
 301 temperature shift. It can also examine and estimate the thermal stability and materials  
 302 properties such as the alteration weight owing to absorption or desorption, decomposition,  
 303 reduction and oxidation. The material composition of polymer is specified by analysing the  
 304 temperatures and the heights of the individual mass steps (Alamawi et al. 2019). **Figure 6**  
 305 shows the TGA and DTG thermograms of polyurethane. The percentage weight loss (%) is

306 listed in **Table 2**. Generally, only a small amount of weight was observed. It is shown in  
 307 **Figure 6** in the region of 45 – 180°C. This is due to the presence of condensation on moisture  
 308 and solvent residues.

309 **Table2** Weight loss percentage of (wt%) polyurethane film

Sample	% Weight loss (wt%)				Total of weight loss (%)	Residue after 550°C (%)
	T <sub>max</sub> , °C	T <sub>d1</sub> , 200 – 290°C	T <sub>d2</sub> , 350 – 500°C	T <sub>d3</sub> , 500 – 550°C		
Polyurethane	240	8.04	39.29	34.37	81.7	18.3

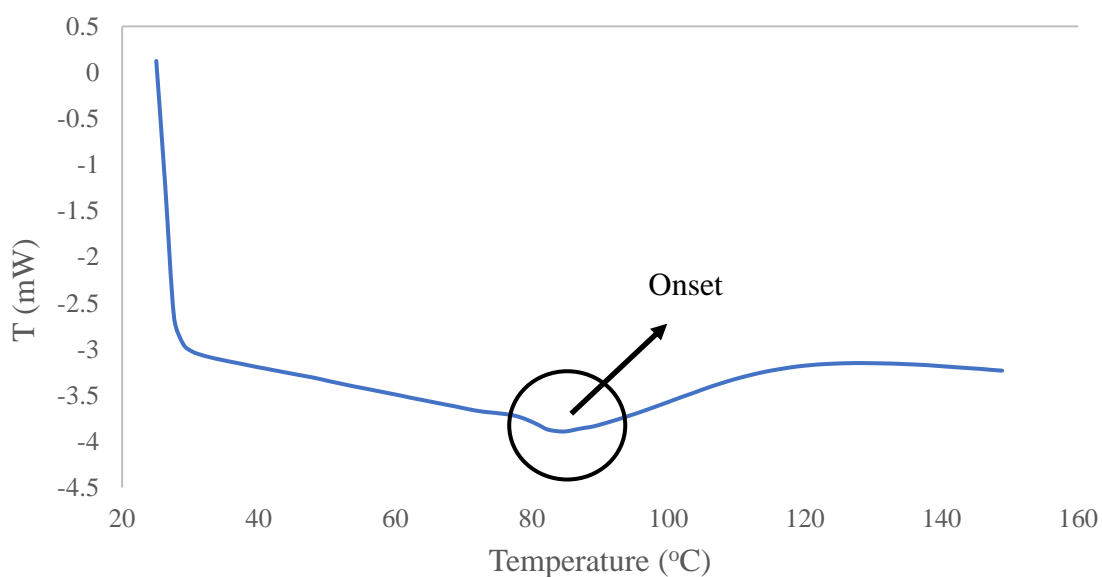
310 The bio polyurethane is thermally stable up to 240 °C before it undergone thermal  
 311 degradation (Agrawal et al. 2017). The first stage of thermal degradation (T<sub>d1</sub>) on  
 312 polyurethane films was shown in the region of 200 – 290 °C as shown in **Figure 6**. The T<sub>d1</sub> is  
 313 associated with degradation of the hard segments of the urethane bond, forming alcohol or  
 314 degradation of the polyol chains and releasing of isocyanates (Berta et al. 2006), primary and  
 315 secondary amines as well as carbon dioxide (Corcuera et al. 2011; Pan & Webster 2012).  
 316 Meanwhile, the second thermal degradation stage (T<sub>d2</sub>) of polyurethane films experienced a  
 317 weight loss of 39.29 %. This endotherm of T<sub>d2</sub> is related to dimerization of isocyanates to  
 318 form carbodiimides and release CO<sub>2</sub>. The formed carbodiimide reacts with alcohol to form  
 319 urea. For the third stage of thermal degradation (T<sub>d3</sub>) is related to the degradation on urea  
 320 (Berta et al. 2006) and the soft segment on polyurethane.



322 **Figure 6.** DTG thermogram of polyurethane film  
 323

324 Generally, DSC analysis exhibited thermal transitions as well as the initial  
325 crystallisation and melting temperatures of the polyurethane (Khairuddin et al. 2018). It  
326 serves to analyse changes in thermal behaviour due to changes occurring in the chemical  
327 chain structure based on the glass transition temperature ( $T_g$ ) of the sample obtained from the  
328 DSC thermogram (**Figure 7**). DSC analysis on polyurethane films was performed in the  
329 temperature at range 100 °C to 200 °C using nitrogen gas as blanket as proposed by  
330 Furtwengler et al. (2017). The glass transition temperature ( $T_g$ ) on polyurethane was above  
331 room temperature, at 78.1 °C indicated the state of glass on polyurethane. The presence of  
332 MDI contributes to the formation of hard segments in polyurethanes. Porcarelli et al. (2017)  
333 stated that possess a low glass transition ( $T_g$ ) may contribute to PU conductivity.

334 During polymerization, this hard segment restricts the mobility of the polymer chain  
335 (Ren et al. 2013) owing to steric effect on benzene ring in hard segment. The endothermic  
336 peak of acetone used as the solvent in this study was supposedly be at 56°C. However, it was  
337 detected in the DSC thermogram nor the TGA thermogram, which indicates that acetone was  
338 removed from the polyurethane during the synthesis process, owing to its volatility nature.  
339 The presence of acetone in the synthesis was to lower the reaction kinetics.



340  
341

**Figure 7.** DSC thermogram of polyurethane film

342 e. The solubility and mechanical properties of the polyurethane film  
 343 The chemical resistivity of a polymer will be the determinant in performing as conductor.  
 344 Thus, its solubility in various solvents was determined by dissolving the polymer in selected  
 345 solvents such as hexane, benzene, acetone, tetrahydrofuran (THF), dimethylformamide  
 346 (DMF) and dimethylformamide (DMSO). On the other hand, the mechanical properties of  
 347 polyurethane were determined based on the standard testing following ASTM D 638  
 348 (Standard Test Method for Tensile Properties of Plastics). The results from the polyurethane  
 349 film solubility and tensile test are shown in **Table 3**. Polyurethane films were insoluble with  
 350 benzene, hexane and acetone and are only slightly soluble in tetrahydrofuran (THF),  
 351 dimethylformamide (DMF) and dimethylformamide (DMSO) solutions. While the tensile  
 352 strength of a PU film indicated how much elongation load the film was capable of  
 353 withstanding the material before breaking.

354 **Table 3** The solubility and mechanical properties of the polyurethane film  
 355

Parameters	Polyurethane film	
Solubility	Benzene	Insoluble
	Hexane	Insoluble
	Acetone	Insoluble
	THF	Less soluble
	DMF	Less soluble
	DMSO	Less soluble
Stress (MPa)	8.53	
Elongation percentage (%)	43.34	
Strain modulus (100) (MPa)	222.10	

356

357 The tensile stress, strain and modulus of polyurethane film also indicated that polyurethane  
358 has good mechanical properties that are capable of being a supporting substrate for the next  
359 stage of study. In the production of polyurethane, the properties of polyurethane are easily  
360 influenced by the content of MDI and polyol used. The length of the chain and its flexibility  
361 are contributed by the polyol which makes it elastic. High crosslinking content can also  
362 produce hard and rigid polymers. MDI is a major component in the formation of hard  
363 segments in polyurethane. It is this hard segment that determines the rigidity of the PU.  
364 Therefore, high isocyanate content results in higher rigidity on PU (Petrovic et al. 2002).  
365 Thus, the polymer has a higher resistance to deformation and more stress can be applied to  
366 the PU.

367

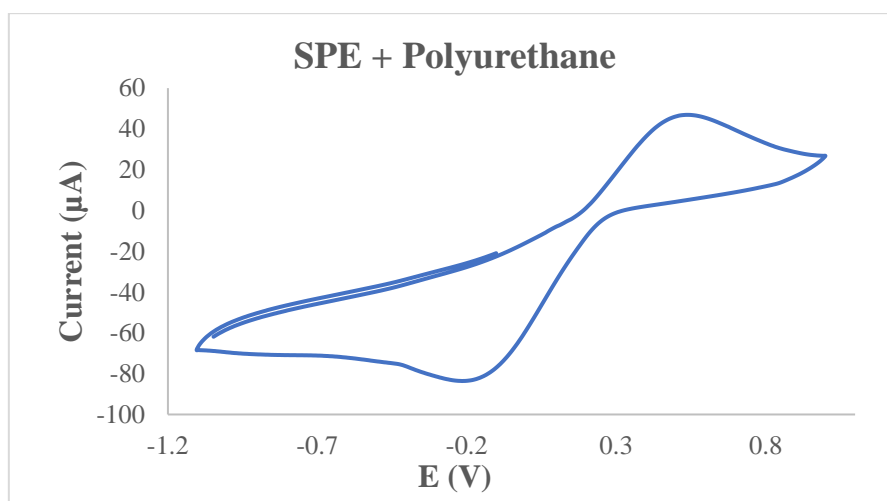
368 f. Conductivity of the polyurethane as polymeric film on SPE

369 Polyurethane film deposited onto the screen printed electrode by casting method as shown in  
370 **Figure 1**. After that, the modified electrode was analysed using cyclic voltammetry (CV) and  
371 differential pulse voltammetry (DPV) in order to study the behaviour of modified electrode.  
372 The modified electrode was tested in a 0.1 mmol/L KCl solution containing 5 mmol/L ( $K_3Fe$   
373  $(CN)_6$ ). The use of potassium ferricyanide is intended to increase the sensitivity of the KCl  
374 solution. The conductivity of the modified electrode was studied. The electrode was analyzed  
375 by cyclic voltametry method with a potential range of -1.00 to +1.00 with a scan rate of 0.05  
376 V/s. The voltamogram at electrode have shown a specific redox reactions. Furthermore, the  
377 conductivity of the modified electrode is lower due to the use of polyurethane. This occurs  
378 due to PU is a natural polymer produced from the polyol of palm kernel oil. The  
379 electrochemical signal at the electrode is low if there is a decrease in electrochemical  
380 conductivity (El - Raheem et al. 2020). It can be concluded that polyurethane is a bio –  
381 polymer with a low conductivity value. The current of modified electrode was found at 5.3 x

382  $10^{-5}$  A or 53  $\mu\text{A}$ . Nevertheless, the electroconductivity of PU in this study shows better  
383 conductivity several times compared to Bahrami et al. (2019) that reported the conductivity  
384 of PU as  $1.26 \times 10^{-6}$  A, whereas Li et al. (2019) reported the PU conductivity in their study  
385 was even very low, namely  $10^{-14}$  A. The conductivity of PU owing to the benzene ring in  
386 hard segment (MDI) could exhibit the conductivity by inducing electron delocalization along  
387 the polyurethane chain (Wong et al. 2014). The conductivity of PU can also caused by PEG.  
388 The application of PEG as polyol has been studied by Porcarelli et al. (2017), that reported  
389 that conductivity of PU based on PEG – polyol was  $9.2 \times 10^{-8}$ .

390 According to **Figure 8**, it can be concluded that the anodic peak present in the modified  
391 electrode was at +0.5 V, it also represented the oxidation process of the modified electrode.  
392 The first oxidation scan on both electrodes ranged from -0.2 to +1.0 V, which showed a  
393 significant anodic peak at a potential of +0.5 V.

394



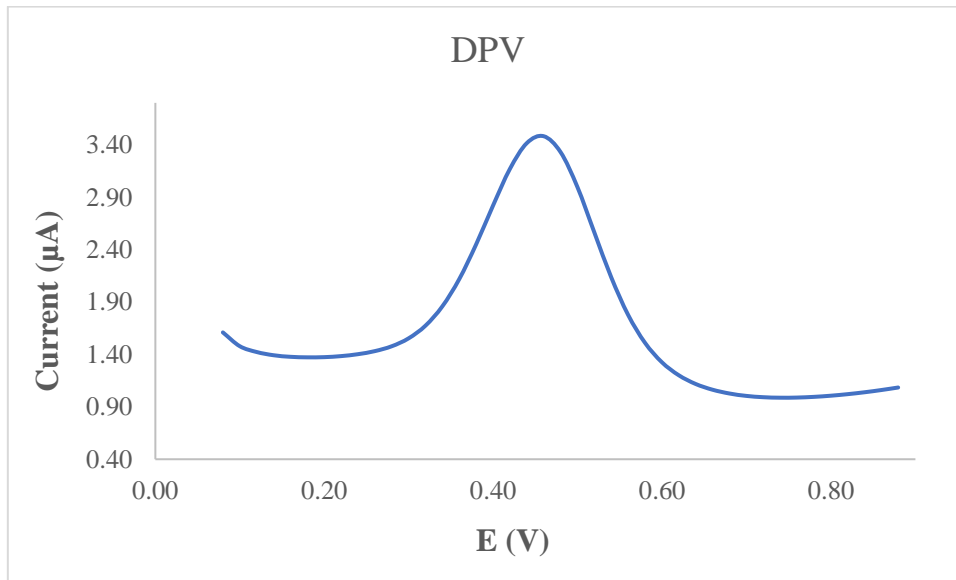
395

396 **Figure 8.** The voltamogram of SPE – PU modified electrode after analysed using cyclic  
397 voltammetry (CV) technique

398

399 **Figure 9** also presents the DPV voltammogram of modified electrode. DPV is a measurement  
400 based on the difference in potential pulses that produce an electric current. Scanning the  
401 capability pulses to the working electrode will produce different currents. Optimal peak

402 currents will be produced to the reduction capacity of the redox material. The peak current  
 403 produced is proportional to the concentration of the redox substance and can be detected up  
 404 to concentration below  $10^{-8}$  M. DPV conducted to obtain the current value that more accurate  
 405 than CV (Lee et al. 2018).



406  
 407 **Figure 9.** The voltammogram of SPE – PU modified electrode after analyzed using  
 408 differential pulse voltammetry (DPV) technique  
 409

410 This study used a redox pair ( $K_3Fe(CN)_6$ ) as a test device (probe). The currents generated by  
 411 SPE-PU and proved by CV and DPV have shown conductivity on polyurethane films. This  
 412 suggests that polyurethane films can conduct electron transfer. The electrochemical area on  
 413 the modified electrode can be calculated using the formula from Randles-Sevcik (Butwong et  
 414 al. 2019), where the electrochemical area for SPE-PU is considered to be A, using Equation  
 415 2:

416 **Current of SPE-PU ,  $I_p = 2.65 \times 10^5 n^{3/2} A v^{1/2} CD^{1/2}$**  (2)

417 Where, n – 1 is the amount of electron transfer involved, while C is the solvent concentration  
 418 used (mmol/L) and the value of D is the diffusion constant of 5 mmol/L at ( $K_3Fe(CN)_6$ )  
 419 dissolved using 0.1 mmol/L KCl. The estimated surface area of the electrode (**Figure 1**) was  
 420  $0.2 \text{ cm}^2$  where the length and width of the electrode used during the study was  $0.44 \text{ cm} \times 0.44$



421 cm while the surface area of the modified electrode was 0.25 cm<sup>2</sup> with the length and width  
422 of the electrode estimated at 0.5 cm × 0.5 cm, and causing the modified electrode has a larger  
423 surface. The corresponding surface concentration ( $\tau$ ) (mol/cm<sup>2</sup>) is calculated using Equation  
424 3.

$$425 \quad I_p = (n^2 F^2 / 4RT) A \tau v \quad (3)$$

426  $I_p$  is the peak current (A), while A is the surface area of the electrode (cm<sup>2</sup>), the value of v is  
427 the applied scan rate (mV/s) and F is the Faraday constant (96,584 C/mol), R is the constant  
428 ideal gas (8.314 J/mol K) and T is the temperature used during the experiment being  
429 conducted (298 K) (Koita et al. 2014). The development of conducting polymer from palm  
430 oil – based biomaterials seems to be one of the potential future applications of palm oil  
431 products, as this novel material has the potential to contribute positively to the analytical  
432 industry. Likewise, other palm oil-based products, such as refined-bleached-deodorised  
433 (RBD) palm oil, palm oil, and palm stearin are abundantly available in Malaysia. They are  
434 known to be economical, sustainable, and environmentally biodegradable. These palm oil-  
435 based products are promising prospects for manufacturing biomaterials that become  
436 alternative products to other polymers from synthetic/chemical-based (Tajao et al. 2021).  
437 Several studies have been reported the application of PU to produce elastic conductive fibres  
438 and films owing to it is highly elastic, scratch resistant and adhesive (Tadese et al. 2019), thus  
439 it is easy for PU to adhere on the screen printed electrode in order to modify the electrode.  
440 PU is also being used as a composite material to make elastic conducting composite films  
441 (Khatoon & Ahmad 2017).

442

#### 443 4. Conclusion

444 Polyurethane film was prepared by pre-polymerization between palm kernel oil-based polyol  
445 (PKO-p) with MDI. The presence of PEG 400 as the chain extender formed freestanding

446 flexible film. Acetone was used as the solvent to lower the reaction kinetics since the pre-  
447 polymerization was carried out at room temperature. The formation of urethane links (NHCO  
448 – backbone) after polymerization was confirmed by the absence of N=C=O peak at 2241 cm<sup>-1</sup>  
449 and the presence of N-H peak at 3300 cm<sup>-1</sup>, carbonyl (C=O) at 1710 cm<sup>-1</sup>, carbamate (C-N) at  
450 1600 cm<sup>-1</sup>, ether (C-O-C) at 1065 cm<sup>-1</sup>, benzene ring (C = C) at 1535 cm<sup>-1</sup> in the bio  
451 polyurethane chain structure. Soxhlet analysis for the determination of crosslinking on  
452 polyurethane films has yielded a high percentage of 99.33 %. This is contributed by the hard  
453 segments formed from the reaction between isocyanates and hydroxyl groups causing  
454 elongation of polymer chains. FESEM analysis exhibited absence of phase separation and  
455 smooth surface. Meanwhile, the current of modified electrode was found at  $5.2 \times 10^{-5}$  A. This  
456 bio polyurethane film can be used as a conducting bio – polymer and it is very useful for  
457 other studies such as electrochemical sensor purpose. **Furthermore, advanced technologies are**  
458 **promising and the future of bio – based polyols looks very bright.**

459

## 460 **5. Acknowledgement**

461 The authors would like to thank Universitas Alma Ata for the sponsorship given to the first  
462 author. We would like to also, thank Department of Chemical Sciences, Universiti  
463 Kebangsaan Malaysia for the laboratory facilities and CRIM, UKM for the analysis  
464 infrastructure.

465

## 466 **6. Conflict of Interest**

467 The authors declare no conflict of interest.

468

469

470

471 **7. References**

- 472 Agrawal, A., Kaur, R., Walia, R. S. (2017). PU foam derived from renewable sources:  
473 Perspective on properties enhancement: An overview. *European Polymer Journal*. 95:  
474 255 – 274.
- 475 Akindoyo, J. O., Beg, M.D.H., Ghazali, S., Islam, M.R., Jeyaratnam, N. & Yuvaraj, A.R.  
476 (2016). Polyurethane types, synthesis and applications – a review. *RSC Advances*. 6:  
477 114453 – 114482.
- 478 Alamawi, M. Y., Khairuddin, F. H., Yusoff, N. I. M., Badri, K., Ceylan, H. (2019).  
479 Investigation on physical, thermal and chemical properties of palm kernel oil polyol bio  
480 – based binder as a replacement for bituminous binder. *Construction and Building*  
481 *Materials*. 204: 122 – 131.
- 482 Alqarni, S. A., Hussein, M. A., Ganash, A. A. & Khan, A. (2020). Composite material –  
483 based conducting polymers for electrochemical sensor applications: a mini review.  
484 *BioNanoScience*. 10: 351 – 364.
- 485 Badan, A., Majka, T. M. (2017). The influence of vegetable – oil based polyols on physico –  
486 mechanical and thermal properties of polyurethane foams. *Proceedings*. 1 – 7.
- 487 Badri, K.H. (2012) Biobased polyurethane from palm kernel oil-based polyol. In  
488 Polyurethane; Zafar, F., Sharmin, E., Eds. InTechOpen: Rijeka, Croatia. pp. 447–470.
- 489 Badri, K.H., Ahmad, S.H. & Zakaria, S. 2000. Production of a high-functionality RBD palm  
490 kernel oil – based polyester polyol. *Journal of Applied Polymer Science* 81(2): 384 –  
491 389.
- 492 Baig, N., Sajid, M. and Saleh, T. A. 2019. Recent trends in nanomaterial – modified  
493 electrodes for electroanalytical applications. *Trends in Analytical Chemistry*. 111: 47 –  
494 61.

495 Berta, M., Lindsay, C., Pans, G., & Camino, G. (2006). Effect of chemical structure on  
496 combustion and thermal behaviour of polyurethane elastomer layered silicate  
497 nanocomposites. *Polymer Degradation and Stability*. **91**: 1179-1191.

498 Borowicz, M., Sadowska, J. P., Lubczak, J. & Czuprynski, B. (2019). Biodegradable, flame –  
499 retardant, and bio – based rigid polyurethane/polyisocyanurate foams for thermal  
500 insulation application. *Polymers*. 11: 1816 – 1839.

501 Butwong, N., Khajonklin, J., Thongbor, A. & Luong, J.H.T. (2019). Electrochemical sensing  
502 of histamine using a glassy carbon electrode modified with multiwalled carbon  
503 nanotubes decorated with Ag – Ag<sub>2</sub>O nanoparticles. *Microchimica Acta*. **186 (11)**: 1 –  
504 10.

505 Clemitson, I. (2008). Castable Polyurethane Elastomers. Taylor & Francis Group, New York.  
506 doi:10.1201/9781420065770.

507 Corcuera, M.A., Rueda, L., Saralegui, A., Martin, M.D., Fernandez-d’Arlas, B., Mondragon,  
508 I. & Eceiza, A. (2011). Effect of diisocyanate structure on the properties and  
509 microstructure of polyurethanes based on polyols derived from renewable resources.  
510 *Journal of Applied Polymer Science*. **122**: 3677-3685.

511 Cuve, L. & Pascault, J.P. (1991). Synthesis and properties of polyurethanes based on  
512 polyolefine: Rigid polyurethanes and amorphous segmented polyurethanes prepared in  
513 polar solvents under homogeneous conditions. *Polymer*. **32 (2)**: 343- 352.

514 Dzulkipli, M. Z., Karim, J., Ahmad, A., Dzulkurnain, N. A., Su’ait, M S., Fujita, M. Y.,  
515 Khoon, L. T. & Hassan, N. H. (2021). The influences of 1-butyl-3-methylimidazolium  
516 tetrafluoroborate on electrochemical, thermal and structural studies as ionic liquid gel  
517 polymer electrolyte. *Polymers*. 13 (8): 1277 – 1294.

518 El-Raheem, H.A., Hassan, R.Y.A., Khaled, R., Farghali, A. & El-Sherbiny, I.M. (2020).  
519 Polyurethane – doped platinum nanoparticles modified carbon paste electrode for the

520 sensitive and selective voltammetric determination of free copper ions in biological  
521 samples. *Microchemical Journal*. **155**: 104765.

522 Fei, T., Li, Y., Liu, B. & Xia, C. (2019). Flexible polyurethane/boron nitride composites with  
523 enhanced thermal conductivity. *High Performance Polymers*. **32** (3): 1 – 10.

524 Furtwengler, P., Perrin R., Redl, A. & Averous, L. (2017). Synthesis and characterization of  
525 polyurethane foams derived of fully renewable polyesters polyols from sorbitol.  
526 *European Polymer Journal*. **97**: 319 – 327.

527 Ghosh, S., Ganguly, S., Remanan, S., Mondal, S., Jana, S., Maji, P. K., Singha, N., Das, N.  
528 C. (2018). Ultra – light weight, water durable and flexible highly electrical conductive  
529 polyurethane foam for superior electromagnetic interference shielding materials.  
530 *Journal of Materials Science: Materials in Electronics*. **29**: 10177 – 10189.

531 Guo, S., Zhang, C., Yang, M., Zhou, Y., Bi, C., Lv, Q. & Ma, N. (2020). A facile and  
532 sensitive electrochemical sensor for non – enzymatic glucose detection based on three –  
533 dimensional flexible polyurethane sponge decorated with nickel hydroxide. *Analytica  
534 Chimica Acta*. **1109**: 130 – 139.

535 Hamuzan, H.A. & Badri, K.H. (2016). The role of isocyanates in determining the viscoelastic  
536 properties of polyurethane. AIP Conference Proceedings. 1784, Issue 1.

537 Herrington, R. & Hock, K. (1997). Flexible polyurethane foams. 2nd Edition. Dow Chemical  
538 Company. Midlan.

539 Janpoung, P., Pattanauwat, P. & Potiyaraj, P. (2020). Improvement of electrical conductivity  
540 of polyurethane/polypyrrole blends by graphene. *Key Engineering Materials*. **831**: 122  
541 – 126.

542 Khairuddin, F.H., Yusof, N. I. M., Badri, K., Ceylan, H., Tawil, S. N. M. (2018). Thermal,  
543 chemical and imaging analysis of polyurethane/cecabase modified bitumen. *IOP Conf.  
544 Series: Materials Science and Engineering*. **512**: 012032.

545 Khatoon, H., Ahmad, S. (2017). A review on conducting polymer reinforced polyurethane  
546 composites. *Journal of Industrial and Engineering Chemistry*. 53: 1 – 22.

547 Koita, D., Tzedakis, T., Kane, C., Diaw, M., Sock, O. & Lavedan, P. (2014). Study of the  
548 histamine electrochemical oxidation catalyzed by nickel sulfate. *Electroanalysis*. **26**  
549 (10): 2224 – 2236.

550 Kotal, M., Srivastava, S.K. & Paramanik, B. (2011). Enhancements in conductivity and  
551 thermal stabilities of polyurethane/polypyrrole nanoblends. *The Journal of Physical*  
552 *Chemistry C*. **115** (5): 1496 – 1505.

553 Ladan, M., Basirun, W.J., Kazi, S.N., Rahman, F.A. (2017). Corrosion protection of AISI  
554 1018 steel using Co – doped TiO<sub>2</sub>/polypyrrole nanocomposites in 3.5% NaCl solution.  
555 *Materials Chemistry and Physics*. **192**: 361 – 373.

556 Lampman, G.M., Pavia, D.L., Kriz, G.S. & Vyvyan, J.R. (2010). Spectroscopy. 4th Edition.  
557 Brooks/Cole Cengage Learning, Belmont, USA.

558 Lee, K.J., Elgrishi, N., Kandemir, B. & Dempsey, J.L. 2018. Electrochemical and  
559 spectroscopic methods for evaluating molecular electrocatalysts. *Nature Reviews*  
560 *Chemistry* 1(5): 1 - 14.

561 Leykin, A., Shapovalov, L. & Figovsky, O. (2016). Non – isocyanate polyurethanes –  
562 Yesterday, today and tomorrow. *Alternative Energy and Ecology*. **191** (3 – 4): 95 – 108.

563 Li, H., Yuan, D., Li, P., He, C. (2019). High conductive and mechanical robust carbon  
564 nanotubes/waterborne polyurethane composite films for efficient electromagnetic  
565 interference shielding. *Composites Part A*. 121: 411 – 417.

566 Nakthong, P., Kondo, T., Chailapakul, O., Siangproh, W. (2020). Development of an  
567 unmodified screen – printed graphene electrode for nonenzymatic histamine detection.  
568 *Analytical Methods*. 12: 5407 – 5414.

569 Mishra, K., Narayan, R., Raju, K.V.S.N. & Aminabhavi, T.M. (2012). Hyperbranched  
570 polyurethane (HBPU)-urea and HBPU-imide coatings: Effect of chain extender and  
571 NCO/OH ratio on their properties. *Progress in Organic Coatings*. **74**: 134 – 141.

572 Mohd Noor, M. A., Tuan Ismail, T. N. M., Ghazali, R. (2020). Bio – based content of  
573 oligomers derived from palm oil: Sample combustion and liquid scintillation counting  
574 technique. *Malaysia Journal of Analytical Science*. **24**: 906 – 917.

575 Mutsuhisa F., Ken, K. & Shohei, N. (2007). Microphase separated structure and mechanical  
576 properties of norbornane diisocyanate – based polyurethane. *Polymer*. **48** (4): 997 –  
577 1004.

578 Mustapha, R., Rahmat, A. R., Abdul Majid, R., Mustapha, S. N. H. (2019). Vegetable oil –  
579 based epoxy resins and their composites with bio – based hardener: A short review.  
580 *Polymer- Plastic Technology and Materials*. **58**: 1311 – 1326.

581 Nohra, B., Candy, L., Blancos, J.F., Guerin, C., Raoul, Y. & Mouloungui, Z. (2013). From  
582 petrochemical polyurethanes to biobased polyhydroxyurethanes. *Macromolecules*. **46**  
583 (10): 3771 – 3792.

584 Pan, T. & Yu, Q. (2016). Anti – corrosion methods and materials comprehensive evaluation  
585 of anti – corrosion capacity of electroactive polyaniline for steels. *Anti – Corrosion*  
586 *Methods and Materials*. **63**: 360 – 368.

587 Pan, X. & Webster, D.C. (2012). New biobased high functionality polyols and their use in  
588 polyurethane coatings. *ChemSusChem*. **5**: 419-429.

589 Petrovic, Z.S. (2008). Polyurethanes from vegetable oils. *Polymer Reviews*. **48** (1): 109 –  
590 155.

591 Porcarelli, L., Manojkumar, K., Sardon, H., Llorente, O., Shaplov, A. S., Vijayakrishna, K.,  
592 Gerbaldi, C., Mecerreyes, D. (2017). Single ion conducting polymer electrolytes based  
593 on versatile polyurethanes. *Electrochimica Acta*. **241**: 526 – 534.

594 Priya, S. S., Karthika, M., Selvasekarapandian, S. & Manjuladevi, R. (2018). Preparation and  
595 characterization of polymer electrolyte based on biopolymer I-carrageenan with  
596 magnesium nitrate. *Solid State Ionics*. **327**: 136 – 149.

597 Ren, D. & Frazier, C.E. (2013). Structure–property behaviour of moisture-cure polyurethane  
598 wood adhesives: Influence of hard segment content. *Adhesion and Adhesives*. **45**: 118-  
599 124.

600 Rogulska, S.K., Kultys, A. & Podkoscielny, W. (2007). Studies on thermoplastic  
601 polyurethanes based on new diphenylethane – derivative diols. II. Synthesis and  
602 characterization of segmented polyurethanes from HDI and MDI. *European Polymer*  
603 *Journal*. **43**: 1402 – 1414.

604 Romaskevicius, T., Budriene, S., Pielichowski, K. & Pielichowski, J. (2006). Application of  
605 polyurethane – based materials for immobilization of enzymes and cells: a review.  
606 *Chemija*. **17**: 74 – 89.

607 Sengodu, P. & Deshmukh, A. D. (2015). Conducting polymers and their inorganic  
608 composites for advanced Li-ion batteries: a review. *RSC Advances*. **5**: 42109 – 42130.

609 Septevani, A. A., Evans, D. A. C., Chaleat, C., Martin, D. J., Annamalai, P. K. (2015). A  
610 systematic study substituting polyether polyol with palm kernel oil based polyester  
611 polyol in rigid polyurethane foam. *Industrial Corrosion and Products*. **66**: 16 – 26.

612 Su'ait, M. S., Ahmad, A., Badri, K. H., Mohamed, N. S., Rahman, M. Y. A., Ricardi, C. L.  
613 A. & Scardi, P. The potential of polyurethane bio – based solid polymer electrolyte for  
614 photoelectrochemical cell application. *International Journal of Hydrogen Energy*. **39**  
615 (6): 3005 – 3017.

616 Tadesse, M. G., Mengistie, D. A., Chen, Y., Wang, L., Loghin, C., Nierstrasz, V. (2019).  
617 Electrically conductive highly elastic polyamide/lycra fabric treated with PEDOT: PSS  
618 and polyurethane. *Journal of Materials Science*. **54**: 9591 – 9602.



619 Tajau, R., R, Rosiah, Alias, M. S., Mudri, N. H., Halim, K. A. A., Harun, M. H., Isa, N. M.,  
620 Ismail, R. C., Faisal, S. M., Talib, M., Zin, M. R. M., Yusoff, I. I., Zaman, N. K., Illias,  
621 I. A. (2021). Emergence of polymeric material utilising sustainable radiation curable  
622 palm oil – based products for advanced technology applications. *Polymers*. 13: 1865 –  
623 1886.

624 Tran, V.H., Kim, J.D., Kim, J.H., Kim, S.K., Lee, J.M. (2020). Influence of cellulose  
625 nanocrystal on the cryogenic mechanical behaviour and thermal conductivity of  
626 polyurethane composite. *Journal of Polymers and The Environment*. **28**: 1169 – 1179.

627 Viera, I.R.S., Costa, L.D.F.D.O., Miranda, G.D.S., Nardehcia, S., Monteiro, M.S.D. S.D.B.,  
628 Junior, E.R. & Delpech, M.C. (2020). Waterborne poly (urethane – urea)s  
629 nanocomposites reinforced with clay, reduced graphene oxide and respective hybrids:  
630 Synthesis, stability and structural characterization. *Journal of Polymers and The  
631 Environment*. **28**: 74 – 90.

632 Wang, B., Wang, L., Li, X., Liu, Y., Zhang, Z., Hedrick, E., Safe, S., Qiu, J., Lu, G. & Wang,  
633 S. (2018). Template – free fabrication of vertically – aligned polymer nanowire array  
634 on the flat – end tip for quantifying the single living cancer cells and nanosurface  
635 interaction. a *Manufacturing Letters*. **16**: 27 – 31.

636 Wang, J., Xiao, L., Du, X., Wang, J. & Ma, H. (2017). Polypyrrole composites with carbon  
637 materials for supercapacitors. *Chemical Papers*. **71 (2)**: 293 – 316.

638 Wong, C.S. & Badri, K.H. (2012). Chemical analyses of palm kernel oil – based  
639 polyurethane prepolymer. *Materials Sciences and Applications*. **3**: 78 – 86.

640 Wong, C. S., Badri, K., Ataollahi, N., Law, K., Su'ait, M. S., Hassan, N. I. (2014). Synthesis  
641 of new bio – based solid polymer electrolyte polyurethane – LiClO<sub>4</sub> via  
642 prepolymerization method: Effect of NCO/OH ratio on their chemical, thermal  
643 properties and ionic conductivity. *World Academy of Science, Engineering and*

644 *Technology, International Journal of Chemical, Molecular, Nuclear, Materials and*  
645 *Metallurgical Engineering. 8: 1243 – 1250.*

646 Yong, Z., Bo, Z.M., Bo, W., Lin, J.Z. & Jun, N. (2009). Synthesis and properties of novel  
647 polyurethane acrylate containing 3-(2-Hydroxyethyl) isocyanurate segment. *Progress*  
648 *in Organic Coatings. 67: 264 – 268*

649 Zia, K. M., Anjum, S., Zuber, M., Mujahid, M. & Jamil, T. (2014). Synthesis and molecular  
650 characterization of chitosan based polyurethane elastomers using aromatic diisocyanate.  
651 *International of Journal of Biological Macromolecules. 66: 26 – 32.*

652

653

654

[← BACK](#) [DASHBOARD / ARTICLE DETAILS](#)

Updated on 2021-11-15

Version 3 ▾

# Design and Synthesis of Conducting Polymer Based on Polyurethane produced from Palm Kernel Oil

VIEWING AN OLDER VERSION

ID 6815187

Muhammad Abdurrahman Munir <sup>SA CA</sup> <sup>1</sup>,  
Khairiah Haji Badri<sup>1</sup>, Lee Yook Heng<sup>1</sup>  
[+ Show Affiliations](#)

## Article Type

Research Article

## Journal

International Journal of  
Polymer Science

Rydz Joanna

Submitted on 2021-06-14 (2 years ago)

[> Abstract](#)[> Author Declaration](#)[> Files](#) 3

## — Editorial Comments

Peter Foot

15.11.2021

**Decision**

Major Revision Requested

**Message for Author**

\* The synthetic chemistry and general polymer characterization are fine.  
\* I am satisfied with the revisions made by the authors, but I agree with the following comments of Reviewer #3:

1. The reported electrical properties are misleading and incorrect. A current of 53 microamps signifies nothing on its own, and it cannot be used as the basis of a comparison of the authors' polymer with other polymers. The mentions of "conductivity" in the following sentences should be corrected or preferably the sentences should be deleted completely:

Lines 432-435: "Nevertheless, the electroconductivity of PU in this study shows better conductivity several times compared to Bahrami et al. (2019) that reported the conductivity of PU as  $1.26 \times 10^{-6}$  A, whereas Li et al. (2019) reported the PU conductivity in their study was even very low, namely  $10^{-14}$  A. "

and in lines 438-440: "The application of PEG as polyol has been studied by Porcarelli et al. (2017), that reported that the conductivity of PU based on PEG – polyol was  $9.2 \times 10^{-8}$ ." (This sentence doesn't even mention the units of the reported conductivity.)

2. The English is still poor and hard to follow in some places. This includes missing verbs, e.g. line 420 "Polyurethane film deposited" should be "Polyurethane film was deposited"; orthographic errors e.g. lines 123-125 "SPE becomes the best solution owing to its frugal manufacture, tiny size, able to produce on large-scale and can be applied for on-site detection".

Typographic errors should be corrected e.g. line 89: change Pus to PUs; and lines 138-139 "Polyurethane is possible to become an advanced frontier material is chemically modified electrodes.."

As noted by the reviewer, in line 299 "spectrums" is an incorrect word, which should change to "spectra".

Also repetitious or awkward sentences should be rewritten or deleted, e.g. line 53 "The application of petroleum as polyol in order to produce polyurethane has been applied." or lines 56-57 "These reasons have been considered and finding utilizing plants that can be used as alternative polyols should be done immediately."

The sentence in lines 37-38 must be deleted; readers of IJPS don't need to be told what a polymer is!

The authors are strongly advised to seek the help of a fluent English speaker when they revise their manuscript, or to use a professional scientific editing service.

**— Response to Revision Request**

Muhammad Abdurrahman Munir

01.10.2021

**Your Reply**

Greetings, Dear Editor, Hope you are doing well. I have attached several documents such as the manuscript edited and the comments for reviewers. Best regards

**File**

Comments for Reviewers.docx 16 kB

[+ Reviewer Reports](#)

---

[Hindawi](#) [Privacy Policy](#) [Terms of Service](#) Support: [help@hindawi.com](mailto:help@hindawi.com)



25 cyclic voltammetry (CV). Cyclic voltammetry was employed to study electro-catalytic  
26 properties of SPE-Polyurethane towards oxidation of PU. Remarkably, SPE-PU exhibited  
27 improved anodic peak current as compared to SPE itself using the differential pulse  
28 voltammetry (DPV) method. Furthermore, the formation of urethane linkages (NHCO  
29 backbone) after polymerization was analysed using FTIR and confirmed by the absence of  
30 N=C=O peak at  $2241\text{ cm}^{-1}$ . The glass transition temperature ( $T_g$ ) of the polyurethane was  
31 detected at  $78.1^\circ\text{C}$ .

32

33 **Keywords:** Polyurethane, polymerization, screen-printed electrode, voltammetry

34

35

## 36 1. Introduction

37 Polymers are molecules composed of many repeated sub-units referred to as monomers  
38 (Sengodu & Deshmukh 2015). Conducting polymers (CPs) are polymers that exhibit electrical  
39 behavior (Alqarni et al. 2020). The conductivity of CPs was first observed in polyacetylene,  
40 nevertheless owing to its instability led to the discovery of other forms of CPs such as  
41 polyaniline (PANI), poly (o-toluidine) (PoT), polythiophene (PTh), polyfluorene (PF) and  
42 polyurethane (PU). Furthermore, natural CPs have low conductivity and are often semi-  
43 conductive. Therefore, it is essential to increase their conductivity mainly for use in  
44 electrochemical sensor programs (Dzulkipli et al. 2021; Wang et al. 2018). Conducting  
45 polymers (CPs) represent a sizeable range of useful organic substances. Their unique electrical,  
46 chemical and physical properties; reasonable price; simple preparation; small dimensions and  
47 large surface area have enabled researchers to discover a wide variety of uses such as sensors,  
48 biochemical applications, solar cells and electrochromic devices (Alqarni et al. 2020; Ghosh et  
49 al. 2018). There are scientific documentation on the use of conductive polymers in various

50 studies such as polyaniline (Pan & Yu 2016), polypyrrole (Ladan et al. 2017) and polyurethane  
51 (Tran et al. 2020; Vieira et al. 2020; Guo et al. 2020; Fei et al. 2020).

52

53 The application of petroleum as polyol in order to produce polyurethane has been applied. Coal  
54 and crude oil were used as raw materials to produce it. Nevertheless, these materials have  
55 become very rare to find and the price is very expensive at the same time required a  
56 sophisticated system to produce it. These reasons have been considered and finding utilizing  
57 plants that can be used as alternative polyols should be done immediately (Badri 2012).  
58 Furthermore, in order to avoid the application of petroleum as raw material for a polyol,  
59 vegetable oils become a better choice as polyol in order to obtain a biodegradable polyol.  
60 Vegetable oils that are generally used for synthesis polyurethane are soybean oil, corn oil,  
61 sunflower seed oil, coconut oil, nuts oil, rapeseed, olive oil and palm oil (Badri 2012; Borowicz  
62 et al. 2019).

63

64 It is very straightforward for vegetable oils to react with a specific group in order to form PU  
65 such as epoxy, hydroxyl, carboxyl and acrylate owing to the existence of (-C=C-) in vegetable  
66 oils. Thus, it has provided appealing profits to vegetable oils compared to petroleum considered  
67 the toxicity, price and harm to the environment (Mustapha et al. 2019; Mohd Noor et al. 2020).  
68 Palm oil becomes the chosen in this study to produce PU owing to it is largely cultivated in  
69 South Asia particularly in Malaysia and Indonesia. It has several profits compared to other  
70 vegetable oils such as the easiest materials obtained, the lowest cost of all the common  
71 vegetable oils and recognized as the plantation that has a low environmental impact and  
72 removing CO<sub>2</sub> from the atmosphere as net sequester (Tajau et al. 2021; Septevani et al. 2015).  
73 Biopolymer, a natural biodegradable polymer has attracted much attention in recent years.  
74 Global environmental awareness and fossil fuel depletion urged researchers to work in the



75 biopolymer field (Priya et al. 2018). Polyurethane is one of the most common, versatile and  
76 researched materials in the world. These materials combine the durability and toughness of  
77 metals with the elasticity of rubber, making them suitable to replace metals, plastics and rubber  
78 in several engineered products. They have been widely applied in biomedical applications,  
79 building and construction applications, automotive, textiles and in several other industries due  
80 to their superior properties in terms of hardness, elongation, strength and modulus (Zia et al.  
81 2014; Romaskevicius et al. 2006). Polyurethanes are also considered to be one of the most useful  
82 materials with many profits such as, possess low conductivity, low density, absorption  
83 capability and dimensional stability. They are clearly a great research subject owing to their  
84 mechanical, physical and chemical properties (Badan & Majka 2017).

85

86 The urethane group is the major repeating unit in PUs and is produced from the reaction  
87 between alcohol (-OH) and isocyanate (NCO); albeit polyurethanes also contain other groups  
88 such as ethers, esters, urea and some aromatic compounds. Due to the wide variety of sources  
89 from which PUs can be synthesized, thus a wide range of specific applications can be generated.  
90 They are grouped into several different classes based on the desired properties: rigid, flexible,  
91 thermoplastic, waterborne, binders, coating, adhesives, sealants and elastomers (Akindoyo et  
92 al. 2016).

93

94 Although, PU has low conductivity, it is lighter than other materials such as metals. The  
95 hardness of PU also relies on the number of the aromatic rings in the polymer structure  
96 (Janpoung et al, 2020; Su'ait et al. 2014), majorly contributed by the isocyanate derivatives.  
97 PU has also a conjugate structure where electrons can move in the main chain that causing  
98 electricity produced even the conductivity is low. The electrical conductivity of conjugated  
99 linear ( $\pi$ ) can be explained by the distance between the highest energy level containing

100 electrons (HOMO) called valence band and the lowest energy level not containing electrons  
101 (LUMO) called the conduction band (Wang et al. 2017; Kotal et al. 2011).

102

103 In the recent past, several conventional methods have been developed such as capillary  
104 electrophoresis, liquid and gas chromatography coupled with several detectors. Nevertheless,  
105 although chromatographic and spectrometric approaches are well developed for qualitative and  
106 quantitative analyses of analytes, several limitations emerged such as complicated  
107 instrumentation, expensive, tedious sample preparations and requiring large amounts of  
108 expensive solvents that will harm the users and environment (Kilele et al. 2020). Therefore, is  
109 is imperative to obtain and develop an alternative material that can be used to analyse a specific  
110 analyte. Electrochemical methods are extremely promising methods in the determination of an  
111 analyte in samples owing to the high selectivities, sensitivities, inexpensive, requirements of  
112 small amounts of solvents and can be operated by people who have no background in analytical  
113 chemistry. In addition, the sample preparation such as separation and extraction steps are not  
114 needed owing to the selectivity of this instrument where no obvious interference on the current  
115 response recorded (Chokkareddy et al. 2020). Few works have been reported on the  
116 electrochemical methods for the determination of analyte using electrode combined with  
117 several electrode modifiers such as carbon nanotube, gold and graphene (Chokkareddy et al.  
118 2020; Kilele et al. 2021). Nevertheless, the materials are costly and the modification procedures  
119 are not straightforward. Thus, an electrochemical approach using inexpensive and easily  
120 available materials as electrode modifiers should be developed (Degefu et al. 2014).

121

122 Nowadays, screen-printed electrodes (SPEs) modified with conducting polymer have been  
123 developed for various electrochemical sensing. SPE becomes the best solution owing to its  
124 frugal manufacture, tiny size, able to produce on large-scale and can be applied for on-site

125 detection (Nakthong et al. 2020). Conducting polymers (CPs) become an alternative to  
126 modifying the screen-printed electrodes due to their electrical conductivity, able to capture  
127 analyte by chemical/physical adsorption, large surface area and making CPs are very appealing  
128 materials from electrochemical perspectives (Baig et al. 2019). Such advantages of SPE  
129 encourage us to construct a new electrode for electrochemical sensing, and no research reported  
130 on the direct electrochemical oxidation of histamine using screen-printed electrode modified  
131 by polyurethane. Therefore, this research is the first to develop a new electrode using (screen  
132 printed polyurethane electrode) SPPE without any conducting materials.

133

134 The purpose of this work was to synthesize, characterize and study the conductivity of  
135 polyurethane using cyclic voltammetry (CV) and differential pulse voltammetry (DPV)  
136 attached to screen-printed electrode (SPE). To the best of our knowledge, this is the first  
137 attempt to use a modified polyurethane electrode. The electrochemistry of polyurethane  
138 mounted onto screen-printed electrode (SPE) is discussed in detail. Polyurethane is possible to  
139 become an advanced frontier material is chemically modified electrodes for bio/chemical  
140 sensing application.

141

## 142 **2. Experimental**

### 143 **2.1 Chemicals**

144 ***Synthesis of polyurethane film:*** Palm kernel oil (PKOp) supplied by UKM Technology Sdn  
145 Bhd through MPOB/UKM station plant, Pekan Bangi Lama, Selangor and prepared using  
146 Badri et al. (2000) method. 4, 4-diphenylmethane diisocyanate (MDI) was acquired from  
147 Cosmopolyurethane (M) Sdn. Bhd., Klang, Malaysia. Solvents and analytical reagents were  
148 benzene ( $\geq 99.8\%$ ), toluene ( $\geq 99.8\%$ ), hexane ( $\geq 99\%$ ), acetone ( $\geq 99\%$ ), tetrahydrofuran  
149 (THF), dimethylformamide (DMF) ( $\geq 99.8\%$ ), dimethylsulfoxide (DMSO) ( $\geq 99.9\%$ ) and

150 polyethylene glycol (PED) with a molecular weight of 400 Da obtained from Sigma Aldrich  
151 Sdn Bhd, Shah Alam.

152

## 153 **2.2 Apparatus**

154 Tensile testing was performed using a universal testing machine model Instron 5566 following  
155 ASTM 638 (Standard Test Method for Tensile Properties of Plastics). The tensile properties of  
156 the polyurethane film were measured at a velocity of 10 mm/min with a cell load of 5 kN.

157 The thermal properties were performed using thermogravimetry analysis (TGA) and  
158 differential scanning calorimetry (DSC) analysis. TGA was performed using a thermal analyzer  
159 of Perkin Elmer Pyris model with a heating rate of 10 °C/minute at a temperature range of 30  
160 to 800 °C under a nitrogen gas atmosphere. The DSC analysis was performed using a thermal  
161 analyzer of Perkin Elmer Pyris model with a heating rate of 10 °C /minute at a temperature  
162 range of -100 to 200 °C under a nitrogen gas atmosphere. Approximately, 5-10 mg of PU was  
163 weighed. The sample was heated from 25 to 150 °C for one minute, then cooled immediately  
164 from 150 -100 °C for another one minute and finally, reheated to 200 °C at a rate of 10 °C /min.  
165 At this point, the polyurethane encounters changes from elastic properties to brittle due to  
166 changes in the movement of the polymer chains. Therefore, the temperature in the middle of  
167 the inclined regions is taken as the glass transition temperature ( $T_g$ ). The melting temperature  
168 ( $T_m$ ) is identified as the maximum endothermic peak by taking the area below the peak as the  
169 enthalpy point ( $\Delta H_m$ ).

170

171 The morphological analysis of PU film was performed by Field Emission Scanning Electron  
172 Microscope (FESEM) model Gemini SEM microscope model 500-70-22. Before the analysis  
173 was carried out, the polyurethane film was coated with a thin layer of gold to increase the  
174 conductivity of the film. The coating method was carried out using a sputter-coater. The

175 observations were conducted at a magnification of 200× and 5000 × with 10.00 kV (Electron  
176 high tension - EHT).

177

178 The crosslinking of PU was determined using the soxhlet extraction method. About 0.60 g of  
179 PU sample was weighed and put in an extractor tube containing 250 ml of toluene, used as a  
180 solvent. This flow of toluene was let running for 24 hours. Mass of the PU was weighed before  
181 and after the reflux process was carried out. Then, the sample was dried in the conventional  
182 oven at 100 °C for 24 hours in order to get a constant mass. The percentage of crosslinking  
183 content known as the gel content can be calculated using Equation (1).

$$184 \quad \text{Gel content (\%)} = \frac{W_0 - W}{W} \times 100 \% \quad (1)$$

185  $W_0$  is the mass of PU before the reflux process (g) and  $W$  is the mass of PU after the reflux  
186 process (g).

187

188 FTIR spectroscopic analysis was performed using a Perkin-Elmer Spectrum BX instrument  
189 using the Diamond Attenuation Total Reflectance (DATR) method to confirm the  
190 polyurethane, PKOp and MDI functional group. FTIR spectroscopic analysis was performed  
191 at a wave number of 4000 to 600  $\text{cm}^{-1}$  to identify the peaks of the major functional groups in  
192 the formation of the polymer such as amide group (-NH), urethane carbonyl group (-C = O)  
193 and carbamate group (-CN).

194

### 195 **2.3 Synthesis of Polyurethane**

196 Palm kernel oil (PKO)p and polyethylene glycol (PEG) 400 (100:40 g/g) were combined and  
197 dissolved by acetone 30% in order to form a polyol prepolymer solution. The mixture was  
198 mixed using centrifuge with 100 rpm for 5 min to acquire a homogenized solution. Whereas,  
199 diisocyanate prepolymer was obtained by mixing 4,4'-diphenyl-methane diisocyanate (MDI)  
200 (100 g) to acetone 30%, afterward the mixture was mixed using centrifuge for 1 min to obtain

201 a homogenized solution. Then, 10 g of diisocyanate solution was poured into a container that  
202 containing 10 g of a polyol prepolymer solution slowly in order to avoid an exothermic reaction  
203 occur. The mixture was mixed for 30 sec until a homogenized solution acquired. Lastly, the  
204 polyurethane solution was poured on the electrode surface by using casting method and dried  
205 at ambient temperature for 12 hours.

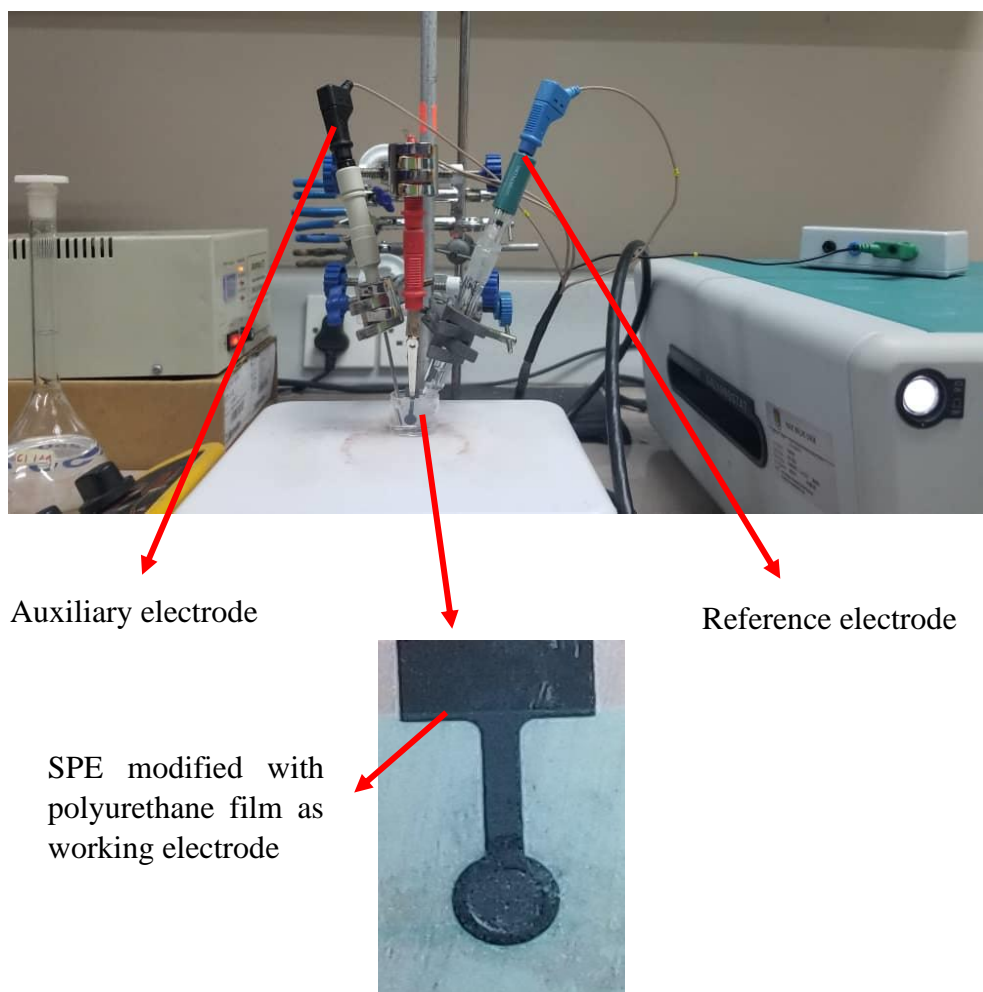
206

#### 207 **2.4 Modification of Electrode**

208 Voltammetric tests were performed using Metrohm Autolab Software (**Figure 1**) analyzer  
209 using cyclic voltammetry (CV) method or known as amperometric mode and differential pulse  
210 voltammetry (DPV). All electrochemical experiments were carried out using screen-printed  
211 electrode (diameter 3 mm) modified using polyurethane film as working electrode, platinum  
212 wire as auxiliary electrode and Ag/AgCl electrode as a reference electrode. All experiments  
213 were conducted at a temperature of  $20 \pm 2^\circ\text{C}$ .

214

215 The PU was cast onto the screen – printed electrode (SPE + PU) and analyzed using a single  
216 voltammetric cycle between -1200 and +1500 mV (vs Ag/AgCl) of ten cycles at a scanning  
217 rate of 100 mV/s in 5 ml of KCl in order to study the activity of SPE and polyurethane film.  
218 Approximately (0.1, 0.3 & 0.5) mg of palm-based prepolyurethane was dropped separately  
219 onto the surface of the SPE and dried at room temperature. The modified palm-based  
220 polyurethane electrodes were then rinsed with deionized water to remove physically adsorbed  
221 impurities and residues of unreacted material on the electrode surface. All electrochemical  
222 materials and calibration measurements were carried out in a 5 mL glass beaker with a  
223 configuration of three electrodes inside it. Platinum wire and silver/silver chloride (Ag/AgCl)  
224 electrodes were used as auxiliary and reference electrodes, while screen-printed electrode that  
225 had been modified with polyurethane was applied as a working electrode.



226 **Figure 1.** Potentiostat instrument to study the conductivity of SPE modified with  
 227 polyurethane film using cyclic voltammetry (CV) and differential pulse voltammetry (DPV)

228

### 229 3. Results and Discussion

230 The synthesis of PU films was carried out using pre-polymerization method which involves  
 231 the formation of urethane polymer at an early stage. The reaction took place between palm  
 232 kernel oil-based polyol (PKOp) and diisocyanate (MDI). **Table 1** presents the PKO-p  
 233 properties used in this study. The structural chain was extended with the aid of polyethylene  
 234 glycol (PEG) to form flexible and elastic polyurethane film. In order to form the urethane  
 235 prepolymer, one of the isocyanate groups (NCO) reacts with one hydroxyl group (OH) of  
 236 polyol while the other isocyanate group attacks another hydroxyl group in the polyol (Wong &  
 237 Badri 2012) as shown in **Figure 2**.

238 **Table 1** The specification of PKO-p (Badri et al. (2000)).

Property	Values
Viscosity at 25°C (cps)	1313.3
Specific gravity (g/mL)	1.114
Moisture content (%)	0.09
pH value	10 – 11
The hydroxyl number mg KOH/g	450 - 470

239

240

241 a. FTIR analysis

242 **Figure 3** shows the FTIR spectrum for polyurethane, exhibiting the important functional group  
 243 peaks. According to a study researched by Wong & Badri 2012, PKO-p reacts with MDI to  
 244 form urethane prepolymers. The NCO group on MDI reacts with the OH group on polyol  
 245 whether PKOp or PEG. It can be seen there are no important peaks of MDI in the FTIR  
 246 spectrums. This is further verified by the absence of peak at the  $2400\text{ cm}^{-1}$  belongs to MDI (-  
 247 NCO groups). This could also confirm that the NCO group on MDI had completely reacted  
 248 with PKO-p to form the urethane -NHC (O) backbone. The presence of amides (-NH),  
 249 carbonyl urethane group (-C = O), carbamate group (C-NH) and -C-O-C confirmed the  
 250 formation of urethane chains. In this study, the peak of carbonyl urethane (C = O) detected at  
 251  $1727\text{ cm}^{-1}$  indicated that the carbonyl urethane group was bonded without hydrogen owing to  
 252 the hydrogen reacted with the carbonyl urethane group.

253

254 The reaction of polyurethane has been studied by Hamuzan & Badri (2016) where the urethane  
 255 carbonyl group was detected at  $1730 - 1735\text{ cm}^{-1}$  while the MDI carbonyl was detected at  $2400$   
 256  $\text{cm}^{-1}$ . The absence of peaks at  $2250 - 2270\text{ cm}^{-1}$  indicates the absence of NCO groups. It shows



257 that the polymerization reaction occurs entirely between NCO groups in MDI with hydroxyl  
258 groups on polyols and PEG (Mishra et al. 2012). The absence of peaks at  $1690\text{ cm}^{-1}$   
259 representing urea ( $\text{C} = \text{O}$ ) in this study indicated, there is no urea formation as a byproduct  
260 (Clemitson 2008) of the polymerization reaction that possibly occurs due to the excessive  
261 water. For the amine (NH) group, hydrogen-bond to NH and oxygen to form ether and  
262 hydrogen bond to NH and oxygen to form carbonyl on urethane can be detected at the peak of  
263  $3301\text{ cm}^{-1}$  and in the wavenumber at range  $3326 - 3428\text{ cm}^{-1}$ . This has also been studied and  
264 detected by Lampman et. al. (2010) and Mutsuhisa et al. (2007). In this study, the hydrogen  
265 bond formed by  $\text{C} = \text{O}$  acts as a proton acceptor whereas NH acts as a proton donor. The  
266 urethane group in the hard segment (MDI) has electrostatic forces on the oxygen, hydrogen  
267 and nitrogen atoms and these charged atoms form dipoles that attract other opposite atoms.  
268 These properties make isocyanates are highly reactive and having different properties (Leykin  
269 et al. 2016).

270

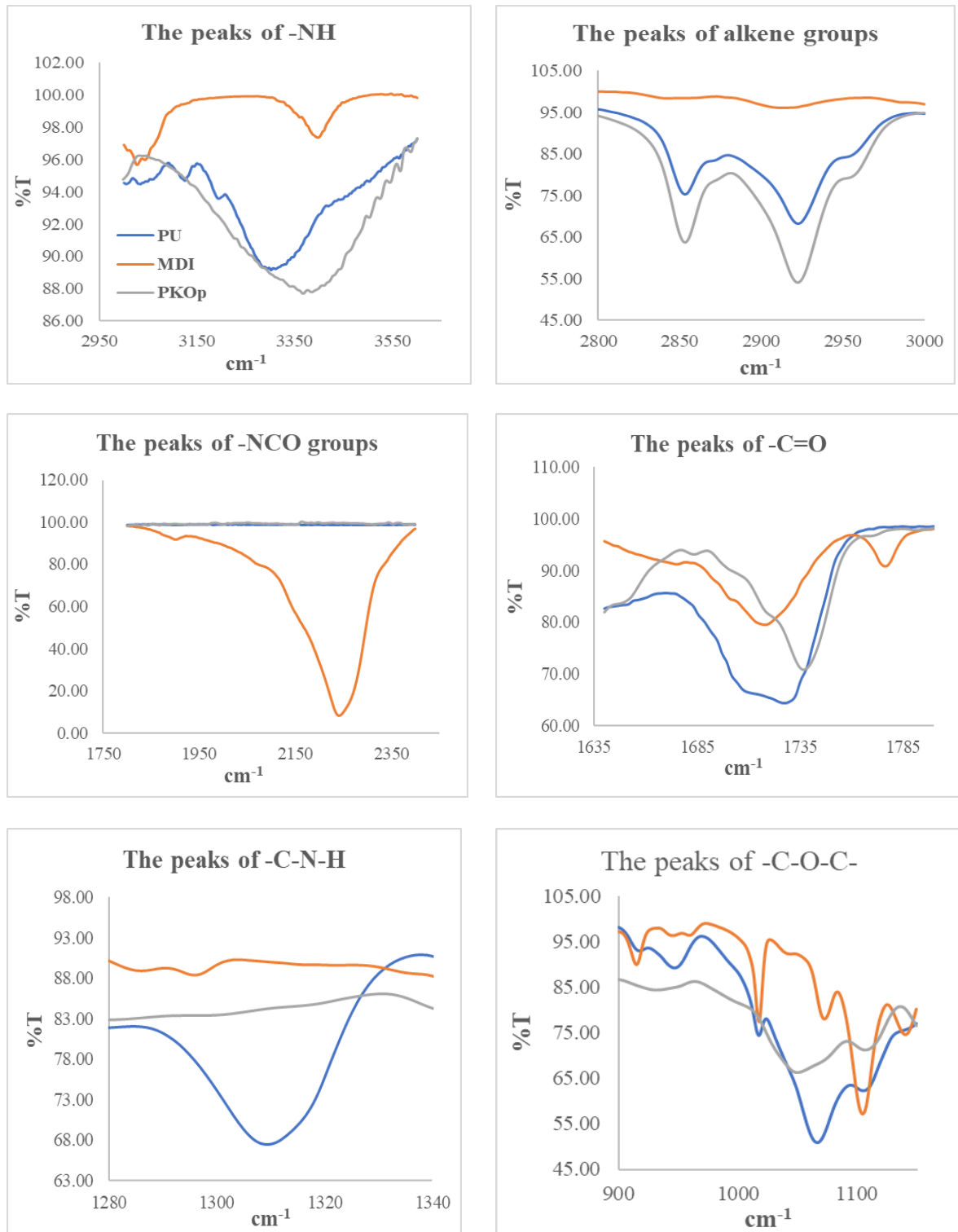
271 MDI was one of the isocyanates used in this study, has an aromatic group and is more  
272 reactive compared to aliphatic group isocyanates such as hexamethylene diisocyanate (HDI)  
273 or isophorone diisocyanate (IPDI). Isocyanates have two groups of isocyanates on each  
274 molecule. Diphenylmethane diisocyanate is an exception owing to its structure consists of two,  
275 three, four or more isocyanate groups (Nohra et al. 2013). The use of PEG 400 in this study as  
276 a chain extender for polyurethane increases the chain mobility of polyurethane at an optimal  
277 amount. The properties of a polyurethane are contributed by hard and soft copolymer segments  
278 of both polyol monomers and MDI. This makes the hard segment of urethane serves as a  
279 crosslinking site between the soft segments of the polyol (Leykin et al. 2016).

280



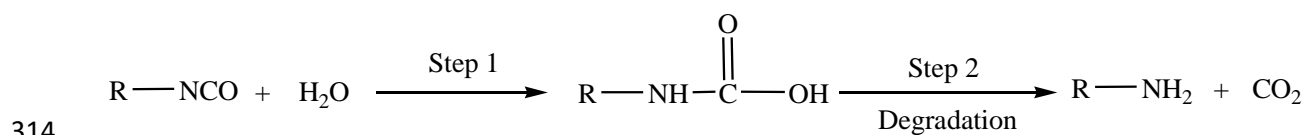
296 dimensional networks with high molecular weight. In some aspects, polyurethane can be a  
297 macromolecule, a giant molecule (Petrovic 2008).

298



299 **Figure 3.** FTIR spectrums of several important peaks between polyurethane, PKO-p and MDI

300 However, the reaction between MDI and PEG as a chain extender where oxygen on the  
 301 nucleophile PEG attacks the NCO group in the MDI to form two intermediate complexes A  
 302 and B can occur. Nevertheless, nucleophilic substitution reactions have a greater tendency to  
 303 occur in PKOp compared to PEG because the presence of nitrogen atoms is more  
 304 electropositive than oxygen atoms in PEG. Amine has a higher probability of reacting  
 305 compared to hydroxyl (Herrington & Hock 1997). Amine with high alkalinity reacts with  
 306 carbon atoms on MDI as proposed by Wong and Badri (2012). PKOp contains long carbon  
 307 chains that can easily stabilize alkyl ions when intermediate complexes are formed. Therefore,  
 308 the polyol is more reactive than PEG to react with MDI. However, the addition of PEG will  
 309 increase the length of the polyurethane chain and prevent side effects such as the formation of  
 310 urea by-products of the NCO group reaction in urethane pre-polymer and water molecules from  
 311 the environment. If the NCO group reacts with the excess water in the environment, the  
 312 formation of urea and carbon dioxide gas will also occur excessively (**Figure 4**). This reaction  
 313 can cause a polyurethane foam, not polyurethane film as we studied the film.



315 **Figure 4.** The reaction between NCO group and water producing carbon dioxide

316

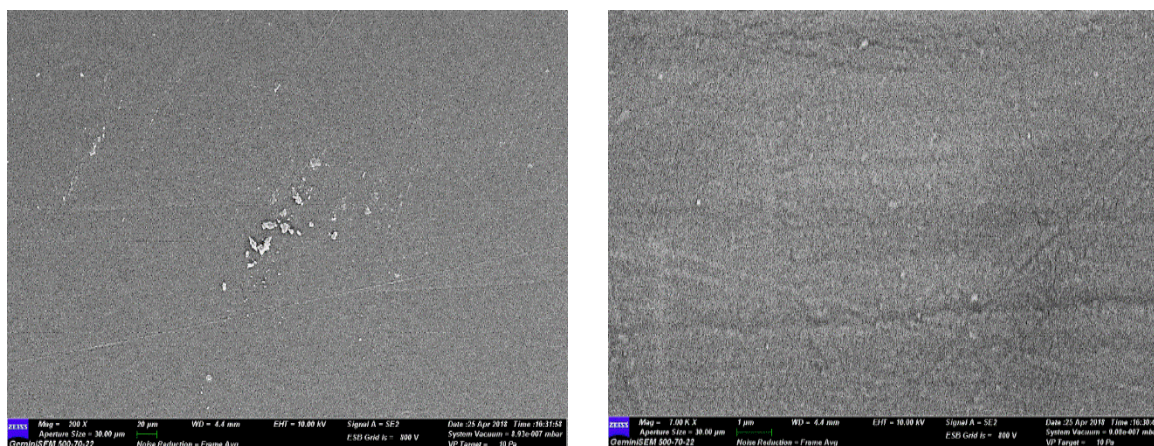
317 Furthermore, the application of PEG can influence the conductivity of PU where  
 318 Porcarelli et al. (2017) have reported the application of PEG using several molecular weights.  
 319 PEG 1500 decreased the conductivity of PU in consequence of the semicrystalline phase of  
 320 PEG 1500 that acted as a poor ion conducting phase for PU. It is also well known that PEG  
 321 with a molecular weight of more than 1000 g·mol<sup>-1</sup> tends to crystallize with deleterious effects  
 322 on room temperature ionic conductivity (Porcarelli et al. 2017).

323

324 b. Morphological analysis

325 The Field Emission Scanning Electron Microscope (FESEM) micrograph in **Figure 5** shows  
326 the formation of a uniform polymer film contributed by the polymerization method applied.  
327 The magnification used for this surface analysis ranged from 200 to 5000  $\times$ . The  
328 polymerization method can also avoid the failure of the reaction in PU polymerization.  
329 Furthermore, no trace of separation was detected by FESEM. This has also been justified by  
330 the wavelengths obtained by the FTIR spectrums above.

331



332 **Figure 5.** The micrograph of polyurethane films analysed by FESEM at (a) 200  $\times$  and (b)  
333 5000 $\times$  magnifications.

334 c. The crosslinking analysis

336 Soxhlet analysis was applied to determine the degree of crosslinking between the hard  
337 segments and the soft segments in the polyurethane. The urethane group on the hard segment  
338 along the polyurethane chain is polar (Cuve & Pascault 1991). Therefore, during the testing, it  
339 was very difficult to dissolve in toluene, as the testing reagent. The degree of crosslinking is  
340 determined by the percentage of the gel content. The analysis result obtained from the Soxhlet  
341 testing indicating a 99.3 % gel content. This is significant in getting a stable polymer at higher  
342 working temperature (Rogulska et al. 2007).

343

$$\text{Gel content (\%)} = \frac{(0.6 - 0.301) \text{ g}}{0.301 \text{ g}} \times 100\% = 99.33\%$$

344

345

346 d. The thermal analysis

347 Thermogravimetric analysis (TGA) can be used to observe the material mass based on

348 temperature shift. It can also examine and estimate the thermal stability and materials

349 properties such as the alteration weight owing to absorption or desorption, decomposition,

350 reduction and oxidation. The material composition of polymer is specified by analysing the

351 temperatures and the heights of the individual mass steps (Alamawi et al. 2019). **Figure 6**

352 shows the TGA and DTG thermograms of polyurethane. The percentage weight loss (%) is

353 listed in **Table 2**. Generally, only a small amount of weight was observed. It is shown in **Figure**

354 **6** in the region of 45 – 180°C. This is due to the presence of condensation on moisture and

355 solvent residues.

356

357 **Table2** Weight loss percentage of (wt%) polyurethane film

Sample	% Weight loss (wt%)				Total of weight loss (%)	Residue after 550°C (%)
	T <sub>max</sub> , °C	T <sub>d1</sub> , 200 – 290°C	T <sub>d2</sub> , 350 – 500°C	T <sub>d3</sub> , 500 – 550°C		
Polyurethane	240	8.04	39.29	34.37	81.7	18.3

358

359 The bio polyurethane is thermally stable up to 240 °C before it has undergone thermal

360 degradation (Agrawal et al. 2017). The first stage of thermal degradation (T<sub>d1</sub>) on polyurethane

361 films was shown in the region of 200 – 290 °C as shown in **Figure 6**. The T<sub>d1</sub> is associated with

362 degradation of the hard segments of the urethane bond, forming alcohol or degradation of the

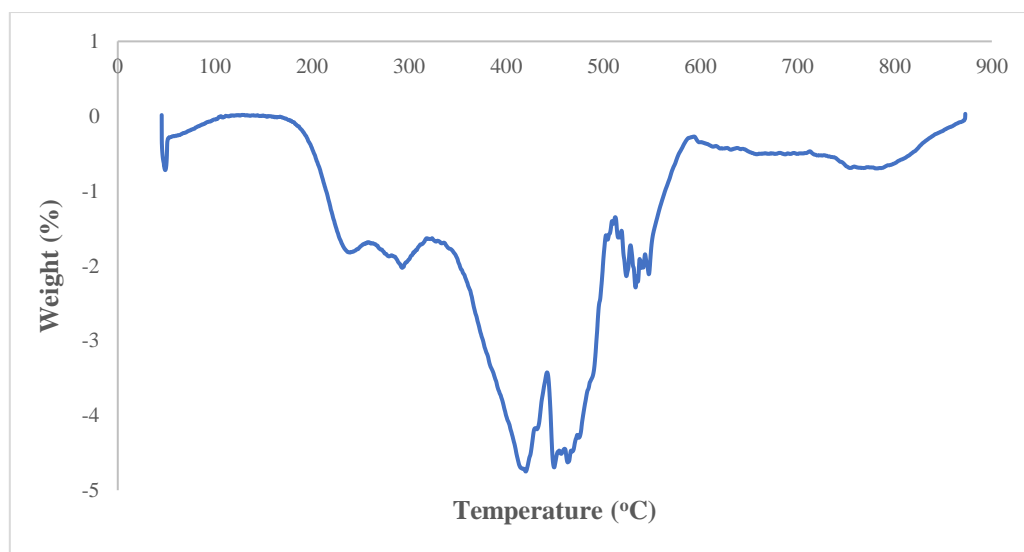
363 polyol chains and releasing of isocyanates (Berta et al. 2006), primary and secondary amines

364 as well as carbon dioxide (Corcuera et al. 2011; Pan & Webster 2012). Meanwhile, the second

365 thermal degradation stage ( $T_{d2}$ ) of polyurethane films experienced a weight loss of 39.29 %.  
366 This endotherm of  $T_{d2}$  is related to the dimerization of isocyanates to form carbodiimides and  
367 release  $CO_2$ . The formed carbodiimide reacts with alcohol to form urea. The third stage of  
368 thermal degradation ( $T_{d3}$ ) is related to the degradation of urea (Berta et al. 2006) and the soft  
369 segment on polyurethane.

370

371 Generally, DSC analysis exhibited thermal transitions as well as the initial  
372 crystallisation and melting temperatures of the polyurethane (Khairuddin et al. 2018). It serves  
373 to analyse changes in thermal behavior due to changes occurring in the chemical chain structure  
374 based on the glass transition temperature ( $T_g$ ) of the sample obtained from the DSC thermogram  
375 (**Figure 7**). DSC analysis on polyurethane film was performed in the temperature at the range  
376 100 °C to 200 °C using nitrogen gas as a blanket as proposed by Furtwengler et al. (2017). The  
377 glass transition temperature ( $T_g$ ) on polyurethane was above room temperature, at 78.1 °C  
378 indicated the state of glass on polyurethane. The presence of MDI contributes to the formation  
379 of hard segments in polyurethanes. Porcarelli et al. (2017) stated that possess a low glass  
380 transition ( $T_g$ ) may contribute to PU conductivity.

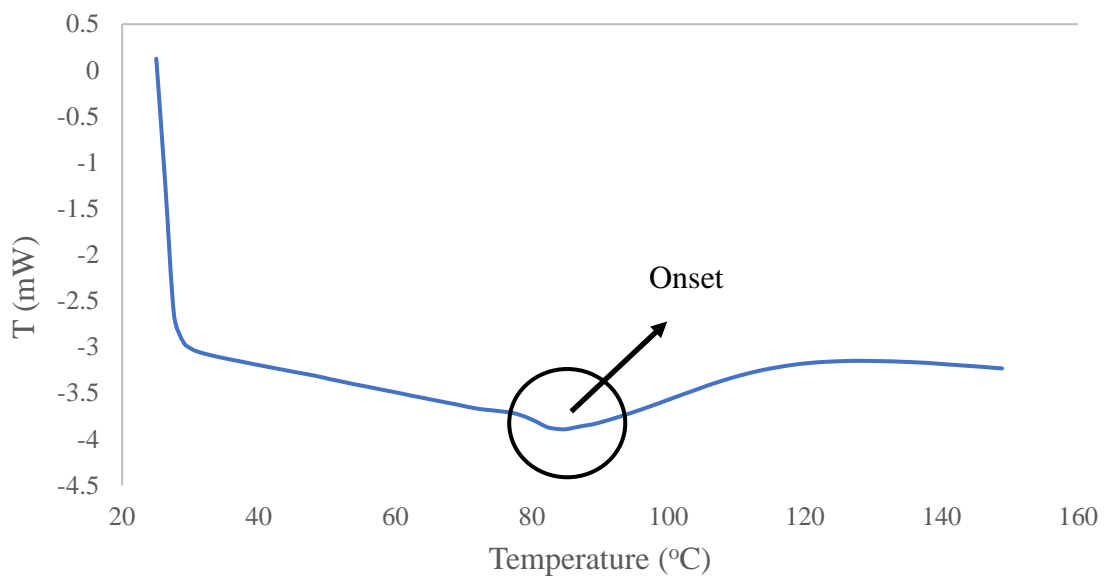


381

382

**Figure 6.** DTG thermogram of polyurethane film

383 During polymerization, this hard segment restricts the mobility of the polymer chain  
384 (Ren et al. 2013) owing to the steric effect on the benzene ring in the hard segment. The  
385 endothermic peak of acetone used as the solvent in this study was supposedly at 56°C.  
386 However, it was detected in the DSC thermogram nor the TGA thermogram, which indicates  
387 that acetone was removed from the polyurethane during the synthesis process, owing to its  
388 volatility nature. The presence of acetone in the synthesis was to lower the reaction kinetics.



389 **Figure 7.** DSC thermogram of polyurethane film

391  
392  
393 e. The solubility and mechanical properties of the polyurethane film  
394 The chemical resistivity of a polymer will be the determinant in performing as a conductor.  
395 Thus, its solubility in various solvents was determined by dissolving the polymer in selected  
396 solvents such as hexane, benzene, acetone, tetrahydrofuran (THF), dimethylformamide (DMF)  
397 and dimethylformamide (DMSO). On the other hand, the mechanical properties of  
398 polyurethane were determined based on the standard testing following ASTM D 638 (Standard  
399 Test Method for Tensile Properties of Plastics). The results from the polyurethane film  
400 solubility and tensile test are shown in **Table 3**. Polyurethane films were insoluble with



401 benzene, hexane and acetone and are only slightly soluble in tetrahydrofuran (THF),  
 402 dimethylformamide (DMF) and dimethylformamide (DMSO) solutions. While the tensile  
 403 strength of a PU film indicated how much elongation load the film was capable of withstanding  
 404 the material before breaking.

405

406 **Table 3** The solubility and mechanical properties of the polyurethane film

407

Parameters	Polyurethane film
Solubility	Benzene Insoluble
	Hexane Insoluble
	Acetone Insoluble
	THF Less soluble
	DMF Less soluble
	DMSO Less soluble
Stress (MPa)	8.53
Elongation percentage (%)	43.34
Strain modulus (100) (MPa)	222.10

408

409 The tensile stress, strain and modulus of polyurethane film also indicated that polyurethane has  
 410 good mechanical properties that are capable of being a supporting substrate for the next stage  
 411 of study. In the production of polyurethane, the properties of a polyurethane are easily  
 412 influenced by the content of MDI and polyol used. The length of the chain and its flexibility  
 413 are contributed by the polyol which makes it elastic. High crosslinking content can also produce  
 414 hard and rigid polymers. MDI is a major component in the formation of hard segments in  
 415 polyurethane. It is this hard segment that determines the rigidity of the PU. Therefore, high

416 isocyanate content results in higher rigidity on PU (Petrovic et al. 2002). Thus, the polymer has  
417 a higher resistance to deformation and more stress can be applied to the PU.

418

419 f. The conductivity of the polyurethane as a polymeric film on SPE

420 Polyurethane film deposited onto the screen-printed electrode by casting method as shown in

421 **Figure 1**. After that, the modified electrode was analysed using cyclic voltammetry (CV) and

422 differential pulse voltammetry (DPV) in order to study the behaviour of modified electrode.

423 The modified electrode was tested in a 0.1 mmol/L KCl solution containing 5 mmol/L ( $K_3Fe$

424  $(CN)_6$ ). The use of potassium ferricyanide is intended to increase the sensitivity of the KCl

425 solution. The conductivity of the modified electrode was studied. The electrode was analyzed

426 by cyclic voltammetry method with a potential range of -1.00 to +1.00 with a scan rate of 0.05

427 V/s. The voltammograms at electrode have shown a specific redox reaction. Furthermore, the

428 conductivity of the modified electrode is lower due to the use of polyurethane. This occurs due

429 to PU is a natural polymer produced from the polyol of palm kernel oil. The electrochemical

430 signal at the electrode is low if there is a decrease in electrochemical conductivity (El - Raheem

431 et al. 2020). It can be concluded that polyurethane is a bio-polymer with a low conductivity

432 value. The current of the modified electrode was found at  $5.3 \times 10^{-5}$  A or 53  $\mu$ A. Nevertheless,

433 the electroconductivity of PU in this study shows better conductivity several times compared

434 to Bahrami et al. (2019) that reported the conductivity of PU as  $1.26 \times 10^{-6}$  A, whereas Li et al.

435 (2019) reported the PU conductivity in their study was even very low, namely  $10^{-14}$  A. The

436 conductivity of PU owing to the benzene ring in the hard segment (MDI) could exhibit the

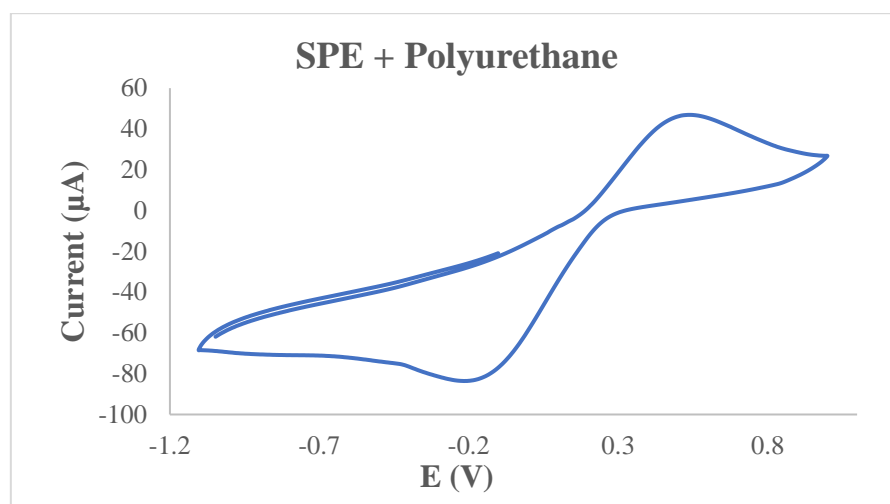
437 conductivity by inducing electron delocalization along the polyurethane chain (Wong et al.

438 2014). The conductivity of PU can also be caused by PEG. The application of PEG as polyol

439 has been studied by Porcarelli et al. (2017), that reported that the conductivity of PU based on

440 PEG – polyol was  $9.2 \times 10^{-8}$ .

441 According to **Figure 8**, it can be concluded that the anodic peak present in the modified  
442 electrode was at +0.5 V, it also represented the oxidation process of the modified electrode.  
443 The first oxidation scan on both electrodes ranged from -0.2 to +1.0 V, which showed a  
444 significant anodic peak at a potential of +0.5 V.  
445



446  
447 **Figure 8.** The voltammogram of SPE – PU modified electrode after analysed using cyclic  
448 voltammetry (CV) technique

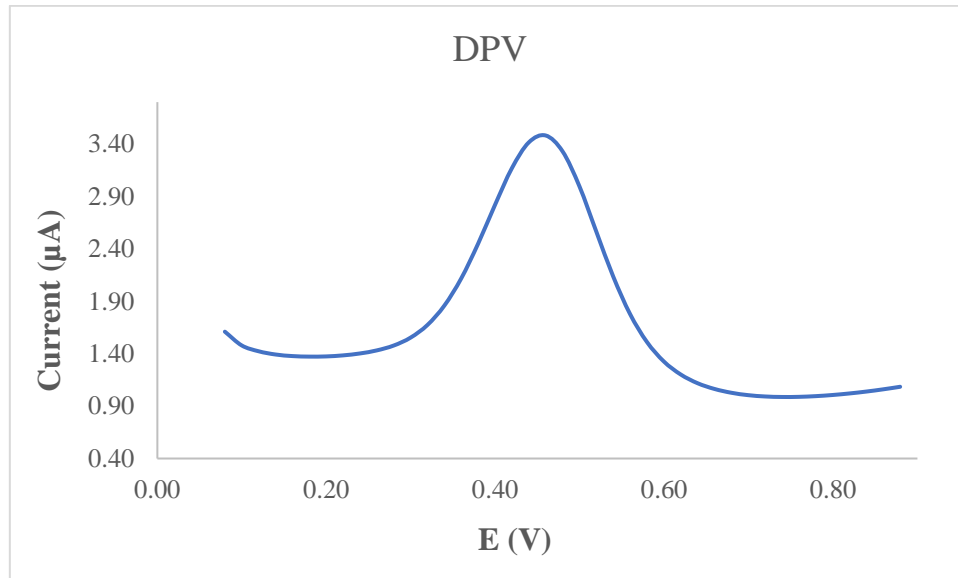
449  
450 **Figure 9** also presents the DPV voltammogram of modified electrode. DPV is a measurement  
451 based on the difference in potential pulses that produce an electric current. Scanning the  
452 capability pulses to the working electrode will produce different currents. Optimal peak  
453 currents will be produced to the reduction capacity of the redox material. The peak current  
454 produced is proportional to the concentration of the redox substance and can be detected up to  
455 concentration below  $10^{-8}$  M. DPV was conducted to obtain the current value that more accurate  
456 than CV (Lee et al. 2018).

457  
458 This study used a redox pair ( $K_3Fe(CN)_6$ ) as a test device (probe). The currents generated by  
459 SPE-PU and proved by CV and DPV have shown conductivity on polyurethane films. This  
460 suggests that polyurethane films can conduct electron transfer. The electrochemical area on the

461 modified electrode can be calculated using the formula from Randles-Sevcik (Butwong et al.  
 462 2019), where the electrochemical area for SPE-PU is considered to be A, using Equation 2:

463 
$$\text{Current of SPE-PU, } I_p = 2.65 \times 10^5 n^{3/2} A v^{1/2} C D^{1/2} \quad (2)$$

464



465

466 **Figure 9.** The voltammogram of SPE – PU modified electrode after analyzed using  
 467 differential pulse voltammetry (DPV) technique

468

469 Where,  $n - 1$  is the amount of electron transfer involved, while C is the solvent concentration  
 470 used (mmol/L) and the value of D is the diffusion constant of 5 mmol/L at  $(K_3Fe(CN)_6)$   
 471 dissolved using 0.1 mmol/L KCl. The estimated surface area of the electrode (**Figure 1**) was  
 472  $0.2 \text{ cm}^2$  where the length and width of the electrode used during the study was  $0.44 \text{ cm} \times 0.44$   
 473 cm while the surface area of the modified electrode was  $0.25 \text{ cm}^2$  with the length and width of  
 474 the electrode estimated at  $0.5 \text{ cm} \times 0.5 \text{ cm}$ , and causing the modified electrode has a larger  
 475 surface. The corresponding surface concentration ( $\tau$ ) ( $\text{mol}/\text{cm}^2$ ) is calculated using Equation 3.

476 
$$I_p = (n^2 F^2 / 4RT) A \tau v \quad (3)$$

477  $I_p$  is the peak current (A), while A is the surface area of the electrode ( $\text{cm}^2$ ), the value of v is  
 478 the applied scan rate (mV/s) and F is the Faraday constant (96,584 C/mol), R is the constant  
 479 ideal gas (8.314 J/mol K) and T is the temperature used during the experiment being conducted

480 (298 K) (Koita et al. 2014). The development of conducting polymer from palm oil-based  
481 biomaterials seems to be one of the potential future applications of palm oil products, as this  
482 novel material has the potential to contribute positively to the analytical industry. Likewise,  
483 other palm oil-based products, such as refined-bleached-deodorised (RBD) palm oil, palm oil,  
484 and palm stearin are abundantly available in Malaysia. They are known to be economical,  
485 sustainable, and environmentally biodegradable. These palm oil-based products are promising  
486 prospects for manufacturing biomaterials that become alternative products to other polymers  
487 from synthetic/chemical-based (Tajao et al. 2021). Several studies have been reported the  
488 application of PU to produce elastic conductive fibres and films owing to it is highly elastic,  
489 scratch resistant and adhesive (Tadese et al. 2019), thus it is easy for PU to adhere on the  
490 screen-printed electrode in order to modify the electrode. PU is also being used as a composite  
491 material to make elastic conducting composite films (Khatoon & Ahmad 2017).

492

#### 493 **4. Conclusion**

494 Polyurethane film was prepared by pre-polymerization between palm kernel oil-based polyol  
495 (PKO-p) with MDI. The presence of PEG 400 as the chain extender formed freestanding  
496 flexible film. Acetone was used as the solvent to lower the reaction kinetics since the pre-  
497 polymerization was carried out at room temperature. The formation of urethane links (NHCO  
498 – backbone) after polymerization was confirmed by the absence of N=C=O peak at  $2241\text{ cm}^{-1}$   
499 and the presence of N-H peak at  $3300\text{ cm}^{-1}$ , carbonyl (C=O) at  $1710\text{ cm}^{-1}$ , carbamate (C-N) at  
500  $1600\text{ cm}^{-1}$ , ether (C-O-C) at  $1065\text{ cm}^{-1}$ , benzene ring (C = C) at  $1535\text{ cm}^{-1}$  in the bio  
501 polyurethane chain structure. Soxhlet analysis for the determination of crosslinking on  
502 polyurethane films has yielded a high percentage of 99.33 %. This is contributed by the hard  
503 segments formed from the reaction between isocyanates and hydroxyl groups causing  
504 elongation of polymer chains. FESEM analysis exhibited an absence of phase separation and

505 smooth surface. Meanwhile, the current of modified electrode was found at  $5.2 \times 10^{-5}$  A. This  
506 bio polyurethane film can be used as a conducting bio-polymer and it is very useful for other  
507 studies such as electrochemical sensor purposes. Furthermore, advanced technologies are  
508 promising and the future of bio-based polyol looks very bright.

509

## 510 **5. Acknowledgment**

511 The authors would like to thank Universitas Alma Ata for the sponsorship given to the first  
512 author. We would like to also, thank The Department of Chemical Sciences, Universiti  
513 Kebangsaan Malaysia for the laboratory facilities and CRIM, UKM for the analysis  
514 infrastructure.

515

## 516 **6. Conflict of Interest**

517 The authors declare no conflict of interest.

518

## 519 **7. References**

- 520 Agrawal, A., Kaur, R., Walia, R. S. (2017). PU foam derived from renewable sources:  
521 Perspective on properties enhancement: An overview. *European Polymer Journal*. 95:  
522 255 – 274.
- 523 Akindoyo, J. O., Beg, M.D.H., Ghazali, S., Islam, M.R., Jeyaratnam, N. & Yuvaraj, A.R.  
524 (2016). Polyurethane types, synthesis and applications – a review. *RSC Advances*. 6:  
525 114453 – 114482.
- 526 Alamawi, M. Y., Khairuddin, F. H., Yusoff, N. I. M., Badri, K., Ceylan, H. (2019).  
527 Investigation on physical, thermal and chemical properties of palm kernel oil polyol bio  
528 – based binder as a replacement for bituminous binder. *Construction and Building*  
529 *Materials*. 204: 122 – 131.

530 Alqarni, S. A., Hussein, M. A., Ganash, A. A. & Khan, A. (2020). Composite material – based  
531 conducting polymers for electrochemical sensor applications: a mini review.  
532 *BioNanoScience*. **10**: 351 – 364.

533 Badan, A., Majka, T. M. (2017). The influence of vegetable – oil based polyols on physico –  
534 mechanical and thermal properties of polyurethane foams. *Proceedings*. 1 – 7.

535 Badri, K.H. (2012) Biobased polyurethane from palm kernel oil-based polyol. In Polyurethane;  
536 Zafar, F., Sharmin, E., Eds. InTechOpen: Rijeka, Croatia. pp. 447–470.

537 Badri, K.H., Ahmad, S.H. & Zakaria, S. 2000. Production of a high-functionality RBD palm  
538 kernel oil – based polyester polyol. *Journal of Applied Polymer Science* 81(2): 384 –  
539 389.

540 Baig, N., Sajid, M. and Saleh, T. A. 2019. Recent trends in nanomaterial – modified electrodes  
541 for electroanalytical applications. *Trends in Analytical Chemistry*. 111: 47 – 61.

542 Berta, M., Lindsay, C., Pans, G., & Camino, G. (2006). Effect of chemical structure on  
543 combustion and thermal behaviour of polyurethane elastomer layered silicate  
544 nanocomposites. *Polymer Degradation and Stability*. **91**: 1179-1191.

545 Borowicz, M., Sadowska, J. P., Lubczak, J. & Czuprynski, B. (2019). Biodegradable, flame –  
546 retardant, and bio – based rigid polyurethane/polyisocyanurate foams for thermal  
547 insulation application. *Polymers*. 11: 1816 – 1839.

548 Butwong, N., Khajonklin, J., Thongbor, A. & Luong, J.H.T. (2019). Electrochemical sensing  
549 of histamine using a glassy carbon electrode modified with multiwalled carbon nanotubes  
550 decorated with Ag – Ag<sub>2</sub>O nanoparticles. *Microchimica Acta*. **186 (11)**: 1 – 10.

551 Chokkareddy, R., Thondavada, N., Kabane, B. & Redhi, G. G. (2020). A novel ionic liquid  
552 based electrochemical sensor for detection of pyrazinamide. *Journal of the Iranian*  
553 *Chemical Society*. 18: 621 – 629.

554 Chokkareddy, R., Kanchi, S. & Inamuddin (2020). Simultaneous detection of ethambutol and  
555 pyrazinamide with IL@CoFe<sub>2</sub>O<sub>4</sub>NPs@MWCNTs fabricated glassy carbon electrode.  
556 *Scientific Reports*. 10: 13563.

557 Clemitson, I. (2008). Castable Polyurethane Elastomers. Taylor & Francis Group, New York.  
558 doi:10.1201/9781420065770.

559 Corcuera, M.A., Rueda, L., Saralegui, A., Martin, M.D., Fernandez-d'Arlas, B., Mondragon,  
560 I. & Eceiza, A. (2011). Effect of diisocyanate structure on the properties and  
561 microstructure of polyurethanes based on polyols derived from renewable resources.  
562 *Journal of Applied Polymer Science*. **122**: 3677-3685.

563 Cuve, L. & Pascault, J.P. (1991). Synthesis and properties of polyurethanes based on  
564 polyolefine: Rigid polyurethanes and amorphous segmented polyurethanes prepared in  
565 polar solvents under homogeneous conditions. *Polymer*. **32** (2): 343- 352.

566 Degefu, H., Amare, M., Tessema, M. & Admassie, S. (2014). Lignin modified glassy carbon  
567 electrode for the electrochemical determination of histamine in human urine and wine  
568 samples. *Electrochimica Acta*. 121: 307 – 314.

569 Dzulkipli, M. Z., Karim, J., Ahmad, A., Dzulkurnain, N. A., Su'ait, M S., Fujita, M. Y., Khoon,  
570 L. T. & Hassan, N. H. (2021). The influences of 1-butyl-3-methylimidazolium  
571 tetrafluoroborate on electrochemical, thermal and structural studies as ionic liquid gel  
572 polymer electrolyte. *Polymers*. 13 (8): 1277 – 1294.

573 El-Raheem, H.A., Hassan, R.Y.A., Khaled, R., Farghali, A. & El-Sherbiny, I.M. (2020).  
574 Polyurethane – doped platinum nanoparticles modified carbon paste electrode for the  
575 sensitive and selective voltammetric determination of free copper ions in biological  
576 samples. *Microchemical Journal*. **155**: 104765.

577 Fei, T., Li, Y., Liu, B. & Xia, C. (2019). Flexible polyurethane/boron nitride composites with  
578 enhanced thermal conductivity. *High Performance Polymers*. **32** (3): 1 – 10.



579 Furtwengler, P., Perrin R., Redl, A. & Averous, L. (2017). Synthesis and characterization of  
580 polyurethane foams derived of fully renewable polyesters polyols from sorbitol.  
581 *European Polymer Journal*. **97**: 319 – 327.

582 Ghosh, S., Ganguly, S., Remanan, S., Mondal, S., Jana, S., Maji, P. K., Singha, N., Das, N. C.  
583 (2018). Ultra – light weight, water durable and flexible highly electrical conductive  
584 polyurethane foam for superior electromagnetic interference shielding materials. *Journal*  
585 *of Materials Science: Materials in Electronics*. 29: 10177 – 10189.

586 Guo, S., Zhang, C., Yang, M., Zhou, Y., Bi, C., Lv, Q. & Ma, N. (2020). A facile and sensitive  
587 electrochemical sensor for non – enzymatic glucose detection based on three –  
588 dimensional flexible polyurethane sponge decorated with nickel hydroxide. *Analytica*  
589 *Chimica Acta*. **1109**: 130 – 139.

590 Hamuzan, H.A. & Badri, K.H. (2016). The role of isocyanates in determining the viscoelastic  
591 properties of polyurethane. AIP Conference Proceedings. 1784, Issue 1.

592 Herrington, R. & Hock, K. (1997). Flexible polyurethane foams. 2nd Edition. Dow Chemical  
593 Company. Midlan.

594 Janpoung, P., Pattanauwat, P. & Potiyaraj, P. (2020). Improvement of electrical conductivity  
595 of polyurethane/polypyrrole blends by graphene. *Key Engineering Materials*. **831**: 122 –  
596 126.

597 Khairuddin, F.H., Yusof, N. I. M., Badri, K., Ceylan, H., Tawil, S. N. M. (2018). Thermal,  
598 chemical and imaging analysis of polyurethane/cecabase modified bitumen. *IOP Conf.*  
599 *Series: Materials Science and Engineering*. 512: 012032.

600 Khatoon, H., Ahmad, S. (2017). A review on conducting polymer reinforced polyurethane  
601 composites. *Journal of Industrial and Engineering Chemistry*. 53: 1 – 22.

602 Kilele, J. C., Chokkareddy, R., Rono, N. & Redhi, G. G. (2020). A novel electrochemical  
603 sensor for selective determination of theophylline in pharmaceutical formulations.  
604 *Journal of the Taiwan Institute of Chemical Engineers.* 1 – 11.

605 Kilele, J. C., Chokkareddy, R. & Redhi, G. G. (2021). Ultra – sensitive electrochemical sensor  
606 for fenitrothion pesticide residues in fruit samples using IL@CoFe<sub>2</sub>ONPs@MWCNTs  
607 nanocomposite. *Microchemical Journal.* 164: 106012.

608 Koita, D., Tzedakis, T., Kane, C., Diaw, M., Sock, O. & Lavedan, P. (2014). Study of the  
609 histamine electrochemical oxidation catalyzed by nickel sulfate. *Electroanalysis.* **26 (10):**  
610 2224 – 2236.

611 Kotal, M., Srivastava, S.K. & Paramanik, B. (2011). Enhancements in conductivity and thermal  
612 stabilities of polyurethane/polypyrrole nanoblends. *The Journal of Physical Chemistry*  
613 *C.* **115 (5):** 1496 – 1505.

614 Ladan, M., Basirun, W.J., Kazi, S.N., Rahman, F.A. (2017). Corrosion protection of AISI 1018  
615 steel using Co – doped TiO<sub>2</sub>/polypyrrole nanocomposites in 3.5% NaCl solution.  
616 *Materials Chemistry and Physics.* **192:** 361 – 373.

617 Lampman, G.M., Pavia, D.L., Kriz, G.S. & Vyvyan, J.R. (2010). Spectroscopy. 4th Edition.  
618 Brooks/Cole Cengage Learning, Belmont, USA.

619 Lee, K.J., Elgrishi, N., Kandemir, B. & Dempsey, J.L. 2018. Electrochemical and spectroscopic  
620 methods for evaluating molecular electrocatalysts. *Nature Reviews Chemistry* 1(5): 1 -  
621 14.

622 Leykin, A., Shapovalov, L. & Figovsky, O. (2016). Non – isocyanate polyurethanes –  
623 Yesterday, today and tomorrow. *Alternative Energy and Ecology.* **191 (3 – 4):** 95 – 108.

624 Li, H., Yuan, D., Li, P., He, C. (2019). High conductive and mechanical robust carbon  
625 nanotubes/waterborne polyurethane composite films for efficient electromagnetic  
626 interference shielding. *Composites Part A.* 121: 411 – 417.

- 627 Nakthong, P., Kondo, T., Chailapakul, O., Siangproh, W. (2020). Development of an  
628 unmodified screen – printed graphene electrode for nonenzymatic histamine detection.  
629 *Analytical Methods*. 12: 5407 – 5414.
- 630 Mishra, K., Narayan, R., Raju, K.V.S.N. & Aminabhavi, T.M. (2012). Hyperbranched  
631 polyurethane (HBPU)-urea and HBPU-imide coatings: Effect of chain extender and  
632 NCO/OH ratio on their properties. *Progress in Organic Coatings*. 74: 134 – 141.
- 633 Mohd Noor, M. A., Tuan Ismail, T. N. M., Ghazali, R. (2020). Bio – based content of oligomers  
634 derived from palm oil: Sample combustion and liquid scintillation counting technique.  
635 *Malaysia Journal of Analytical Science*. 24: 906 – 917.
- 636 Mutsuhisa F., Ken, K. & Shohei, N. (2007). Microphase separated structure and mechanical  
637 properties of norbornane diisocyanate – based polyurethane. *Polymer*. 48 (4): 997 – 1004.
- 638 Mustapha, R., Rahmat, A. R., Abdul Majid, R., Mustapha, S. N. H. (2019). Vegetable oil –  
639 based epoxy resins and their composites with bio – based hardener: A short review.  
640 *Polymer- Plastic Technology and Materials*. 58: 1311 – 1326.
- 641 Nohra, B., Candy, L., Blancos, J.F., Guerin, C., Raoul, Y. & Mouloungui, Z. (2013). From  
642 petrochemical polyurethanes to biobased polyhydroxyurethanes. *Macromolecules*. 46  
643 (10): 3771 – 3792.
- 644 Pan, T. & Yu, Q. (2016). Anti – corrosion methods and materials comprehensive evaluation of  
645 anti – corrosion capacity of electroactive polyaniline for steels. *Anti – Corrosion Methods  
646 and Materials*. 63: 360 – 368.
- 647 Pan, X. & Webster, D.C. (2012). New biobased high functionality polyols and their use in  
648 polyurethane coatings. *ChemSusChem*. 5: 419-429.
- 649 Petrovic, Z.S. (2008). Polyurethanes from vegetable oils. *Polymer Reviews*. 48 (1): 109 – 155.

650 Porcarelli, L., Manojkumar, K., Sardon, H., Llorente, O., Shaplov, A. S., Vijayakrishna, K.,  
651 Gerbaldi, C., Mecerreyes, D. (2017). Single ion conducting polymer electrolytes based  
652 on versatile polyurethanes. *Electrochimica Acta*. 241: 526 – 534.

653 Priya, S. S., Karthika, M., Selvasekarapandian, S. & Manjuladevi, R. (2018). Preparation and  
654 characterization of polymer electrolyte based on biopolymer I-carrageenan with  
655 magnesium nitrate. *Solid State Ionics*. **327**: 136 – 149.

656 Ren, D. & Frazier, C.E. (2013). Structure–property behaviour of moisture-cure polyurethane  
657 wood adhesives: Influence of hard segment content. *Adhesion and Adhesives*. **45**: 118-  
658 124.

659 Rogulska, S.K., Kultys, A. & Podkoscielny, W. (2007). Studies on thermoplastic polyurethanes  
660 based on new diphenylethane – derivative diols. II. Synthesis and characterization of  
661 segmented polyurethanes from HDI and MDI. *European Polymer Journal*. **43**: 1402 –  
662 1414.

663 Romaskevicius, T., Budriene, S., Pielichowski, K. & Pielichowski, J. (2006). Application of  
664 polyurethane – based materials for immobilization of enzymes and cells: a review.  
665 *Chemija*. **17**: 74 – 89.

666 Sengodu, P. & Deshmukh, A. D. (2015). Conducting polymers and their inorganic composites  
667 for advanced Li-ion batteries: a review. *RSC Advances*. **5**: 42109 – 42130.

668 Septevani, A. A., Evans, D. A. C., Chaleat, C., Martin, D. J., Annamalai, P. K. (2015). A  
669 systematic study substituting polyether polyol with palm kernel oil based polyester  
670 polyol in rigid polyurethane foam. *Industrial Corps and Products*. 66: 16 – 26.

671 Su'ait, M. S., Ahmad, A., Badri, K. H., Mohamed, N. S., Rahman, M. Y. A., Ricardi, C. L. A.  
672 & Scardi, P. The potential of polyurethane bio – based solid polymer electrolyte for  
673 photoelectrochemical cell application. *International Journal of Hydrogen Energy*. 39 (6):  
674 3005 – 3017.

675 Tadesse, M. G., Mengistie, D. A., Chen, Y., Wang, L., Loghin, C., Nierstrasz, V. (2019).  
676 Electrically conductive highly elastic polyamide/lycra fabric treated with PEDOT: PSS  
677 and polyurethane. *Journal of Materials Science*. 54: 9591 – 9602.

678 Tajau, R., R, Rosiah, Alias, M. S., Mudri, N. H., Halim, K. A. A., Harun, M. H., Isa, N. M.,  
679 Ismail, R. C., Faisal, S. M., Talib, M., Zin, M. R. M., Yusoff, I. I., Zaman, N. K., Illias,  
680 I. A. (2021). Emergence of polymeric material utilising sustainable radiation curable  
681 palm oil – based products for advanced technology applications. *Polymers*. 13: 1865 –  
682 1886.

683 Tran, V.H., Kim, J.D., Kim, J.H., Kim, S.K., Lee, J.M. (2020). Influence of cellulose  
684 nanocrystal on the cryogenic mechanical behaviour and thermal conductivity of  
685 polyurethane composite. *Journal of Polymers and The Environment*. **28**: 1169 – 1179.

686 Viera, I.R.S., Costa, L.D.F.D.O., Miranda, G.D.S., Nardehcia, S., Monteiro, M.S.D. S.D.B.,  
687 Junior, E.R. & Delpech, M.C. (2020). Waterborne poly (urethane – urea)s  
688 nanocomposites reinforced with clay, reduced graphene oxide and respective hybrids:  
689 Synthesis, stability and structural characterization. *Journal of Polymers and The  
690 Environment*. **28**: 74 – 90.

691 Wang, B., Wang, L., Li, X., Liu, Y., Zhang, Z., Hedrick, E., Safe, S., Qiu, J., Lu, G. & Wang,  
692 S. (2018). Template – free fabrication of vertically – aligned polymer nanowire array on  
693 the flat – end tip for quantifying the single living cancer cells and nanosurface interaction.  
694 *a Manufacturing Letters*. **16**: 27 – 31.

695 Wang, J., Xiao, L., Du, X., Wang, J. & Ma, H. (2017). Polypyrrole composites with carbon  
696 materials for supercapacitors. *Chemical Papers*. **71** (2): 293 – 316.

697 Wong, C.S. & Badri, K.H. (2012). Chemical analyses of palm kernel oil – based polyurethane  
698 prepolymer. *Materials Sciences and Applications*. **3**: 78 – 86.

- 699 Wong, C. S., Badri, K., Ataollahi, N., Law, K., Su'ait, M. S., Hassan, N. I. (2014). Synthesis  
700 of new bio – based solid polymer electrolyte polyurethane – LiClO<sub>4</sub> via  
701 prepolymerization method: Effect of NCO/OH ratio on their chemical, thermal properties  
702 and ionic conductivity. *World Academy of Science, Engineering and Technology,*  
703 *International Journal of Chemical, Molecular, Nuclear, Materials and Metallurgical*  
704 *Engineering.* 8: 1243 – 1250.
- 705 Yong, Z., Bo, Z.M., Bo, W., Lin, J.Z. & Jun, N. (2009). Synthesis and properties of novel  
706 polyurethane acrylate containing 3-(2-Hydroxyethyl) isocyanurate segment. *Progress in*  
707 *Organic Coatings.* **67**: 264 – 268
- 708 Zia, K. M., Anjum, S., Zuber, M., Mujahid, M. & Jamil, T. (2014). Synthesis and molecular  
709 characterization of chitosan based polyurethane elastomers using aromatic diisocyanate.  
710 *International of Journal of Biological Macromolecules.* **66**: 26 – 32.

[← BACK](#) [DASHBOARD / ARTICLE DETAILS](#)

Updated on 2022-02-02

Version 4 ▾

# Design and Synthesis of Conducting Polymer Based on Polyurethane produced from Palm Kernel Oil

VIEWING AN OLDER VERSION

ID 6815187

Muhammad Abdurrahman Munir <sup>SA CA</sup> <sup>1</sup>,  
Khairiah Haji Badri<sup>1</sup>, Lee Yook Heng<sup>1</sup>  
[+ Show Affiliations](#)

## Article Type

Research Article

## Journal

International Journal of  
Polymer Science

Rydz Joanna

Submitted on 2021-06-14 (2 years ago)

[> Abstract](#)[> Author Declaration](#)[> Files](#) 3[- Editorial Comments](#)

Joanna Rydz

02.02.2022

**Decision**

Major Revision Requested

**Message for Author**

Dear Authors,

The reviewers have raised points that were not fully taken into consideration and revision of the manuscript before it is suitable for publication is still required.

The journal should follow certain standards, such as compliance with general recommendations (IUPAC, SI, manual for authors), so please review and correct manuscript again.

Comments have been entered into the manuscript as a track changes with comments and will be sent additionally.

We look forward to receiving your revised manuscript.

**— Response to Revision Request**

Muhammad Abdurrahman Munir

02.12.2021

**Your Reply**

Greetings, Dear Dr. Peter Foot, Thank you so much for your suggestions to the manuscript. For your information, we have followed your suggestion and ensured the manuscript has been followed the journal regulation. The file contains the revised manuscript and the answer for the reviewer. Please check the manuscript and inform us if there is any revision that should be made. We hope this study can be published in this journal. Best Regards.

**File**

Manuscript - Munir.docx 873 kB







25 cyclic voltammetry (CV). Cyclic voltammetry was employed to study electro-catalytic  
26 properties of SPE-Polyurethane towards oxidation of PU. Remarkably, SPE-PU exhibited  
27 improved anodic peak current as compared to SPE itself using the differential pulse  
28 voltammetry (DPV) method. Furthermore, the formation of urethane linkages (NHCO  
29 backbone) after polymerization was analysed using FTIR and confirmed by the absence of  
30 N=C=O peak at  $2241\text{ cm}^{-1}$ . The glass transition temperature ( $T_g$ ) of the polyurethane was  
31 detected at  $78.1^\circ\text{C}$ .

32

33 **Keywords:** Polyurethane, polymerization, screen-printed electrode, voltammetry

34

35

## 36 1. Introduction

37 Polymers are molecules composed of many repeated sub-units referred to as monomers  
38 (Sengodu & Deshmukh 2015). Conducting polymers (CPs) are polymers that exhibit electrical  
39 behavior (Alqarni et al. 2020). The conductivity of CPs was first observed in polyacetylene,  
40 nevertheless owing to its instability led to the discovery of other forms of CPs such as  
41 polyaniline (PANI), poly (o-toluidine) (PoT), polythiophene (PTh), polyfluorene (PF) and  
42 polyurethane (PU). Furthermore, natural CPs have low conductivity and are often semi-  
43 conductive. Therefore, it is essential to increase their conductivity mainly for use in  
44 electrochemical sensor programs (Dzulkipli et al. 2021; Wang et al. 2018). Conducting  
45 polymers (CPs) represent a sizeable range of useful organic substances. Their unique electrical,  
46 chemical and physical properties; reasonable price; simple preparation; small dimensions and  
47 large surface area have enabled researchers to discover a wide variety of uses such as sensors,  
48 biochemical applications, solar cells and electrochromic devices (Alqarni et al. 2020; Ghosh et  
49 al. 2018). There are scientific documentation on the use of conductive polymers in various

50 studies such as polyaniline (Pan & Yu 2016), polypyrrole (Ladan et al. 2017) and polyurethane  
51 (Tran et al. 2020; Vieira et al. 2020; Guo et al. 2020; Fei et al. 2020).

52

53 The application of petroleum as polyol in order to produce polyurethane has been applied. Coal  
54 and crude oil were used as raw materials to produce it. Nevertheless, these materials have  
55 become very rare to find and the price is very expensive at the same time required a  
56 sophisticated system to produce it. These reasons have been considered and finding utilizing  
57 plants that can be used as alternative polyols should be done immediately (Badri 2012).  
58 Furthermore, in order to avoid the application of petroleum as raw material for a polyol,  
59 vegetable oils become a better choice as polyol in order to obtain a biodegradable polyol.  
60 Vegetable oils that are generally used for synthesis polyurethane are soybean oil, corn oil,  
61 sunflower seed oil, coconut oil, nuts oil, rapeseed, olive oil and palm oil (Badri 2012; Borowicz  
62 et al. 2019).

63

64 It is very straightforward for vegetable oils to react with a specific group in order to form PU  
65 such as epoxy, hydroxyl, carboxyl and acrylate owing to the existence of (-C=C-) in vegetable  
66 oils. Thus, it has provided appealing profits to vegetable oils compared to petroleum considered  
67 the toxicity, price and harm to the environment (Mustapha et al. 2019; Mohd Noor et al. 2020).  
68 Palm oil becomes the chosen in this study to produce PU owing to it is largely cultivated in  
69 South Asia particularly in Malaysia and Indonesia. It has several profits compared to other  
70 vegetable oils such as the easiest materials obtained, the lowest cost of all the common  
71 vegetable oils and recognized as the plantation that has a low environmental impact and  
72 removing CO<sub>2</sub> from the atmosphere as net sequester (Tajau et al. 2021; Septevani et al. 2015).  
73 Biopolymer, a natural biodegradable polymer has attracted much attention in recent years.  
74 Global environmental awareness and fossil fuel depletion urged researchers to work in the

75 biopolymer field (Priya et al. 2018). Polyurethane is one of the most common, versatile and  
76 researched materials in the world. These materials combine the durability and toughness of  
77 metals with the elasticity of rubber, making them suitable to replace metals, plastics and rubber  
78 in several engineered products. They have been widely applied in biomedical applications,  
79 building and construction applications, automotive, textiles and in several other industries due  
80 to their superior properties in terms of hardness, elongation, strength and modulus (Zia et al.  
81 2014; Romaskevicius et al. 2006). Polyurethanes are also considered to be one of the most useful  
82 materials with many profits such as, possess low conductivity, low density, absorption  
83 capability and dimensional stability. They are clearly a great research subject owing to their  
84 mechanical, physical and chemical properties (Badan & Majka 2017).

85

86 The urethane group is the major repeating unit in PUs and is produced from the reaction  
87 between alcohol (-OH) and isocyanate (NCO); albeit polyurethanes also contain other groups  
88 such as ethers, esters, urea and some aromatic compounds. Due to the wide variety of sources  
89 from which PUs can be synthesized, thus a wide range of specific applications can be generated.  
90 They are grouped into several different classes based on the desired properties: rigid, flexible,  
91 thermoplastic, waterborne, binders, coating, adhesives, sealants and elastomers (Akindoyo et  
92 al. 2016).

93

94 Although, PU has low conductivity, it is lighter than other materials such as metals. The  
95 hardness of PU also relies on the number of the aromatic rings in the polymer structure  
96 (Janpoung et al, 2020; Su'ait et al. 2014), majorly contributed by the isocyanate derivatives.  
97 PU has also a conjugate structure where electrons can move in the main chain that causing  
98 electricity produced even the conductivity is low. The electrical conductivity of conjugated  
99 linear ( $\pi$ ) can be explained by the distance between the highest energy level containing

100 electrons (HOMO) called valence band and the lowest energy level not containing electrons  
101 (LUMO) called the conduction band (Wang et al. 2017; Kotal et al. 2011).

102

103 In the recent past, several conventional methods have been developed such as capillary  
104 electrophoresis, liquid and gas chromatography coupled with several detectors. Nevertheless,  
105 although chromatographic and spectrometric approaches are well developed for qualitative and  
106 quantitative analyses of analytes, several limitations emerged such as complicated  
107 instrumentation, expensive, tedious sample preparations and requiring large amounts of  
108 expensive solvents that will harm the users and environment (Kilele et al. 2020). Therefore, is  
109 is imperative to obtain and develop an alternative material that can be used to analyse a specific  
110 analyte. Electrochemical methods are extremely promising methods in the determination of an  
111 analyte in samples owing to the high selectivities, sensitivities, inexpensive, requirements of  
112 small amounts of solvents and can be operated by people who have no background in analytical  
113 chemistry. In addition, the sample preparation such as separation and extraction steps are not  
114 needed owing to the selectivity of this instrument where no obvious interference on the current  
115 response recorded (Chokkareddy et al. 2020). Few works have been reported on the  
116 electrochemical methods for the determination of analyte using electrode combined with  
117 several electrode modifiers such as carbon nanotube, gold and graphene (Chokkareddy et al.  
118 2020; Kilele et al. 2021). Nevertheless, the materials are costly and the modification procedures  
119 are not straightforward. Thus, an electrochemical approach using inexpensive and easily  
120 available materials as electrode modifiers should be developed (Degefu et al. 2014).

121

122 Nowadays, screen-printed electrodes (SPEs) modified with conducting polymer have been  
123 developed for various electrochemical sensing. SPE becomes the best solution owing to its  
124 frugal manufacture, tiny size, able to produce on large-scale and can be applied for on-site

125 detection (Nakthong et al. 2020). Conducting polymers (CPs) become an alternative to  
126 modifying the screen-printed electrodes due to their electrical conductivity, able to capture  
127 analyte by chemical/physical adsorption, large surface area and making CPs are very appealing  
128 materials from electrochemical perspectives (Baig et al. 2019). Such advantages of SPE  
129 encourage us to construct a new electrode for electrochemical sensing, and no research reported  
130 on the direct electrochemical oxidation of histamine using screen-printed electrode modified  
131 by polyurethane. Therefore, this research is the first to develop a new electrode using (screen  
132 printed polyurethane electrode) SPPE without any conducting materials.

133

134 The purpose of this work was to synthesize, characterize and study the conductivity of  
135 polyurethane using cyclic voltammetry (CV) and differential pulse voltammetry (DPV)  
136 attached to screen-printed electrode (SPE). To the best of our knowledge, this is the first  
137 attempt to use a modified polyurethane electrode. The electrochemistry of polyurethane  
138 mounted onto screen-printed electrode (SPE) is discussed in detail. Polyurethane is possible to  
139 become an advanced frontier material is chemically modified electrodes for bio/chemical  
140 sensing application.

141

## 142 **2. Experimental**

### 143 **2.1 Chemicals**

144 ***Synthesis of polyurethane film:*** Palm kernel oil (PKOp) supplied by UKM Technology Sdn  
145 Bhd through MPOB/UKM station plant, Pekan Bangi Lama, Selangor and prepared using  
146 Badri et al. (2000) method. 4, 4-diphenylmethane diisocyanate (MDI) was acquired from  
147 Cosmopolyurethane (M) Sdn. Bhd., Klang, Malaysia. Solvents and analytical reagents were  
148 benzene ( $\geq 99.8\%$ ), toluene ( $\geq 99.8\%$ ), hexane ( $\geq 99\%$ ), acetone ( $\geq 99\%$ ), tetrahydrofuran  
149 (THF), dimethylformamide (DMF) ( $\geq 99.8\%$ ), dimethylsulfoxide (DMSO) ( $\geq 99.9\%$ ) and

150 polyethylene glycol (PED) with a molecular weight of 400 Da obtained from Sigma Aldrich  
151 Sdn Bhd, Shah Alam.

152

## 153 **2.2 Apparatus**

154 Tensile testing was performed using a universal testing machine model Instron 5566 following  
155 ASTM 638 (Standard Test Method for Tensile Properties of Plastics). The tensile properties of  
156 the polyurethane film were measured at a velocity of 10 mm/min with a cell load of 5 kN.

157 The thermal properties were performed using thermogravimetry analysis (TGA) and  
158 differential scanning calorimetry (DSC) analysis. TGA was performed using a thermal analyzer  
159 of Perkin Elmer Pyris model with a heating rate of 10 °C/minute at a temperature range of 30  
160 to 800 °C under a nitrogen gas atmosphere. The DSC analysis was performed using a thermal  
161 analyzer of Perkin Elmer Pyris model with a heating rate of 10 °C /minute at a temperature  
162 range of -100 to 200 °C under a nitrogen gas atmosphere. Approximately, 5-10 mg of PU was  
163 weighed. The sample was heated from 25 to 150 °C for one minute, then cooled immediately  
164 from 150 -100 °C for another one minute and finally, reheated to 200 °C at a rate of 10 °C /min.  
165 At this point, the polyurethane encounters changes from elastic properties to brittle due to  
166 changes in the movement of the polymer chains. Therefore, the temperature in the middle of  
167 the inclined regions is taken as the glass transition temperature ( $T_g$ ). The melting temperature  
168 ( $T_m$ ) is identified as the maximum endothermic peak by taking the area below the peak as the  
169 enthalpy point ( $\Delta H_m$ ).

170

171 The morphological analysis of PU film was performed by Field Emission Scanning Electron  
172 Microscope (FESEM) model Gemini SEM microscope model 500-70-22. Before the analysis  
173 was carried out, the polyurethane film was coated with a thin layer of gold to increase the  
174 conductivity of the film. The coating method was carried out using a sputter-coater. The

175 observations were conducted at a magnification of 200× and 5000 × with 10.00 kV (Electron  
176 high tension - EHT).

177

178 The crosslinking of PU was determined using the soxhlet extraction method. About 0.60 g of  
179 PU sample was weighed and put in an extractor tube containing 250 ml of toluene, used as a  
180 solvent. This flow of toluene was let running for 24 hours. Mass of the PU was weighed before  
181 and after the reflux process was carried out. Then, the sample was dried in the conventional  
182 oven at 100 °C for 24 hours in order to get a constant mass. The percentage of crosslinking  
183 content known as the gel content can be calculated using Equation (1).

$$184 \quad \text{Gel content (\%)} = \frac{W_0 - W}{W} \times 100 \% \quad (1)$$

185  $W_0$  is the mass of PU before the reflux process (g) and  $W$  is the mass of PU after the reflux  
186 process (g).

187

188 FTIR spectroscopic analysis was performed using a Perkin-Elmer Spectrum BX instrument  
189 using the Diamond Attenuation Total Reflectance (DATR) method to confirm the  
190 polyurethane, PKOp and MDI functional group. FTIR spectroscopic analysis was performed  
191 at a wave number of 4000 to 600  $\text{cm}^{-1}$  to identify the peaks of the major functional groups in  
192 the formation of the polymer such as amide group (-NH), urethane carbonyl group (-C = O)  
193 and carbamate group (-CN).

194

### 195 **2.3 Synthesis of Polyurethane**

196 Palm kernel oil (PKO)p and polyethylene glycol (PEG) 400 (100:40 g/g) were combined and  
197 dissolved by acetone 30% in order to form a polyol prepolymer solution. The mixture was  
198 mixed using centrifuge with 100 rpm for 5 min to acquire a homogenized solution. Whereas,  
199 diisocyanate prepolymer was obtained by mixing 4,4'-diphenyl-methane diisocyanate (MDI)  
200 (100 g) to acetone 30%, afterward the mixture was mixed using centrifuge for 1 min to obtain



201 a homogenized solution. Then, 10 g of diisocyanate solution was poured into a container that  
202 containing 10 g of a polyol prepolymer solution slowly in order to avoid an exothermic reaction  
203 occur. The mixture was mixed for 30 sec until a homogenized solution acquired. Lastly, the  
204 polyurethane solution was poured on the electrode surface by using casting method and dried  
205 at ambient temperature for 12 hours.

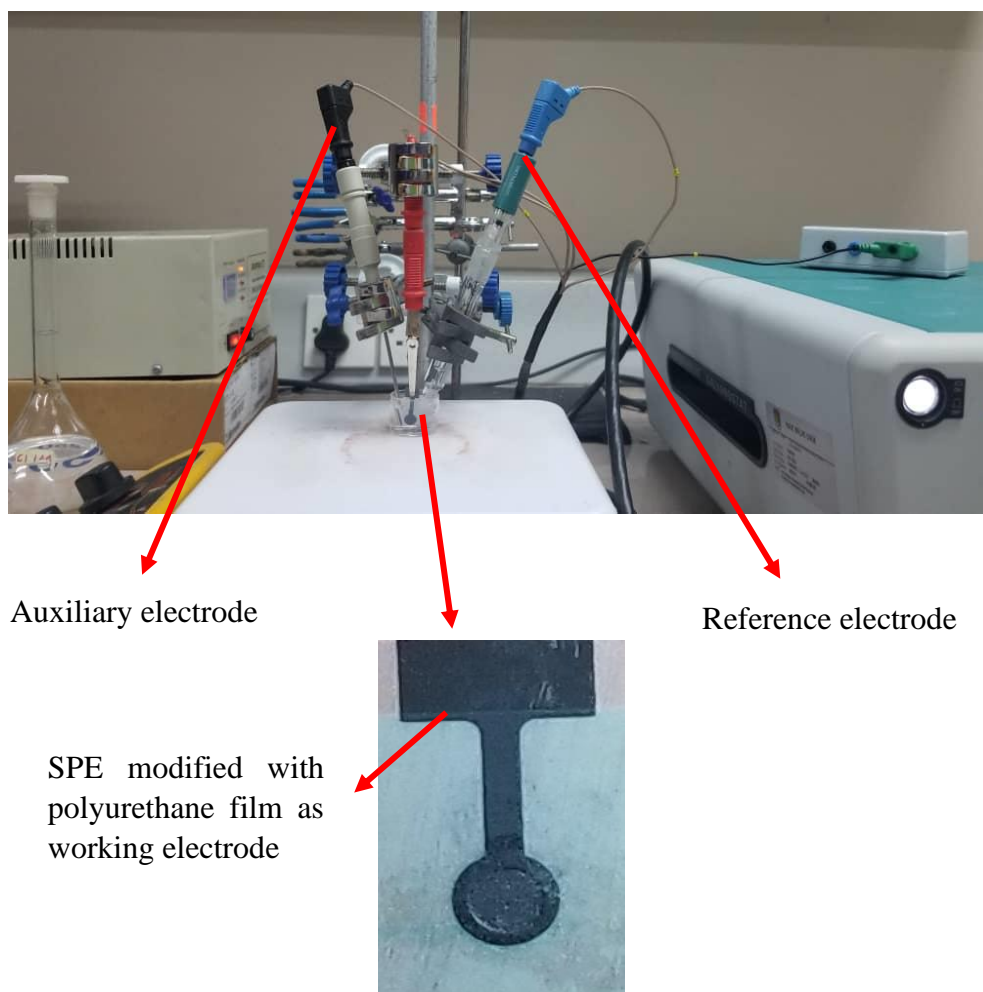
206

#### 207 **2.4 Modification of Electrode**

208 Voltammetric tests were performed using Metrohm Autolab Software (**Figure 1**) analyzer  
209 using cyclic voltammetry (CV) method or known as amperometric mode and differential pulse  
210 voltammetry (DPV). All electrochemical experiments were carried out using screen-printed  
211 electrode (diameter 3 mm) modified using polyurethane film as working electrode, platinum  
212 wire as auxiliary electrode and Ag/AgCl electrode as a reference electrode. All experiments  
213 were conducted at a temperature of  $20 \pm 2^\circ\text{C}$ .

214

215 The PU was cast onto the screen – printed electrode (SPE + PU) and analyzed using a single  
216 voltammetric cycle between -1200 and +1500 mV (vs Ag/AgCl) of ten cycles at a scanning  
217 rate of 100 mV/s in 5 ml of KCl in order to study the activity of SPE and polyurethane film.  
218 Approximately (0.1, 0.3 & 0.5) mg of palm-based prepolyurethane was dropped separately  
219 onto the surface of the SPE and dried at room temperature. The modified palm-based  
220 polyurethane electrodes were then rinsed with deionized water to remove physically adsorbed  
221 impurities and residues of unreacted material on the electrode surface. All electrochemical  
222 materials and calibration measurements were carried out in a 5 mL glass beaker with a  
223 configuration of three electrodes inside it. Platinum wire and silver/silver chloride (Ag/AgCl)  
224 electrodes were used as auxiliary and reference electrodes, while screen-printed electrode that  
225 had been modified with polyurethane was applied as a working electrode.



226 **Figure 1.** Potentiostat instrument to study the conductivity of SPE modified with  
 227 polyurethane film using cyclic voltammetry (CV) and differential pulse voltammetry (DPV)

228

### 229 3. Results and Discussion

230 The synthesis of PU films was carried out using pre-polymerization method which involves  
 231 the formation of urethane polymer at an early stage. The reaction took place between palm  
 232 kernel oil-based polyol (PKOp) and diisocyanate (MDI). **Table 1** presents the PKO-p  
 233 properties used in this study. The structural chain was extended with the aid of polyethylene  
 234 glycol (PEG) to form flexible and elastic polyurethane film. In order to form the urethane  
 235 prepolymer, one of the isocyanate groups (NCO) reacts with one hydroxyl group (OH) of  
 236 polyol while the other isocyanate group attacks another hydroxyl group in the polyol (Wong &  
 237 Badri 2012) as shown in **Figure 2**.

238 **Table 1** The specification of PKO-p (Badri et al. (2000)).

Property	Values
Viscosity at 25°C (cps)	1313.3
Specific gravity (g/mL)	1.114
Moisture content (%)	0.09
pH value	10 – 11
The hydroxyl number mg KOH/g	450 - 470

239

240

241 a. FTIR analysis

242 **Figure 3** shows the FTIR spectrum for polyurethane, exhibiting the important functional group  
 243 peaks. According to a study researched by Wong & Badri 2012, PKO-p reacts with MDI to  
 244 form urethane prepolymers. The NCO group on MDI reacts with the OH group on polyol  
 245 whether PKOp or PEG. It can be seen there are no important peaks of MDI in the FTIR  
 246 spectrums. This is further verified by the absence of peak at the  $2400\text{ cm}^{-1}$  belongs to MDI (-  
 247 NCO groups). This could also confirm that the NCO group on MDI had completely reacted  
 248 with PKO-p to form the urethane -NHC (O) backbone. The presence of amides (-NH),  
 249 carbonyl urethane group (-C = O), carbamate group (C-NH) and -C-O-C confirmed the  
 250 formation of urethane chains. In this study, the peak of carbonyl urethane (C = O) detected at  
 251  $1727\text{ cm}^{-1}$  indicated that the carbonyl urethane group was bonded without hydrogen owing to  
 252 the hydrogen reacted with the carbonyl urethane group.

253

254 The reaction of polyurethane has been studied by Hamuzan & Badri (2016) where the urethane  
 255 carbonyl group was detected at  $1730 - 1735\text{ cm}^{-1}$  while the MDI carbonyl was detected at  $2400$   
 256  $\text{cm}^{-1}$ . The absence of peaks at  $2250 - 2270\text{ cm}^{-1}$  indicates the absence of NCO groups. It shows

257 that the polymerization reaction occurs entirely between NCO groups in MDI with hydroxyl  
258 groups on polyols and PEG (Mishra et al. 2012). The absence of peaks at  $1690\text{ cm}^{-1}$   
259 representing urea ( $\text{C} = \text{O}$ ) in this study indicated, there is no urea formation as a byproduct  
260 (Clemitson 2008) of the polymerization reaction that possibly occurs due to the excessive  
261 water. For the amine (NH) group, hydrogen-bond to NH and oxygen to form ether and  
262 hydrogen bond to NH and oxygen to form carbonyl on urethane can be detected at the peak of  
263  $3301\text{ cm}^{-1}$  and in the wavenumber at range  $3326 - 3428\text{ cm}^{-1}$ . This has also been studied and  
264 detected by Lampman et. al. (2010) and Mutsuhisa et al. (2007). In this study, the hydrogen  
265 bond formed by  $\text{C} = \text{O}$  acts as a proton acceptor whereas NH acts as a proton donor. The  
266 urethane group in the hard segment (MDI) has electrostatic forces on the oxygen, hydrogen  
267 and nitrogen atoms and these charged atoms form dipoles that attract other opposite atoms.  
268 These properties make isocyanates are highly reactive and having different properties (Leykin  
269 et al. 2016).

270

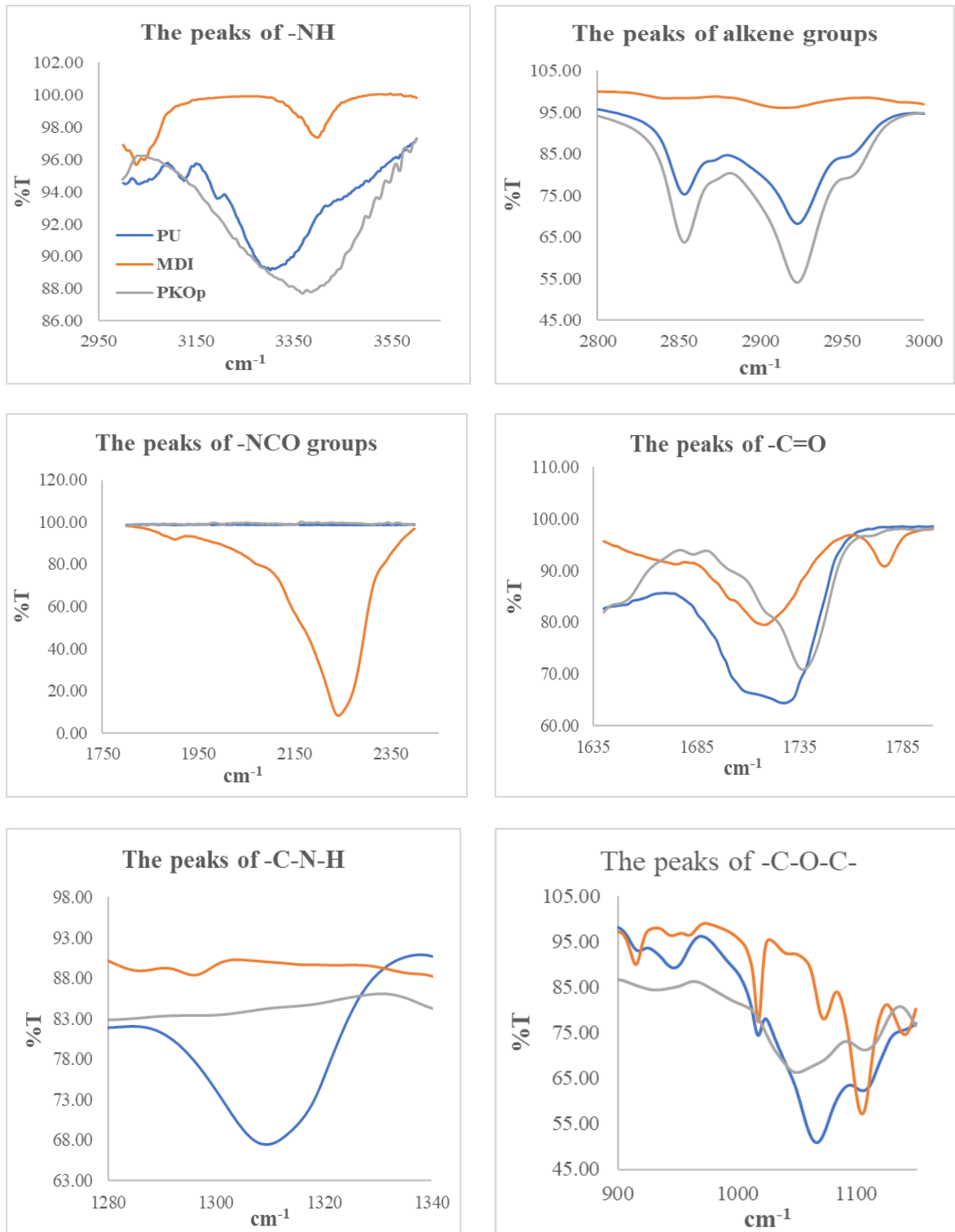
271 MDI was one of the isocyanates used in this study, has an aromatic group and is more  
272 reactive compared to aliphatic group isocyanates such as hexamethylene diisocyanate (HDI)  
273 or isophorone diisocyanate (IPDI). Isocyanates have two groups of isocyanates on each  
274 molecule. Diphenylmethane diisocyanate is an exception owing to its structure consists of two,  
275 three, four or more isocyanate groups (Nohra et al. 2013). The use of PEG 400 in this study as  
276 a chain extender for polyurethane increases the chain mobility of polyurethane at an optimal  
277 amount. The properties of a polyurethane are contributed by hard and soft copolymer segments  
278 of both polyol monomers and MDI. This makes the hard segment of urethane serves as a  
279 crosslinking site between the soft segments of the polyol (Leykin et al. 2016).

280



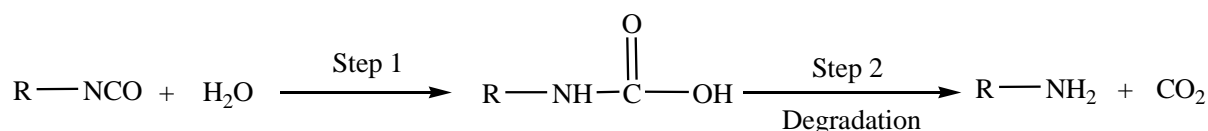
296 dimensional networks with high molecular weight. In some aspects, polyurethane can be a  
297 macromolecule, a giant molecule (Petrovic 2008).

298



299 **Figure 3.** FTIR spectrums of several important peaks between polyurethane, PKO-p and MDI

300 However, the reaction between MDI and PEG as a chain extender where oxygen on the  
 301 nucleophile PEG attacks the NCO group in the MDI to form two intermediate complexes A  
 302 and B can occur. Nevertheless, nucleophilic substitution reactions have a greater tendency to  
 303 occur in PKOp compared to PEG because the presence of nitrogen atoms is more  
 304 electropositive than oxygen atoms in PEG. Amine has a higher probability of reacting  
 305 compared to hydroxyl (Herrington & Hock 1997). Amine with high alkalinity reacts with  
 306 carbon atoms on MDI as proposed by Wong and Badri (2012). PKOp contains long carbon  
 307 chains that can easily stabilize alkyl ions when intermediate complexes are formed. Therefore,  
 308 the polyol is more reactive than PEG to react with MDI. However, the addition of PEG will  
 309 increase the length of the polyurethane chain and prevent side effects such as the formation of  
 310 urea by-products of the NCO group reaction in urethane pre-polymer and water molecules from  
 311 the environment. If the NCO group reacts with the excess water in the environment, the  
 312 formation of urea and carbon dioxide gas will also occur excessively (**Figure 4**). This reaction  
 313 can cause a polyurethane foam, not polyurethane film as we studied the film.



314  
 315 **Figure 4.** The reaction between NCO group and water producing carbon dioxide  
 316

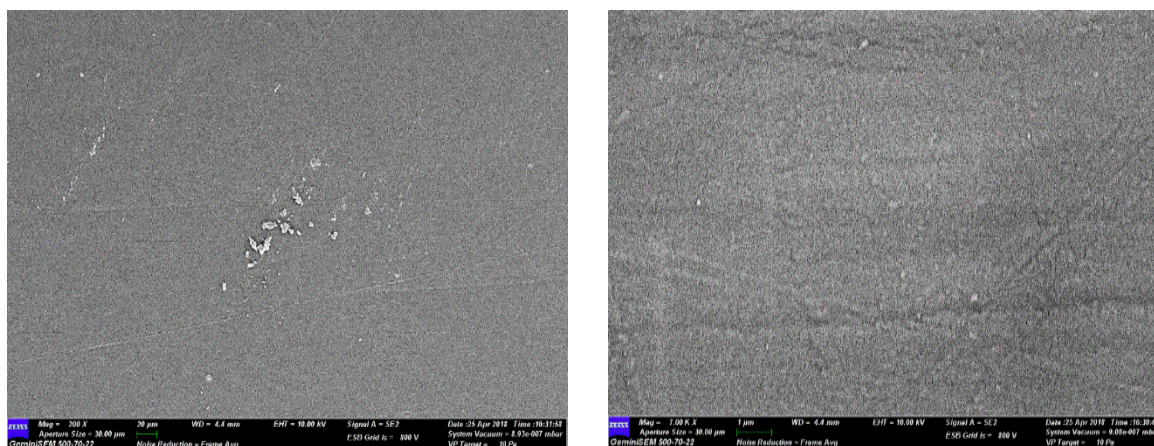
317 Furthermore, the application of PEG can influence the conductivity of PU where  
 318 Porcarelli et al. (2017) have reported the application of PEG using several molecular weights.  
 319 PEG 1500 decreased the conductivity of PU in consequence of the semicrystalline phase of  
 320 PEG 1500 that acted as a poor ion conducting phase for PU. It is also well known that PEG  
 321 with a molecular weight of more than 1000 g·mol<sup>-1</sup> tends to crystallize with deleterious effects  
 322 on room temperature ionic conductivity (Porcarelli et al. 2017).

323

324 b. Morphological analysis

325 The Field Emission Scanning Electron Microscope (FESEM) micrograph in **Figure 5** shows  
326 the formation of a uniform polymer film contributed by the polymerization method applied.  
327 The magnification used for this surface analysis ranged from 200 to 5000  $\times$ . The  
328 polymerization method can also avoid the failure of the reaction in PU polymerization.  
329 Furthermore, no trace of separation was detected by FESEM. This has also been justified by  
330 the wavelengths obtained by the FTIR spectrums above.

331



332 **Figure 5.** The micrograph of polyurethane films analysed by FESEM at (a) 200  $\times$  and (b)  
333 5000 $\times$  magnifications.

334 c. The crosslinking analysis

336 Soxhlet analysis was applied to determine the degree of crosslinking between the hard  
337 segments and the soft segments in the polyurethane. The urethane group on the hard segment  
338 along the polyurethane chain is polar (Cuve & Pascault 1991). Therefore, during the testing, it  
339 was very difficult to dissolve in toluene, as the testing reagent. The degree of crosslinking is  
340 determined by the percentage of the gel content. The analysis result obtained from the Soxhlet  
341 testing indicating a 99.3 % gel content. This is significant in getting a stable polymer at higher  
342 working temperature (Rogulska et al. 2007).

343



$$\text{Gel content (\%)} = \frac{(0.6 - 0.301) \text{ g}}{0.301 \text{ g}} \times 100\% = 99.33\%$$

344

345

346 d. The thermal analysis

347 Thermogravimetric analysis (TGA) can be used to observe the material mass based on

348 temperature shift. It can also examine and estimate the thermal stability and materials

349 properties such as the alteration weight owing to absorption or desorption, decomposition,

350 reduction and oxidation. The material composition of polymer is specified by analysing the

351 temperatures and the heights of the individual mass steps (Alamawi et al. 2019). **Figure 6**

352 shows the TGA and DTG thermograms of polyurethane. The percentage weight loss (%) is

353 listed in **Table 2**. Generally, only a small amount of weight was observed. It is shown in **Figure**

354 **6** in the region of 45 – 180°C. This is due to the presence of condensation on moisture and

355 solvent residues.

356

357 **Table2** Weight loss percentage of (wt%) polyurethane film

Sample	% Weight loss (wt%)				Total of weight loss (%)	Residue after 550°C (%)
	T <sub>max</sub> , °C	T <sub>d1</sub> , 200 – 290°C	T <sub>d2</sub> , 350 – 500°C	T <sub>d3</sub> , 500 – 550°C		
Polyurethane	240	8.04	39.29	34.37	81.7	18.3

358

359 The bio polyurethane is thermally stable up to 240 °C before it has undergone thermal

360 degradation (Agrawal et al. 2017). The first stage of thermal degradation (T<sub>d1</sub>) on polyurethane

361 films was shown in the region of 200 – 290 °C as shown in **Figure 6**. The T<sub>d1</sub> is associated with

362 degradation of the hard segments of the urethane bond, forming alcohol or degradation of the

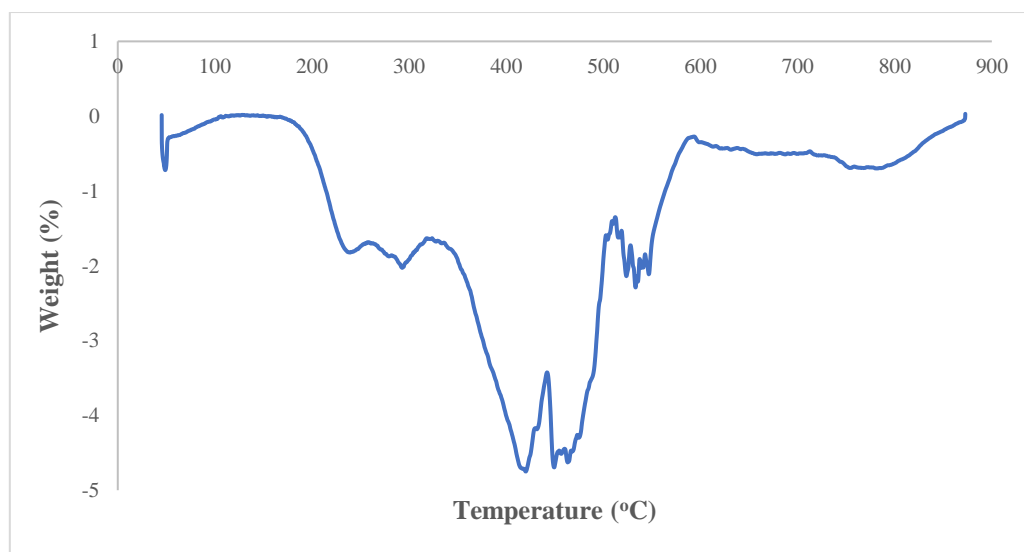
363 polyol chains and releasing of isocyanates (Berta et al. 2006), primary and secondary amines

364 as well as carbon dioxide (Corcuera et al. 2011; Pan & Webster 2012). Meanwhile, the second

365 thermal degradation stage ( $T_{d2}$ ) of polyurethane films experienced a weight loss of 39.29 %.  
366 This endotherm of  $T_{d2}$  is related to the dimerization of isocyanates to form carbodiimides and  
367 release  $CO_2$ . The formed carbodiimide reacts with alcohol to form urea. The third stage of  
368 thermal degradation ( $T_{d3}$ ) is related to the degradation of urea (Berta et al. 2006) and the soft  
369 segment on polyurethane.

370

371 Generally, DSC analysis exhibited thermal transitions as well as the initial  
372 crystallisation and melting temperatures of the polyurethane (Khairuddin et al. 2018). It serves  
373 to analyse changes in thermal behavior due to changes occurring in the chemical chain structure  
374 based on the glass transition temperature ( $T_g$ ) of the sample obtained from the DSC thermogram  
375 (Figure 7). DSC analysis on polyurethane film was performed in the temperature at the range  
376 100 °C to 200 °C using nitrogen gas as a blanket as proposed by Furtwengler et al. (2017). The  
377 glass transition temperature ( $T_g$ ) on polyurethane was above room temperature, at 78.1 °C  
378 indicated the state of glass on polyurethane. The presence of MDI contributes to the formation  
379 of hard segments in polyurethanes. Porcarelli et al. (2017) stated that possess a low glass  
380 transition ( $T_g$ ) may contribute to PU conductivity.

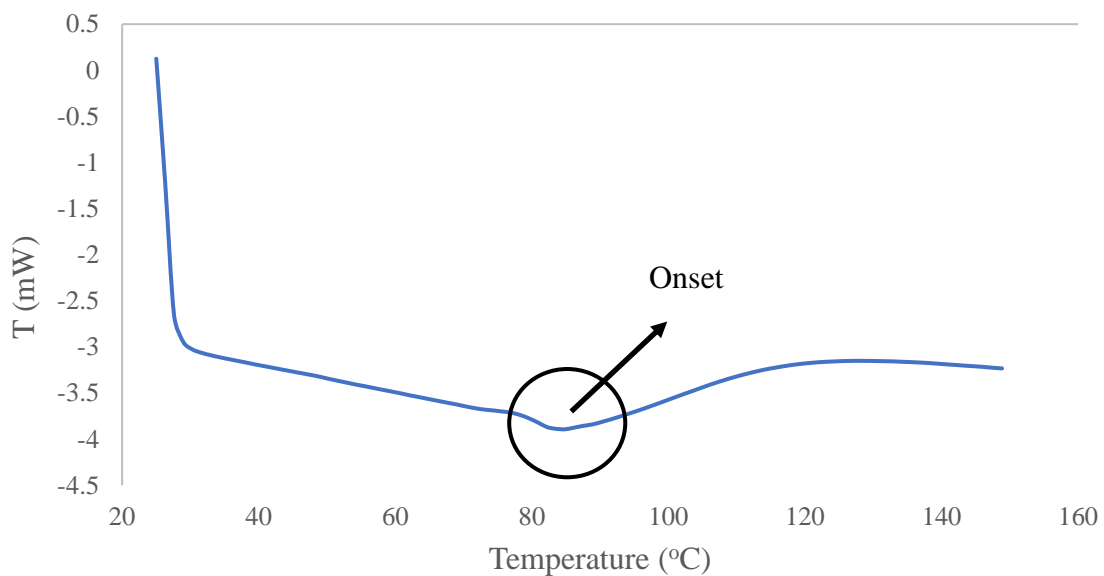


381

382

**Figure 6.** DTG thermogram of polyurethane film

383 During polymerization, this hard segment restricts the mobility of the polymer chain  
384 (Ren et al. 2013) owing to the steric effect on the benzene ring in the hard segment. The  
385 endothermic peak of acetone used as the solvent in this study was supposedly at 56°C.  
386 However, it was detected in the DSC thermogram nor the TGA thermogram, which indicates  
387 that acetone was removed from the polyurethane during the synthesis process, owing to its  
388 volatility nature. The presence of acetone in the synthesis was to lower the reaction kinetics.



389 **Figure 7.** DSC thermogram of polyurethane film

390  
391  
392  
393 e. The solubility and mechanical properties of the polyurethane film

394 The chemical resistivity of a polymer will be the determinant in performing as a conductor.  
395 Thus, its solubility in various solvents was determined by dissolving the polymer in selected  
396 solvents such as hexane, benzene, acetone, tetrahydrofuran (THF), dimethylformamide (DMF)  
397 and dimethylformamide (DMSO). On the other hand, the mechanical properties of of  
398 polyurethane were determined based on the standard testing following ASTM D 638 (Standard  
399 Test Method for Tensile Properties of Plastics). The results from the polyurethane film  
400 solubility and tensile test are shown in **Table 3**. Polyurethane films were insoluble with

401 benzene, hexane and acetone and are only slightly soluble in tetrahydrofuran (THF),  
 402 dimethylformamide (DMF) and dimethylformamide (DMSO) solutions. While the tensile  
 403 strength of a PU film indicated how much elongation load the film was capable of withstanding  
 404 the material before breaking.

405

406 **Table 3** The solubility and mechanical properties of the polyurethane film

407

Parameters	Polyurethane film
Solubility	
Benzene	Insoluble
Hexane	Insoluble
Acetone	Insoluble
THF	Less soluble
DMF	Less soluble
DMSO	Less soluble
Stress (MPa)	8.53
Elongation percentage (%)	43.34
Strain modulus (100) (MPa)	222.10

408

409 The tensile stress, strain and modulus of polyurethane film also indicated that polyurethane has  
 410 good mechanical properties that are capable of being a supporting substrate for the next stage  
 411 of study. In the production of polyurethane, the properties of a polyurethane are easily  
 412 influenced by the content of MDI and polyol used. The length of the chain and its flexibility  
 413 are contributed by the polyol which makes it elastic. High crosslinking content can also produce  
 414 hard and rigid polymers. MDI is a major component in the formation of hard segments in  
 415 polyurethane. It is this hard segment that determines the rigidity of the PU. Therefore, high

416 isocyanate content results in higher rigidity on PU (Petrovic et al. 2002). Thus, the polymer has  
417 a higher resistance to deformation and more stress can be applied to the PU.

418

419 f. The conductivity of the polyurethane as a polymeric film on SPE

420 Polyurethane film deposited onto the screen-printed electrode by casting method as shown in

421 **Figure 1**. After that, the modified electrode was analysed using cyclic voltammetry (CV) and

422 differential pulse voltammetry (DPV) in order to study the behaviour of modified electrode.

423 The modified electrode was tested in a 0.1 mmol/L KCl solution containing 5 mmol/L ( $K_3Fe$

424  $(CN)_6$ ). The use of potassium ferricyanide is intended to increase the sensitivity of the KCl

425 solution. The conductivity of the modified electrode was studied. The electrode was analyzed

426 by cyclic voltammetry method with a potential range of -1.00 to +1.00 with a scan rate of 0.05

427 V/s. The voltammograms at electrode have shown a specific redox reaction. Furthermore, the

428 conductivity of the modified electrode is lower due to the use of polyurethane. This occurs due

429 to PU is a natural polymer produced from the polyol of palm kernel oil. The electrochemical

430 signal at the electrode is low if there is a decrease in electrochemical conductivity (El - Raheem

431 et al. 2020). It can be concluded that polyurethane is a bio-polymer with a low conductivity

432 value. The current of the modified electrode was found at  $5.3 \times 10^{-5}$  A or 53  $\mu$ A. Nevertheless,

433 the electroconductivity of PU in this study shows better conductivity several times compared

434 to Bahrami et al. (2019) that reported the conductivity of PU as  $1.26 \times 10^{-6}$  A, whereas Li et al.

435 (2019) reported the PU conductivity in their study was even very low, namely  $10^{-14}$  A. The

436 conductivity of PU owing to the benzene ring in the hard segment (MDI) could exhibit the

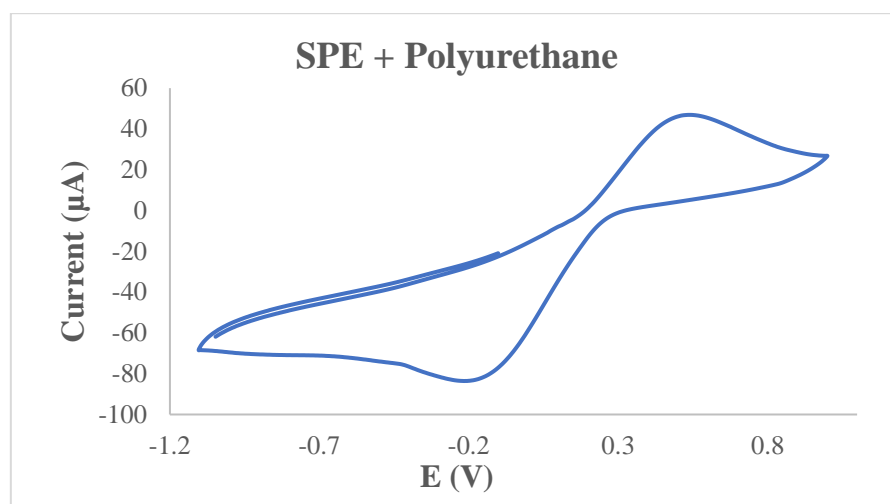
437 conductivity by inducing electron delocalization along the polyurethane chain (Wong et al.

438 2014). The conductivity of PU can also be caused by PEG. The application of PEG as polyol

439 has been studied by Porcarelli et al. (2017), that reported that the conductivity of PU based on

440 PEG – polyol was  $9.2 \times 10^{-8}$ .

441 According to **Figure 8**, it can be concluded that the anodic peak present in the modified  
442 electrode was at +0.5 V, it also represented the oxidation process of the modified electrode.  
443 The first oxidation scan on both electrodes ranged from -0.2 to +1.0 V, which showed a  
444 significant anodic peak at a potential of +0.5 V.  
445



446  
447 **Figure 8.** The voltammogram of SPE – PU modified electrode after analysed using cyclic  
448 voltammetry (CV) technique

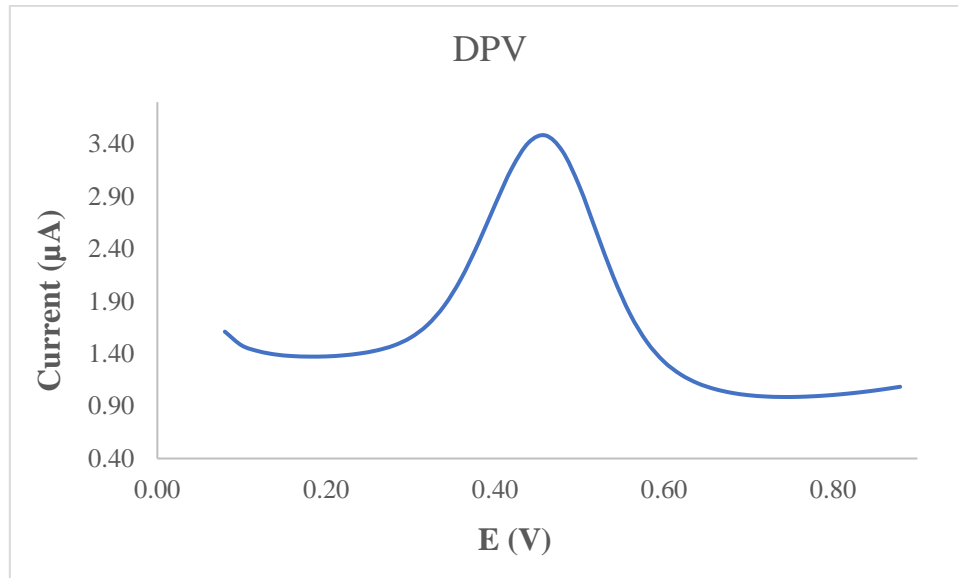
449  
450 **Figure 9** also presents the DPV voltammogram of modified electrode. DPV is a measurement  
451 based on the difference in potential pulses that produce an electric current. Scanning the  
452 capability pulses to the working electrode will produce different currents. Optimal peak  
453 currents will be produced to the reduction capacity of the redox material. The peak current  
454 produced is proportional to the concentration of the redox substance and can be detected up to  
455 concentration below  $10^{-8}$  M. DPV was conducted to obtain the current value that more accurate  
456 than CV (Lee et al. 2018).

457  
458 This study used a redox pair ( $K_3Fe(CN)_6$ ) as a test device (probe). The currents generated by  
459 SPE-PU and proved by CV and DPV have shown conductivity on polyurethane films. This  
460 suggests that polyurethane films can conduct electron transfer. The electrochemical area on the

461 modified electrode can be calculated using the formula from Randles-Sevcik (Butwong et al.  
 462 2019), where the electrochemical area for SPE-PU is considered to be A, using Equation 2:

463 
$$\text{Current of SPE-PU, } I_p = 2.65 \times 10^5 n^{3/2} A v^{1/2} C D^{1/2} \quad (2)$$

464



465

466 **Figure 9.** The voltammogram of SPE – PU modified electrode after analyzed using  
 467 differential pulse voltammetry (DPV) technique

468

469 Where,  $n - 1$  is the amount of electron transfer involved, while C is the solvent concentration  
 470 used (mmol/L) and the value of D is the diffusion constant of 5 mmol/L at  $(K_3Fe(CN)_6)$   
 471 dissolved using 0.1 mmol/L KCl. The estimated surface area of the electrode (**Figure 1**) was  
 472  $0.2 \text{ cm}^2$  where the length and width of the electrode used during the study was  $0.44 \text{ cm} \times 0.44$   
 473 cm while the surface area of the modified electrode was  $0.25 \text{ cm}^2$  with the length and width of  
 474 the electrode estimated at  $0.5 \text{ cm} \times 0.5 \text{ cm}$ , and causing the modified electrode has a larger  
 475 surface. The corresponding surface concentration ( $\tau$ ) ( $\text{mol}/\text{cm}^2$ ) is calculated using Equation 3.

476 
$$I_p = (n^2 F^2 / 4RT) A \tau v \quad (3)$$

477  $I_p$  is the peak current (A), while A is the surface area of the electrode ( $\text{cm}^2$ ), the value of v is  
 478 the applied scan rate (mV/s) and F is the Faraday constant (96,584 C/mol), R is the constant  
 479 ideal gas (8.314 J/mol K) and T is the temperature used during the experiment being conducted

480 (298 K) (Koita et al. 2014). The development of conducting polymer from palm oil-based  
481 biomaterials seems to be one of the potential future applications of palm oil products, as this  
482 novel material has the potential to contribute positively to the analytical industry. Likewise,  
483 other palm oil-based products, such as refined-bleached-deodorised (RBD) palm oil, palm oil,  
484 and palm stearin are abundantly available in Malaysia. They are known to be economical,  
485 sustainable, and environmentally biodegradable. These palm oil-based products are promising  
486 prospects for manufacturing biomaterials that become alternative products to other polymers  
487 from synthetic/chemical-based (Tajao et al. 2021). Several studies have been reported the  
488 application of PU to produce elastic conductive fibres and films owing to it is highly elastic,  
489 scratch resistant and adhesive (Tadese et al. 2019), thus it is easy for PU to adhere on the  
490 screen-printed electrode in order to modify the electrode. PU is also being used as a composite  
491 material to make elastic conducting composite films (Khatoon & Ahmad 2017).

492

#### 493 **4. Conclusion**

494 Polyurethane film was prepared by pre-polymerization between palm kernel oil-based polyol  
495 (PKO-p) with MDI. The presence of PEG 400 as the chain extender formed freestanding  
496 flexible film. Acetone was used as the solvent to lower the reaction kinetics since the pre-  
497 polymerization was carried out at room temperature. The formation of urethane links (NHCO  
498 – backbone) after polymerization was confirmed by the absence of N=C=O peak at  $2241\text{ cm}^{-1}$   
499 and the presence of N-H peak at  $3300\text{ cm}^{-1}$ , carbonyl (C=O) at  $1710\text{ cm}^{-1}$ , carbamate (C-N) at  
500  $1600\text{ cm}^{-1}$ , ether (C-O-C) at  $1065\text{ cm}^{-1}$ , benzene ring (C = C) at  $1535\text{ cm}^{-1}$  in the bio  
501 polyurethane chain structure. Soxhlet analysis for the determination of crosslinking on  
502 polyurethane films has yielded a high percentage of 99.33 %. This is contributed by the hard  
503 segments formed from the reaction between isocyanates and hydroxyl groups causing  
504 elongation of polymer chains. FESEM analysis exhibited an absence of phase separation and



505 smooth surface. Meanwhile, the current of modified electrode was found at  $5.2 \times 10^{-5}$  A. This  
506 bio polyurethane film can be used as a conducting bio-polymer and it is very useful for other  
507 studies such as electrochemical sensor purposes. Furthermore, advanced technologies are  
508 promising and the future of bio-based polyol looks very bright.

509

## 510 **5. Acknowledgment**

511 The authors would like to thank Universitas Alma Ata for the sponsorship given to the first  
512 author. We would like to also, thank The Department of Chemical Sciences, Universiti  
513 Kebangsaan Malaysia for the laboratory facilities and CRIM, UKM for the analysis  
514 infrastructure.

515

## 516 **6. Conflict of Interest**

517 The authors declare no conflict of interest.

518

## 519 **7. References**

- 520 Agrawal, A., Kaur, R., Walia, R. S. (2017). PU foam derived from renewable sources:  
521 Perspective on properties enhancement: An overview. *European Polymer Journal*. 95:  
522 255 – 274.
- 523 Akindoyo, J. O., Beg, M.D.H., Ghazali, S., Islam, M.R., Jeyaratnam, N. & Yuvaraj, A.R.  
524 (2016). Polyurethane types, synthesis and applications – a review. *RSC Advances*. 6:  
525 114453 – 114482.
- 526 Alamawi, M. Y., Khairuddin, F. H., Yusoff, N. I. M., Badri, K., Ceylan, H. (2019).  
527 Investigation on physical, thermal and chemical properties of palm kernel oil polyol bio  
528 – based binder as a replacement for bituminous binder. *Construction and Building*  
529 *Materials*. 204: 122 – 131.

530 Alqarni, S. A., Hussein, M. A., Ganash, A. A. & Khan, A. (2020). Composite material – based  
531 conducting polymers for electrochemical sensor applications: a mini review.  
532 *BioNanoScience*. **10**: 351 – 364.

533 Badan, A., Majka, T. M. (2017). The influence of vegetable – oil based polyols on physico –  
534 mechanical and thermal properties of polyurethane foams. *Proceedings*. 1 – 7.

535 Badri, K.H. (2012) Biobased polyurethane from palm kernel oil-based polyol. In Polyurethane;  
536 Zafar, F., Sharmin, E., Eds. InTechOpen: Rijeka, Croatia. pp. 447–470.

537 Badri, K.H., Ahmad, S.H. & Zakaria, S. 2000. Production of a high-functionality RBD palm  
538 kernel oil – based polyester polyol. *Journal of Applied Polymer Science* 81(2): 384 –  
539 389.

540 Baig, N., Sajid, M. and Saleh, T. A. 2019. Recent trends in nanomaterial – modified electrodes  
541 for electroanalytical applications. *Trends in Analytical Chemistry*. 111: 47 – 61.

542 Berta, M., Lindsay, C., Pans, G., & Camino, G. (2006). Effect of chemical structure on  
543 combustion and thermal behaviour of polyurethane elastomer layered silicate  
544 nanocomposites. *Polymer Degradation and Stability*. **91**: 1179-1191.

545 Borowicz, M., Sadowska, J. P., Lubczak, J. & Czuprynski, B. (2019). Biodegradable, flame –  
546 retardant, and bio – based rigid polyurethane/polyisocyanurate foams for thermal  
547 insulation application. *Polymers*. 11: 1816 – 1839.

548 Butwong, N., Khajonklin, J., Thongbor, A. & Luong, J.H.T. (2019). Electrochemical sensing  
549 of histamine using a glassy carbon electrode modified with multiwalled carbon nanotubes  
550 decorated with Ag – Ag<sub>2</sub>O nanoparticles. *Microchimica Acta*. **186** (11): 1 – 10.

551 Chokkareddy, R., Thondavada, N., Kabane, B. & Redhi, G. G. (2020). A novel ionic liquid  
552 based electrochemical sensor for detection of pyrazinamide. *Journal of the Iranian*  
553 *Chemical Society*. 18: 621 – 629.

554 Chokkareddy, R., Kanchi, S. & Inamuddin (2020). Simultaneous detection of ethambutol and  
555 pyrazinamide with IL@CoFe<sub>2</sub>O<sub>4</sub>NPs@MWCNTs fabricated glassy carbon electrode.  
556 *Scientific Reports*. 10: 13563.

557 Clemitson, I. (2008). Castable Polyurethane Elastomers. Taylor & Francis Group, New York.  
558 doi:10.1201/9781420065770.

559 Corcuera, M.A., Rueda, L., Saralegui, A., Martin, M.D., Fernandez-d'Arlas, B., Mondragon,  
560 I. & Eceiza, A. (2011). Effect of diisocyanate structure on the properties and  
561 microstructure of polyurethanes based on polyols derived from renewable resources.  
562 *Journal of Applied Polymer Science*. **122**: 3677-3685.

563 Cuve, L. & Pascault, J.P. (1991). Synthesis and properties of polyurethanes based on  
564 polyolefine: Rigid polyurethanes and amorphous segmented polyurethanes prepared in  
565 polar solvents under homogeneous conditions. *Polymer*. **32** (2): 343- 352.

566 Degefu, H., Amare, M., Tessema, M. & Admassie, S. (2014). Lignin modified glassy carbon  
567 electrode for the electrochemical determination of histamine in human urine and wine  
568 samples. *Electrochimica Acta*. 121: 307 – 314.

569 Dzulkipli, M. Z., Karim, J., Ahmad, A., Dzulkurnain, N. A., Su'ait, M S., Fujita, M. Y., Khoon,  
570 L. T. & Hassan, N. H. (2021). The influences of 1-butyl-3-methylimidazolium  
571 tetrafluoroborate on electrochemical, thermal and structural studies as ionic liquid gel  
572 polymer electrolyte. *Polymers*. 13 (8): 1277 – 1294.

573 El-Raheem, H.A., Hassan, R.Y.A., Khaled, R., Farghali, A. & El-Sherbiny, I.M. (2020).  
574 Polyurethane – doped platinum nanoparticles modified carbon paste electrode for the  
575 sensitive and selective voltammetric determination of free copper ions in biological  
576 samples. *Microchemical Journal*. **155**: 104765.

577 Fei, T., Li, Y., Liu, B. & Xia, C. (2019). Flexible polyurethane/boron nitride composites with  
578 enhanced thermal conductivity. *High Performance Polymers*. **32** (3): 1 – 10.

579 Furtwengler, P., Perrin R., Redl, A. & Averous, L. (2017). Synthesis and characterization of  
580 polyurethane foams derived of fully renewable polyesters polyols from sorbitol.  
581 *European Polymer Journal*. **97**: 319 – 327.

582 Ghosh, S., Ganguly, S., Remanan, S., Mondal, S., Jana, S., Maji, P. K., Singha, N., Das, N. C.  
583 (2018). Ultra – light weight, water durable and flexible highly electrical conductive  
584 polyurethane foam for superior electromagnetic interference shielding materials. *Journal*  
585 *of Materials Science: Materials in Electronics*. 29: 10177 – 10189.

586 Guo, S., Zhang, C., Yang, M., Zhou, Y., Bi, C., Lv, Q. & Ma, N. (2020). A facile and sensitive  
587 electrochemical sensor for non – enzymatic glucose detection based on three –  
588 dimensional flexible polyurethane sponge decorated with nickel hydroxide. *Analytica*  
589 *Chimica Acta*. **1109**: 130 – 139.

590 Hamuzan, H.A. & Badri, K.H. (2016). The role of isocyanates in determining the viscoelastic  
591 properties of polyurethane. AIP Conference Proceedings. 1784, Issue 1.

592 Herrington, R. & Hock, K. (1997). Flexible polyurethane foams. 2nd Edition. Dow Chemical  
593 Company. Midlan.

594 Janpoung, P., Pattanauwat, P. & Potiyaraj, P. (2020). Improvement of electrical conductivity  
595 of polyurethane/polypyrrole blends by graphene. *Key Engineering Materials*. **831**: 122 –  
596 126.

597 Khairuddin, F.H., Yusof, N. I. M., Badri, K., Ceylan, H., Tawil, S. N. M. (2018). Thermal,  
598 chemical and imaging analysis of polyurethane/cecabase modified bitumen. *IOP Conf.*  
599 *Series: Materials Science and Engineering*. 512: 012032.

600 Khatoon, H., Ahmad, S. (2017). A review on conducting polymer reinforced polyurethane  
601 composites. *Journal of Industrial and Engineering Chemistry*. 53: 1 – 22.

602 Kilele, J. C., Chokkareddy, R., Rono, N. & Redhi, G. G. (2020). A novel electrochemical  
603 sensor for selective determination of theophylline in pharmaceutical formulations.  
604 *Journal of the Taiwan Institute of Chemical Engineers*. 1 – 11.

605 Kilele, J. C., Chokkareddy, R. & Redhi, G. G. (2021). Ultra – sensitive electrochemical sensor  
606 for fenitrothion pesticide residues in fruit samples using IL@CoFe<sub>2</sub>ONPs@MWCNTs  
607 nanocomposite. *Microchemical Journal*. 164: 106012.

608 Koita, D., Tzedakis, T., Kane, C., Diaw, M., Sock, O. & Lavedan, P. (2014). Study of the  
609 histamine electrochemical oxidation catalyzed by nickel sulfate. *Electroanalysis*. **26 (10)**:  
610 2224 – 2236.

611 Kotal, M., Srivastava, S.K. & Paramanik, B. (2011). Enhancements in conductivity and thermal  
612 stabilities of polyurethane/polypyrrole nanoblends. *The Journal of Physical Chemistry*  
613 *C*. **115 (5)**: 1496 – 1505.

614 Ladan, M., Basirun, W.J., Kazi, S.N., Rahman, F.A. (2017). Corrosion protection of AISI 1018  
615 steel using Co – doped TiO<sub>2</sub>/polypyrrole nanocomposites in 3.5% NaCl solution.  
616 *Materials Chemistry and Physics*. **192**: 361 – 373.

617 Lampman, G.M., Pavia, D.L., Kriz, G.S. & Vyvyan, J.R. (2010). Spectroscopy. 4th Edition.  
618 Brooks/Cole Cengage Learning, Belmont, USA.

619 Lee, K.J., Elgrishi, N., Kandemir, B. & Dempsey, J.L. 2018. Electrochemical and spectroscopic  
620 methods for evaluating molecular electrocatalysts. *Nature Reviews Chemistry* 1(5): 1 -  
621 14.

622 Leykin, A., Shapovalov, L. & Figovsky, O. (2016). Non – isocyanate polyurethanes –  
623 Yesterday, today and tomorrow. *Alternative Energy and Ecology*. **191 (3 – 4)**: 95 – 108.

624 Li, H., Yuan, D., Li, P., He, C. (2019). High conductive and mechanical robust carbon  
625 nanotubes/waterborne polyurethane composite films for efficient electromagnetic  
626 interference shielding. *Composites Part A*. 121: 411 – 417.

627 Nakthong, P., Kondo, T., Chailapakul, O., Siangproh, W. (2020). Development of an  
628 unmodified screen – printed graphene electrode for nonenzymatic histamine detection.  
629 *Analytical Methods*. 12: 5407 – 5414.

630 Mishra, K., Narayan, R., Raju, K.V.S.N. & Aminabhavi, T.M. (2012). Hyperbranched  
631 polyurethane (HBPU)-urea and HBPU-imide coatings: Effect of chain extender and  
632 NCO/OH ratio on their properties. *Progress in Organic Coatings*. **74**: 134 – 141.

633 Mohd Noor, M. A., Tuan Ismail, T. N. M., Ghazali, R. (2020). Bio – based content of oligomers  
634 derived from palm oil: Sample combustion and liquid scintillation counting technique.  
635 *Malaysia Journal of Analytical Science*. 24: 906 – 917.

636 Mutsuhisa F., Ken, K. & Shohei, N. (2007). Microphase separated structure and mechanical  
637 properties of norbornane diisocyanate – based polyurethane. *Polymer*. **48** (4): 997 – 1004.

638 Mustapha, R., Rahmat, A. R., Abdul Majid, R., Mustapha, S. N. H. (2019). Vegetable oil –  
639 based epoxy resins and their composites with bio – based hardener: A short review.  
640 *Polymer- Plastic Technology and Materials*. 58: 1311 – 1326.

641 Nohra, B., Candy, L., Blancos, J.F., Guerin, C., Raoul, Y. & Mouloungui, Z. (2013). From  
642 petrochemical polyurethanes to biobased polyhydroxyurethanes. *Macromolecules*. **46**  
643 (10): 3771 – 3792.

644 Pan, T. & Yu, Q. (2016). Anti – corrosion methods and materials comprehensive evaluation of  
645 anti – corrosion capacity of electroactive polyaniline for steels. *Anti – Corrosion Methods*  
646 *and Materials*. **63**: 360 – 368.

647 Pan, X. & Webster, D.C. (2012). New biobased high functionality polyols and their use in  
648 polyurethane coatings. *ChemSusChem*. **5**: 419-429.

649 Petrovic, Z.S. (2008). Polyurethanes from vegetable oils. *Polymer Reviews*. **48** (1): 109 – 155.

650 Porcarelli, L., Manojkumar, K., Sardon, H., Llorente, O., Shaplov, A. S., Vijayakrishna, K.,  
651 Gerbaldi, C., Mecerreyes, D. (2017). Single ion conducting polymer electrolytes based  
652 on versatile polyurethanes. *Electrochimica Acta*. 241: 526 – 534.

653 Priya, S. S., Karthika, M., Selvasekarapandian, S. & Manjuladevi, R. (2018). Preparation and  
654 characterization of polymer electrolyte based on biopolymer I-carrageenan with  
655 magnesium nitrate. *Solid State Ionics*. **327**: 136 – 149.

656 Ren, D. & Frazier, C.E. (2013). Structure–property behaviour of moisture-cure polyurethane  
657 wood adhesives: Influence of hard segment content. *Adhesion and Adhesives*. **45**: 118-  
658 124.

659 Rogulska, S.K., Kultys, A. & Podkoscielny, W. (2007). Studies on thermoplastic polyurethanes  
660 based on new diphenylethane – derivative diols. II. Synthesis and characterization of  
661 segmented polyurethanes from HDI and MDI. *European Polymer Journal*. **43**: 1402 –  
662 1414.

663 Romaskevicius, T., Budriene, S., Pielichowski, K. & Pielichowski, J. (2006). Application of  
664 polyurethane – based materials for immobilization of enzymes and cells: a review.  
665 *Chemija*. **17**: 74 – 89.

666 Sengodu, P. & Deshmukh, A. D. (2015). Conducting polymers and their inorganic composites  
667 for advanced Li-ion batteries: a review. *RSC Advances*. **5**: 42109 – 42130.

668 Septevani, A. A., Evans, D. A. C., Chaleat, C., Martin, D. J., Annamalai, P. K. (2015). A  
669 systematic study substituting polyether polyol with palm kernel oil based polyester  
670 polyol in rigid polyurethane foam. *Industrial Corps and Products*. 66: 16 – 26.

671 Su'ait, M. S., Ahmad, A., Badri, K. H., Mohamed, N. S., Rahman, M. Y. A., Ricardi, C. L. A.  
672 & Scardi, P. The potential of polyurethane bio – based solid polymer electrolyte for  
673 photoelectrochemical cell application. *International Journal of Hydrogen Energy*. 39 (6):  
674 3005 – 3017.

675 Tadesse, M. G., Mengistie, D. A., Chen, Y., Wang, L., Loghin, C., Nierstrasz, V. (2019).  
676 Electrically conductive highly elastic polyamide/lycra fabric treated with PEDOT: PSS  
677 and polyurethane. *Journal of Materials Science*. 54: 9591 – 9602.

678 Tajau, R., R, Rosiah, Alias, M. S., Mudri, N. H., Halim, K. A. A., Harun, M. H., Isa, N. M.,  
679 Ismail, R. C., Faisal, S. M., Talib, M., Zin, M. R. M., Yusoff, I. I., Zaman, N. K., Illias,  
680 I. A. (2021). Emergence of polymeric material utilising sustainable radiation curable  
681 palm oil – based products for advanced technology applications. *Polymers*. 13: 1865 –  
682 1886.

683 Tran, V.H., Kim, J.D., Kim, J.H., Kim, S.K., Lee, J.M. (2020). Influence of cellulose  
684 nanocrystal on the cryogenic mechanical behaviour and thermal conductivity of  
685 polyurethane composite. *Journal of Polymers and The Environment*. **28**: 1169 – 1179.

686 Viera, I.R.S., Costa, L.D.F.D.O., Miranda, G.D.S., Nardehcia, S., Monteiro, M.S.D. S.D.B.,  
687 Junior, E.R. & Delpech, M.C. (2020). Waterborne poly (urethane – urea)s  
688 nanocomposites reinforced with clay, reduced graphene oxide and respective hybrids:  
689 Synthesis, stability and structural characterization. *Journal of Polymers and The  
690 Environment*. **28**: 74 – 90.

691 Wang, B., Wang, L., Li, X., Liu, Y., Zhang, Z., Hedrick, E., Safe, S., Qiu, J., Lu, G. & Wang,  
692 S. (2018). Template – free fabrication of vertically – aligned polymer nanowire array on  
693 the flat – end tip for quantifying the single living cancer cells and nanosurface interaction.  
694 *a Manufacturing Letters*. **16**: 27 – 31.

695 Wang, J., Xiao, L., Du, X., Wang, J. & Ma, H. (2017). Polypyrrole composites with carbon  
696 materials for supercapacitors. *Chemical Papers*. **71** (2): 293 – 316.

697 Wong, C.S. & Badri, K.H. (2012). Chemical analyses of palm kernel oil – based polyurethane  
698 prepolymer. *Materials Sciences and Applications*. **3**: 78 – 86.



- 699 Wong, C. S., Badri, K., Ataollahi, N., Law, K., Su'ait, M. S., Hassan, N. I. (2014). Synthesis  
700 of new bio – based solid polymer electrolyte polyurethane – LiClO<sub>4</sub> via  
701 prepolymerization method: Effect of NCO/OH ratio on their chemical, thermal properties  
702 and ionic conductivity. *World Academy of Science, Engineering and Technology,*  
703 *International Journal of Chemical, Molecular, Nuclear, Materials and Metallurgical*  
704 *Engineering.* 8: 1243 – 1250.
- 705 Yong, Z., Bo, Z.M., Bo, W., Lin, J.Z. & Jun, N. (2009). Synthesis and properties of novel  
706 polyurethane acrylate containing 3-(2-Hydroxyethyl) isocyanurate segment. *Progress in*  
707 *Organic Coatings.* **67**: 264 – 268
- 708 Zia, K. M., Anjum, S., Zuber, M., Mujahid, M. & Jamil, T. (2014). Synthesis and molecular  
709 characterization of chitosan based polyurethane elastomers using aromatic diisocyanate.  
710 *International of Journal of Biological Macromolecules.* **66**: 26 – 32.

[← BACK](#) [DASHBOARD / ARTICLE DETAILS](#)

Updated on 2022-02-10

Version 5 ▼

# Design and Synthesis of Conducting Polymer Based on Polyurethane produced from Palm Kernel Oil

VIEWING AN OLDER VERSION

ID 6815187

Muhammad Abdurrahman Munir <sup>SA CA</sup> <sup>1</sup>,  
Khairiah Haji Badri<sup>2</sup>, Lee Yook Heng<sup>2</sup>  
[+ Show Affiliations](#)

## Article Type

Research Article

## Journal

International Journal of  
Polymer Science

Rydz Joanna

Submitted on 2021-06-14 (2 years ago)

[> Abstract](#)[> Author Declaration](#)[> Files](#) 2[- Editorial Comments](#)

Joanna Rydz

10.02.2022

**Decision**

Minor Revision Requested

**Message for Author**

Dear authors,

The text still needs to be improved.

1. Please properly describe the results from FTIR throughout the text also in Conclusion.

"N=C=O is not a peak. Functional groups give characteristic signals in a spectrum. Please use scientific language throughout your text and please describe the FTIR spectra properly"

"Thank you for your suggestion. Nevertheless, the reading of this spectrum based on Spectroscopy book 4th Edition by Lampman et al. It is written on Page 29, 77 and 78 (Figure 2.64) about the spectrum of N=C=O. According to their research, the isocyanates have sp-hybridized carbon atoms similar to the C≡C bond. The absorption occurs in 2100-2270 cm<sup>-1</sup>"

Exactly, then why do you write "N=C=O peak"? It is a scientific work and that is the language it should use.

"and confirmed by the absence of peak at 2241 cm<sup>-1</sup> attributed to the sp-hybridized carbon atoms of ....."/or "absorption bands at 2241 cm<sup>-1</sup> associated with N=C=O bond stretching...." Please correct.

2. "bio based" is one word and should be spelled the same way throughout the text, see lines 21 and 75 (correct). Please correct throughout the text (It is best to use the find options throughout the text).

3. Line 150-152: The reagent purity record was perfectly correct and please restore it. The note was about DMSO, which was 2 times.

4. Line 220: the parenthesis is missing.

5. Line 369, 507, 513: "bio polyurethane". Should be bio-based polyurethane. A single comment applies to the entire text!

6. Table 2: Please explain variables such as Tmax, etc. under the table.

The table has not been corrected and is still incomprehensible. It not only shows the "weight loss percentage" as its caption suggests, but also other parameters. Please properly title it. Right now, the table shows that the weight loss percentage of sample Tmax has changed by 240!

The first row should be discarded. The table shows the TGA parameters of one sample, so there is no need to put it in the table. Please correct.

**— Response to Revision Request**

Muhammad Abdurrahman Munir

10.02.2022

**Your Reply**

Greetings, Dear Dr. Joanna Rydz We would like to inform you that the manuscript has been revised according to the reviewer's comments. Journal: International

Journal of Polymer Science Manuscript ID: 6815187 Title: "Design and Synthesis of Conducting Polymer Based on Polyurethane produced from Palm Kernel Oil"  
Comments and track changes are attached. We look forward to receiving your revision if any. Best Regards.

**File**

Manuscript - Munir.docx 916 kB



---

[Hindawi](#) [Privacy Policy](#) [Terms of Service](#) Support: [help@hindawi.com](mailto:help@hindawi.com)



25 adhesion on the SPE surface. The synthesized polyurethane was characterized using  
26 thermogravimetry analysis (TGA), differential scanning calorimetry (DSC), Fourier –  
27 transform infrared spectroscopy (FTIR), surface area analysis by field emission scanning  
28 electron microscope (FESEM), and cyclic voltammetry (CV). Cyclic voltammetry was  
29 employed to study electro-catalytic properties of SPE-Polyurethane towards oxidation of PU.  
30 Remarkably, SPE-PU exhibited improved anodic peak current as compared to SPE itself using  
31 the differential pulse voltammetry (DPV) method. Furthermore, the formation of urethane  
32 linkages (NHCO backbone) after polymerization was analyzed using FTIR and confirmed by  
33 the absence of N=C=O peak at  $2241\text{ cm}^{-1}$ . The glass transition temperature ( $T_g$ ) of the  
34 polyurethane was detected at  $78.1^\circ\text{C}$ .

35

36 **Keywords:** Polyurethane, polymerization, screen-printed electrode, voltammetry

37

38

### 39 **1. Introduction**

40 Conducting polymers (CPs) are polymers that can release a current (Alqarni et al. 2020). The  
41 conductivity of CPs was first observed in polyacetylene, nevertheless owing to its instability,  
42 the invention of various CPs have been studied and reported such as polyaniline (PANI), poly  
43 (o-toluidine) (PoT), polythiophene (PTH), polyfluorene (PF), and polyurethane (PU).  
44 Furthermore, natural CPs have low conductivity and are often semi-conductive. Therefore, it  
45 is imperative to improve their conductivity for electrochemical sensor purposes (Sengodu &  
46 Deshmukh 2015; Dzulkipli et al. 2021; Wang et al. 2018). The CPs can be produced from many  
47 organic materials and they have several advantages such as having an electrical current,  
48 inexpensive materials, massive surface area, small dimensions, and the production is  
49 straightforward. Furthermore, according to these properties, many studies have been reported

50 by researchers to study and report the variety of CPs applications such as sensors, biochemical  
51 applications, electrochromic devices, and solar cells (Alqarni et al. 2020; Ghosh et al. 2018).  
52 There is scientific documentation on the use of conductive polymers in various studies such as  
53 polyaniline (Pan & Yu 2016), polypyrrole (Ladan et al. 2017), and polyurethane (Tran et al.  
54 2020; Vieira et al. 2020; Guo et al. 2020; Fei et al. 2020).

55

56 Polyurethane productions can be obtained by using several materials as polyols such as  
57 petroleum, coal, and crude oils. Nevertheless, these materials have become very rare to find  
58 and the price is very expensive at the same time required a sophisticated system to produce it.  
59 The reasons such as price and time consuming to produce polyols have been considered by  
60 many researchers, furthermore, finding utilizing plants that can be used as alternative polyols  
61 should be done immediately (Badri 2012). Thus, to avoid the use of petroleum, coal, and crude  
62 oils as raw materials for a polyol, vegetable oils become a better choice to produce polyol in  
63 order to obtain a biodegradable polymer. Vegetable oils that are generally used for  
64 polyurethane synthesis are soybean oil, corn oil, sunflower seed oil, coconut oil, nuts oil,  
65 rapeseed, olive oil, and palm oil (Badri 2012; Borowicz et al. 2019).

66

67 It is very straightforward for vegetable oils to react with a specific group to produce a PU such  
68 as epoxy, hydroxyl, carboxyl, and acrylate owing to the existence of (-C=C-) in vegetable oils.  
69 Thus, it provides appealing profits to vegetable oils compared to petroleum considering the  
70 toxicity, price, and harm to the environment (Mustapha et al. 2019; Mohd Noor et al. 2020).  
71 Palm oil becomes the chosen in this study to produce PU owing to it being largely cultivated  
72 in South Asia particularly in Malaysia and Indonesia. It has several profits compared to other  
73 vegetable oils such as the easiest materials obtained, the lowest cost of all the common

74 vegetable oils, and recognized as the plantation that has a low environmental impact and  
75 removing CO<sub>2</sub> from the atmosphere as a net sequester (Tajau et al. 2021; Septevani et al. 2015).

76

77 The application of biopolymer has appealed much attention until now. Global environmental  
78 activists have forced researchers to discover another material producing biopolymers (Priya et  
79 al. 2018). PUs have many advantages that have been used by many researchers, they are not  
80 merely versatile materials but also have the durability of metal and the flexibility of rubber.  
81 Furthermore, they can be promoted to replace rubber, metals, and plastics in several aspects.  
82 Several applications of Pus have been reported and studied such as textiles, automotive,  
83 building and construction applications, and biomedical applications (Zia et al. 2014;  
84 Romaskevic et al. 2006). Polyurethanes are also considered to be one of the most useful  
85 materials with many profits such as; possessing low conductivity, low density, absorption  
86 capability, and dimensional stability. They are a great research subject due to their mechanical,  
87 physical, and chemical properties (Badan & Majka 2017; Munir et al. 2021).

88

89 PU structure contains the urethane group that can be formed from the reaction between  
90 isocyanate groups (-NCO) and hydroxyl group (-OH). Nevertheless, several groups can be  
91 found in PU structure such as urea, esters, ethers, and several aromatic groups. Furthermore,  
92 PUs can be produced from different sources as long as they contain specific materials (polyol  
93 & MDI) and making them very useful for specific applications. Thus, according to the desired  
94 properties, PUs can be divided into several types such as waterborne, flexible, rigid, coating,  
95 binding, sealants, adhesives, and elastomers (Akindoyo et al. 2016).

96

97 PUs have low conductivity and are lighter than other materials such as metals, gold, and  
98 platinum. The hardness of PU also relies on the number of the aromatic rings in the polymer



99 structure (Janpoung et al, 2020; Su'ait et al. 2014), majorly contributed by the isocyanate  
100 derivatives. PUs have also a conjugate structure where electrons can move in the main chain  
101 that causes electricity produced even the current is low. The current of conjugated linear ( $\pi$ )  
102 can be elaborated by the gap between the valence band and the conduction band, or called high  
103 energy level containing electrons (HOMO) and lowest energy level not containing electrons  
104 (LUMO), respectively (Wang et al. 2017; Kotal et al. 2011).

105

106 In the recent past, several conventional methods have been developed such as capillary  
107 electrophoresis, liquid, and gas chromatography coupled with several detectors. Nevertheless,  
108 although chromatographic and spectrometric approaches are well developed for qualitative and  
109 quantitative analyses of analytes, several limitations emerged such as complicated  
110 instrumentation, expensive, tedious sample preparations, and requiring large amounts of  
111 expensive solvents that will harm the users and environment (Kilele et al. 2020; Inayatullah et  
112 al. 2021; Munir et al. 2021; Harmayani et al. 2014; Nurwanti et al. 2018). Therefore, it is  
113 imperative to obtain and develop an alternative material that can be used to analyze a specific  
114 analyte. Electrochemical methods are extremely promising methods in the determination of an  
115 analyte in samples owing to the high selectivities, sensitivities, inexpensive, requirements of  
116 small amounts of solvents, and can be operated by people who have no background in analytical  
117 chemistry. In addition, sample preparation such as separation and extraction steps are not  
118 needed owing to the selectivity of this instrument where no obvious interference on the current  
119 response is recorded (Chokkareddy et al. 2020). Few works have been reported on the  
120 electrochemical methods for the determination of analyte using electrodes combined with  
121 several electrode modifiers such as carbon nanotube, gold, and graphene (Chokkareddy et al.  
122 2020; Kilele et al. 2021). Nevertheless, the materials are expensive and the production is

123 difficult. Thus, an electrochemical approach using inexpensive and easily available materials  
124 as electrode modifiers should be developed (Degefu et al. 2014).

125

126 Nowadays, screen-printed electrodes (SPEs) modified with conducting polymer have been  
127 developed for various electrochemical sensing. SPE becomes the best solution owing to the  
128 electrode having several advantages such as frugal manufacture, tiny size, being able to  
129 produce on a large scale, and can be applied for on-site detection (Nakthong et al. 2020).  
130 Conducting polymers (CPs) become an alternative to modifying the screen-printed electrodes  
131 due to their electrical conductivity, able to capture analyte by chemical/physical adsorption,  
132 large surface area, and making CPs are very appealing materials from electrochemical  
133 perspectives (Baig et al. 2019). Such advantages of SPE encourage us to construct a new  
134 electrode for electrochemical sensing, and no research reported on the direct electrochemical  
135 oxidation of histamine using a screen-printed electrode modified by polyurethane. Therefore,  
136 this research is the first to develop a new electrode using (screen printed polyurethane  
137 electrode) SPPE without any conducting materials.

138

139 The purpose of this work was to synthesize, characterize and study the electro behavior of  
140 polyurethane using cyclic voltammetry (CV) and differential pulse voltammetry (DPV)  
141 attached to the screen-printed electrode (SPE). To the best of our knowledge, this is the first  
142 attempt to use a modified polyurethane electrode. The electrochemistry of polyurethane  
143 mounted onto screen-printed electrode (SPE) is discussed in detail. PUs are possible to become  
144 an advanced frontier material that has been chemically modified the specific electrodes for  
145 bio/chemical sensing application.

146

147

## 148 2. Experimental

### 149 2.1 Chemicals

150 *Synthesis of polyurethane film:* Palm kernel oil (PKOp) supplied by UKM Technology Sdn  
151 Bhd through MPOB/UKM station plant, Pekan Bangi Lama, Selangor and prepared using  
152 Badri et al. (2000) method. 4, 4-diphenylmethane diisocyanate (MDI) was acquired from  
153 Cosmopolyurethane (M) Sdn. Bhd., Klang, Malaysia. Solvents and analytical reagents were  
154 benzene ( $\geq 99.8\%$ ), toluene ( $\geq 99.8\%$ ), hexane ( $\geq 99\%$ ), acetone ( $\geq 99\%$ ), dimethylsulfoxide  
155 (DMSO) ( $\geq 99.9\%$ ), dimethylformamide (DMF) ( $\geq 99.8\%$ ), tetrahydrofuran (THF) ( $\geq 99.8\%$ ),  
156 dimethylsulfoxide (DMSO) ( $\geq 99.9\%$ ), and polyethylene glycol (PEG) with a molecular weight  
157 of 400 Da obtained from Sigma Aldrich Sdn Bhd, Shah Alam.

158

### 159 2.2 Apparatus

160 Tensile testing was performed using a universal testing machine model Instron 5566 following  
161 ASTM 638 (Standard Test Method for Tensile Properties of Plastics). The tensile properties of  
162 the polyurethane film were measured at a velocity of 10 mm/min with a cell load of 5 kN.

163 The thermal properties were performed using thermogravimetry analysis (TGA) and  
164 differential scanning calorimetry (DSC) analysis. TGA was performed using a thermal analyzer  
165 of the Perkin Elmer Pyris model with a heating rate of 10 °C/min at a temperature range of 30  
166 to 800 °C under a nitrogen gas atmosphere. The DSC analysis was performed using a thermal  
167 analyzer of the Perkin Elmer Pyris model with a heating rate of 10 °C /minute at a temperature  
168 range of -100 to 200 °C under a nitrogen gas atmosphere. Approximately, 5-10 mg of PU was  
169 weighed. The sample was heated from 25 to 150 °C for one minute, then cooled immediately  
170 from 150 -100 °C for another one minute and finally, reheated to 200 °C at a rate of 10 °C /min.  
171 At this point, the polyurethane encounters changes from elastic properties to brittle due to  
172 changes in the movement of the polymer chains. Therefore, the temperature in the middle of

173 the inclined regions is taken as the glass transition temperature ( $T_g$ ). The melting temperature  
174 ( $T_m$ ) is identified as the maximum endothermic peak by taking the area below the peak as the  
175 enthalpy point ( $\Delta H_m$ ).

176

177 The morphological analysis of PU film was performed by Field Emission Scanning Electron  
178 Microscope (FESEM) model Gemini SEM microscope model 500-70-22. Before the analysis  
179 was carried out, the polyurethane film was coated with a thin layer of gold to increase the  
180 conductivity of the film. The coating method was carried out using a sputter-coater. The  
181 observations were conducted at a magnification of 200 $\times$  and 5000  $\times$  with 10.00 kV (Electron  
182 high tension - EHT).

183

184 The crosslinking of PU was determined using the soxhlet extraction method. About 0.60 g of  
185 PU sample was weighed and put in an extractor tube containing 250 ml of toluene, used as a  
186 solvent. This flow of toluene was let running for 24 hours. Mass of the PU was weighed before  
187 and after the reflux process was carried out. Then, the sample was dried in the conventional  
188 oven at 100 °C for 24 hours in order to get a constant mass. The percentage of crosslinking  
189 content known as the gel content can be calculated using Equation (1).

$$190 \quad \text{Gel content (\%)} = \frac{W_0 - W}{W} \times 100 \% \quad (1)$$

191  $W_0$  is the mass of PU before the reflux process (g) and  $W$  is the mass of PU after the reflux  
192 process (g).

193

194 FTIR spectroscopic analysis was performed using a Perkin-Elmer Spectrum BX instrument  
195 using the Diamond Attenuation Total Reflectance (DATR) method to confirm the  
196 polyurethane, PKOp, and MDI functional group. FTIR spectroscopic analysis was performed  
197 at a wavenumber of 4000 to 600  $\text{cm}^{-1}$  to identify the peaks of the major functional groups in

198 the formation of the polymer such as amide group (-NH), urethane carbonyl group (-C = O),  
199 and carbamate group (-CN).

200

### 201 **2.3 Synthesis of Polyurethane**

202 Firstly, the polyol prepolymer solution was produced by combining palm kernel oil (PKO)p  
203 and polyethylene glycol (PEG) 400 (100:40 g/g), acetone 30% was used as a solution. The  
204 compound was homogenized using a centrifuge (100 rpm) for 5 min. Whereas diisocyanate  
205 prepolymer was obtained by mixing 4,4'-diphenylmethane diisocyanate (MDI) (100 g) to  
206 acetone 30%, afterward the mixture was mixed using a centrifuge for 1 min to obtain a  
207 homogenized solution. Afterward, diisocyanate solution (10 g) was poured into a container that  
208 contains polyol prepolymer solution (10 g) slowly to avoid an exothermic reaction occurring.  
209 The mixture was mixed for 30 sec until a homogenized solution was acquired. Lastly, the  
210 polyurethane solution was poured on the electrode surface by using the casting method and  
211 dried at ambient temperature for 12 hours.

212

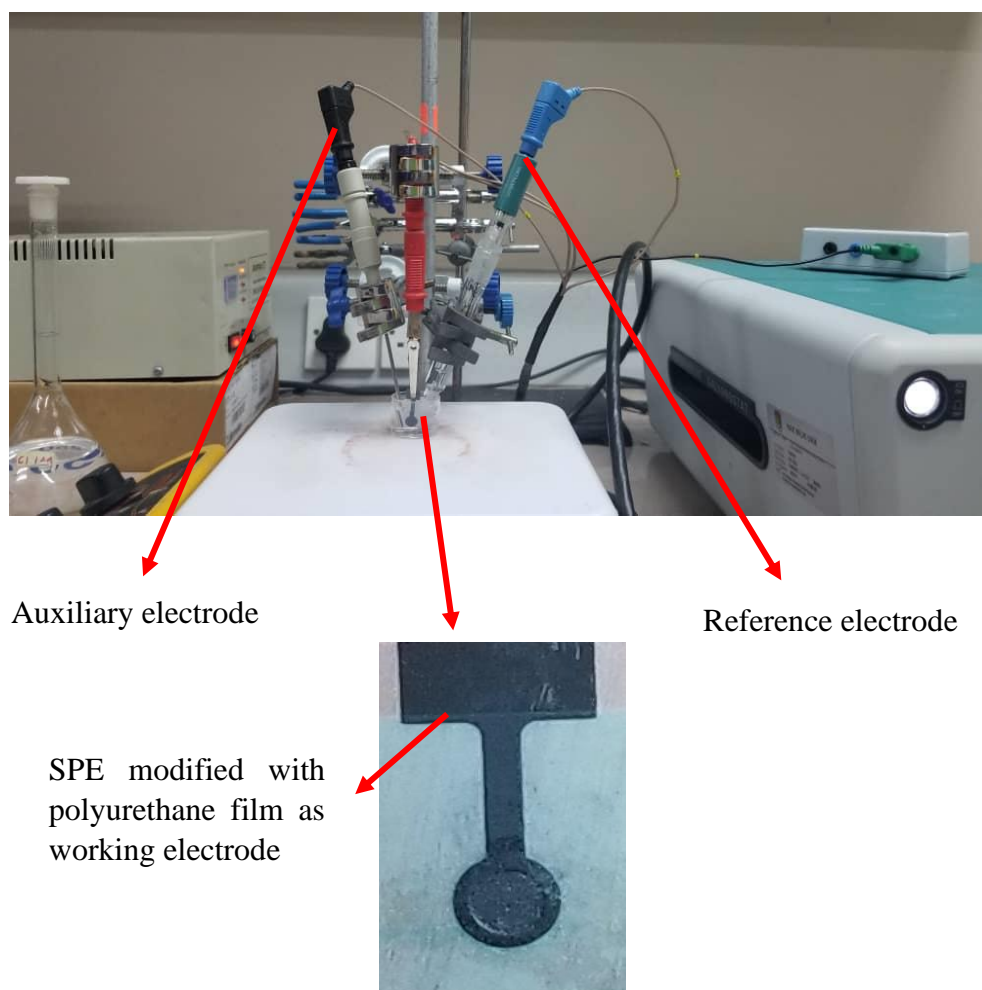
### 213 **2.4 Modification of Electrode**

214 Voltammetric tests were performed using Metrohm Autolab Software (**Figure 1**) analyzer  
215 using cyclic voltammetry (CV) method or known as amperometric mode and differential pulse  
216 voltammetry (DPV). All electrochemical experiments were carried out using screen-printed  
217 electrode (diameter 3 mm) modified using polyurethane film as working electrode, platinum  
218 wire as the auxiliary electrode, and Ag/AgCl electrode as a reference electrode. All experiments  
219 were conducted at a temperature of  $20 \pm 2^\circ\text{C}$ .

220

221 The PU was cast onto the screen-printed electrode (SPE + PU) and analyzed using a single  
222 voltammetric cycle between -1200 and +1500 mV (vs Ag/AgCl) of ten cycles at a scanning

223 rate of 100 mV/s in 5 ml of KCl in order to study the activity of SPE and polyurethane film.  
224 Approximately (0.1, 0.3 & 0.5) mg of palm-based pre-polyurethane was dropped separately  
225 onto the surface of the SPE and dried at room temperature. The modified palm-based  
226 polyurethane electrodes were then rinsed with deionized water to remove physically adsorbed  
227 impurities and residues of unreacted material on the electrode surface. All electrochemical  
228 materials and calibration measurements were carried out in a 5 mL glass beaker with a  
229 configuration of three electrodes inside it. Platinum wire and silver/silver chloride (Ag/AgCl)  
230 electrodes were used as auxiliary and reference electrodes, while a screen-printed electrode  
231 that had been modified with polyurethane was applied as a working electrode.



232 **Figure 1.** Potentiostat instrument to study the conductivity of SPE modified with  
233 polyurethane film using voltammetric approach: CV and DPV

234

235 **3. Results and Discussion**

236 The synthesis of PU films was carried out using a pre-polymerization method which involves  
237 the formation of urethane polymer at an early stage. The reaction took place between  
238 diisocyanate (MDI) and palm kernel oil-based polyol (PKOp). **Table 1** presents the PKO-p  
239 properties used in this study. The structural chain was extended with the aid of polyethylene  
240 glycol (PEG) to form flexible and elastic polyurethane film. In order to produce the urethane  
241 prepolymer, the isocyanate group (NCO) attacks with the hydroxyl group (OH) of polyol  
242 (PKOp) while the other hydroxyl group of the polyol is attacked by the other isocyanate group  
243 (Wong & Badri 2012) as shown in **Figure 2**.

244 **Table 1** The specification of PKO-p (Badri et al. (2000)).

Property	Values
Viscosity at 25°C (cps)	1313.3
Specific gravity (g/mL)	1.114
Moisture content (%)	0.09
pH value	10 – 11
The hydroxyl number mg KOH/g	450 - 470

245

246

247 a. FTIR analysis

248 **Figure 3** shows the FTIR spectra for polyurethane, exhibiting the important functional group  
249 peaks. According to a study researched by Wong & Badri 2012, PKO-p reacts with MDI to  
250 form urethane prepolymers. The NCO group on MDI reacts with the OH group on polyol  
251 whether PKOp or PEG. It can be seen there are no important peaks of MDI in the FTIR spectra.  
252 This is further verified by the absence of a peak at the 2400 cm<sup>-1</sup> belonging to MDI (-NCO  
253 groups). This could also confirm that the NCO group on MDI had completely reacted with

254 PKO-p to form the urethane –NHC (O) backbone. The presence of amides (-NH), carbonyl  
255 urethane group (-C = O), carbamate group (C-NH), and -C-O-C confirmed the formation of  
256 urethane chains. In this study, the peak of carbonyl urethane (C = O) detected at 1727 cm<sup>-1</sup>  
257 indicated that the carbonyl urethane group was bonded without hydrogen owing to the  
258 hydrogen reacts with the carbonyl urethane group.

259

260 The reaction of polyurethane has been studied by Hamuzan & Badri (2016) where the urethane  
261 carbonyl group was detected at 1730 – 1735 cm<sup>-1</sup> while the MDI carbonyl was detected at 2400  
262 cm<sup>-1</sup>. The absence of peaks at 2250 – 2270 cm<sup>-1</sup> indicates the absence of NCO groups. It shows  
263 that the polymerization reaction occurs entirely between NCO groups in MDI with hydroxyl  
264 groups on polyols and PEG (Mishra et al. 2012). The absence of peaks at 1690 cm<sup>-1</sup>  
265 representing urea (C = O) in this study indicated, there is no urea formation as a byproduct  
266 (Clemitson 2008) of the polymerization reaction that possibly occurs due to the excessive  
267 water. For the amine (NH) group, hydrogen-bond to NH and oxygen to form ether and  
268 hydrogen bond to NH and oxygen to form carbonyl on urethane can be detected at the peak of  
269 3301 cm<sup>-1</sup> and in the wavenumber at range 3326 – 3428 cm<sup>-1</sup>. This has also been studied and  
270 detected by Mutsuhisa et al. (2007) and Lampman et. al. (2010). In this research, the proton  
271 acceptor is carbonyl (-C=O) while the proton donor is an amine (-NH) to form a hydrogen  
272 bond. The MDI chemical structure has the electrostatic capability that produces dipoles from  
273 several atoms such as hydrogen, oxygen, and nitrogen atoms. These properties make  
274 isocyanates are highly reactive, and have different properties (Leykin et al. 2016).

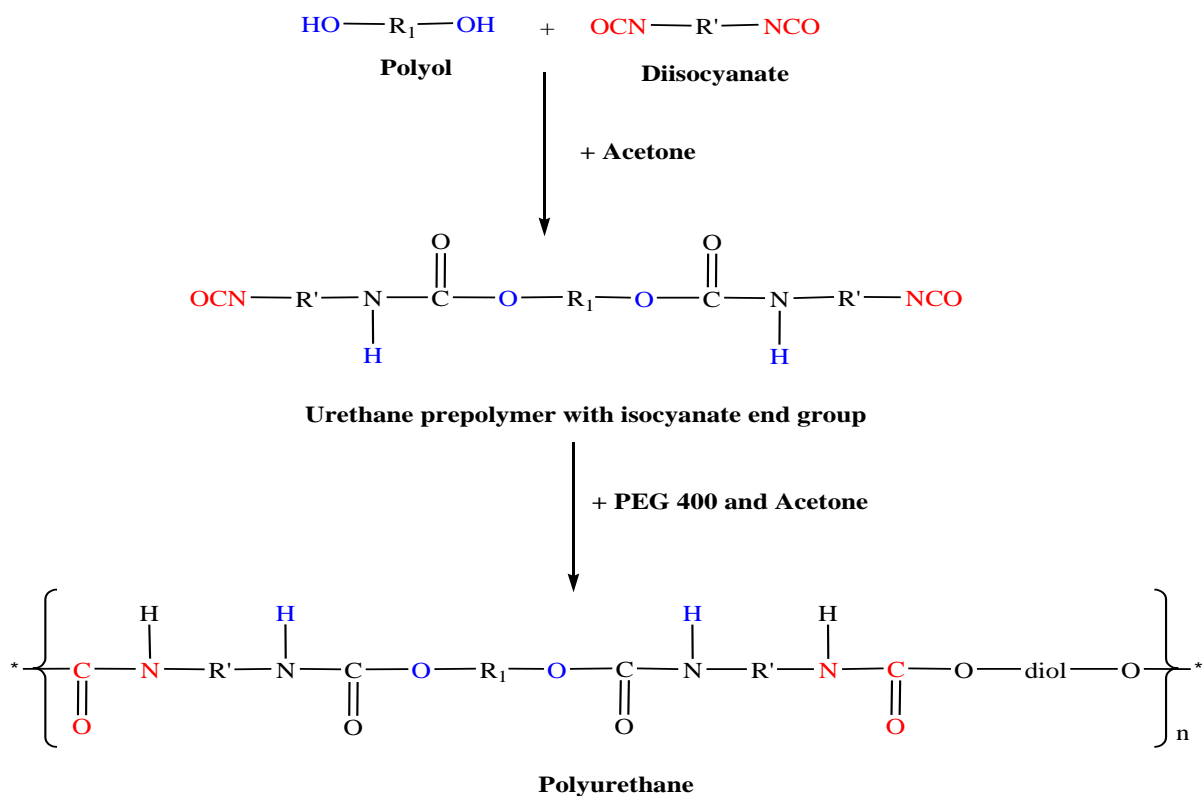
275

276 MDI was one of the isocyanates used in this study, has an aromatic group, and is more  
277 reactive compared to aliphatic group isocyanates such as hexamethylene diisocyanate (HDI)  
278 or isophorone diisocyanate (IPDI). Isocyanates have two groups of isocyanates on each



279 molecule. Diphenylmethane diisocyanate is an exception owing to its structure consisting of  
 280 two, three, four, or more isocyanate groups (Nohra et al. 2013). The use of PEG 400 in this  
 281 study as a chain extender for polyurethane increases the chain mobility of polyurethane at an  
 282 optimal amount. The properties of polyurethane are contributed by hard and soft copolymer  
 283 segments of both polyol monomers and MDI. This makes the hard segment of urethane serves  
 284 as a crosslinking site between the soft segments of the polyol (Leykin et al. 2016).

285



286

287 **Figure 2.** PU production via the pre-polymerization method (Wong & Badri 2012).

288

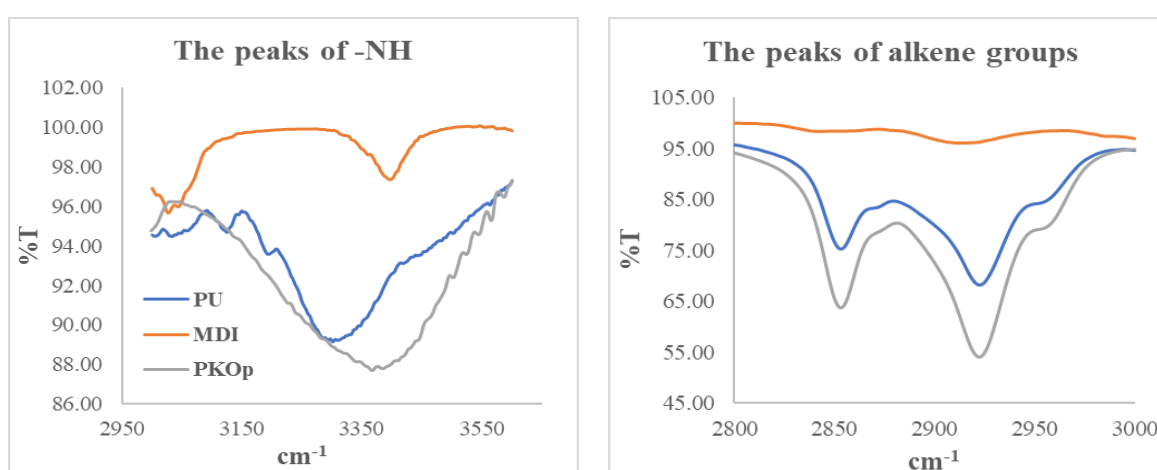
289 The mechanism of the pre-polymerization in urethane chains formation is a  
 290 nucleophilic substitution reaction as studied by Yong et al. (2009). However, this study found  
 291 amines as nucleophiles. Amine attacks carbonyl on isocyanate in MDI in order to form two  
 292 resonance structures of intermediate complexes A and B. Intermediate complex B has a greater  
 293 tendency to react with polyols due to stronger carbonyl (C = O) bonds than C = N bonds on

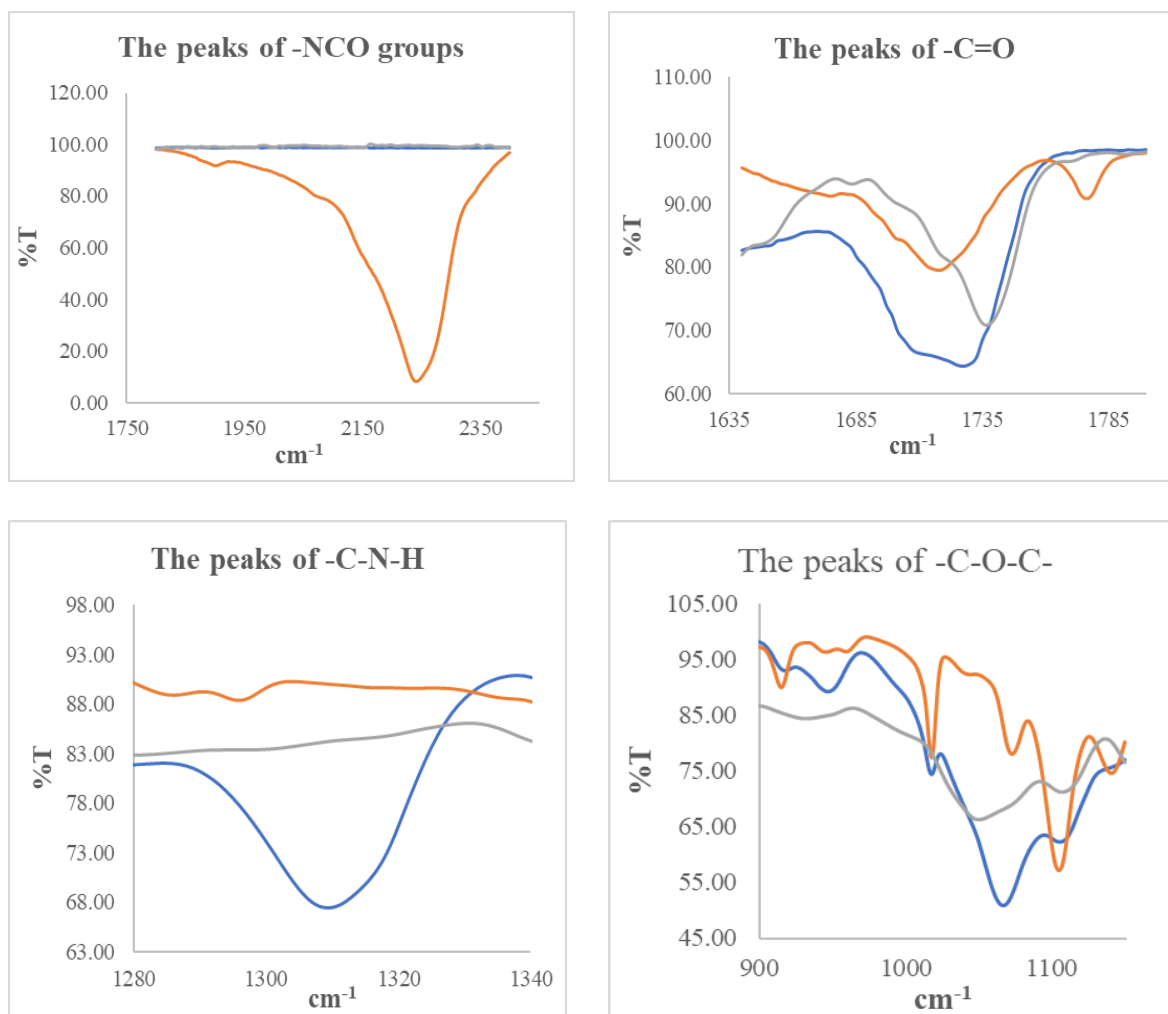
294 intermediate complexes A. Thus, intermediate complex B is more stable than intermediate  
295 complex A, as suggested by previous researchers who have conducted by Wong and Badri  
296 (2012). Moreover, oxygen is more electronegative than nitrogen causing cations ( $H^+$ ) to tend  
297 to attack  $-CN$  bonds compared to  $-CO$ . The combination between long polymer chain and low  
298 cross-linking content gives the polymer elastic properties whereas short-chain and high cross-  
299 linking produce hard and rigid polymers. Cross-linking in polymers consists of three-  
300 dimensional networks with high molecular weight. In some aspects, polyurethane can be a  
301 macromolecule, a giant molecule (Petrovic 2008).

302

303 However, complexes A and B intermediate were produced after the nucleophile of PEG  
304 attacking the isocyanate group in the MDI. However, PEG contains oxygen atoms that are more  
305 electronegative than nitrogen atoms inside the PKOp chemical structure causing the reaction  
306 of nucleophilic substitution that occurs in PKOp. Furthermore, amine has a higher probability  
307 of reacting compared to hydroxyl (Herrington & Hock 1997). Amine with high alkalinity reacts  
308 with carbon atoms on MDI as proposed by Wong and Badri (2012).

309





310 **Figure 3.** FTIR spectra of several important peaks between polyurethane, PKO-p, and MDI

311

312

313

314 The production of intermediate complexes unstabilizes the alkyl ions, nevertheless, the

315 long carbon chains of PKOp ensure the stability of alkyl ions. The addition of PEG in this study

316 is imperative, not merely to increase the chain length of PU but also to avoid the production of

317 urea as a by-product after the NCO group reacts with  $\text{H}_2\text{O}$  from the environment. If the NCO

318 group reacts with the excess water in the environment, the formation of urea and carbon dioxide

319 gas will also occur excessively (**Figure 4**). This reaction can cause a polyurethane foam, not

320 polyurethane film as we studied the film.

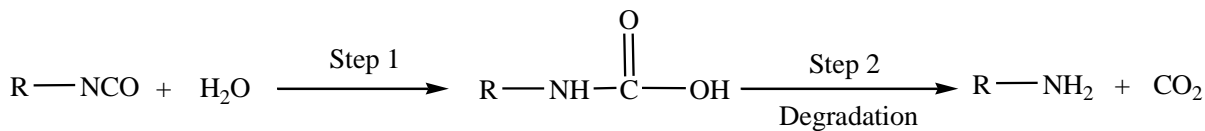
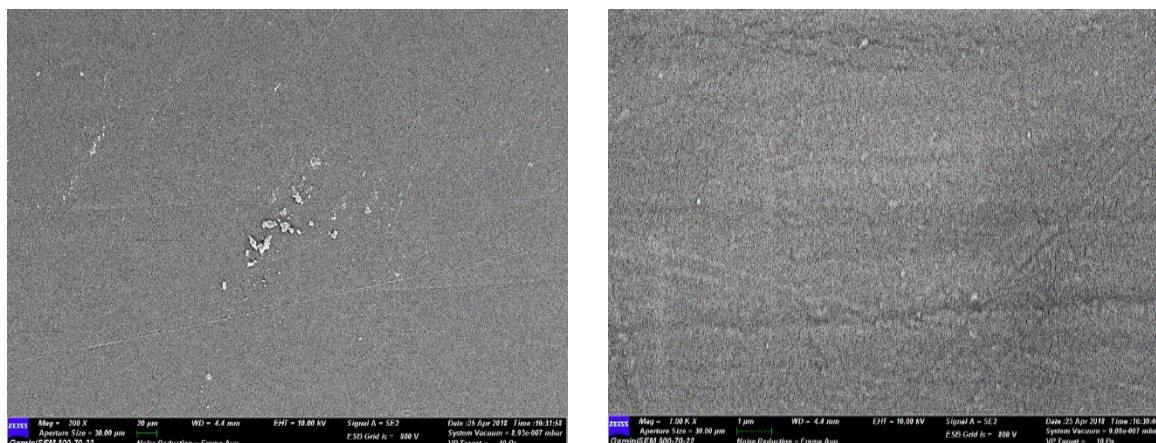


**Figure 4.** The reaction between the NCO group and water producing carbon dioxide

Furthermore, the application of PEG can influence the conductivity of PU whereby Porcarelli et al. (2017) have reported the application of PEG using several molecular weights. PEG 1500 decreased the conductivity of PU in consequence of the semicrystalline phase of PEG 1500 that acted as a poor ion-conducting phase for PU. It is also well known that PEG with a molecular weight of more than 1000 g·mol<sup>-1</sup> tends to crystallize with deleterious effects on room temperature ionic conductivity (Porcarelli et al. 2017).

#### b. Morphological analysis

The Field Emission Scanning Electron Microscope (FESEM) micrograph in **Figure 5** shows the formation of a uniform polymer film contributed by the polymerization method applied. The magnification used for this surface analysis ranged from 200 to 5000 ×. The polymerization method can also avoid the failure of the reaction in PU polymerization. Furthermore, no trace of separation was detected by FESEM. This has also been justified by the wavelengths obtained by the FTIR spectra above.



339 **Figure 5.** The micrograph of polyurethane films was analyzed by FESEM at (a) 200 × and  
340 (b) 5000× magnifications.

341  
342 c. The crosslinking analysis

343 Soxhlet analysis was applied to determine the degree of crosslinking between the hard  
344 segments and the soft segments in the polyurethane. The urethane group on the hard segment  
345 along the polyurethane chain is polar (Cuve & Pascault 1991). Therefore, during the testing, it  
346 was very difficult to dissolve in toluene, as the testing reagent. The degree of crosslinking is  
347 determined by the percentage of the gel content. The analysis result obtained from the Soxhlet  
348 testing indicated a 99.3 % gel content. This is significant in getting a stable polymer at a higher  
349 working temperature (Rogulska et al. 2007).

350

$$\text{Gel content (\%)} = \frac{(0.6 - 0.301) \text{ g}}{0.301 \text{ g}} \times 100\% = 99.33\%$$

351

352

353

354

355

356

357 d. The thermal analysis

358 Thermogravimetric analysis (TGA) can be used to observe the material mass based on  
359 temperature shift. It can also examine and estimate the thermal stability and materials  
360 properties such as the alteration weight owing to absorption or desorption, decomposition,  
361 reduction, and oxidation. The material composition of polymer is specified by analyzing the  
362 temperatures and the heights of the individual mass steps (Alamawi et al. 2019). **Figure 6**  
363 shows the TGA and DTG thermograms of polyurethane. The percentage weight loss (%) is

364 listed in **Table 2**. Generally, only a small amount of weight was observed. It is shown in **Figure**  
 365 **6** in the region of 45 – 180°C. This is due to the presence of condensation on moisture and  
 366 solvent residues.

367

368

**Table2** Weight loss percentage of (wt%) polyurethane film

Sample	% Weight loss (wt%)				Total of weight loss (%)	Residue after 550°C (%)
	T <sub>max</sub> ,	T <sub>d1</sub> ,	T <sub>d2</sub> ,	T <sub>d3</sub> ,		
	°C	200 – 290°C	350 – 500°C	500 – 550°C		
Polyurethane	240	8.04	39.29	34.37	81.7	18.3

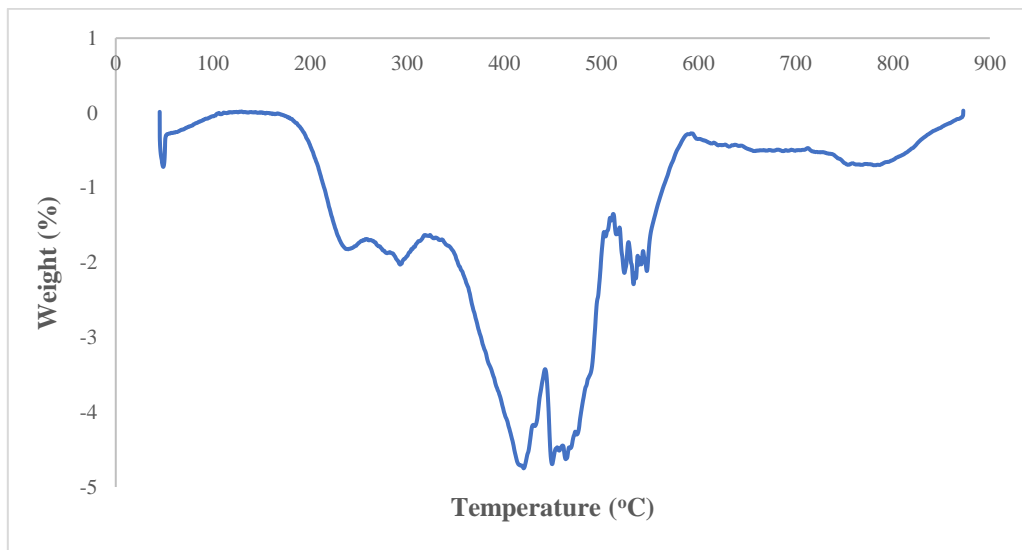
369

370 The bio polyurethane is thermally stable up to 240 °C before it has undergone thermal  
 371 degradation (Agrawal et al. 2017). The first stage of thermal degradation (T<sub>d1</sub>) on polyurethane  
 372 films was shown in the region of 200 – 290 °C as shown in **Figure 6**. The T<sub>d1</sub> is associated with  
 373 degradation of the hard segments of the urethane bond, forming alcohol or degradation of the  
 374 polyol chains and releasing of isocyanates (Berta et al. 2006), primary and secondary amines  
 375 as well as carbon dioxide (Corcuera et al. 2011; Pan & Webster 2012). Meanwhile, the second  
 376 thermal degradation stage (T<sub>d2</sub>) of polyurethane films experienced a weight loss of 39.29 %.  
 377 This endotherm of T<sub>d2</sub> is related to the dimerization of isocyanates to form carbodiimides and  
 378 release CO<sub>2</sub>. The formed carbodiimide reacts with alcohol to form urea. The third stage of  
 379 thermal degradation (T<sub>d3</sub>) is related to the degradation of urea (Berta et al. 2006) and the soft  
 380 segment on polyurethane.

381

382 Generally, DSC analysis exhibited thermal transitions as well as the initial  
 383 crystallization and melting temperatures of the polyurethane (Khairuddin et al. 2018). It serves  
 384 to analyze changes in thermal behavior due to changes occurring in the chemical chain structure  
 385 based on the glass transition temperature (T<sub>g</sub>) of the sample obtained from the DSC thermogram

386 (Figure 7). DSC analysis on polyurethane film was performed in the temperature at the range  
387 100 °C to 200 °C of using nitrogen gas as a blanket as proposed by Furtwengler et al. (2017).  
388 The glass transition temperature ( $T_g$ ) on polyurethane was above room temperature, at 78.1 °C  
389 indicated the state of glass on polyurethane. The presence of MDI contributes to the formation  
390 of hard segments in polyurethanes. Porcarelli et al. (2017) stated that possessing a low glass  
391 transition ( $T_g$ ) may contribute to PU conductivity.



392  
393  
394

**Figure 6.** DTG thermogram of polyurethane film

395 During polymerization, this hard segment restricts the mobility of the polymer chain  
396 (Ren et al. 2013) owing to the steric effect on the benzene ring in the hard segment. The  
397 endothermic peak of acetone used as the solvent in this study was supposedly at 56°C.  
398 However, it was detected in the DSC thermogram nor the TGA thermogram, which indicates  
399 that acetone was removed from the polyurethane during the synthesis process, owing to its  
400 volatile nature. The presence of acetone in the synthesis was to lower the reaction kinetics.

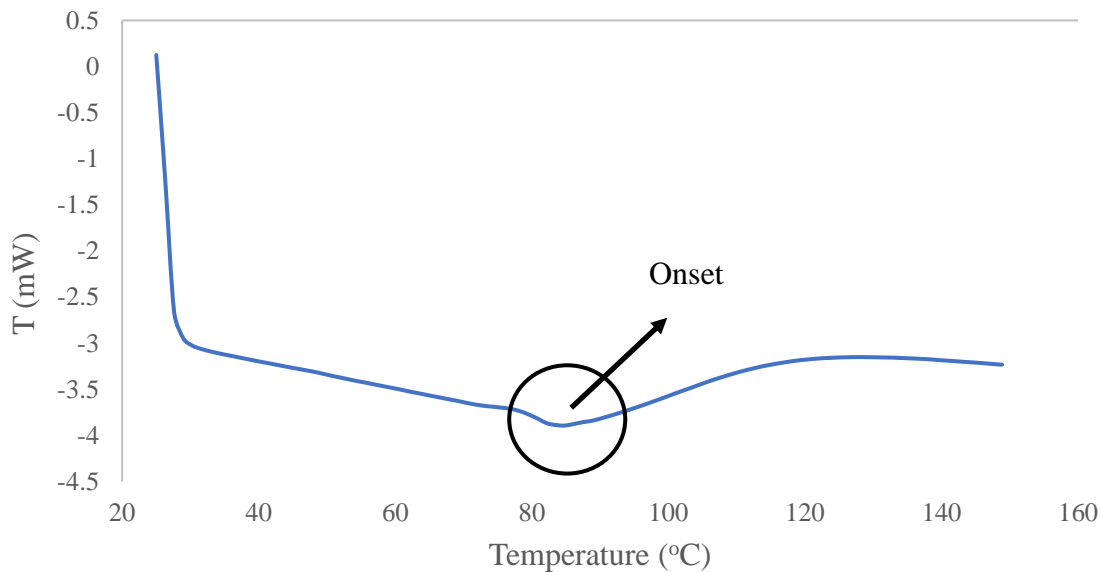


**Figure 7.** DSC thermogram of polyurethane film

e. The solubility and mechanical properties of the polyurethane film

The chemical resistivity of a polymer will be the determinant in performing as a conductor. Thus, its solubility in various solvents was determined by dissolving the polymer in selected solvents such as hexane, benzene, acetone, tetrahydrofuran (THF), dimethylformamide (DMF), and dimethyl sulfoxide (DMSO). On the other hand, the mechanical properties of polyurethane were determined based on the standard testing following ASTM D 638 (Standard Test Method for Tensile Properties of Plastics). The results from the polyurethane film solubility and tensile test are shown in **Table 3**. Polyurethane films were insoluble with acetone, hexane, and benzene and are only slightly soluble in tetrahydrofuran (THF), dimethylformamide (DMF), and dimethyl sulfoxide (DMSO) solutions. While the tensile strength of a PU film indicated how much elongation load the film was capable of withstanding the material before breaking.

**Table 3** The solubility and mechanical properties of the polyurethane film

Parameters	Polyurethane film
------------	-------------------



	Benzene	Insoluble
	Hexane	Insoluble
	Acetone	Insoluble
Solubility	THF	Less soluble
	DMF	Less soluble
	DMSO	Less soluble
Stress (MPa)		8.53
Elongation percentage (%)		43.34
Strain modulus (100) (MPa)		222.10

418

419 The tensile stress, strain, and modulus of polyurethane film also indicated that polyurethane  
420 has good mechanical properties that are capable of being a supporting substrate for the next  
421 stage of the study. In the production of polyurethane, the properties of polyurethane are easily  
422 influenced by the content of MDI and polyol used. The length of the chain and its flexibility  
423 are contributed by the polyol which makes it elastic. High crosslinking content can also produce  
424 hard and rigid polymers. MDI is a major component in the formation of hard segments in  
425 polyurethane. It is this hard segment that determines the rigidity of the PU. Therefore, high  
426 isocyanate content results in higher rigidity on PU (Petrovic et al. 2002). Thus, the polymer has  
427 a higher resistance to deformation and more stress can be applied to the PU.

428

429

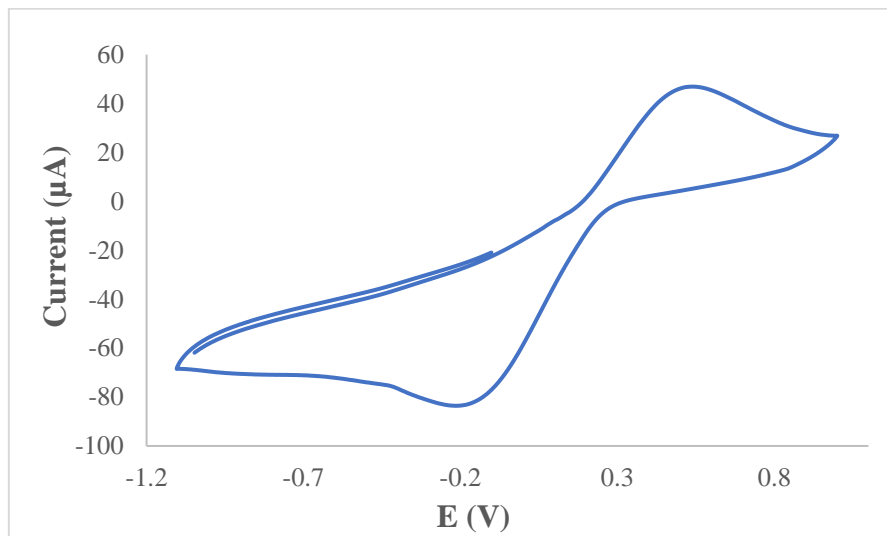
430

431

432 f. The conductivity of the polyurethane as a polymeric film on SPE

433 Polyurethane film was deposited onto the screen-printed electrode by casting method as shown  
434 in **Figure 1**. After that, the modified electrode was analyzed using cyclic voltammetry (CV)  
435 and differential pulse voltammetry (DPV) in order to study the behavior of the modified  
436 electrode. The modified electrode was tested in a  $0.1 \text{ mmol}\cdot\text{L}^{-1}$  KCl solution containing  $5$   
437  $\text{mmol}\cdot\text{L}^{-1}$  ( $\text{K}_3\text{Fe}(\text{CN})_6$ ). The use of potassium ferricyanide is intended to increase the sensitivity  
438 of the KCl solution. The conductivity of the modified electrode was studied. The electrode was  
439 analyzed by cyclic voltammetry method with a potential range of  $-1.00$  to  $+1.00$  with a scan  
440 rate of  $0.05 \text{ V}\cdot\text{s}^{-1}$ . The voltammograms at the electrode have shown a specific redox reaction.  
441 Furthermore, the conductivity of the modified electrode is lower due to the use of polyurethane.  
442 This occurs due to PU being a natural polymer produced from the polyol of palm kernel oil.  
443 The electrochemical signal at the electrode is low if there is a decrease in electrochemical  
444 conductivity (El - Raheem et al. 2020). It can be concluded that polyurethane is a bio-polymer  
445 with a low current value. The current of the modified electrode was found at  $5.3 \times 10^{-5} \text{ A}$  or  $53$   
446  $\mu\text{A}$ . Nevertheless, the current of PU in this study showed better results compared to Bahrami  
447 et al. (2019) that reported the current of PU as  $1.26 \times 10^{-6} \text{ A}$ , whereas Li et al. (2019) reported  
448 the PU current in their study was even very low, namely  $10^{-14} \text{ A}$ . The PU can obtain a current  
449 owing to the benzene ring in the hard segment (MDI) could exhibit the current by inducing  
450 electron delocalization along the polyurethane chain (Wong et al. 2014). The PU can also  
451 release a current caused by PEG. The application of PEG as polyol has been studied by  
452 Porcarelli et al. (2017), that reported that the current of PU based on PEG – polyol was  $9.2 \times$   
453  $10^{-8} \text{ A}$ .

454 According to **Figure 8**, it can be concluded that the anodic peak present in the modified  
455 electrode was at  $+0.5 \text{ V}$ , it also represented the anodic peak of the SPE-PU. The first oxidation  
456 signal on both electrodes ranged from  $-0.2$  to  $+1.0 \text{ V}$ , which revealed a particular oxidative  
457 peak at a potential of  $+0.5 \text{ V}$ .



459

460 **Figure 8.** The voltammogram of SPE – PU modified electrode after analyzed using cyclic  
 461 voltammetry (CV) technique

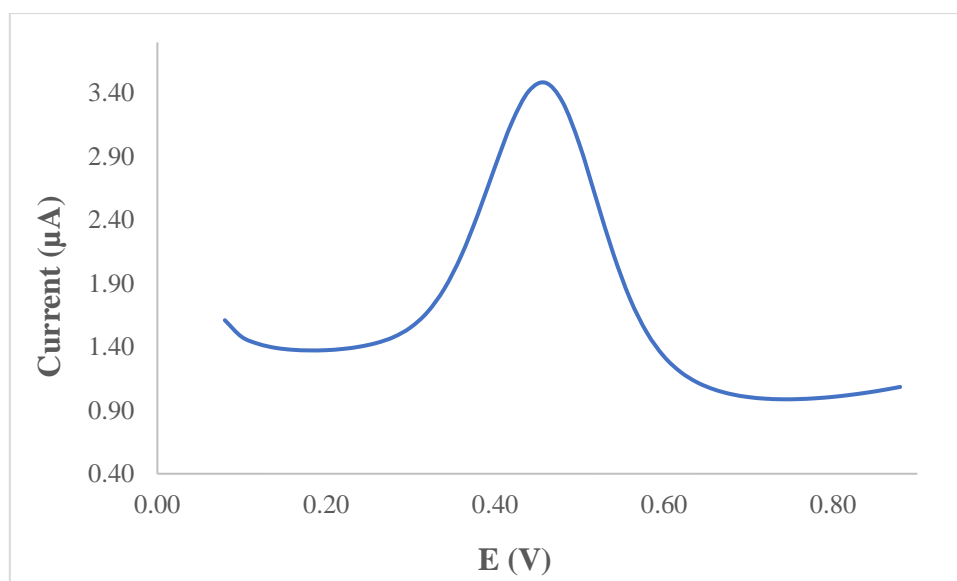
462

463 **Figure 9** also presents the DPV voltammogram of the modified electrode. DPV is a  
 464 measurement based on the difference in potential pulses that produce an electric current.  
 465 Scanning the capability pulses to the working electrode will produce different currents. Optimal  
 466 peak currents will be produced to the reduction capacity of the redox material. The peak current  
 467 produced is proportional to the concentration of the redox substance and can be detected up to  
 468 a concentration below  $10^{-8}$  M. DPV was conducted to obtain the current value that is more  
 469 accurate than CV (Lee et al. 2018).

470 This study used a redox pair ( $K_3Fe(CN)_6$ ) as a test device (probe). The currents generated by  
 471 SPE-PU and proved by CV and DPV have shown conductivity on polyurethane films. This  
 472 suggests that polyurethane films can conduct electron transfer. The electrochemical area on the  
 473 modified electrode can be calculated using the formula from Randles-Sevcik (Butwong et al.  
 474 2019), where the electrochemical area for SPE-PU is considered to be A, using Equation 2:

475

$$\text{Current of SPE-PU, } I_p = 2.65 \times 10^5 A C n^{3/2} \nu^{1/2} D^{1/2} \quad (2)$$



476  
477 **Figure 9.** The voltammogram of SPE – PU modified electrode after analyzed using  
478 differential pulse voltammetry (DPV) technique  
479

480 Where,  $n - 1$  is the amount of electron transfer involved, while  $C$  is the solvent concentration  
481 used ( $\text{mmol}\cdot\text{L}^{-1}$ ) and the value of  $D$  is the diffusion constant of  $5 \text{ mmol}\cdot\text{L}^{-1}$  at  $(\text{K}_3\text{Fe}(\text{CN})_6)$   
482 dissolved using  $0.1 \text{ mmol}\cdot\text{L}^{-1}$  KCl. The estimated surface area of the electrode (**Figure 1**) was  
483  $0.2 \text{ cm}^2$  where the length and width of the electrode used during the study was  $0.44 \text{ cm} \times 0.44$   
484  $\text{cm}$  while the surface area of the SPE-PU was  $0.25 \text{ cm}^2$  with the length and width of the  
485 electrode estimated at  $0.5 \text{ cm} \times 0.5 \text{ cm}$ , and causing the SPE-PU has a larger surface. The  
486 corresponding surface concentration ( $\tau$ ) ( $\text{mol}/\text{cm}^2$ ) is measured using Equation 3.

$$487 \quad I_p = (n^2 F^2 / 4RT) A \tau v \quad (3)$$

488  $I_p$  is the peak current (A), while  $A$  is the surface area of the electrode ( $\text{cm}^2$ ), the value of  $v$  is  
489 the applied scan rate (mV/s) and  $F$  is the Faraday constant ( $96,584 \text{ C}/\text{mol}$ ),  $R$  is the constant  
490 ideal gas ( $8.314 \text{ J}/\text{mol K}$ ) and  $T$  is the temperature used during the experiment being conducted  
491 ( $298 \text{ K}$ ) (Koita et al. 2014). The application of PKOp to produce a conducting polymer will be  
492 a great prospect as this material can be employed in the analytical industry in order to modify  
493 electrodes for electrochemical purposes.

494 Furthermore, number of palm oils is abundant in Malaysia and Indonesia such as palm stearin  
495 and refined-bleached-deodorized (RBD) palm oil. They have several benefits such as being  
496 sustainable, cheap, and environmentally biodegradable. These palms are the potential to  
497 produce biomaterials that can be used to replace other polymers that are chemical-based (Tajao  
498 et al. 2021). Several studies have been reported the application of PU to produce elastic  
499 conductive fibres and films owing to it being highly elastic, scratch-resistant, and adhesive  
500 (Tadese et al. 2019), thus it is easy for PU to adhere to the screen-printed electrode to modify  
501 the electrode. PU is also being used as a composite material to make elastic conducting  
502 composite films (Khatoon & Ahmad 2017).

503

#### 504 **4. Conclusion**

505 Polyurethane film was prepared by pre-polymerization between palm kernel oil-based polyol  
506 (PKO-p) with MDI. The presence of PEG 400 as the chain extender formed freestanding  
507 flexible film. Acetone was used as the solvent to lower the reaction kinetics since the pre-  
508 polymerization was carried out at room temperature. The formation of urethane links (NHCO  
509 – backbone) after polymerization was confirmed by the absence of N=C=O peak at  $2241\text{ cm}^{-1}$   
510 and the presence of N-H peak at  $3300\text{ cm}^{-1}$ , carbonyl (C=O) at  $1710\text{ cm}^{-1}$ , carbamate (C-N) at  
511  $1600\text{ cm}^{-1}$ , ether (C-O-C) at  $1065\text{ cm}^{-1}$ , benzene ring (C = C) at  $1535\text{ cm}^{-1}$  in the bio  
512 polyurethane chain structure. Soxhlet analysis for the determination of crosslinking on  
513 polyurethane films has yielded a high percentage of 99.33 %. This is contributed by the hard  
514 segments formed from the reaction between isocyanates and hydroxyl groups causing  
515 elongation of polymer chains. FESEM analysis exhibited an absence of phase separation and  
516 smooth surface. Meanwhile, the current of the modified electrode was found at  $5.2 \times 10^{-5}\text{ A}$ .  
517 This bio polyurethane film can be used as a conducting bio-polymer and it is very useful for

518 other studies such as electrochemical sensor purposes. Furthermore, advanced technologies are  
519 promising and the future of bio-based polyol looks very bright.

## 520 **5. Acknowledgment**

521 The authors would like to thank Alma Ata University for the sponsorship given to the first  
522 author. We would like to also, thank The Department of Chemical Sciences, Universiti  
523 Kebangsaan Malaysia for the laboratory facilities and CRIM, UKM for the analysis  
524 infrastructure.

525

## 526 **6. Conflict of Interest**

527 The authors declare no conflict of interest.

528

## 529 **7. References**

530 Agrawal, A., Kaur, R., Walia, R. S. (2017). PU foam derived from renewable sources:  
531 Perspective on properties enhancement: An overview. *European Polymer Journal*. **95**:  
532 255 – 274.

533 Akindoyo, J. O., Beg, M.D.H., Ghazali, S., Islam, M.R., Jeyaratnam, N. & Yuvaraj, A.R.  
534 (2016). Polyurethane types, synthesis, and applications – a review. *RSC Advances*. **6**:  
535 114453 – 114482.

536 Alamawi, M. Y., Khairuddin, F. H., Yusoff, N. I. M., Badri, K., Ceylan, H. (2019).  
537 Investigation on physical, thermal, and chemical properties of palm kernel oil polyobio-  
538 based binder as a replacement for bituminous binder. *Construction and Building*  
539 *Materials*. **204**: 122 – 131.

540 Alqarni, S. A., Hussein, M. A., Ganash, A. A. & Khan, A. (2020). Composite material-based  
541 conducting polymers for electrochemical sensor applications: a mini-review.  
542 *BioNanoScience*. **10**: 351 – 364.

543 Badan, A., Majka, T. M. (2017). The influence of vegetable – oil based polyols on physico –  
544 mechanical and thermal properties of polyurethane foams. *Proceedings*. 1 – 7.

545 Badri, K.H. (2012) Biobased polyurethane from palm kernel oil-based polyol. In Polyurethane;  
546 Zafar, F., Sharmin, E., Eds. InTechOpen: Rijeka, Croatia. pp. 447–470.

547 Badri, K.H., Ahmad, S.H. & Zakaria, S. 2000. Production of a high-functionality RBD palm  
548 kernel oil-based polyester polyol. *Journal of Applied Polymer Science*. **81**(2): 384 – 389.

549 Baig, N., Sajid, M. and Saleh, T. A. 2019. Recent trends in nanomaterial–modified electrodes  
550 for electroanalytical applications. *Trends in Analytical Chemistry*. **111**: 47 – 61.

551 Berta, M., Lindsay, C., Pans, G., & Camino, G. (2006). Effect of chemical structure on  
552 combustion and thermal behaviour of polyurethane elastomer layered silicate  
553 nanocomposites. *Polymer Degradation and Stability*. **91**: 1179-1191.

554 Borowicz, M., Sadowska, J. P., Lubczak, J. & Czuprynski, B. (2019). Biodegradable, flame–  
555 retardant, and bio-based rigid polyurethane/polyisocyanurate foams for thermal  
556 insulation application. *Polymers*. **11**: 1816 – 1839.

557 Butwong, N., Khajonklin, J., Thongbor, A. & Luong, J.H.T. (2019). Electrochemical sensing  
558 of histamine using a glassy carbon electrode modified with multiwalled carbon nanotubes  
559 decorated with Ag – Ag<sub>2</sub>O nanoparticles. *Microchimica Acta*. **186** (11): 1 – 10.

560 Chokkareddy, R., Thondavada, N., Kabane, B. & Redhi, G. G. (2020). A novel ionic liquid  
561 based electrochemical sensor for detection of pyrazinamide. *Journal of the Iranian*  
562 *Chemical Society*. **18**: 621 – 629.

563 Chokkareddy, R., Kanchi, S. & Inamuddin (2020). Simultaneous detection of ethambutol and  
564 pyrazinamide with IL@CoFe<sub>2</sub>O<sub>4</sub>NPs@MWCNTs fabricated glassy carbon electrode.  
565 *Scientific Reports*. **10**: 13563.

566 Clemitson, I. (2008). Castable Polyurethane Elastomers. Taylor & Francis Group, New York.  
567 doi:10.1201/9781420065770.

568 Corcuera, M.A., Rueda, L., Saralegui, A., Martin, M.D., Fernandez-d'Arlas, B., Mondragon,  
569 I. & Eceiza, A. (2011). Effect of diisocyanate structure on the properties and  
570 microstructure of polyurethanes based on polyols derived from renewable resources.  
571 *Journal of Applied Polymer Science*. **122**: 3677-3685.

572 Cuve, L. & Pascault, J.P. (1991). Synthesis and properties of polyurethanes based on  
573 polyolefine: Rigid polyurethanes and amorphous segmented polyurethanes prepared in  
574 polar solvents under homogeneous conditions. *Polymer*. **32** (2): 343- 352.

575 Degefu, H., Amare, M., Tessema, M. & Admassie, S. (2014). Lignin modified glassy carbon  
576 electrode for the electrochemical determination of histamine in human urine and wine  
577 samples. *Electrochimica Acta*. **121**: 307 – 314.

578 Dzulkipli, M. Z., Karim, J., Ahmad, A., Dzulkurnain, N. A., Su'ait, M S., Fujita, M. Y., Khoon,  
579 L. T. & Hassan, N. H. (2021). The influences of 1-butyl-3-methylimidazolium  
580 tetrafluoroborate on electrochemical, thermal and structural studies as ionic liquid gel  
581 polymer electrolyte. *Polymers*. **13** (8): 1277 – 1294.

582 El-Raheem, H.A., Hassan, R.Y.A., Khaled, R., Farghali, A. & El-Sherbiny, I.M. (2020).  
583 Polyurethane-doped platinum nanoparticles modified carbon paste electrode for the  
584 sensitive and selective voltammetric determination of free copper ions in biological  
585 samples. *Microchemical Journal*. **155**: 104765.

586 Fei, T., Li, Y., Liu, B. & Xia, C. (2019). Flexible polyurethane/boron nitride composites with  
587 enhanced thermal conductivity. *High Performance Polymers*. **32** (3): 1 – 10.

588 Furtwengler, P., Perrin R., Redl, A. & Averous, L. (2017). Synthesis and characterization of  
589 polyurethane foams derived of fully renewable polyesters polyols from sorbitol.  
590 *European Polymer Journal*. **97**: 319 – 327.

591 Ghosh, S., Ganguly, S., Remanan, S., Mondal, S., Jana, S., Maji, P. K., Singha, N., Das, N. C.  
592 (2018). Ultra-light weight, water durable and flexible highly electrical conductive



593 polyurethane foam for superior electromagnetic interference shielding materials. *Journal*  
594 *of Materials Science: Materials in Electronics*. **29**: 10177 – 10189.

595 Guo, S., Zhang, C., Yang, M., Zhou, Y., Bi, C., Lv, Q. & Ma, N. (2020). A facile and sensitive  
596 electrochemical sensor for non – enzymatic glucose detection based on three –  
597 dimensional flexible polyurethane sponge decorated with nickel hydroxide. *Analytica*  
598 *Chimica Acta*. **1109**: 130 – 139.

599 Hamuzan, H.A. & Badri, K.H. (2016). The role of isocyanates in determining the viscoelastic  
600 properties of polyurethane. *AIP Conference Proceedings*. 1784, Issue 1.

601 Harmayani, E., Aprilia, V. & Marsono, Y. (2014). Characterization of glucomannan from  
602 *Amorphophallus oncophyllus* and its prebiotic activity in vivo. *Carbohydrate Polymers*.  
603 **112**: 475-79.

604 Herrington, R. & Hock, K. (1997). Flexible polyurethane foams. 2nd Edition. Dow Chemical  
605 Company. Midlan.

606 Inayatullah, A., Badrul, H.A., Munir, M.A. (2021). Fish analysis containing biogenic amines  
607 using gas chromatography flame ionization detector. *Science and Technology Indonesia*.  
608 **6** (1): 1-7.

609 Janpoung, P., Pattanauwat, P. & Potiyaraj, P. (2020). Improvement of electrical conductivity  
610 of polyurethane/polypyrrole blends by graphene. *Key Engineering Materials*. **831**: 122 –  
611 126.

612 Khairuddin, F.H., Yusof, N. I. M., Badri, K., Ceylan, H., Tawil, S. N. M. (2018). Thermal,  
613 chemical and imaging analysis of polyurethane/cecabase modified bitumen. *IOP Conf.*  
614 *Series: Materials Science and Engineering*. **512**: 012032.

615 Khatoun, H., Ahmad, S. (2017). A review on conducting polymer reinforced polyurethane  
616 composites. *Journal of Industrial and Engineering Chemistry*. **53**: 1 – 22.

617 Kilele, J. C., Chokkareddy, R., Rono, N. & Redhi, G. G. (2020). A novel electrochemical  
618 sensor for selective determination of theophylline in pharmaceutical formulations.  
619 *Journal of the Taiwan Institute of Chemical Engineers*. 111: 228-238.

620 Kilele, J. C., Chokkareddy, R. & Redhi, G. G. (2021). Ultra-sensitive electrochemical sensor  
621 for fenitrothion pesticide residues in fruit samples using IL@CoFe<sub>2</sub>ONPs@MWCNTs  
622 nanocomposite. *Microchemical Journal*. **164**: 106012.

623 Koita, D., Tzedakis, T., Kane, C., Diaw, M., Sock, O. & Lavedan, P. (2014). Study of the  
624 histamine electrochemical oxidation catalyzed by nickel sulfate. *Electroanalysis*. **26 (10)**:  
625 2224 – 2236.

626 Kotal, M., Srivastava, S.K. & Paramanik, B. (2011). Enhancements in conductivity and thermal  
627 stabilities of polyurethane/polypyrrole nanoblends. *The Journal of Physical Chemistry*  
628 *C*. **115 (5)**: 1496 – 1505.

629 Ladan, M., Basirun, W.J., Kazi, S.N., Rahman, F.A. (2017). Corrosion protection of AISI 1018  
630 steel using Co-doped TiO<sub>2</sub>/polypyrrole nanocomposites in 3.5% NaCl solution.  
631 *Materials Chemistry and Physics*. **192**: 361 – 373.

632 Lampman, G.M., Pavia, D.L., Kriz, G.S. & Vyvyan, J.R. (2010). Spectroscopy. 4th Edition.  
633 Brooks/Cole Cengage Learning, Belmont, USA.

634 Lee, K.J., Elgrishi, N., Kandemir, B. & Dempsey, J.L. 2018. Electrochemical and spectroscopic  
635 methods for evaluating molecular electrocatalysts. *Nature Reviews Chemistry*. **1(5)**: 1 -  
636 14.

637 Leykin, A., Shapovalov, L. & Figovsky, O. (2016). Non – isocyanate polyurethanes –  
638 Yesterday, today and tomorrow. *Alternative Energy and Ecology*. **191 (3 – 4)**: 95 – 108.

639 Li, H., Yuan, D., Li, P., He, C. (2019). High conductive and mechanical robust carbon  
640 nanotubes/waterborne polyurethane composite films for efficient electromagnetic  
641 interference shielding. *Composites Part A*. **121**: 411 – 417.

642 Nakthong, P., Kondo, T., Chailapakul, O., Siangproh, W. (2020). Development of an  
643 unmodified screen-printed electrode for nonenzymatic histamine detection. *Analytical*  
644 *Methods*. **12**: 5407 – 5414.

645 Mishra, K., Narayan, R., Raju, K.V.S.N. & Aminabhavi, T.M. (2012). Hyperbranched  
646 polyurethane (HBPU)-urea and HBPU-imide coatings: Effect of chain extender and  
647 NCO/OH ratio on their properties. *Progress in Organic Coatings*. **74**: 134 – 141.

648 Mohd Noor, M. A., Tuan Ismail, T. N. M., Ghazali, R. (2020). Bio-based content of oligomers  
649 derived from palm oil: Sample combustion and liquid scintillation counting technique.  
650 *Malaysia Journal of Analytical Science*. **24**: 906 – 917.

651 Munir, M. A., Heng, L. Y., Badri, K. H. (2021). Polyurethane modified screen-printed  
652 electrode for the electrochemical detection of histamine in fish. *IOP Conference Series:*  
653 *Earth and Environmental Science*. **880**: 012032.

654 Munir, M.A., Mackeen, M.M.M., Heng, L.Y. Badri, K.H. (2021). Study of histamine detection  
655 using liquid chromatography and gas chromatography. *ASM Science Journal*. **16**: 1-9.

656 Mutsuhisa F., Ken, K. & Shohei, N. (2007). Microphase separated structure and mechanical  
657 properties of norbornane diisocyanate-based polyurethane. *Polymer*. **48 (4)**: 997 – 1004.

658 Mustapha, R., Rahmat, A. R., Abdul Majid, R., Mustapha, S. N. H. (2019). Vegetable oil-based  
659 epoxy resins and their composites with bio-based hardener: A short review. *Polymer-*  
660 *Plastic Technology and Materials*. **58**: 1311 – 1326.

661 Nohra, B., Candy, L., Blancos, J.F., Guerin, C., Raoul, Y. & Mouloungui, Z. (2013). From  
662 petrochemical polyurethanes to bio-based polyhydroxyurethanes. *Macromolecules*. **46**  
663 **(10)**: 3771 – 3792.

664 Nurwanti, E., Uddin, M., Chang, J.S., Hadi, H., Abdul, S.S., Su, E.C.Y., Nursetyo, A.A.,  
665 Masud, J.H.B. & Bai, C.H. (2018). Roles of sedentary behaviors and unhealthy foods in

666 increasing the obesity risk in adult men and women: A cross-sectional national study.  
667 *Nutrients*. **10** (6): 704-715.

668 Pan, T. & Yu, Q. (2016). Anti-corrosion methods and materials comprehensive evaluation of  
669 anti-corrosion capacity of electroactive polyaniline for steels. *Anti – Corrosion Methods  
670 and Materials*. **63**: 360 – 368.

671 Pan, X. & Webster, D.C. (2012). New biobased high functionality polyols and their use in  
672 polyurethane coatings. *ChemSusChem*. **5**: 419-429.

673 Petrovic, Z.S. (2008). Polyurethanes from vegetable oils. *Polymer Reviews*. **48** (1): 109 – 155.

674 Porcarelli, L., Manojkumar, K., Sardon, H., Llorente, O., Shaplov, A. S., Vijayakrishna, K.,  
675 Gerbaldi, C., Mecerreyes, D. (2017). Single ion conducting polymer electrolytes based  
676 on versatile polyurethanes. *Electrochimica Acta*. **241**: 526 – 534.

677 Priya, S. S., Karthika, M., Selvasekarapandian, S. & Manjuladevi, R. (2018). Preparation and  
678 characterization of polymer electrolyte based on biopolymer I-carrageenan with  
679 magnesium nitrate. *Solid State Ionics*. **327**: 136 – 149.

680 Ren, D. & Frazier, C.E. (2013). Structure–property behaviour of moisture-cure polyurethane  
681 wood adhesives: Influence of hard segment content. *Adhesion and Adhesives*. **45**: 118-  
682 124.

683 Rogulska, S.K., Kultys, A. & Podkoscielny, W. (2007). Studies on thermoplastic polyurethanes  
684 based on newdiphe – derivative diols. II. Synthesis and characterization of segmented  
685 polyurethanes from HDI and MDI. *European Polymer Journal*. **43**: 1402 – 1414.

686 Romaskevicius, T., Budriene, S., Pielichowski, K. & Pielichowski, J. (2006). Application of  
687 polyurethane-based materials for immobilization of enzymes and cells: a review.  
688 *Chemija*. **17**: 74 – 89.

689 Sengodu, P. & Deshmukh, A. D. (2015). Conducting polymers and their inorganic composites  
690 for advanced Li-ion battery electrolytes: a review. *RSC Advances*. **5**: 42109 – 42130.

691 Septevani, A. A., Evans, D. A. C., Chaleat, C., Martin, D. J., Annamalai, P. K. (2015). A  
692 systematic study substituting polyether polyol with palm kernel oil based polyester  
693 polyol in rigid polyurethane foam. *Industrial Crops and Products*. **66**: 16 – 26.

694 Su'ait, M. S., Ahmad, A., Badri, K. H., Mohamed, N. S., Rahman, M. Y. A., Ricardi, C. L. A.  
695 & Scardi, P. The potential of polyurethane bio-based solid polymer electrolyte for  
696 photoelectrochemical cell application. *International Journal of Hydrogen Energy*. **39** (6):  
697 3005 – 3017.

698 Tadesse, M. G., Mengistie, D. A., Chen, Y., Wang, L., Loghin, C., Nierstrasz, V. (2019).  
699 Electrically conductive highly elastic polyamide/lycra fabric treated with PEDOT: PSS  
700 and polyurethane. *Journal of Materials Science*. **54**: 9591 – 9602.

701 Tajau, R., R, Rosiah, Alias, M. S., Mudri, N. H., Halim, K. A. A., Harun, M. H., Isa, N. M.,  
702 Ismail, R. C., Faisal, S. M., Talib, M., Zin, M. R. M., Yusoff, I. I., Zaman, N. K., Illias,  
703 I. A. (2021). Emergence of polymeric material utilising sustainable radiation curable  
704 palm oil-based products for advanced technology applications. *Polymers*. **13**: 1865 –  
705 1886.

706 Tran, V.H., Kim, J.D., Kim, J.H., Kim, S.K., Lee, J.M. (2020). Influence of cellulose  
707 nanocrystal on the cryogenic mechanical behaviour and thermal conductivity of  
708 polyurethane composite. *Journal of Polymers and The Environment*. **28**: 1169 – 1179.

709 Viera, I.R.S., Costa, L.D.F.D.O., Miranda, G.D.S., Nardehhcia, S., Monteiro, M.S.D. S.D.B.,  
710 Junior, E.R. & Delpech, M.C. (2020). Waterborne poly (urethane – urea)s  
711 nanocomposites reinforced with clay, reduced graphene oxide and respective hybrids:  
712 Synthesis, stability and structural characterization. *Journal of Polymers and The  
713 Environment*. **28**: 74 – 90.

714 Wang, B., Wang, L., Li, X., Liu, Y., Zhang, Z., Hedrick, E., Safe, S., Qiu, J., Lu, G. & Wang,  
715 S. (2018). Template-free fabrication of vertically–aligned polymer nanowire array on the

716 flat–end tip for quantifying the single living cancer cells and nanosurface interaction. a  
717 *Manufacturing Letters*. **16**: 27 – 31.

718 Wang, J., Xiao, L., Du, X., Wang, J. & Ma, H. (2017). Polypyrrole composites with carbon  
719 materials for supercapacitors. *Chemical Papers*. **71** (2): 293 – 316.

720 Wong, C.S. & Badri, K.H. (2012). Chemical analyses of palm kernel oil-based polyurethane  
721 prepolymer. *Materials Sciences and Applications*. **3**: 78 – 86.

722 Wong, C. S., Badri, K., Ataollahi, N., Law, K., Su'ait, M. S., Hassan, N. I. (2014). Synthesis  
723 of new bio–based solid polymer electrolyte polyurethane – LiClO<sub>4</sub> via prepolymerization  
724 method: Effect of NCO/OH ratio on their chemical, thermal properties and ionic  
725 conductivity. *World Academy of Science, Engineering and Technology, International*  
726 *Journal of Chemical, Molecular, Nuclear, Materials and Metallurgical Engineering*. **8**:  
727 1243 – 1250.

728 Yong, Z., Bo, Z.M., Bo, W., Lin, J.Z. & Jun, N. (2009). Synthesis and properties of novel  
729 polyurethane acrylate containing 3-(2-Hydroxyethyl) isocyanurate segment. *Progress in*  
730 *Organic Coatings*. **67**: 264 – 268

731 Zia, K. M., Anjum, S., Zuber, M., Mujahid, M. & Jamil, T. (2014). Synthesis and molecular  
732 characterization of chitosan based polyurethane elastomers using aromatic diisocyanate.  
733 *International of Journal of Biological Macromolecules*. **66**: 26 – 32.

734  
735  
736  
737  
738  
739  
740

## Comments for Reviewers

741

742

743 1. The reported electrical properties are misleading and incorrect. A current of 53 microamps  
744 signifies nothing on its own, and it cannot be used as the basis of a comparison of the  
745 authors' polymer with other polymers. The mentions of "conductivity" in the following  
746 sentences should be corrected or preferably the sentences should be deleted completely:

747

748 **Answer:**

749

750 The corrections have been made following the suggestion from reviewers.

751

752 2. Lines 432-435: "Nevertheless, the electroconductivity of PU in this study shows better  
753 conductivity several times compared to Bahrami et al. (2019) that reported the conductivity  
754 of PU as  $1.26 \times 10^{-6}$  A, whereas Li et al. (2019) reported the PU conductivity in their study  
755 was even very low, namely 10-14 A. "

756

757 **Answer:**

758

759 The corrections have been made following the suggestion from reviewers.

760 So, these lines have been revised according to the reviewer's suggestions.

761

762 3. and in lines 438-440: "The application of PEG as polyol has been studied by Porcarelli et  
763 al. (2017), that reported that the conductivity of PU based on PEG – polyol was  $9.2 \times 10^{-8}$ .  
764 (This sentence doesn't even mention the units of the reported conductivity.)

765

766 **Answer:**

767

768 The units of the reported conductivity have been added and revised based on the reviewer's  
769 suggestion.

770

771 4. The English is still poor and hard to follow in some places. This includes missing verbs,  
772 e.g. line 420 "Polyurethane film deposited" should be "Polyurethane film was deposited".;  
773 orthographic errors e.g. lines 123-125 "SPE becomes the best solution owing to its frugal  
774 manufacture, tiny size, able to produce on large-scale and can be applied for on-site  
775 detection".

776

777 **Answer:**

778

779 The grammars in this manuscript have been revised. The missing verb in Line 436 has been  
780 added.

781 Lines 126-128 have been rephrased.

782

783 5. Typographic errors should be corrected e.g. line 89: change Pus to PUs; and lines 138-139  
784 "Polyurethane is possible to become an advanced frontier material is chemically modified

785 electrodes." As noted by the reviewer, in line 299 "spectrums" is an incorrect word, which  
786 should change to "spectra".

787

788 **Answer:**

789

790 Lines 138-139 have been revised and they are shown in lines 141-143.

791

792 The spectrum words in this manuscript have been changed to spectra and the correction can  
793 be seen at lines: 250, 253, 315, and 342.

794

795

796 6. Also repetitious or awkward sentences should be rewritten or deleted, e.g. line 53 "The  
797 application of petroleum as a polyol in order to produce polyurethane has been applied." or  
798 lines 56-57 "These reasons have been considered and finding utilizing plants that can be  
799 used as alternative polyols should be done immediately."

800

801 **Answer:**

802

803 Lines 55-64 have been rephrased.

804

805

806 7. The sentence in lines 37-38 must be deleted; readers of IJPS don't need to be told what a  
807 polymer is! The authors are strongly advised to seek the help of a fluent English speaker  
808 when they revise their manuscript, or to use a professional scientific editing service.

809

810 **Answer:**

811

812 The suggestion of the reviewer has been followed.

813



[← BACK](#) [DASHBOARD / ARTICLE DETAILS](#)

Updated on 2022-02-15

Version 6

# Design and Synthesis of Conducting Polymer Bio-Based Polyurethane Produced from Palm Kernel Oil

VIEWING AN OLDER VERSION

ID 6815187

Muhammad Abdurrahman Munir <sup>SA CA</sup> <sup>1</sup>,  
Khairiah Haji Badri<sup>2</sup>, Lee Yook Heng<sup>2</sup>  
[+ Show Affiliations](#)

## Article Type

Research Article

## Journal

International Journal of  
Polymer Science

Rydz Joanna

Submitted on 2021-06-14 (2 years ago)

[> Abstract](#)[> Author Declaration](#)[> Files](#) 2[- Editorial Comments](#)



## Decision

Minor Revision Requested

## Message for Author

1. "bio based" is one word and should be spelled the same way throughout the text. Please correct throughout the text.

"Please correct throughout the text" means using the search option to find "bio based" throughout the text. The reviewer only has to point out what is wrong. Please correct in lines 77 and 518.

2. Conclusion: "and the presence of N-H peak at 3300 cm<sup>-1</sup>"

N-H is also not a peak. Neither linkage is a peak.

Please correct on: "and the presence of absorption bands associated with N-H at 3300 cm<sup>-1</sup>"

Please also correct throughout the text!

3. Table 2.

The table shows the "Thermal degradation parameters determined by TGA".

Please remove "% Weight loss (wt%) and thermal degradation (Td)" from the table and leave only two rows with variables (first) and data (second).

Thermogravimetric analysis is measurement of thermal stability of materials. In this method, changes in the weight of a specimen are measured while its temperature is increased. It does not need to be written in the row of table.

In this section (d. The thermal analysis), the authors write both mass and weight.

Please change everything to mass.

Line 369 "Tmax: The temperature of polyurethane started to degrade"

Tmax represents the temperature at the maximum mass-loss rate. "The temperature of material started to degrade" is onset temperature usually given for 5% (T5%) because it is difficult to accurately determine the beginning (Tonset). What temperature did the authors mean?

The authors rightly speak of "individual mass steps"

Td1 is probably temperature at the first onset or at the first Tmax (at the first mass loss step).

Please use the IUPAC nomenclature and correctly present and describe the TGA variables (<https://www.degruyter.com/database/iupac/html>).

## — Response to Revision Request

Muhammad Abdurrahman Munir

13.02.2022

### Your Reply

Dear Dr. Joanna, Thank you for your comments and we have done revisions based on your comments above. Nevertheless, for the comment no. 6, we want to elaborate about the Tmax, where according to Figure 7. DTG thermogram of PU film, Page 19. The temperature was started to degrade at 240 C, that's why we called it as Tmax. So, the Td1, Td2 and Td3 in this manuscript are the thermal degradation

that we have plotted based on the specific region. However, if the revisions we have made are not sufficient, please guide us to improve this manuscript so it can be published to this Journal. We are looking forward to hear from you. Best Regards.

**File**

Manuscript - Munir.docx 902 kB



---

[Hindawi](#) [Privacy Policy](#) [Terms of Service](#) Support: [help@hindawi.com](mailto:help@hindawi.com)

1 **Design and Synthesis of Conducting Polymer Based on Polyurethane**  
2 **Produced from Palm Kernel Oil**

3  
4 Muhammad Abdurrahman Munir<sup>1\*</sup>, Khairiah Haji Badri<sup>2,3</sup>, Lee Yook Heng<sup>2</sup>, Ahlam  
5 Inayatullah<sup>4</sup>, Ari Susiana Wulandari<sup>1</sup>, Emelda<sup>1</sup>, Eliza Dwinta<sup>1</sup>, Veriani Aprillia<sup>5</sup>, Rachmad  
6 Bagas Yahya Supriyono<sup>1</sup>

7  
8 <sup>1</sup>Department of Pharmacy, Faculty of Health Science, Alma Ata University, Daerah Istimewa  
9 Yogyakarta, 55183, Indonesia

10 <sup>2</sup>Department of Chemical Sciences, Faculty of Science and Technology, Universiti  
11 Kebangsaan Malaysia, Bangi, 43600, Malaysia

12 <sup>3</sup>Polymer Research Center, Universiti Kebangsaan Malaysia, Bangi, 43600, Malaysia

13 <sup>4</sup>Faculty of Science and Technology, Universiti Sains Islam Malaysia, Nilai, 71800, Malaysia

14 <sup>5</sup>Department of Nutrition Science, Alma Ata School of Health Sciences, Alma Ata  
15 University, Daerah Istimewa Yogyakarta, 55183, Indonesia

16  
17 \*Email: [muhammad@almaata.ac.id](mailto:muhammad@almaata.ac.id)

18  
19 **Abstract**

20 Polyurethane (PU) is a unique polymer that has versatile processing methods and mechanical  
21 properties upon the inclusion of selected additives. In this study, a freestanding **bio based**  
22 **polyurethane** film the screen-printed electrode (SPE) was prepared by the solution casting  
23 technique, using acetone as solvent. It was a one-pot synthesis between major reactants namely,  
24 palm kernel oil-based polyol and 4,4-methylene diisocyanate. The PU has strong adhesion on

**Commented [j1]:** What the authors mean by "bio-polyurethane"? Bio-based or for medical purpose? The title given should be bio-based. Please correct.

**Commented [MAM2R1]:** The use of bio in this statement owing to the application of palm kernel oil acts as a polyol.

25 the SPE surface. The synthesized polyurethane was characterized using thermogravimetry  
26 analysis, differential scanning calorimetry, Fourier-transform infrared spectroscopy (FTIR),  
27 surface area analysis by field emission scanning electron microscope, and cyclic voltammetry.  
28 Cyclic voltammetry was employed to study electro-catalytic properties of SPE-polyurethane  
29 towards oxidation of PU. Remarkably, SPE-PU exhibited improved anodic peak current as  
30 compared to SPE itself using the differential pulse voltammetry method. Furthermore, the  
31 formation of urethane linkages ( $-\text{NHC}(\text{O})$  backbone) after polymerization was analyzed using  
32 FTIR and confirmed by the absence of  $\text{N}=\text{C}=\text{O}$  peak at  $2241\text{ cm}^{-1}$ . The glass transition  
33 temperature of the polyurethane was detected at  $78.1\text{ }^{\circ}\text{C}$ .

35 **Keywords:** polyurethane, polymerization, screen-printed electrode, voltammetry

## 38 1. Introduction

39 Conducting polymers (CPs) are polymers that can release a current (Alqarni et al. 2020). The  
40 conductivity of CPs was first observed in polyacetylene, nevertheless owing to its instability,  
41 the invention of various CPs have been studied and reported such as polyaniline (PANI),  
42 poly(*o*-toluidine) (PoT), polythiophene (PTH), polyfluorene (PF), and polyurethane (PU).  
43 Furthermore, natural CPs have low conductivity and are often semi-conductive. Therefore, it  
44 is imperative to improve their conductivity for electrochemical sensor purposes (Sengodu &  
45 Deshmukh 2015; Dzulkipli et al. 2021; Wang et al. 2018). The CPs can be produced from many  
46 organic materials and they have several advantages such as having an electrical current,  
47 inexpensive materials, massive surface area, small dimensions, and the production is  
48 straightforward. Furthermore, according to these properties, many studies have been reported  
49 by researchers to study and report the variety of CPs applications such as sensors, biochemical

**Commented [j3]:** Please clean up the groups and backbones that are presented differently each time. For example -NHC(O)

**Commented [MAM4R3]:** Done

**Commented [j5]:**  $\text{N}=\text{C}=\text{O}$  is not a peak. Functional groups give characteristic signals in a spectrum. Please use scientific language throughout your text and please describe the FTIR spectra properly.

**Commented [MAM6R5]:** Thank you for your suggestion. Nevertheless, the reading of this spectrum based on Spectroscopy book 4<sup>th</sup> Edition by Lampman et al. It is written on Page 29, 77 and 78 (Figure 2.64) about the spectrum of  $\text{N}=\text{C}=\text{O}$ . According to their research, the isocyanates have *sp*-hybridized carbon atoms similar to the  $\text{C}\equiv\text{C}$  bond. The absorption occurs in  $2100\text{-}2270\text{ cm}^{-1}$ .

**Commented [j7]:** What do "natural CPs" mean? Natural polymers occurring in nature?

**Commented [MAM8R7]:** This statement about natural polymers, we acquired from the manuscript that studied by Bharadwaz & Jayasuriya 2020 (doi.org/10.1016/j.msec.2020.110698).

This paper has studied about the natural polymer and the synthetic polymer.

50 applications, electrochromic devices, and solar cells (Alqarni et al. 2020; Ghosh et al. 2018).  
51 There is scientific documentation on the use of conductive polymers in various studies such as  
52 polyaniline (Pan & Yu 2016), polypyrrole (Ladan et al. 2017), and polyurethane (Tran et al.  
53 2020; Vieira et al. 2020; Guo et al. 2020; Fei et al. 2020).

54  
55 Polyurethane productions can be obtained by using several materials as polyols such as  
56 petroleum, coal, and crude oils. Nevertheless, these materials have become very rare to find  
57 and the price is very expensive at the same time required a sophisticated system to produce it.

58 The reasons such as price and time consuming to produce polyols have been considered by  
59 many researchers, furthermore, finding utilizing plants that can be used as alternative polyols  
60 should be done immediately (Badri 2012). Thus, to avoid the use of petroleum, coal, and crude  
61 oils as raw materials for a polyol, vegetable oils become a better choice to produce polyol in  
62 order to obtain a biodegradable polymer. Vegetable oils that are generally used for  
63 polyurethane synthesis are soybean oil, corn oil, sunflower seed oil, coconut oil, nuts oil,  
64 rapeseed, olive oil, and palm oil (Badri 2012; Borowicz et al. 2019).

65  
66 It is very straightforward for vegetable oils to react with a specific group to produce a PU such  
67 as epoxy, hydroxyl, carboxyl, and acrylate owing to the existence of (-C=C-) in vegetable oils.  
68 Thus, it provides appealing profits to vegetable oils compared to petroleum considering the  
69 toxicity, price, and harm to the environment (Mustapha et al. 2019; Mohd Noor et al. 2020).

70 Palm oil becomes the chosen in this study to produce PU owing to it being largely cultivated  
71 in South Asia particularly in Malaysia and Indonesia. It has several profits compared to other  
72 vegetable oils such as the easiest materials obtained, the lowest cost of all the common  
73 vegetable oils, and recognized as the plantation that has a low environmental impact and  
74 removing CO<sub>2</sub> from the atmosphere as a net sequester (Tajau et al. 2021; Septevani et al. 2015).

75  
76 The application of bio-based polymer has appealed much attention until now. Global  
77 environmental activists have forced researchers to discover another material producing  
78 polymers (Priya et al. 2018). PUs have many advantages that have been used by many  
79 researchers, they are not merely versatile materials but also have the durability of metal and  
80 the flexibility of rubber. Furthermore, they can be promoted to replace rubber, metals, and  
81 plastics in several aspects. Several applications of PUs have been reported and studied such as  
82 textiles, automotive, building and construction applications, and biomedical applications (Zia  
83 et al. 2014; Romaskevicius et al. 2006). Polyurethanes are also considered to be one of the most  
84 useful materials with many profits such as; possessing low conductivity, low density,  
85 absorption capability, and dimensional stability. They are a great research subject due to their  
86 mechanical, physical, and chemical properties (Badan & Majka 2017; Munir et al. 2021).

87  
88 PU structure contains the urethane group that can be formed from the reaction between  
89 isocyanate groups (-NCO) and hydroxyl group (-OH). Nevertheless, several groups can be  
90 found in PU structure such as urea, esters, ethers, and several aromatic groups. Furthermore,  
91 PUs can be produced from different sources as long as they contain specific materials (polyol  
92 and methylene diphenyl diisocyanate (MDI) and making them very useful for specific  
93 applications. Thus, according to the desired properties, PUs can be divided into several types  
94 such as waterborne, flexible, rigid, coating, binding, sealants, adhesives, and elastomers  
95 (Akindoyo et al. 2016).

96  
97 PUs are lighter than other materials such as metals, gold, and platinum. The hardness of PU  
98 also relies on the number of the aromatic rings in the polymer structure (Janpoung et al, 2020;  
99 Su'ait et al. 2014), majorly contributed by the isocyanate derivatives. PUs have also a conjugate

**Commented [j9]:** Authors should be careful when using the prefix "bio", as it gives words a strictly defined meaning (biopolymers, bioplastics, biomaterials). According IUPAC biopolymers are macromolecules formed by living organisms (including proteins, nucleic acids and polysaccharides). The authors, however, probably mean something else. Please correct.

**Commented [MAM10R9]:** Done. The authors want to stated the biopolymer owing to the bio polyol was applied in this study, namely palm kernel oil

**Commented [j11]:** Reviewer's note 5 was not taken into account. Please correct.

**Commented [MAM12R11]:** Done

**Commented [j13]:** The abbreviation should be explained where it is first used.

**Commented [MAM14R13]:** Done

100 structure where electrons can move in the main chain that causes electricity produced even the  
101 current is low. The current of conjugated linear ( $\pi$ ) can be elaborated by the gap between the  
102 valence band and the conduction band, or called high energy level containing electrons  
103 (HOMO) and lowest energy level not containing electrons (LUMO), respectively (Wang et al.  
104 2017; Kotal et al. 2011).

105  
106 In the recent past, several conventional methods have been developed such as capillary  
107 electrophoresis, liquid, and gas chromatography coupled with several detectors. Nevertheless,  
108 although chromatographic and spectrometric approaches are well developed for qualitative and  
109 quantitative analyses of analytes, several limitations emerged such as complicated  
110 instrumentation, expensive, tedious sample preparations, and requiring large amounts of  
111 expensive solvents that will harm the users and environment (Kilele et al. 2020; Inayatullah et  
112 al. 2021; Munir et al. 2021; Harmayani et al. 2014; Nurwanti et al. 2018). Therefore, it is  
113 imperative to obtain and develop an alternative material that can be used to analyze a specific  
114 analyte. Electrochemical methods are extremely promising methods in the determination of an  
115 analyte in samples owing to the high selectivities, sensitivities, inexpensive, requirements of  
116 small amounts of solvents, and can be operated by people who have no background in analytical  
117 chemistry. In addition, sample preparation such as separation and extraction steps are not  
118 needed owing to the selectivity of this instrument where no obvious interference on the current  
119 response is recorded (Chokkareddy et al. 2020). Few works have been reported on the  
120 electrochemical methods for the determination of analyte using electrodes combined with  
121 several electrode modifiers such as carbon nanotube, gold, and graphene (Chokkareddy et al.  
122 2020; Kilele et al. 2021). Nevertheless, the materials are expensive and the production is  
123 difficult. Thus, an electrochemical approach using inexpensive and easily available materials  
124 as electrode modifiers should be developed (Degefu et al. 2014; Munir et al. 2022).



125 Nowadays, screen-printed electrodes (SPEs) modified with conducting polymer have been  
126 developed for various electrochemical sensing. SPE becomes the best solution owing to the  
127 electrode having several advantages such as frugal manufacture, tiny size, being able to  
128 produce on a large scale, and can be applied for on-site detection (Nakthong et al. 2020).  
129 Conducting polymers (CPs) become an alternative to modifying the screen-printed electrodes  
130 due to their electrical conductivity, able to capture analyte by chemical/physical adsorption,  
131 large surface area, and making CPs are very appealing materials from electrochemical  
132 perspectives (Baig et al. 2019). Such advantages of SPE encourage us to construct a new  
133 electrode for electrochemical sensing, and no research reported on the direct electrochemical  
134 oxidation of histamine using a screen-printed electrode modified by polyurethane. Therefore,  
135 this research is the first to develop a new electrode using (screen printed polyurethane  
136 electrode) SPPE without any conducting materials.

137

138 The purpose of this work was to synthesise, characterize and study the electro behavior of  
139 polyurethane using cyclic voltammetry (CV) and differential pulse voltammetry (DPV)  
140 attached to the screen-printed electrode. To the best of our knowledge, this is the first attempt  
141 to use a modified polyurethane electrode. The electrochemistry of polyurethane mounted onto  
142 SPE is discussed in detail. PUs are possible to become an advanced frontier material that has  
143 been chemically modified the specific electrodes for bio/chemical sensing application.

144

## 145 2. Experimental

### 146 2.1 Chemicals

147 *Synthesis of polyurethane film:* Palm kernel oil (PKOp) based polyol supplied by UKM  
148 Technology Sdn Bhd through MPOB/UKM station plant, Pekan Bangi Lama, Selangor and  
149 prepared using Badri et al. (2000) method. 4, 4-diphenylmethane diisocyanate (MDI) was

**Commented [j15]:** Is this palm kernel oil-based polyol? Please select one writing option also for the abbreviation. There are 3 types in the text. And please explain the abbreviation only once. This applies to all abbreviations. Please correct it throughout.

**Commented [MAM16R15]:** Yes, the Palm Kernel Oil acts as polyol for this study. The revisions have been followed.

150 acquired from Cosmopolyurethane (M) Sdn. Bhd., Klang, Malaysia. Solvents and analytical  
151 reagents were benzene, toluene, hexane, acetone, dimethylsulfoxide (DMSO),  
152 dimethylformamide (DMF), tetrahydrofuran (THF), (the purity of solvents is  $\geq 99.8\%$ ), and  
153 polyethylene glycol (PEG) with a molecular weight of 400 Da obtained from Sigma Aldrich  
154 Sdn Bhd, Shah Alam.

155

## 156 2.2 Apparatus

157 Tensile testing was performed using a universal testing machine model Instron 5566 following  
158 ASTM D638 (Standard Test Method for Tensile Properties of Plastics). The tensile properties  
159 of the polyurethane film were measured at a velocity of 10 mm/min with a cell load of 5 kN.

160 The thermal properties were performed using thermogravimetry analysis (TGA) and  
161 differential scanning calorimetry (DSC) analysis. TGA was performed using a thermal analyzer  
162 of the Perkin Elmer Pyris model with a heating rate of 10 °C/min at a temperature range of 30  
163 to 800 °C under a nitrogen gas atmosphere. The DSC analysis was performed using a thermal  
164 analyzer of the Perkin Elmer Pyris model with a heating rate of 10 °C /minute at a temperature  
165 range of -100 to 200 °C under a nitrogen gas atmosphere. Approximately, 5–10 mg of PU was  
166 weighed. The sample was heated from 25 to 150 °C for one minute, then cooled immediately  
167 from 150 to 100 °C for another one minute and finally, reheated to 200 °C at a rate of 10 °C  
168 /min. At this point, the polyurethane encounters changing from elastic properties to brittle due  
169 to changes in the movement of the polymer chains. Therefore, the temperature in the middle of  
170 the inclined regions is taken as the glass transition temperature ( $T_g$ ). The melting temperature  
171 ( $T_m$ ) is identified as the maximum endothermic peak by taking the area below the peak as the  
172 enthalpy point ( $\Delta H_m$ ).

173

Commented [j17]: Different purity?

Commented [MAM18R17]: Similar purity, yet different solvents. that's why the authors write all of solvents purity.

174 The morphological analysis of PU film was performed by field emission scanning electron  
175 microscope (FESEM) model Gemini SEM microscope model 500-70-22. Before the analysis  
176 was carried out, the polyurethane film was coated with a thin layer of gold to increase the  
177 conductivity of the film. The coating method was carried out using a sputter-coater. The  
178 observations were conducted at a magnification of 200× and 5000× with 10.00 kV (Electron  
179 high tension – EHT).

**Commented [j19]:** The notation should be the same.  
Please correct through the text

**Commented [MAM20R19]:** Done.

180  
181 The crosslinking of PU was determined using the soxhlet extraction method. About 0.60 g of  
182 PU sample was weighed and put in an extractor tube containing 250 ml of toluene, used as a  
183 solvent. This flow of toluene was let running for 24 h. Mass of the PU was weighed before and  
184 after the reflux process was carried out. Then, the sample was dried in the conventional oven  
185 at 100 °C for 24 h in order to get a constant mass. The percentage of crosslinking content  
186 known as the gel content can be calculated using Equation (1).

$$187 \quad \text{Gel content (\%)} = \frac{W_0 - W}{W} \times 100 \% \quad (1)$$

188  $W_0$  is the mass of PU before the reflux process (g) and  $W$  is the mass of PU after the reflux  
189 process (g).

190  
191 FTIR spectroscopic analysis was performed using a Perkin-Elmer Spectrum BX instrument  
192 using the diamond attenuation total reflectance (DATR) method to confirm the polyurethane,  
193 PKOp, and MDI functional group. FTIR spectroscopic analysis was performed at a  
194 wavenumber of 4000 to 600  $\text{cm}^{-1}$  to identify the peaks of the major functional groups in the  
195 formation of the polymer such as amide group (-NH), urethane carbonyl group (-C=O),  
196 isocyanate group (-O=C=N-), and carbamate group (-CN).

197

198

199

### 200 2.3 Synthesis of Polyurethane

201 Firstly, the polyol prepolymer solution was produced by combining palm kernel oil-based  
202 polyol and poly(ethylene glycol) (PEG) 400 (100:40 g/g), acetone 30% was used as a solution.

203 The compound was homogenized using a centrifuge (100 rpm) for 5 min. Whereas diisocyanate  
204 prepolymer was obtained by mixing 4,4'-diphenylmethane diisocyanate (100 g) to acetone  
205 30%, afterward the mixture was mixed using a centrifuge for 1 min to obtain a homogenized  
206 solution. Afterward, diisocyanate solution (10 g) was poured into a container that contains  
207 polyol prepolymer solution (10 g) slowly to avoid an exothermic reaction occurring. The  
208 mixture was mixed for 30 sec until a homogenized solution was acquired. Lastly, the  
209 polyurethane solution was poured on the electrode surface by using the casting method and  
210 dried at ambient temperature for 12 h.

211

### 212 2.4 Modification of Electrode

213 Voltammetric tests were performed using Metrohm Autolab Software (**Figure 1**) analyzer  
214 using cyclic voltammetry method or known as amperometric mode and differential pulse  
215 voltammetry. All electrochemical experiments were carried out using screen-printed electrode  
216 (diameter 3 mm) modified using polyurethane film as working electrode, platinum wire as the  
217 auxiliary electrode, and Ag/AgCl electrode as a reference electrode. All experiments were  
218 conducted at a temperature of  $20 \pm 2$  °C.

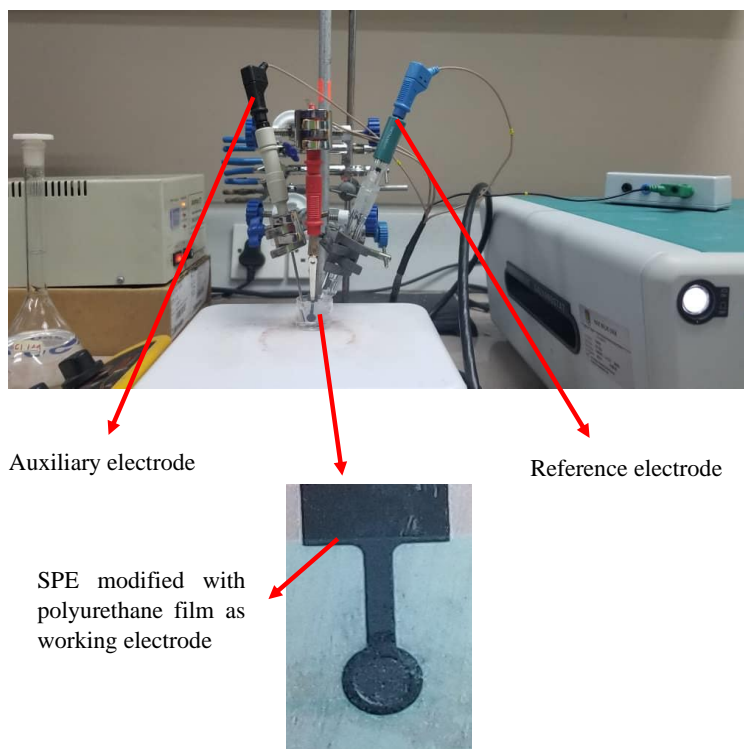
219

220 The PU was cast onto the screen-printed electrode (SPE) and analyzed using a single  
221 voltammetric cycle between -1200 and +1500 mV (vs Ag/AgCl) of ten cycles at a scanning  
222 rate of 100 mV/s in 5 ml of KCl in order to study the activity of SPE and polyurethane film.

223 Approximately (0.1, 0.3 and 0.5) mg of palm-based pre-polyurethane was dropped separately  
224 onto the surface of the SPE and dried at room temperature. The modified palm-based

**Commented [j21]:** According IUPAC nomenclature names of polymers whose monomers consist of two words or more are written with parentheses

225 polyurethane electrodes were then rinsed with deionized water to remove physically adsorbed  
226 impurities and residues of unreacted material on the electrode surface. All electrochemical  
227 materials and calibration measurements were carried out in a 5 mL glass beaker with a  
228 configuration of three electrodes inside it. Platinum wire and silver/silver chloride (Ag/AgCl)  
229 electrodes were used as auxiliary and reference electrodes, while a screen-printed electrode  
230 that had been modified with polyurethane was applied as a working electrode.



231 **Figure 1.** Potentiostat instrument to study the conductivity of SPE modified with  
232 polyurethane film using voltammetric approach: CV and DPV

233

### 234 3. Results and Discussion

235 The synthesis of PU films was carried out using a pre-polymerization method which involves  
236 the formation of urethane polymer at an early stage. The reaction took place between

237 diisocyanate (MDI) and palm kernel oil-based polyol. **Table 1** presents the PKO-p properties  
238 used in this study.

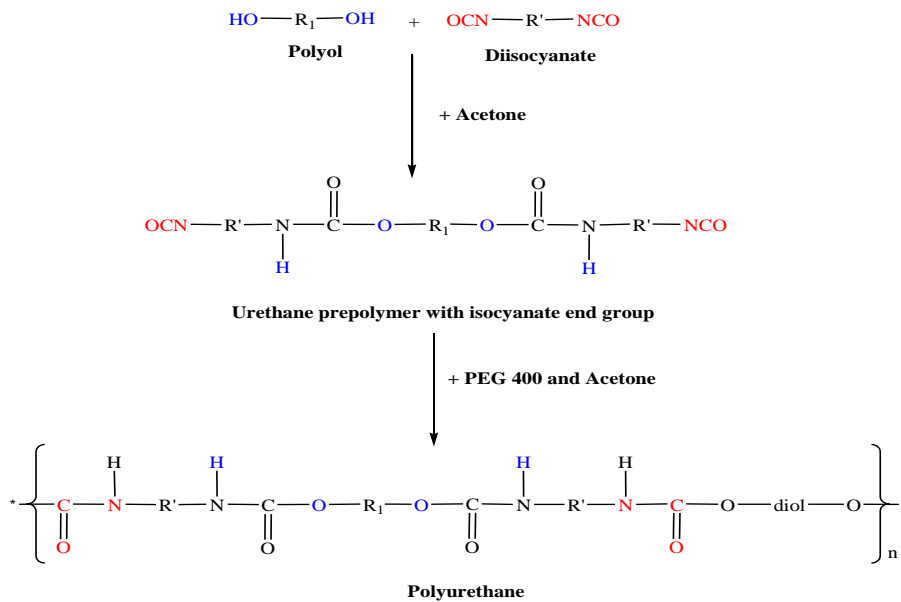
239 **Table 1** The specification of PKO-p (Badri et al. (2000)).

Property	Values
Viscosity at 25 °C (cps)	1313.3
Specific gravity (g/mL)	1.114
Moisture content (%)	0.09
pH value	10–11
The hydroxyl number mg KOH/g	450–470

240

241 The structural chain was extended with the aid of poly(ethylene glycol) to form flexible and  
242 elastic polyurethane film. In order to produce the urethane prepolymer, the isocyanate group (-  
243 NCO) attacks with the hydroxyl group (-OH) of polyol (PKOp) while the other hydroxyl group  
244 of the polyol is attacked by the other isocyanate group (Wong & Badri 2012) as shown in  
245 **Figure 2**.

246



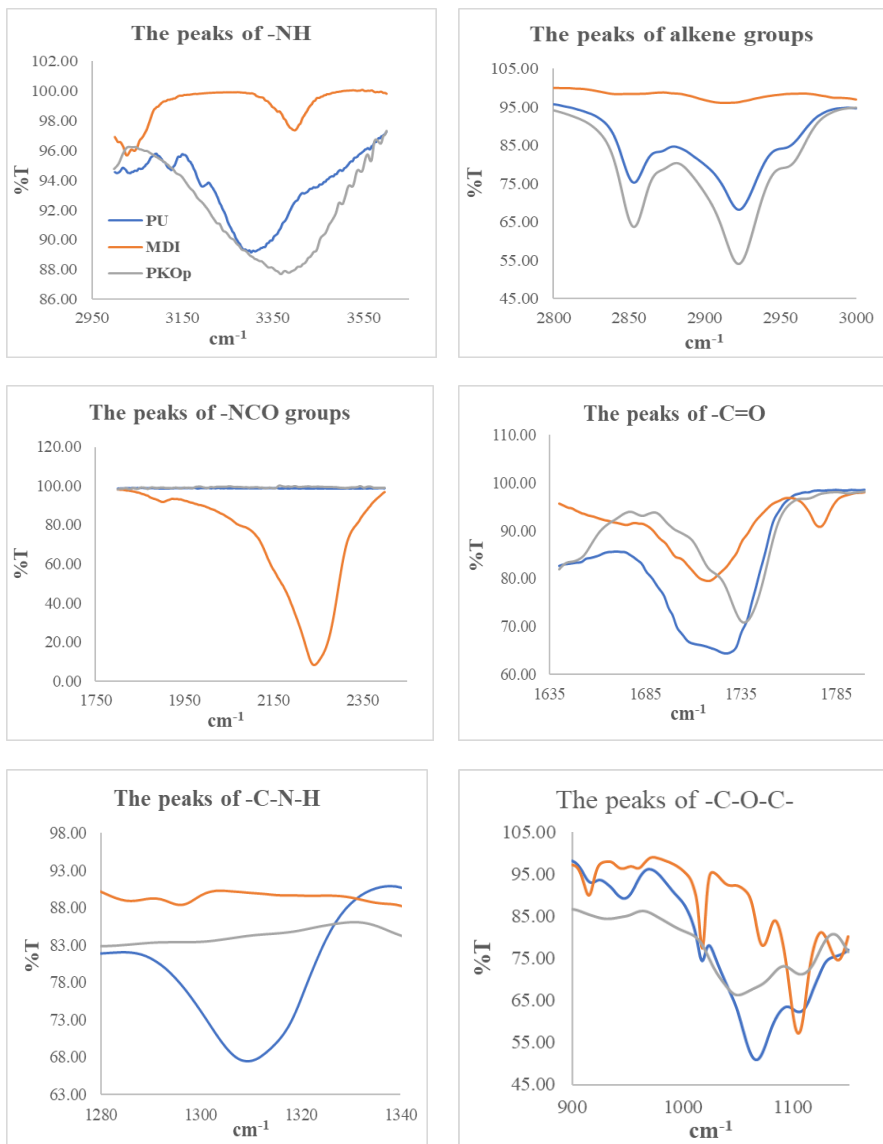
247

248 **Figure 2.** PU production via the pre-polymerization method (Wong & Badri 2012).

249

250 a. FTIR analysis

251 **Figure 3** shows the FTIR spectra for polyurethane, exhibiting the important functional group  
252 peaks. According to a study researched by Wong & Badri 2012, PKO-p reacts with MDI to  
253 form urethane prepolymers. The NCO group on MDI reacts with the OH group on polyol  
254 whether PKOp or PEG. It can be seen there are no important peaks of MDI in the FTIR spectra.  
255 This is further verified by the absence of a peak at the  $2400 \text{ cm}^{-1}$  belonging to MDI (-NCO  
256 groups). This could also confirm that the -NCO group on MDI had completely reacted with  
257 PKO-p to form the urethane -NHC(O) backbone. The presence of amides (-NH), carbonyl  
258 urethane group (-C=O), carbamate group (C-NH), and -C-O-C confirmed the formation of  
259 urethane chains. In this study, the peak of carbonyl urethane (-C=O) detected at  $1727 \text{ cm}^{-1}$   
260 indicated that the carbonyl urethane group was bonded without hydrogen owing to the  
261 hydrogen reacts with the carbonyl urethane group.



262 **Figure 3.** FTIR spectra of several important peaks between polyurethane, PKO-p, and MDI  
 263  
 264 The reaction of polyurethane has been studied by Hamuzan & Badri (2016) where the urethane  
 265 carbonyl group was detected at 1730–1735  $\text{cm}^{-1}$  while the MDI carbonyl was detected at 2400



266  $\text{cm}^{-1}$ . The absence of peaks at 2250–2270  $\text{cm}^{-1}$  indicates the absence of NCO groups. It shows  
267 that the polymerization reaction occurs entirely between NCO groups in MDI with hydroxyl  
268 groups on polyols and PEG (Mishra et al. 2012). The absence of peaks at 1690  $\text{cm}^{-1}$   
269 representing urea (C=O) in this study indicated, there is no urea formation as a byproduct  
270 (Clemitsen 2008) of the polymerization reaction that possibly occurs due to the excessive  
271 water. For the amine (-NH) group, hydrogen-bond to -NH and oxygen to form ether and  
272 hydrogen bond to NH and oxygen to form carbonyl on urethane can be detected at the peak of  
273 3301  $\text{cm}^{-1}$  and in the wavenumber at range 3326–3428  $\text{cm}^{-1}$ . This has also been studied and  
274 detected by Mutsuhisa et al. (2007) and Lampman et. al. (2010). In this research, the proton  
275 acceptor is carbonyl (-C=O) while the proton donor is an amine (-NH) to form a hydrogen  
276 bond. The MDI chemical structure has the electrostatic capability that produces dipoles from  
277 several atoms such as hydrogen, oxygen, and nitrogen atoms. These properties make  
278 isocyanates are highly reactive, and have different properties (Leykin et al. 2016).

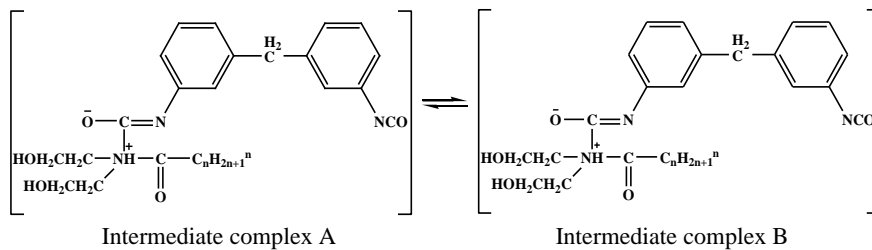
279  
280 MDI was one of the isocyanates used in this study, has an aromatic group, and is more  
281 reactive compared to aliphatic group isocyanates such as hexamethylene diisocyanate (HDI)  
282 or isophorone diisocyanate (IPDI). Isocyanates have two groups of isocyanates on each  
283 molecule. Diphenylmethane diisocyanate is an exception owing to its structure consisting of  
284 two, three, four, or more isocyanate groups (Nohra et al. 2013). The use of PEG 400 in this  
285 study as a chain extender for polyurethane increases the chain mobility of polyurethane at an  
286 optimal amount. The properties of polyurethane are contributed by hard and soft copolymer  
287 segments of both polyol monomers and MDI. This makes the hard segment of urethane serves  
288 as a crosslinking site between the soft segments of the polyol (Leykin et al. 2016).

289

290

291 The mechanism of the pre-polymerization in urethane chains formation is a  
 292 nucleophilic substitution reaction as studied by Yong et al. (2009). However, this study found  
 293 amines as nucleophiles. Amine attacks carbonyl on isocyanate in MDI in order to form two  
 294 resonance structures of intermediate complexes A and B (Figure 4). Intermediate complex B  
 295 has a greater tendency to react with polyols due to stronger carbonyl (C=O) bonds than C=N  
 296 bonds on intermediate complexes A. Thus, intermediate complex B is more stable than  
 297 intermediate complex A, as suggested by previous researchers who have conducted by Wong  
 298 and Badri (2012).

299



300

**Figure 4.** The formation of intermediate complexes

301 Moreover, oxygen is more electronegative than nitrogen causing cations (H+) to tend  
 302 to attack -CN bonds compared to -CO. The combination between long polymer chain and low  
 303 cross-linking content gives the polymer elastic properties whereas short-chain and high cross-  
 304 linking produce hard and rigid polymers. Cross-linking in polymers consists of three-  
 305 dimensional networks with high molecular weight. In some aspects, polyurethane can be a  
 306 macromolecule, a giant molecule (Petrovic 2008).

307

308 However, complexes A and B intermediate were produced after the nucleophile of PEG  
 309 attacking the isocyanate group in the MDI. However, PEG contains oxygen atoms that are more  
 310 electronegative than nitrogen atoms inside the PKOp chemical structure causing the reaction  
 311 of nucleophilic substitution that occurs in PKOp. Furthermore, amine has a higher probability

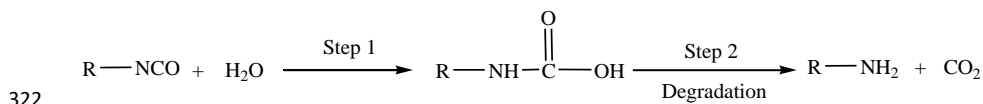
Commented [jj22]: There is no A and B in the Figure. Is this about something else?

Commented [MAM23R22]: Done.

312 of reacting compared to hydroxyl (Herrington & Hock 1997). Amine with high alkalinity reacts  
313 with carbon atoms on MDI as proposed by Wong and Badri (2012).

314

315 The production of intermediate complexes unstabilizes the alkyl ions, nevertheless, the  
316 long carbon chains of PKOp ensure the stability of alkyl ions. The addition of PEG in this study  
317 is imperative, not merely to increase the chain length of PU but also to avoid the production of  
318 urea as a by-product after the NCO group reacts with H<sub>2</sub>O from the environment. If the NCO  
319 group reacts with the excess water in the environment, the formation of urea and carbon dioxide  
320 gas will also occur excessively (**Figure 5**). This reaction can cause a polyurethane foam, not  
321 polyurethane film as we studied the film.



323 **Figure 5.** The reaction between the NCO group and water producing carbon dioxide

324

325 Furthermore, the application of PEG can influence the conductivity of PU whereby  
326 Porcarelli et al. (2017) have reported the application of PEG using several molecular weights.  
327 PEG 1500 decreased the conductivity of PU in consequence of the semicrystalline phase of  
328 PEG 1500 that acted as a poor ion-conducting phase for PU. It is also well known that PEG  
329 with a molecular weight of more than 1000 g·mol<sup>-1</sup> tends to crystallize with deleterious effects  
330 on room temperature ionic conductivity (Porcarelli et al. 2017).

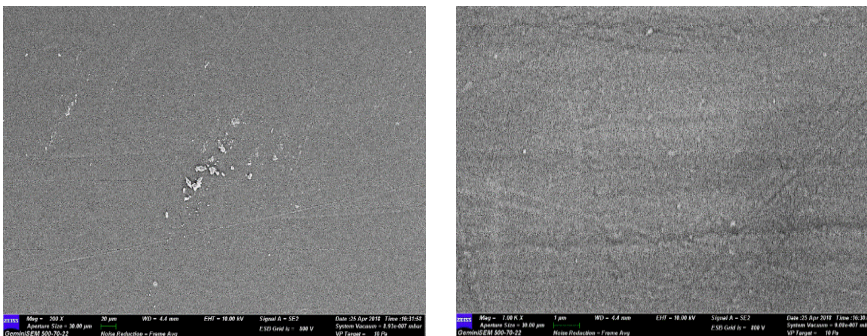
331

#### 332 b. Morphological analysis

333 The field emission scanning electron microscope micrograph in **Figure 6** shows the formation  
334 of a uniform polymer film contributed by the polymerization method applied. The  
335 magnification used for this surface analysis ranged from 200 to 5000×. The polymerization

336 method can also avoid the failure of the reaction in PU polymerization. Furthermore, no trace  
337 of separation was detected by FESEM. This has also been justified by the wavelengths obtained  
338 by the FTIR spectra above.

339



340 **Figure 6.** The micrograph of polyurethane films was analyzed by FESEM at (a) 200× and (b)  
341 5000× magnifications.

342

343 c. The crosslinking analysis

344 Soxhlet analysis was applied to determine the degree of crosslinking between the hard  
345 segments and the soft segments in the polyurethane. The urethane group on the hard segment  
346 along the polyurethane chain is polar (Cuve & Pascault 1991). Therefore, during the testing, it  
347 was very difficult to dissolve in toluene, as the testing reagent. The degree of crosslinking is  
348 determined by the percentage of the gel content. The analysis result obtained from the Soxhlet  
349 testing indicated a 99.3% gel content. This is significant in getting a stable polymer at a higher  
350 working temperature (Rogulska et al. 2007).

351

$$\text{Gel content (\%)} = \frac{(0.6 - 0.301) \text{ g}}{0.301 \text{ g}} \times 100\% = 99.33\%$$

352

353

354

355 d. The thermal analysis

356 Thermogravimetric analysis can be used to observe the material mass based on temperature  
 357 shift. It can also examine and estimate the thermal stability and materials properties such as the  
 358 alteration weight owing to absorption or desorption, decomposition, reduction, and oxidation.  
 359 The material composition of polymer is specified by analyzing the temperatures and the heights  
 360 of the individual mass steps (Alamawi et al. 2019). **Figure 7** shows the TGA and derivative  
 361 thermogravimetry (DTG) thermograms of polyurethane. The percentage weight loss (%) is  
 362 listed in **Table 2**. Generally, only a small amount of weight was observed. It is shown in **Figure**  
 363 **7** in the region of 45–180 °C. This is due to the presence of condensation on moisture and  
 364 solvent residues.

366 **Table2** Weight loss percentage of (wt%) polyurethane film

Sample	% Weight loss (wt%)				Total of weight loss (%)	Residue after 550 °C (%)
	$T_{max}$ , (°C)	$T_{d1}$ , 200–90 °C	$T_{d2}$ , 350–500 °C	$T_{d3}$ , 500–550 °C		
Polyurethane	240	8.04	39.29	34.37	81.7	18.3

367 The bio polyurethane is thermally stable up to 240 °C before it has undergone thermal  
 368 degradation (Agrawal et al. 2017). The first stage of thermal degradation ( $T_{d1}$ ) on polyurethane  
 369 films was shown in the region of 200–290 °C as shown in **Figure 7**. The  $T_{d1}$  is associated with  
 370 degradation of the hard segments of the urethane bond, forming alcohol or degradation of the  
 371 polyol chains and releasing of isocyanates (Berta et al. 2006), primary and secondary amines  
 372 as well as carbon dioxide (Corcuera et al. 2011; Pan & Webster 2012). Meanwhile, the second  
 373 thermal degradation stage ( $T_{d2}$ ) of polyurethane films experienced a weight loss of 39.29%.  
 374 This endotherm of  $T_{d2}$  is related to the dimerization of isocyanates to form carbodiimides and  
 375 release CO<sub>2</sub>. The formed carbodiimide reacts with alcohol to form urea. The third stage of  
 376

Commented [j24]: please explain

Commented [MAM25R24]: Done

Commented [j26]: These are different samples?

Commented [j27]: Please use the correct sign for the grades

Commented [MAM28R27]: Done

Commented [j29]: Is this the % Weight loss. The table is illegible, please rewrite it. Variables should be explained and written in italic.

Commented [MAM30R29]: Yes, this is the weight loss.

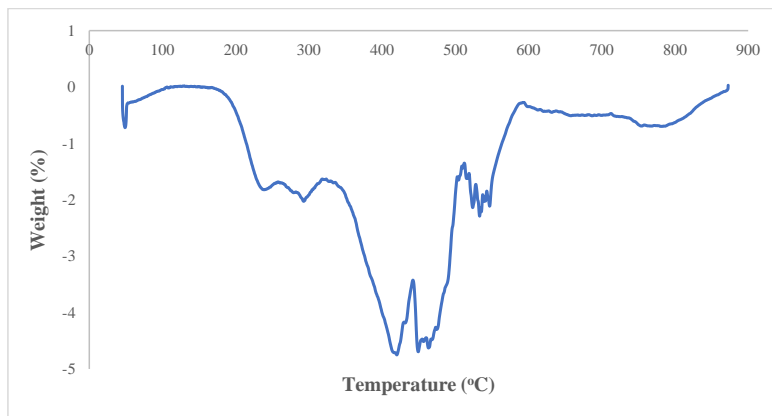
Commented [j31]: Before % was without a gap. Please standardize.

Commented [MAM32R31]: Done.

377 thermal degradation ( $T_{d3}$ ) is related to the degradation of urea (Berta et al. 2006) and the soft  
378 segment on polyurethane.

379

380 Generally, DSC analysis exhibited thermal transitions as well as the initial  
381 crystallization and melting temperatures of the polyurethane (Khairuddin et al. 2018). It serves  
382 to analyze changes in thermal behavior due to changes occurring in the chemical chain structure  
383 based on the  $T_g$  of the sample obtained from the DSC thermogram (**Figure 8**). DSC analysis  
384 on polyurethane film was performed in the temperature at the range 100 °C to 200 °C of using  
385 nitrogen gas as a blanket as proposed by Furtwengler et al. (2017). The glass transition  
386 temperature on polyurethane was above room temperature, at 78.1 °C indicated the state of  
387 glass on polyurethane. The presence of MDI contributes to the formation of hard segments in  
388 polyurethanes. Porcarelli et al. (2017) stated that possessing a low  $T_g$  may contribute to PU  
389 conductivity.



390

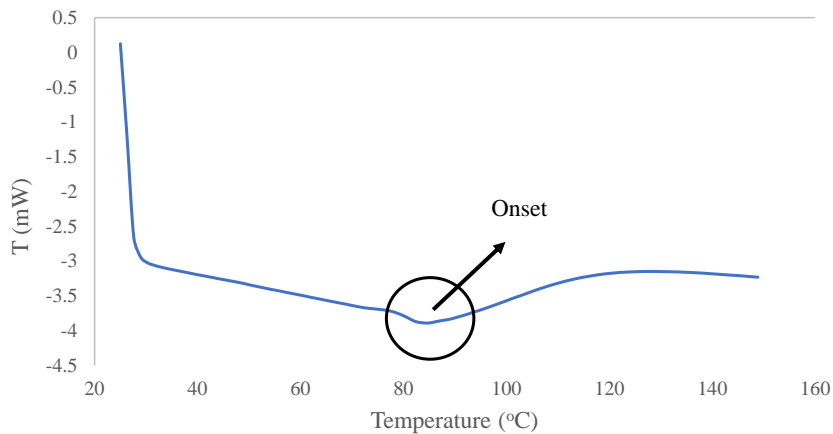
**Figure 7.** DTG thermogram of polyurethane film

391

392

393 During polymerization, this hard segment restricts the mobility of the polymer chain  
394 (Ren et al. 2013) owing to the steric effect on the benzene ring in the hard segment. The  
395 endothermic peak of acetone used as the solvent in this study was supposedly at 56 °C.

396 However, it was detected in the DSC thermogram nor the TGA thermogram, which indicates  
397 that acetone was removed from the polyurethane during the synthesis process, owing to its  
398 volatile nature. The presence of acetone in the synthesis was to lower the reaction kinetics.



399 **Figure 8.** DSC thermogram of polyurethane film

401  
402  
403 e. The solubility and mechanical properties of the polyurethane film

404 The chemical resistivity of a polymer will be the determinant in performing as a conductor.  
405 Thus, its solubility in various solvents was determined by dissolving the polymer in selected  
406 solvents such as hexane, benzene, acetone, THF, DMF, and DMSO. On the other hand, the  
407 mechanical properties of polyurethane were determined based on the standard testing following  
408 ASTM D638. The results from the polyurethane film solubility and tensile test are shown in  
409 **Table 3.** Polyurethane films were insoluble with acetone, hexane, and benzene and are only  
410 slightly soluble in THF, DMF, and DMSO solutions. While the tensile strength of a PU film  
411 indicated how much elongation load the film was capable of withstanding the material before  
412 breaking.

413

414 **Table 3** The solubility and mechanical properties of the polyurethane film

415

Parameters	Polyurethane film	
Solubility	Benzene	Insoluble
	Hexane	Insoluble
	Acetone	Insoluble
	THF	Less soluble
	DMF	Less soluble
	DMSO	Less soluble
	Stress (MPa)	8.53
Elongation percentage (%)	43.34	
Strain modulus (100) (MPa)	222.10	

416

417 The tensile stress, strain, and modulus of polyurethane film also indicated that polyurethane

418 has good mechanical properties that are capable of being a supporting substrate for the next

419 stage of the study. In the production of polyurethane, the properties of polyurethane are easily

420 influenced by the content of MDI and polyol used. The length of the chain and its flexibility

421 are contributed by the polyol which makes it elastic. High crosslinking content can also produce

422 hard and rigid polymers. MDI is a major component in the formation of hard segments in

423 polyurethane. It is this hard segment that determines the rigidity of the PU. Therefore, high

424 isocyanate content results in higher rigidity on PU (Petrovic et al. 2002). Thus, the polymer has

425 a higher resistance to deformation and more stress can be applied to the PU.

426

427 f. The conductivity of the polyurethane as a polymeric film on SPE

428 Polyurethane film was deposited onto the screen-printed electrode by casting method as shown

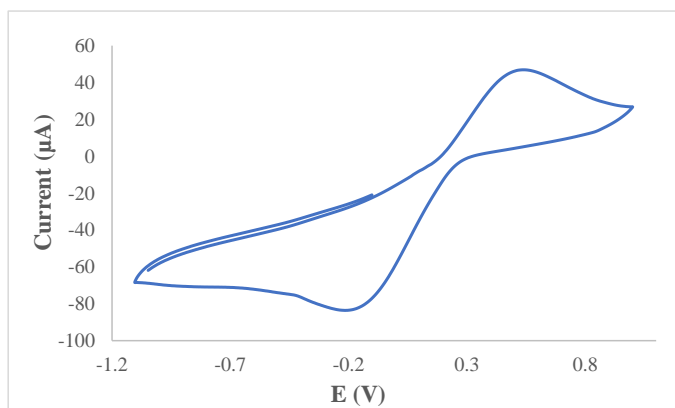
429 in **Figure 1**. After that, the modified electrode was analyzed using cyclic voltammetry and



430 differential pulse voltammetry in order to study the behavior of the modified electrode. The  
431 modified electrode was tested in a 0.1 mmol·L<sup>-1</sup> KCl solution containing 5 mmol·L<sup>-1</sup>  
432 (K<sub>3</sub>Fe(CN)<sub>6</sub>). The use of potassium ferricyanide is intended to increase the sensitivity of the  
433 KCl solution. The conductivity of the modified electrode was studied. The electrode was  
434 analyzed by cyclic voltammetry method with a potential range of -1.00 to +1.00 with a scan  
435 rate of 0.05 V·s<sup>-1</sup>. The voltammograms at the electrode have shown a specific redox reaction.  
436 Furthermore, the conductivity of the modified electrode is lower due to the use of polyurethane.  
437 This occurs due to PU being a natural polymer produced from the polyol of palm kernel oil-  
438 based polyol. The electrochemical signal at the electrode is low if there is a decrease in  
439 electrochemical conductivity (El - Raheem et al. 2020). It can be concluded that polyurethane  
440 is a bio-polymer with a low current value. The current of the modified electrode was found at  
441 5.3 x 10<sup>-5</sup> A or 53 μA. Nevertheless, the current of PU in this study showed better results  
442 compared to Bahrami et al. (2019) that reported the current of PU as 1.26 x 10<sup>-6</sup> A, whereas Li  
443 et al. (2019) reported the PU current in their study was even very low, namely 10<sup>-14</sup> A. The PU  
444 can obtain a current owing to the benzene ring in the hard segment (MDI) could exhibit the  
445 current by inducing electron delocalization along the polyurethane chain (Wong et al. 2014).  
446 The PU can also release a current caused by PEG. The application of PEG as polyol has been  
447 studied by Porcarelli et al. (2017), that reported that the current of PU based on PEG – polyol  
448 was 9.2 x 10<sup>-8</sup> A.

449 According to **Figure 9**, it can be concluded that the anodic peak present in the modified  
450 electrode was at +0.5 V, it also represented the anodic peak of the SPE-PU. The first oxidation  
451 signal on both electrodes ranged from -0.2 to +1.0 V, which revealed a particular oxidative  
452 peak at a potential of +0.5 V.

453

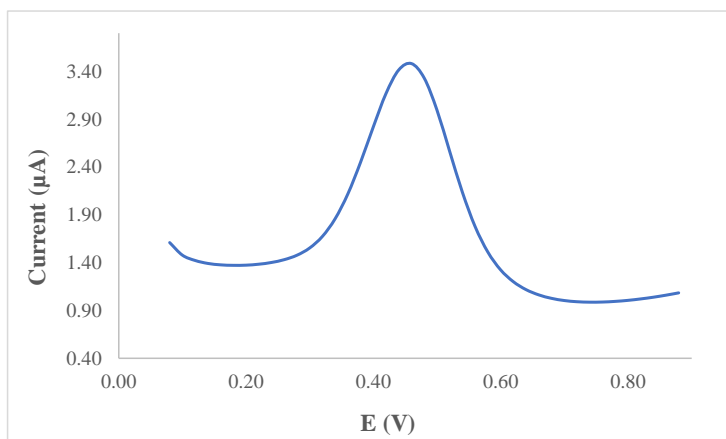


454 **Figure 9.** The voltammogram of SPE-PU modified electrode after analyzed using cyclic  
 455 voltammetry technique  
 456

457 **Figure 10** also presents the DPV voltammogram of the modified electrode. DPV is a  
 458 measurement based on the difference in potential pulses that produce an electric current.  
 459 Scanning the capability pulses to the working electrode will produce different currents. Optimal  
 460 peak currents will be produced to the reduction capacity of the redox material. The peak current  
 461 produced is proportional to the concentration of the redox substance and can be detected up to  
 462 a concentration below  $10^{-8}$  M. DPV was conducted to obtain the current value that is more  
 463 accurate than CV (Lee et al. 2018).  
 464

465 This study used a redox pair ( $K_3Fe(CN)_6$ ) as a test device (probe). The currents generated by  
 466 SPE-PU and proved by CV and DPV have shown conductivity on polyurethane films. This  
 467 suggests that polyurethane films can conduct electron transfer. The electrochemical area on the  
 468 modified electrode can be calculated using the formula from Randles-Sevcik (Butwong et al.  
 469 2019), where the electrochemical area for SPE-PU is considered to be A, using Equation 2:

470 **Current of SPE-PU,  $I_p = 2.65 \times 10^5 A C n^{3/2} \nu^{1/2} D^{1/2}$**  (2)



471 **Figure 10.** The voltammogram of SPE – PU modified electrode after analyzed using  
 472 differential pulse voltammetry technique  
 473

474  
 475 Where,  $n - 1$  is the amount of electron transfer involved, while  $C$  is the solvent concentration  
 476 used ( $\text{mmol}\cdot\text{L}^{-1}$ ) and the value of  $D$  is the diffusion constant of  $5 \text{ mmol}\cdot\text{L}^{-1}$  at  $(\text{K}_3\text{Fe}(\text{CN})_6)$   
 477 dissolved using  $0.1 \text{ mmol}\cdot\text{L}^{-1}$  KCl. The estimated surface area of the electrode (**Figure 1**) was  
 478  $0.2 \text{ cm}^2$  where the length and width of the electrode used during the study was  $0.44 \text{ cm} \times 0.44$   
 479  $\text{cm}$  while the surface area of the SPE-PU was  $0.25 \text{ cm}^2$  with the length and width of the  
 480 electrode estimated at  $0.5 \text{ cm} \times 0.5 \text{ cm}$ , and causing the SPE-PU has a larger surface. The  
 481 corresponding surface concentration ( $\tau$ ) ( $\text{mol}/\text{cm}^2$ ) is measured using Equation 3.

$$482 \quad I_p = \frac{(n^2 F^2 / 4RT) A \tau v}{\quad} \quad (3)$$

483  $I_p$  is the peak current (A), while  $A$  is the surface area of the electrode ( $\text{cm}^2$ ), the value of  $v$  is  
 484 the applied scan rate (mV/s) and  $F$  is the Faraday constant ( $96,584 \text{ C}/\text{mol}$ ),  $R$  is the constant  
 485 ideal gas ( $8.314 \text{ J}/\text{mol K}$ ) and  $T$  is the temperature used during the experiment being conducted  
 486 ( $298 \text{ K}$ ) (Koita et al. 2014). The application of PKOp to produce a conducting polymer will be  
 487 a great prospect as this material can be employed in the analytical industry in order to modify  
 488 electrodes for electrochemical purposes.

489 Furthermore, number of palm oils is abundant in Malaysia and Indonesia such as palm stearin  
490 and refined-bleached-deodorized (RBD) palm oil. They have several benefits such as being  
491 sustainable, cheap, and environmentally biodegradable. These palms are the potential to  
492 produce biomaterials that can be used to replace other polymers that are chemical-based (Tajao  
493 et al. 2021). Several studies have been reported the application of PU to produce elastic  
494 conductive fibres and films owing to it being highly elastic, scratch-resistant, and adhesive  
495 (Tadese et al. 2019), thus it is easy for PU to adhere to the screen-printed electrode to modify  
496 the electrode. PU is also being used as a composite material to make elastic conducting  
497 composite films (Khatoon & Ahmad 2017).

498

#### 499 **4. Conclusion**

500 Polyurethane film was prepared by pre-polymerization between palm kernel oil-based polyol  
501 (PKO-p) with MDI. The presence of PEG 400 as the chain extender formed freestanding  
502 flexible film. Acetone was used as the solvent to lower the reaction kinetics since the pre-  
503 polymerization was carried out at room temperature. The formation of urethane links (-  
504 NHC(O) backbone) after polymerization was confirmed by the absence of N=C=O peak at  
505  $2241\text{ cm}^{-1}$  and the presence of N-H peak at  $3300\text{ cm}^{-1}$ , carbonyl (C=O) at  $1710\text{ cm}^{-1}$ , carbamate  
506 (C-N) at  $1600\text{ cm}^{-1}$ , ether (C-O-C) at  $1065\text{ cm}^{-1}$ , benzene ring (C=C) at  $1535\text{ cm}^{-1}$  in the bio  
507 polyurethane chain structure. Soxhlet analysis for the determination of crosslinking on  
508 polyurethane films has yielded a high percentage of 99.33%. This is contributed by the hard  
509 segments formed from the reaction between isocyanates and hydroxyl groups causing  
510 elongation of polymer chains. FESEM analysis exhibited an absence of phase separation and  
511 smooth surface. Meanwhile, the current of the modified electrode was found at  $5.2 \times 10^{-5}\text{ A}$ .  
512 This bio polyurethane film can be used as a conducting bio-polymer and it is very useful for

513 other studies such as electrochemical sensor purposes. Furthermore, advanced technologies are  
514 promising and the future of bio-based polyol looks very bright.

515

## 516 **5. Acknowledgment**

517 The authors would like to thank Alma Ata University for the sponsorship given to the first  
518 author. We would like to also, thank The Department of Chemical Sciences, Universiti  
519 Kebangsaan Malaysia for the laboratory facilities and CRIM, UKM for the analysis  
520 infrastructure.

521

## 522 **6. Conflict of Interest**

523 The authors declare no conflict of interest.

524

## 525 **7. References**

526 Agrawal, A., Kaur, R., Walia, R. S. (2017). PU foam derived from renewable sources:  
527 Perspective on properties enhancement: An overview. *European Polymer Journal*. **95**:  
528 255 – 274.

529 Akindoyo, J. O., Beg, M.D.H., Ghazali, S., Islam, M.R., Jeyaratnam, N. & Yuvaraj, A.R.  
530 (2016). Polyurethane types, synthesis, and applications – a review. *RSC Advances*. **6**:  
531 114453 – 114482.

532 Alamawi, M. Y., Khairuddin, F. H., Yusoff, N. I. M., Badri, K., Ceylan, H. (2019).  
533 Investigation on physical, thermal, and chemical properties of palm kernel oil polybio-  
534 based binder as a replacement for bituminous binder. *Construction and Building*  
535 *Materials*. **204**: 122 – 131.

536 Alqarni, S. A., Hussein, M. A., Ganash, A. A. & Khan, A. (2020). Composite material-based  
537 conducting polymers for electrochemical sensor applications: a mini-review.  
538 *BioNanoScience*. **10**: 351 – 364.

539 Badan, A., Majka, T. M. (2017). The influence of vegetable – oil based polyols on physico –  
540 mechanical and thermal properties of polyurethane foams. *Proceedings*. 1 – 7.

541 Badri, K.H. (2012) Biobased polyurethane from palm kernel oil-based polyol. In Polyurethane;  
542 Zafar, F., Sharmin, E., Eds. InTechOpen: Rijeka, Croatia. pp. 447–470.

543 Badri, K.H., Ahmad, S.H. & Zakaria, S. 2000. Production of a high-functionality RBD palm  
544 kernel oil-based polyester polyol. *Journal of Applied Polymer Science*. **81**(2): 384 – 389.

545 Baig, N., Sajid, M. and Saleh, T. A. 2019. Recent trends in nanomaterial–modified electrodes  
546 for electroanalytical applications. *Trends in Analytical Chemistry*. **111**: 47 – 61.

547 Berta, M., Lindsay, C., Pans, G., & Camino, G. (2006). Effect of chemical structure on  
548 combustion and thermal behaviour of polyurethane elastomer layered silicate  
549 nanocomposites. *Polymer Degradation and Stability*. **91**: 1179-1191.

550 Borowicz, M., Sadowska, J. P., Lubczak, J. & Czuprynski, B. (2019). Biodegradable, flame–  
551 retardant, and bio-based rigid polyurethane/polyisocyanurate foams for thermal  
552 insulation application. *Polymers*. **11**: 1816 – 1839.

553 Butwong, N., Khajonklin, J., Thongbor, A. & Luong, J.H.T. (2019). Electrochemical sensing  
554 of histamine using a glassy carbon electrode modified with multiwalled carbon nanotubes  
555 decorated with Ag – Ag<sub>2</sub>O nanoparticles. *Microchimica Acta*. **186** (11): 1 – 10.

556 Chokkareddy, R., Thondavada, N., Kabane, B. & Redhi, G. G. (2020). A novel ionic liquid  
557 based electrochemical sensor for detection of pyrazinamide. *Journal of the Iranian*  
558 *Chemical Society*. **18**: 621 – 629.

559 Chokkareddy, R., Kanchi, S. & Inamuddin (2020). Simultaneous detection of ethambutol and  
560 pyrazinamide with IL@CoFe<sub>2</sub>O<sub>4</sub>NPs@MWCNTs fabricated glassy carbon electrode.  
561 *Scientific Reports*. **10**: 13563.

562 Clemitson, I. (2008). Castable Polyurethane Elastomers. Taylor & Francis Group, New York.  
563 doi:10.1201/9781420065770.

564 Corcuera, M.A., Rueda, L., Saralegui, A., Martin, M.D., Fernandez-d'Arlas, B., Mondragon,  
565 I. & Eceiza, A. (2011). Effect of diisocyanate structure on the properties and  
566 microstructure of polyurethanes based on polyols derived from renewable resources.  
567 *Journal of Applied Polymer Science*. **122**: 3677-3685.

568 Cuve, L. & Pascault, J.P. (1991). Synthesis and properties of polyurethanes based on  
569 polyolefine: Rigid polyurethanes and amorphous segmented polyurethanes prepared in  
570 polar solvents under homogeneous conditions. *Polymer*. **32** (2): 343- 352.

571 Degefu, H., Amare, M., Tessema, M. & Admassie, S. (2014). Lignin modified glassy carbon  
572 electrode for the electrochemical determination of histamine in human urine and wine  
573 samples. *Electrochimica Acta*. **121**: 307 – 314.

574 Dzulkipli, M. Z., Karim, J., Ahmad, A., Dzulkurnain, N. A., Su'ait, M S., Fujita, M. Y., Khoon,  
575 L. T. & Hassan, N. H. (2021). The influences of 1-butyl-3-methylimidazolium  
576 tetrafluoroborate on electrochemical, thermal and structural studies as ionic liquid gel  
577 polymer electrolyte. *Polymers*. **13** (8): 1277 – 1294.

578 El-Raheem, H.A., Hassan, R.Y.A., Khaled, R., Farghali, A. & El-Sherbiny, I.M. (2020).  
579 Polyurethane-doped platinum nanoparticles modified carbon paste electrode for the  
580 sensitive and selective voltammetric determination of free copper ions in biological  
581 samples. *Microchemical Journal*. **155**: 104765.

582 Fei, T., Li, Y., Liu, B. & Xia, C. (2019). Flexible polyurethane/boron nitride composites with  
583 enhanced thermal conductivity. *High Performance Polymers*. **32** (3): 1 – 10.

584 Furtwengler, P., Perrin R., Redl, A. & Averous, L. (2017). Synthesis and characterization of  
585 polyurethane foams derived of fully renewable polyesters polyols from sorbitol.  
586 *European Polymer Journal*. **97**: 319 – 327.

587 Ghosh, S., Ganguly, S., Remanan, S., Mondal, S., Jana, S., Maji, P. K., Singha, N., Das, N. C.  
588 (2018). Ultra-light weight, water durable and flexible highly electrical conductive  
589 polyurethane foam for superior electromagnetic interference shielding materials. *Journal*  
590 *of Materials Science: Materials in Electronics*. **29**: 10177 – 10189.

591 Guo, S., Zhang, C., Yang, M., Zhou, Y., Bi, C., Lv, Q. & Ma, N. (2020). A facile and sensitive  
592 electrochemical sensor for non – enzymatic glucose detection based on three –  
593 dimensional flexible polyurethane sponge decorated with nickel hydroxide. *Analytica*  
594 *Chimica Acta*. **1109**: 130 – 139.

595 Hamuzan, H.A. & Badri, K.H. (2016). The role of isocyanates in determining the viscoelastic  
596 properties of polyurethane. *AIP Conference Proceedings*. 1784, Issue 1.

597 Harmayani, E., Aprilia, V. & Marsono, Y. (2014). Characterization of glucomannan from  
598 *Amorphophallus oncophyllus* and its prebiotic activity in vivo. *Carbohydrate Polymers*.  
599 **112**: 475-79.

600 Herrington, R. & Hock, K. (1997). Flexible polyurethane foams. 2nd Edition. Dow Chemical  
601 Company. Midlan.

602 Inayatullah, A., Badrul, H.A., Munir, M.A. (2021). Fish analysis containing biogenic amines  
603 using gas chromatography flame ionization detector. *Science and Technology Indonesia*.  
604 **6** (1): 1-7.

605 Janpoung, P., Pattanauwat, P. & Potiyaraj, P. (2020). Improvement of electrical conductivity  
606 of polyurethane/polypyrrole blends by graphene. *Key Engineering Materials*. **831**: 122 –  
607 126.



608 Khairuddin, F.H., Yusof, N. I. M., Badri, K., Ceylan, H., Tawil, S. N. M. (2018). Thermal,  
609 chemical and imaging analysis of polyurethane/cecabase modified bitumen. *IOP Conf.*  
610 *Series: Materials Science and Engineering*. **512**: 012032.

611 Khatoon, H., Ahmad, S. (2017). A review on conducting polymer reinforced polyurethane  
612 composites. *Journal of Industrial and Engineering Chemistry*. **53**: 1 – 22.

613 Kilele, J. C., Chokkareddy, R., Rono, N. & Redhi, G. G. (2020). A novel electrochemical  
614 sensor for selective determination of theophylline in pharmaceutical formulations.  
615 *Journal of the Taiwan Institute of Chemical Engineers*. 111: 228-238.

616 Kilele, J. C., Chokkareddy, R. & Redhi, G. G. (2021). Ultra-sensitive electrochemical sensor  
617 for fenitrothion pesticide residues in fruit samples using IL@CoFe<sub>2</sub>ONPs@MWCNTs  
618 nanocomposite. *Microchemical Journal*. **164**: 106012.

619 Koita, D., Tzedakis, T., Kane, C., Diaw, M., Sock, O. & Lavedan, P. (2014). Study of the  
620 histamine electrochemical oxidation catalyzed by nickel sulfate. *Electroanalysis*. **26 (10)**:  
621 2224 – 2236.

622 Kotal, M., Srivastava, S.K. & Paramanik, B. (2011). Enhancements in conductivity and thermal  
623 stabilities of polyurethane/polypyrrole nanoblends. *The Journal of Physical Chemistry*  
624 *C*. **115 (5)**: 1496 – 1505.

625 Ladan, M., Basirun, W.J., Kazi, S.N., Rahman, F.A. (2017). Corrosion protection of AISI 1018  
626 steel using Co-doped TiO<sub>2</sub>/polypyrrole nanocomposites in 3.5% NaCl solution.  
627 *Materials Chemistry and Physics*. **192**: 361 – 373.

628 Lampman, G.M., Pavia, D.L., Kriz, G.S. & Vyvyan, J.R. (2010). Spectroscopy. 4th Edition.  
629 Brooks/Cole Cengage Learning, Belmont, USA.

630 Lee, K.J., Elgrishi, N., Kandemir, B. & Dempsey, J.L. 2018. Electrochemical and spectroscopic  
631 methods for evaluating molecular electrocatalysts. *Nature Reviews Chemistry*. **1(5)**: 1 -  
632 14.

633 Leykin, A., Shapovalov, L. & Figovsky, O. (2016). Non – isocyanate polyurethanes –  
634 Yesterday, today and tomorrow. *Alternative Energy and Ecology*. **191** (3 – 4): 95 – 108.

635 Li, H., Yuan, D., Li, P., He, C. (2019). High conductive and mechanical robust carbon  
636 nanotubes/waterborne polyurethane composite films for efficient electromagnetic  
637 interference shielding. *Composites Part A*. **121**: 411 – 417.

638 Nakthong, P., Kondo, T., Chailapakul, O., Siangproh, W. (2020). Development of an  
639 unmodified screen-printed electrode for nonenzymatic histamine detection. *Analytical*  
640 *Methods*. **12**: 5407 – 5414.

641 Mishra, K., Narayan, R., Raju, K.V.S.N. & Aminabhavi, T.M. (2012). Hyperbranched  
642 polyurethane (HBPU)-urea and HBPU-imide coatings: Effect of chain extender and  
643 NCO/OH ratio on their properties. *Progress in Organic Coatings*. **74**: 134 – 141.

644 Mohd Noor, M. A., Tuan Ismail, T. N. M., Ghazali, R. (2020). Bio-based content of oligomers  
645 derived from palm oil: Sample combustion and liquid scintillation counting technique.  
646 *Malaysia Journal of Analytical Science*. **24**: 906 – 917.

647 Munir, M. A., Badri, K. H., Heng, L. Y., Inayatullah, A., Nurinda, E., Estiningsih, D.,  
648 Fatmawati, A., Aprilia, V., Syafitri, N. (2022). The application of polyurethane-LiClO<sub>4</sub>  
649 to modify screen-printed electrodes analyzing histamine in mackerel using a  
650 voltammetric approach. *ACS Omega*. Doi.org/10.1021/acsomega.1c06295.

651 Munir, M. A., Heng, L. Y., Sage, E. E., Mackeen, M. M. M., Badri, K. H. (2021). Histaine  
652 detection in mackerel (*Scomberomorus* Sp.) and its products derivatized with 9-  
653 fluorenilmethylchloroformate. *Pakistan Journal of Analytical and Environmental*  
654 *Chemistry*. **22** (2): 243-251.

655 Munir, M. A., Heng, L. Y., Badri, K. H. (2021). Polyurethane modified screen-printed  
656 electrode for the electrochemical detection of histamine in fish. *IOP Conference Series:*  
657 *Earth and Environmental Science*. **880**: 012032.

658 Munir, M.A., Mackeen, M.M.M., Heng, L.Y. Badri, K.H. (2021). Study of histamine detection  
659 using liquid chromatography and gas chromatography. *ASM Science Journal*. **16**: 1-9.

660 Mutsuhisa F., Ken, K. & Shohei, N. (2007). Microphase separated structure and mechanical  
661 properties of norbornane diisocyanate-based polyurethane. *Polymer*. **48** (4): 997 – 1004.

662 Mustapha, R., Rahmat, A. R., Abdul Majid, R., Mustapha, S. N. H. (2019). Vegetable oil-based  
663 epoxy resins and their composites with bio-based hardener: A short review. *Polymer-*  
664 *Plastic Technology and Materials*. **58**: 1311 – 1326.

665 Nohra, B., Candy, L., Blancos, J.F., Guerin, C., Raoul, Y. & Mouloungui, Z. (2013). From  
666 petrochemical polyurethanes to bio-based polyhydroxyurethanes. *Macromolecules*. **46**  
667 (10): 3771 – 3792.

668 Nurwanti, E., Uddin, M., Chang, J.S., Hadi, H., Abdul, S.S., Su, E.C.Y., Nursetyo, A.A.,  
669 Masud, J.H.B. & Bai, C.H. (2018). Roles of sedentary behaviors and unhealthy foods in  
670 increasing the obesity risk in adult men and women: A cross-sectional national study.  
671 *Nutrients*. **10** (6): 704-715.

672 Pan, T. & Yu, Q. (2016). Anti-corrosion methods and materials comprehensive evaluation of  
673 anti-corrosion capacity of electroactive polyaniline for steels. *Anti – Corrosion Methods*  
674 *and Materials*. **63**: 360 – 368.

675 Pan, X. & Webster, D.C. (2012). New biobased high functionality polyols and their use in  
676 polyurethane coatings. *ChemSusChem*. **5**: 419-429.

677 Petrovic, Z.S. (2008). Polyurethanes from vegetable oils. *Polymer Reviews*. **48** (1): 109 – 155.

678 Porcarelli, L., Manojkumar, K., Sardon, H., Llorente, O., Shaplov, A. S., Vijayakrishna, K.,  
679 Gerbaldi, C., Mecerreyes, D. (2017). Single ion conducting polymer electrolytes based  
680 on versatile polyurethanes. *Electrochimica Acta*. **241**: 526 – 534.

681 Priya, S. S., Karthika, M., Selvasekarapandian, S. & Manjuladevi, R. (2018). Preparation and  
682 characterization of polymer electrolyte based on biopolymer I-carrageenan with  
683 magnesium nitrate. *Solid State Ionics*. **327**: 136 – 149.

684 Ren, D. & Frazier, C.E. (2013). Structure–property behaviour of moisture-cure polyurethane  
685 wood adhesives: Influence of hard segment content. *Adhesion and Adhesives*. **45**: 118-  
686 124.

687 Rogulska, S.K., Kultys, A. & Podkoscielny, W. (2007). Studies on thermoplastic polyurethanes  
688 based on newdiphe – derivative diols. II. Synthesis and characterization of segmented  
689 polyurethanes from HDI and MDI. *European Polymer Journal*. **43**: 1402 – 1414.

690 Romaskevicius, T., Budriene, S., Pielichowski, K. & Pielichowski, J. (2006). Application of  
691 polyurethane-based materials for immobilization of enzymes and cells: a review.  
692 *Chemija*. **17**: 74 – 89.

693 Sengodu, P. & Deshmukh, A. D. (2015). Conducting polymers and their inorganic composites  
694 for advanced Li-ion battery electrolytes: a review. *RSC Advances*. **5**: 42109 – 42130.

695 Septevani, A. A., Evans, D. A. C., Chaleat, C., Martin, D. J., Annamalai, P. K. (2015). A  
696 systematic study substituting polyether polyol with palm kernel oil based polyester  
697 polyol in rigid polyurethane foam. *Industrial Crops and Products*. **66**: 16 – 26.

698 Su'ait, M. S., Ahmad, A., Badri, K. H., Mohamed, N. S., Rahman, M. Y. A., Ricardi, C. L. A.  
699 & Scardi, P. The potential of polyurethane bio-based solid polymer electrolyte for  
700 photoelectrochemical cell application. *International Journal of Hydrogen Energy*. **39** (6):  
701 3005 – 3017.

702 Tadesse, M. G., Mengistie, D. A., Chen, Y., Wang, L., Loghin, C., Nierstrasz, V. (2019).  
703 Electrically conductive highly elastic polyamide/lycra fabric treated with PEDOT: PSS  
704 and polyurethane. *Journal of Materials Science*. **54**: 9591 – 9602.

705 Tajau, R., R. Rosiah, Alias, M. S., Mudri, N. H., Halim, K. A. A., Harun, M. H., Isa, N. M.,  
706 Ismail, R. C., Faisal, S. M., Talib, M., Zin, M. R. M., Yusoff, I. I., Zaman, N. K., Ilias,  
707 I. A. (2021). Emergence of polymeric material utilising sustainable radiation curable  
708 palm oil-based products for advanced technology applications. *Polymers*. **13**: 1865 –  
709 1886.

710 Tran, V.H., Kim, J.D., Kim, J.H., Kim, S.K., Lee, J.M. (2020). Influence of cellulose  
711 nanocrystal on the cryogenic mechanical behaviour and thermal conductivity of  
712 polyurethane composite. *Journal of Polymers and The Environment*. **28**: 1169 – 1179.

713 Viera, I.R.S., Costa, L.D.F.D.O., Miranda, G.D.S., Nardehcia, S., Monteiro, M.S.D. S.D.B.,  
714 Junior, E.R. & Delpesch, M.C. (2020). Waterborne poly (urethane – urea)s  
715 nanocomposites reinforced with clay, reduced graphene oxide and respective hybrids:  
716 Synthesis, stability and structural characterization. *Journal of Polymers and The*  
717 *Environment*. **28**: 74 – 90.

718 Wang, B., Wang, L., Li, X., Liu, Y., Zhang, Z., Hedrick, E., Safe, S., Qiu, J., Lu, G. & Wang,  
719 S. (2018). Template-free fabrication of vertically–aligned polymer nanowire array on the  
720 flat–end tip for quantifying the single living cancer cells and nanosurface interaction. a  
721 *Manufacturing Letters*. **16**: 27 – 31.

722 Wang, J., Xiao, L., Du, X., Wang, J. & Ma, H. (2017). Polypyrrole composites with carbon  
723 materials for supercapacitors. *Chemical Papers*. **71** (2): 293 – 316.

724 Wong, C.S. & Badri, K.H. (2012). Chemical analyses of palm kernel oil-based polyurethane  
725 prepolymer. *Materials Sciences and Applications*. **3**: 78 – 86.

726 Wong, C. S., Badri, K., Ataollahi, N., Law, K., Su'ait, M. S., Hassan, N. I. (2014). Synthesis  
727 of new bio–based solid polymer electrolyte polyurethane – LiClO<sub>4</sub> via prepolymerization  
728 method: Effect of NCO/OH ratio on their chemical, thermal properties and ionic  
729 conductivity. *World Academy of Science, Engineering and Technology, International*

- 730 *Journal of Chemical, Molecular, Nuclear, Materials and Metallurgical Engineering*. **8**:  
731 1243 – 1250.
- 732 Yong, Z., Bo, Z.M., Bo, W., Lin, J.Z. & Jun, N. (2009). Synthesis and properties of novel  
733 polyurethane acrylate containing 3-(2-Hydroxyethyl) isocyanurate segment. *Progress in*  
734 *Organic Coatings*. **67**: 264 – 268.
- 735 Zia, K. M., Anjum, S., Zuber, M., Mujahid, M. & Jamil, T. (2014). Synthesis and molecular  
736 characterization of chitosan based polyurethane elastomers using aromatic diisocyanate.  
737 *International of Journal of Biological Macromolecules*. **66**: 26 – 32.

[← BACK](#) [DASHBOARD / ARTICLE DETAILS](#)

Updated on 2022-03-24

Version 7 ▾

# Design and Synthesis of Conducting Polymer Bio-Based Polyurethane Produced from Palm Kernel Oil

VIEWING AN OLDER VERSION

ID 6815187

Muhammad Abdurrahman Munir <sup>SA CA</sup> <sup>1</sup>,  
Khairiah Haji Badri<sup>2</sup>, Lee Yook Heng<sup>2</sup>  
[+ Show Affiliations](#)

## Article Type

Research Article

## Journal

International Journal of  
Polymer Science

Rydz Joanna

Submitted on 2021-06-14 (2 years ago)

[> Abstract](#)[> Author Declaration](#)[> Files](#) 2

## — Editorial Comments

Joanna Rydz

22.03.2022

Decision

Publish

## — Response to Revision Request

Muhammad Abdurrahman Munir

18.02.2022

**Your Reply**

Dear Dr. Joanna, We are thank you so much for you suggestion to this manuscript. We have followed your revisions and looking forward to hear from you. We apologize for the inconvenience during the revision process. Please check the revision and inform us if there is any revision. Best Regards.

**File**Manuscript - Munir.docx 902 kB [+ Reviewer Reports](#)

---

[Hindawi](#) [Privacy Policy](#) [Terms of Service](#) Support: [help@hindawi.com](mailto:help@hindawi.com)



# 1      **Design and Synthesis of Conducting Polymer Bio-Based Polyurethane**

## 2                      **Produced from Palm Kernel Oil**

3

4      Muhammad Abdurrahman Munir<sup>1\*</sup>, Khairiah Haji Badri<sup>2,3</sup>, Lee Yook Heng<sup>2</sup>, Ahlam  
5      Inayatullah<sup>4</sup>, Ari Susiana Wulandari<sup>1</sup>, Emelda<sup>1</sup>, Eliza Dwinta<sup>1</sup>, Veriani Aprillia<sup>5</sup>, Rachmad  
6                      Bagus Yahya Supriyono<sup>1</sup>

7

8      <sup>1</sup>Department of Pharmacy, Faculty of Health Science, Alma Ata University, Daerah Istimewa  
9                      Yogyakarta, 55183, Indonesia

10      <sup>2</sup>Department of Chemical Sciences, Faculty of Science and Technology, Universiti  
11                      Kebangsaan Malaysia, Bangi, 43600, Malaysia

12      <sup>3</sup>Polymer Research Center, Universiti Kebangsaan Malaysia, Bangi, 43600, Malaysia

13      <sup>4</sup>Faculty of Science and Technology, Universiti Sains Islam Malaysia, Nilai, 71800, Malaysia

14      <sup>5</sup>Department of Nutrition Science, Alma Ata School of Health Sciences, Alma Ata  
15                      University, Daerah Istimewa Yogyakarta, 55183, Indonesia

16

17                      \*Email: [muhammad@almaata.ac.id](mailto:muhammad@almaata.ac.id)

### 18

### 19                      **Abstract**

20      Polyurethane (PU) is a unique polymer that has versatile processing methods and mechanical  
21      properties upon the inclusion of selected additives. In this study, a freestanding bio-based  
22      polyurethane film the screen-printed electrode (SPE) was prepared by the solution casting  
23      technique, using acetone as solvent. It was a one-pot synthesis between major reactants namely,  
24      palm kernel oil-based polyol and 4,4-methylene diisocyanate. The PU has strong adhesion on

25 the SPE surface. The synthesized bio-based polyurethane was characterized using  
26 thermogravimetry analysis, differential scanning calorimetry, Fourier-transform infrared  
27 spectroscopy (FTIR), surface area analysis by field emission scanning electron microscope,  
28 and cyclic voltammetry. Cyclic voltammetry was employed to study electro-catalytic  
29 properties of SPE-polyurethane towards oxidation of PU. Remarkably, SPE-PU exhibited  
30 improved anodic peak current as compared to SPE itself using the differential pulse  
31 voltammetry method. Furthermore, the formation of urethane linkages (-NHC(O) backbone)  
32 after polymerization was analyzed using FTIR and confirmed by the absence of peak at 2241  
33  $\text{cm}^{-1}$  attributed to the sp-hybridized carbons atoms of  $\text{C}\equiv\text{C}$  bonds . The glass transition  
34 temperature of the polyurethane was detected at 78.1 °C.

35

36 **Keywords:** polyurethane, polymerization, screen-printed electrode, voltammetry

37

38

### 39 **1. Introduction**

40 Conducting polymers (CPs) are polymers that can release a current (Alqarni et al. 2020). The  
41 conductivity of CPs was first observed in polyacetylene, nevertheless owing to its instability,  
42 the invention of various CPs have been studied and reported such as polyaniline (PANI),  
43 poly(*o*-toluidine) (PoT), polythiophene (PTH), polyfluorene (PF), and polyurethane (PU).  
44 Furthermore, natural CPs have low conductivity and are often semi-conductive. Therefore, it  
45 is imperative to improve their conductivity for electrochemical sensor purposes (Sengodu &  
46 Deshmukh 2015; Dzulkipli et al. 2021; Wang et al. 2018). The CPs can be produced from many  
47 organic materials and they have several advantages such as having an electrical current,  
48 inexpensive materials, massive surface area, small dimensions, and the production is  
49 straightforward. Furthermore, according to these properties, many studies have been reported

50 by researchers to study and report the variety of CPs applications such as sensors, biochemical  
51 applications, electrochromic devices, and solar cells (Alqarni et al. 2020; Ghosh et al. 2018).  
52 There is scientific documentation on the use of conductive polymers in various studies such as  
53 polyaniline (Pan & Yu 2016), polypyrrole (Ladan et al. 2017), and polyurethane (Tran et al.  
54 2020; Vieira et al. 2020; Guo et al. 2020; Fei et al. 2020).

55

56 Polyurethane productions can be obtained by using several materials as polyols such as  
57 petroleum, coal, and crude oils. Nevertheless, these materials have become very rare to find  
58 and the price is very expensive at the same time required a sophisticated system to produce it.  
59 The reasons such as price and time consuming to produce polyols have been considered by  
60 many researchers, furthermore, finding utilizing plants that can be used as alternative polyols  
61 should be done immediately (Badri 2012). Thus, to avoid the use of petroleum, coal, and crude  
62 oils as raw materials for a polyol, vegetable oils become a better choice to produce polyol in  
63 order to obtain a biodegradable polymer. Vegetable oils that are generally used for  
64 polyurethane synthesis are soybean oil, corn oil, sunflower seed oil, coconut oil, nuts oil,  
65 rapeseed, olive oil, and palm oil (Badri 2012; Borowicz et al. 2019).

66

67 It is very straightforward for vegetable oils to react with a specific group to produce a PU such  
68 as epoxy, hydroxyl, carboxyl, and acrylate owing to the existence of (-C=C-) in vegetable oils.  
69 Thus, it provides appealing profits to vegetable oils compared to petroleum considering the  
70 toxicity, price, and harm to the environment (Mustapha et al. 2019; Mohd Noor et al. 2020).  
71 Palm oil becomes the chosen in this study to produce PU owing to it being largely cultivated  
72 in South Asia particularly in Malaysia and Indonesia. It has several profits compared to other  
73 vegetable oils such as the easiest materials obtained, the lowest cost of all the common

74 vegetable oils, and recognized as the plantation that has a low environmental impact and  
75 removing CO<sub>2</sub> from the atmosphere as a net sequester (Tajau et al. 2021; Septevani et al. 2015).

76

77 The application of bio based polymer has appealed much attention until now. Global  
78 environmental activists have forced researchers to discover another material producing  
79 polymers (Priya et al. 2018). PUs have many advantages that have been used by many  
80 researchers, they are not merely versatile materials but also have the durability of metal and  
81 the flexibility of rubber. Furthermore, they can be promoted to replace rubber, metals, and  
82 plastics in several aspects. Several applications of PUs have been reported and studied such as  
83 textiles, automotive, building and construction applications, and biomedical applications (Zia  
84 et al. 2014; Romaskevicius et al. 2006). Polyurethanes are also considered to be one of the most  
85 useful materials with many profits such as; possessing low conductivity, low density,  
86 absorption capability, and dimensional stability. They are a great research subject due to their  
87 mechanical, physical, and chemical properties (Badan & Majka 2017; Munir et al. 2021).

88

89 PU structure contains the urethane group that can be formed from the reaction between  
90 isocyanate groups (-NCO) and hydroxyl group (-OH). Nevertheless, several groups can be  
91 found in PU structure such as urea, esters, ethers, and several aromatic groups. Furthermore,  
92 PUs can be produced from different sources as long as they contain specific materials (polyol  
93 and methylene diphenyl diisocyanate (MDI) and making them very useful for specific  
94 applications. Thus, according to the desired properties, PUs can be divided into several types  
95 such as waterborne, flexible, rigid, coating, binding, sealants, adhesives, and elastomers  
96 (Akindoyo et al. 2016).

97

98 PUs are lighter than other materials such as metals, gold, and platinum. The hardness of PU  
99 also relies on the number of the aromatic rings in the polymer structure (Janpoung et al, 2020;  
100 Su'ait et al. 2014), majorly contributed by the isocyanate derivatives. PUs have also a conjugate  
101 structure where electrons can move in the main chain that causes electricity produced even the  
102 current is low. The current of conjugated linear ( $\pi$ ) can be elaborated by the gap between the  
103 valence band and the conduction band, or called high energy level containing electrons  
104 (HOMO) and lowest energy level not containing electrons (LUMO), respectively (Wang et al.  
105 2017; Kotal et al. 2011).

106  
107 In the recent past, several conventional methods have been developed such as capillary  
108 electrophoresis, liquid, and gas chromatography coupled with several detectors. Nevertheless,  
109 although chromatographic and spectrometric approaches are well developed for qualitative and  
110 quantitative analyses of analytes, several limitations emerged such as complicated  
111 instrumentation, expensive, tedious sample preparations, and requiring large amounts of  
112 expensive solvents that will harm the users and environment (Kilele et al. 2020; Inayatullah et  
113 al. 2021; Munir et al. 2021; Harmayani et al. 2014; Nurwanti et al. 2018). Therefore, it is  
114 imperative to obtain and develop an alternative material that can be used to analyze a specific  
115 analyte. Electrochemical methods are extremely promising methods in the determination of an  
116 analyte in samples owing to the high selectivities, sensitivities, inexpensive, requirements of  
117 small amounts of solvents, and can be operated by people who have no background in analytical  
118 chemistry. In addition, sample preparation such as separation and extraction steps are not  
119 needed owing to the selectivity of this instrument where no obvious interference on the current  
120 response is recorded (Chokkareddy et al. 2020). Few works have been reported on the  
121 electrochemical methods for the determination of analyte using electrodes combined with  
122 several electrode modifiers such as carbon nanotube, gold, and graphene (Chokkareddy et al.

123 2020; Kilele et al. 2021). Nevertheless, the materials are expensive and the production is  
124 difficult. Thus, an electrochemical approach using inexpensive and easily available materials  
125 as electrode modifiers should be developed (Degefu et al. 2014; Munir et al. 2022).

126

127 Nowadays, screen-printed electrodes (SPEs) modified with conducting polymer have been  
128 developed for various electrochemical sensing. SPE becomes the best solution owing to the  
129 electrode having several advantages such as frugal manufacture, tiny size, being able to  
130 produce on a large scale, and can be applied for on-site detection (Nakthong et al. 2020).

131 Conducting polymers (CPs) become an alternative to modifying the screen-printed electrodes  
132 due to their electrical conductivity, able to capture analyte by chemical/physical adsorption,  
133 large surface area, and making CPs are very appealing materials from electrochemical  
134 perspectives (Baig et al. 2019). Such advantages of SPE encourage us to construct a new  
135 electrode for electrochemical sensing, and no research reported on the direct electrochemical  
136 oxidation of histamine using a screen-printed electrode modified by bio-based polyurethane.  
137 Therefore, this research is the first to develop a new electrode using (screen printed  
138 polyurethane electrode) SPPE without any conducting materials.

139

140 The purpose of this work was to synthesize, characterize and study the electro behavior of  
141 polyurethane using cyclic voltammetry (CV) and differential pulse voltammetry (DPV)  
142 attached to the screen-printed electrode. To the best of our knowledge, this is the first attempt  
143 to use a modified polyurethane electrode. The electrochemistry of polyurethane mounted onto  
144 SPE is discussed in detail. PUs are possible to become an advanced frontier material that has  
145 been chemically modified the specific electrodes for bio/chemical sensing application.

146

147

## 148 **2. Experimental**

### 149 **2.1 Chemicals**

150 *Synthesis of bio-based polyurethane film:* Palm kernel oil (PKOp) based polyol supplied by  
151 UKM Technology Sdn Bhd through MPOB/UKM station plant, Pekan Bangi Lama, Selangor  
152 and prepared using Badri et al. (2000) method. 4, 4-diphenylmethane diisocyanate (MDI) was  
153 acquired from Cosmopolyurethane (M) Sdn. Bhd., Klang, Malaysia. Solvents and analytical  
154 reagents were benzene ( $\geq 99.8\%$ ), toluene ( $\geq 99.8\%$ ), hexane ( $\geq 99\%$ ), acetone ( $\geq 99\%$ ),  
155 dimethylsulfoxide (DMSO) ( $\geq 99.9\%$ ), dimethylformamide (DMF) ( $\geq 99.8\%$ ), tetrahydrofuran  
156 (THF) ( $\geq 99.8\%$ ), and polyethylene glycol (PEG) with a molecular weight of 400 Da obtained  
157 from Sigma Aldrich Sdn Bhd, Shah Alam.

158

### 159 **2.2 Apparatus**

160 Tensile testing was performed using a universal testing machine model Instron 5566 following  
161 ASTM D638 (Standard Test Method for Tensile Properties of Plastics). The tensile properties  
162 of the polyurethane film were measured at a velocity of 10 mm/min with a cell load of 5 kN.  
163 The thermal properties were performed using thermogravimetry analysis (TGA) and  
164 differential scanning calorimetry (DSC) analysis. TGA was performed using a thermal analyzer  
165 of the Perkin Elmer Pyris model with a heating rate of 10 °C/min at a temperature range of 30  
166 to 800 °C under a nitrogen gas atmosphere. The DSC analysis was performed using a thermal  
167 analyzer of the Perkin Elmer Pyris model with a heating rate of 10 °C /minute at a temperature  
168 range of -100 to 200 °C under a nitrogen gas atmosphere. Approximately, 5–10 mg of PU was  
169 weighed. The sample was heated from 25 to 150 °C for one minute, then cooled immediately  
170 from 150 to 100 °C for another one minute and finally, reheated to 200 °C at a rate of 10 °C  
171 /min. At this point, the polyurethane encounters changing from elastic properties to brittle due  
172 to changes in the movement of the polymer chains. Therefore, the temperature in the middle of

173 the inclined regions is taken as the glass transition temperature ( $T_g$ ). The melting temperature  
174 ( $T_m$ ) is identified as the maximum endothermic peak by taking the area below the peak as the  
175 enthalpy point ( $\Delta H_m$ ).

176

177 The morphological analysis of PU film was performed by field emission scanning electron  
178 microscope (FESEM) model Gemini SEM microscope model 500-70-22. Before the analysis  
179 was carried out, the polyurethane film was coated with a thin layer of gold to increase the  
180 conductivity of the film. The coating method was carried out using a sputter-coater. The  
181 observations were conducted at a magnification of 200× and 5000× with 10.00 kV (Electron  
182 high tension – EHT).

183

184 The crosslinking of PU was determined using the soxhlet extraction method. About 0.60 g of  
185 PU sample was weighed and put in an extractor tube containing 250 ml of toluene, used as a  
186 solvent. This flow of toluene was let running for 24 h. Mass of the PU was weighed before and  
187 after the reflux process was carried out. Then, the sample was dried in the conventional oven  
188 at 100 °C for 24 h in order to get a constant mass. The percentage of crosslinking content  
189 known as the gel content can be calculated using Equation (1).

$$190 \quad \text{Gel content (\%)} = \frac{W_0 - W}{W} \times 100 \% \quad (1)$$

191  $W_0$  is the mass of PU before the reflux process (g) and  $W$  is the mass of PU after the reflux  
192 process (g).

193

194 FTIR spectroscopic analysis was performed using a Perkin-Elmer Spectrum BX instrument  
195 using the diamond attenuation total reflectance (DATR) method to confirm the polyurethane,  
196 PKOp, and MDI functional group. FTIR spectroscopic analysis was performed at a  
197 wavenumber of 4000 to 600  $\text{cm}^{-1}$  to identify the peaks of the major functional groups in the



198 formation of the polymer such as amide group (-NH), urethane carbonyl group (-C=O),  
199 isocyanate group (-O=C=N-), and carbamate group (-CN).

200

### 201 **2.3 Synthesis of Polyurethane**

202 Firstly, the polyol prepolymer solution was produced by combining palm kernel oil-based  
203 polyol and poly(ethylene glycol) (PEG) 400 (100:40 g/g), acetone 30% was used as a solution.

204 The compound was homogenized using a centrifuge (100 rpm) for 5 min. Whereas diisocyanate  
205 prepolymer was obtained by mixing 4,4'-diphenylmethane diisocyanate (100 g) to acetone

206 30%, afterward the mixture was mixed using a centrifuge for 1 min to obtain a homogenized

207 solution. Afterward, diisocyanate solution (10 g) was poured into a container that contains

208 polyol prepolymer solution (10 g) slowly to avoid an exothermic reaction occurring. The

209 mixture was mixed for 30 sec until a homogenized solution was acquired. Lastly, the

210 polyurethane solution was poured on the electrode surface by using the casting method and

211 dried at ambient temperature for 12 h.

212

### 213 **2.4 Modification of Electrode**

214 Voltammetric tests were performed using Metrohm Autolab Software (**Figure 1**) analyzer

215 using cyclic voltammetry method or known as amperometric mode and differential pulse

216 voltammetry. All electrochemical experiments were carried out using screen-printed electrode

217 (diameter 3 mm) modified using polyurethane film as working electrode, platinum wire as the

218 auxiliary electrode, and Ag/AgCl electrode as a reference electrode. All experiments were

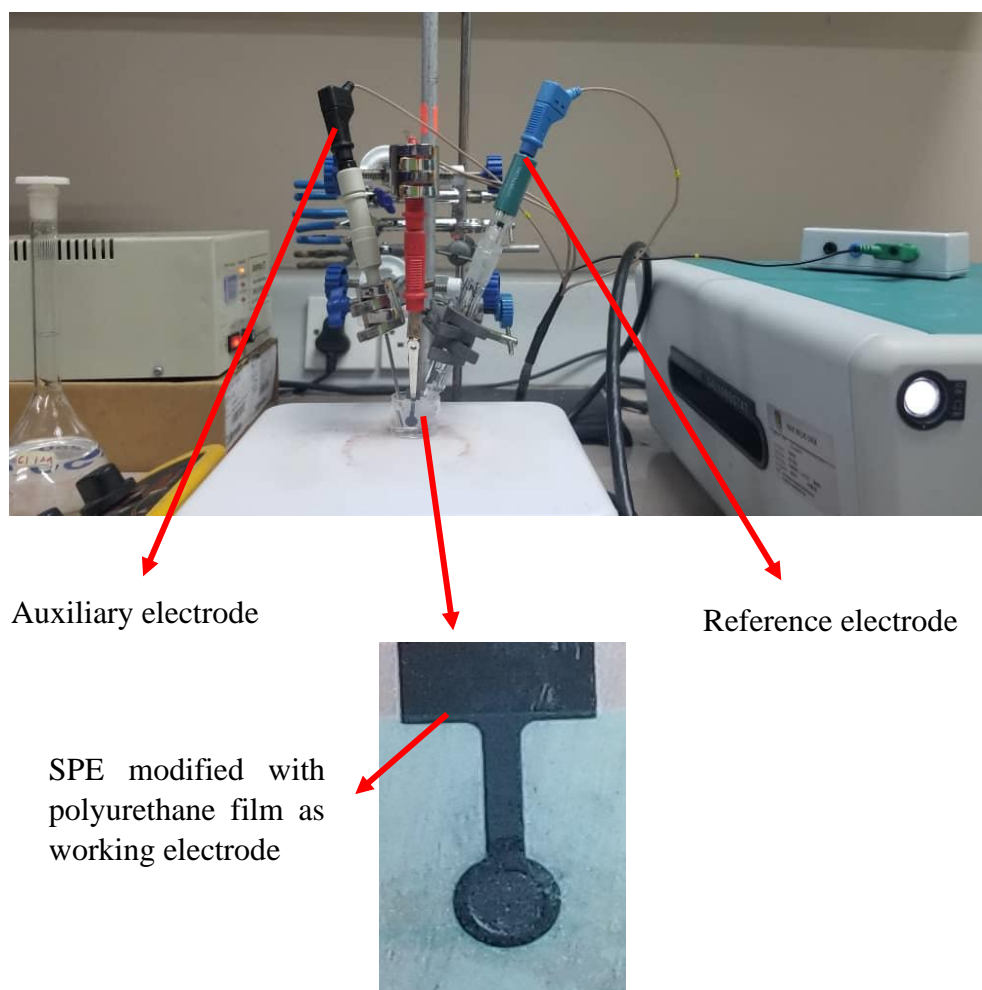
219 conducted at a temperature of  $20 \pm 2$  °C.

220

221 The PU was cast onto the screen-printed electrode (SPE) and analyzed using a single

222 voltammetric cycle between -1200 and +1500 mV (vs Ag/AgCl) of ten cycles at a scanning

223 rate of 100 mV/s in 5 ml of KCl in order to study the activity of SPE and polyurethane film.  
224 Approximately (0.1, 0.3 and 0.5) mg of bio-based polyurethane was dropped separately onto  
225 the surface of the SPE and dried at room temperature. The modified palm-based polyurethane  
226 electrodes were then rinsed with deionized water to remove physically adsorbed impurities and  
227 residues of unreacted material on the electrode surface. All electrochemical materials and  
228 calibration measurements were carried out in a 5 mL glass beaker with a configuration of three  
229 electrodes inside it. Platinum wire and silver/silver chloride (Ag/AgCl) electrodes were used  
230 as auxiliary and reference electrodes, while a screen-printed electrode that had been modified  
231 with polyurethane was applied as a working electrode.



232 **Figure 1.** Potentiostat instrument to study the conductivity of SPE modified with  
233 polyurethane film using voltammetric approach: CV and DPV

234

235 **3. Results and Discussion**

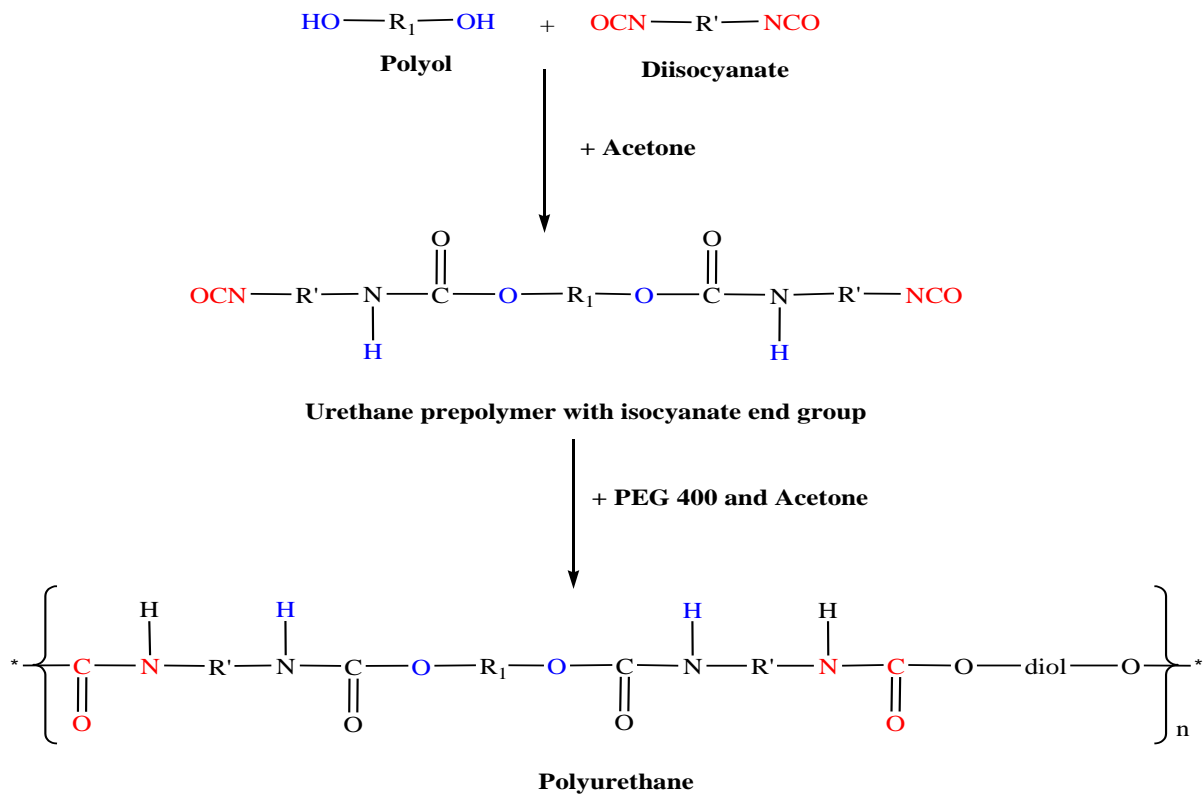
236 The synthesis of PU films was carried out using a pre-polymerization method which involves  
237 the formation of urethane polymer at an early stage. The reaction took place between  
238 diisocyanate (MDI) and palm kernel oil-based polyol. **Table 1** presents the PKO-p properties  
239 used in this study.

240 **Table 1** The specification of PKO-p (Badri et al. (2000)).

Property	Values
Viscosity at 25 °C (cps)	1313.3
Specific gravity (g/mL)	1.114
Moisture content (%)	0.09
pH value	10–11
The hydroxyl number mg KOH/g	450–470

241  
242 The structural chain was extended with the aid of poly(ethylene glycol) to form flexible and  
243 elastic polyurethane film. In order to produce the urethane prepolymer, the isocyanate group (-  
244 NCO) attacks with the hydroxyl group (-OH) of polyol (PKOp) while the other hydroxyl group  
245 of the polyol is attacked by the other isocyanate group (Wong & Badri 2012) as shown in  
246 **Figure 2.**

247



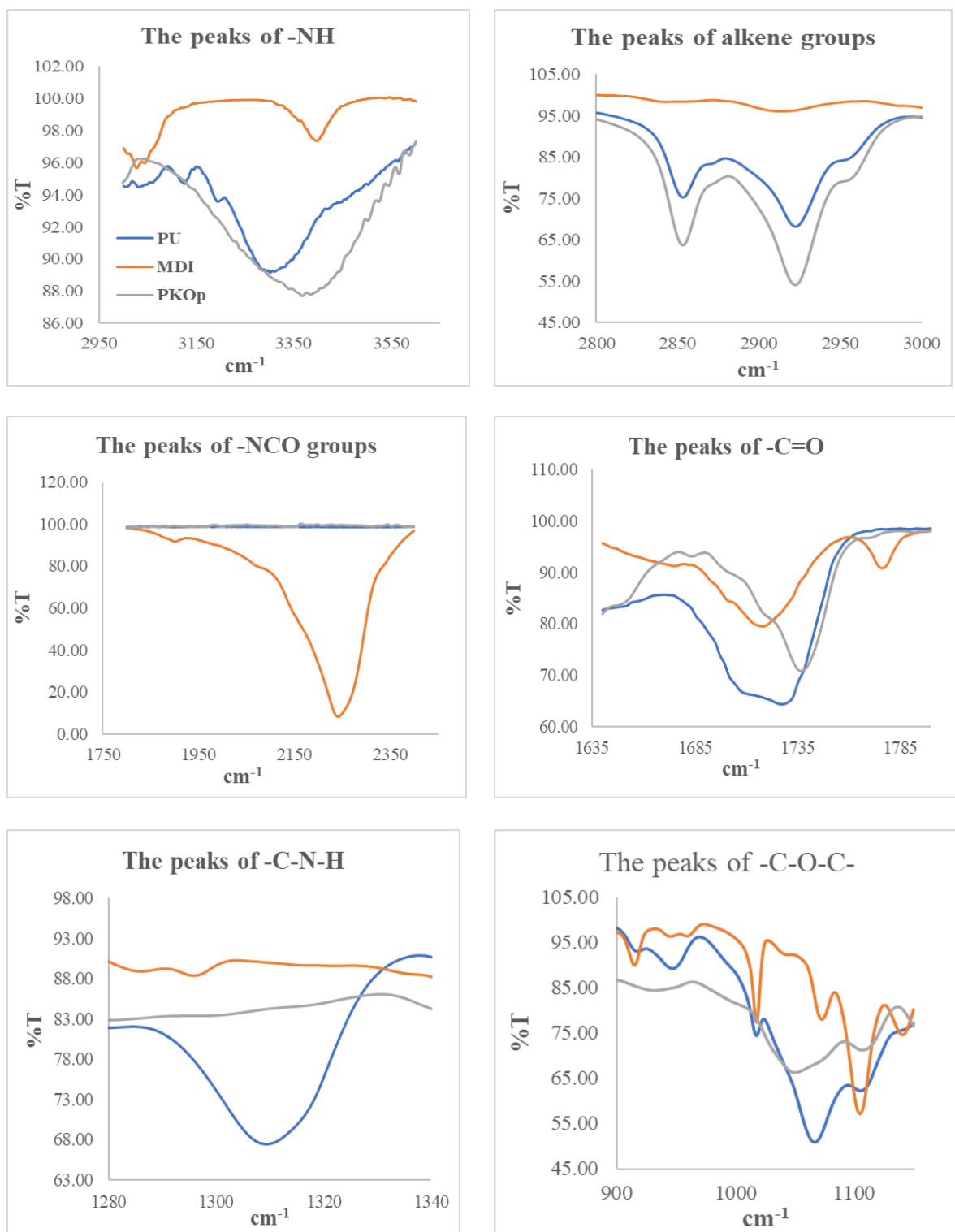
248

249 **Figure 2.** PU production via the pre-polymerization method (Wong & Badri 2012).

250

251 a. FTIR analysis

252 **Figure 3** shows the FTIR spectra for polyurethane, exhibiting the important functional group  
 253 peaks. According to a study researched by Wong & Badri 2012, PKO-p reacts with MDI to  
 254 form urethane prepolymers. The NCO group on MDI reacts with the OH group on polyol  
 255 whether PKOp or PEG. It can be seen there are no important peaks of MDI in the FTIR spectra.  
 256 This is further verified by the absence of an absorption bands at the  $2400 \text{ cm}^{-1}$  belonging to  
 257 MDI (-NCO groups). This could also confirm that the -NCO group on MDI had completely  
 258 reacted with PKO-p to form the urethane -NHC(O) backbone. The presence of amides (-NH),  
 259 carbonyl urethane group (-C=O), carbamate group (C-NH), and -C-O-C confirmed the  
 260 formation of urethane chains. In this study, the peak of carbonyl urethane (-C=O) detected at  
 261  $1727 \text{ cm}^{-1}$  indicated that the carbonyl urethane group was bonded without hydrogen owing to  
 262 the hydrogen reacts with the carbonyl urethane group.



263 **Figure 3.** FTIR spectra of several important peaks between polyurethane, PKO-p, and MDI  
 264  
 265 The reaction of polyurethane has been studied by Hamuzan & Badri (2016) where the urethane  
 266 carbonyl group was detected at 1730–1735  $\text{cm}^{-1}$  while the MDI carbonyl was detected at 2400

267  $\text{cm}^{-1}$ . The absence of absorption bands at  $2250\text{--}2270\text{ cm}^{-1}$  associated with  $\text{N}=\text{C}=\text{O}$  bond  
268 stretching indicates the absence of NCO groups. It shows that the polymerization reaction  
269 occurs entirely between NCO groups in MDI with hydroxyl groups on polyols and PEG  
270 (Mishra et al. 2012). The absence of peaks at  $1690\text{ cm}^{-1}$  representing urea ( $\text{C}=\text{O}$ ) in this study  
271 indicated, there is no urea formation as a byproduct (Clemitson 2008) of the polymerization  
272 reaction that possibly occurs due to the excessive water. For the amine ( $-\text{NH}$ ) group, hydrogen-  
273 bond to  $-\text{NH}$  and oxygen to form ether and hydrogen bond to  $\text{NH}$  and oxygen to form carbonyl  
274 on urethane can be detected at the peak of  $3301\text{ cm}^{-1}$  and in the wavenumber at range  $3326\text{--}$   
275  $3428\text{ cm}^{-1}$ . This has also been studied and detected by Mutsuhisa et al. (2007) and Lampman  
276 et. al. (2010). In this research, the proton acceptor is carbonyl ( $-\text{C}=\text{O}$ ) while the proton donor  
277 is an amine ( $-\text{NH}$ ) to form a hydrogen bond. The MDI chemical structure has the electrostatic  
278 capability that produces dipoles from several atoms such as hydrogen, oxygen, and nitrogen  
279 atoms. These properties make isocyanates are highly reactive, and have different properties  
280 (Leykin et al. 2016).

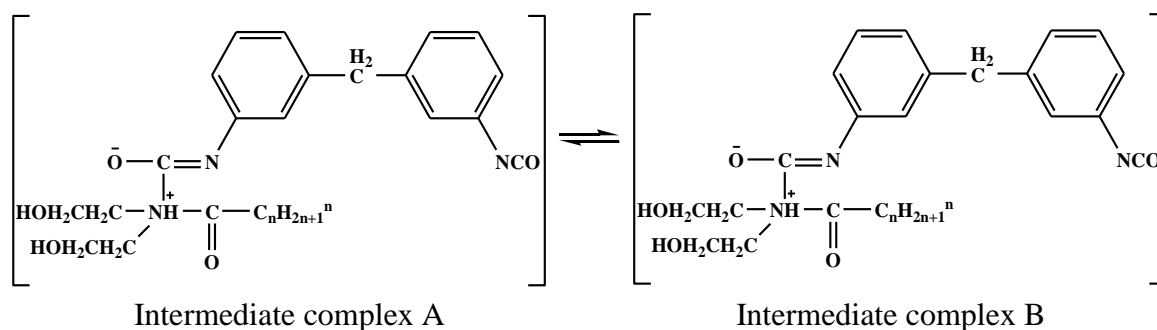
281

282 MDI was one of the isocyanates used in this study, has an aromatic group, and is more  
283 reactive compared to aliphatic group isocyanates such as hexamethylene diisocyanate (HDI)  
284 or isophorone diisocyanate (IPDI). Isocyanates have two groups of isocyanates on each  
285 molecule. Diphenylmethane diisocyanate is an exception owing to its structure consisting of  
286 two, three, four, or more isocyanate groups (Nohra et al. 2013). The use of PEG 400 in this  
287 study as a chain extender for polyurethane increases the chain mobility of polyurethane at an  
288 optimal amount. The properties of polyurethane are contributed by hard and soft copolymer  
289 segments of both polyol monomers and MDI. This makes the hard segment of urethane serves  
290 as a crosslinking site between the soft segments of the polyol (Leykin et al. 2016).

291

292 The mechanism of the pre-polymerization in urethane chains formation is a  
 293 nucleophilic substitution reaction as studied by Yong et al. (2009). However, this study found  
 294 amines as nucleophiles. Amine attacks carbonyl on isocyanate in MDI in order to form two  
 295 resonance structures of intermediate complexes A and B (**Figure 4**). Intermediate complex B  
 296 has a greater tendency to react with polyols due to stronger carbonyl (C=O) bonds than C=N  
 297 bonds on intermediate complexes A. Thus, intermediate complex B is more stable than  
 298 intermediate complex A, as suggested by previous researchers who have conducted by Wong  
 299 and Badri (2012).

300



301

**Figure 4.** The formation of intermediate complexes

302

303 Moreover, oxygen is more electronegative than nitrogen causing cations (H<sup>+</sup>) to tend  
 304 to attack -CN bonds compared to -CO. The combination between long polymer chain and low  
 305 cross-linking content gives the polymer elastic properties whereas short-chain and high cross-  
 306 linking produce hard and rigid polymers. Cross-linking in polymers consists of three-  
 307 dimensional networks with high molecular weight. In some aspects, polyurethane can be a  
 308 macromolecule, a giant molecule (Petrovic 2008).

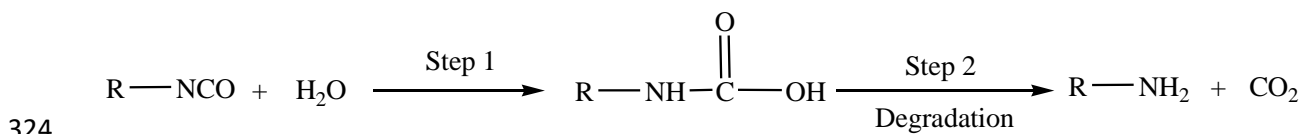
309

310 However, complexes A and B intermediate were produced after the nucleophile of PEG  
 311 attacking the isocyanate group in the MDI. However, PEG contains oxygen atoms that are more  
 312 electronegative than nitrogen atoms inside the PKOp chemical structure causing the reaction

313 of nucleophilic substitution that occurs in PKOp. Furthermore, amine has a higher probability  
314 of reacting compared to hydroxyl (Herrington & Hock 1997). Amine with high alkalinity reacts  
315 with carbon atoms on MDI as proposed by Wong and Badri (2012).

316

317 The production of intermediate complexes unstabilizes the alkyl ions, nevertheless, the  
318 long carbon chains of PKOp ensure the stability of alkyl ions. The addition of PEG in this study  
319 is imperative, not merely to increase the chain length of PU but also to avoid the production of  
320 urea as a by-product after the NCO group reacts with H<sub>2</sub>O from the environment. If the NCO  
321 group reacts with the excess water in the environment, the formation of urea and carbon dioxide  
322 gas will also occur excessively (**Figure 5**). This reaction can cause a polyurethane foam, not  
323 polyurethane film as we studied the film.



325 **Figure 5.** The reaction between the NCO group and water producing carbon dioxide

326

327 Furthermore, the application of PEG can influence the conductivity of PU whereby  
328 Porcarelli et al. (2017) have reported the application of PEG using several molecular weights.  
329 PEG 1500 decreased the conductivity of PU in consequence of the semicrystalline phase of  
330 PEG 1500 that acted as a poor ion-conducting phase for PU. It is also well known that PEG  
331 with a molecular weight of more than 1000 g·mol<sup>-1</sup> tends to crystallize with deleterious effects  
332 on room temperature ionic conductivity (Porcarelli et al. 2017).

333

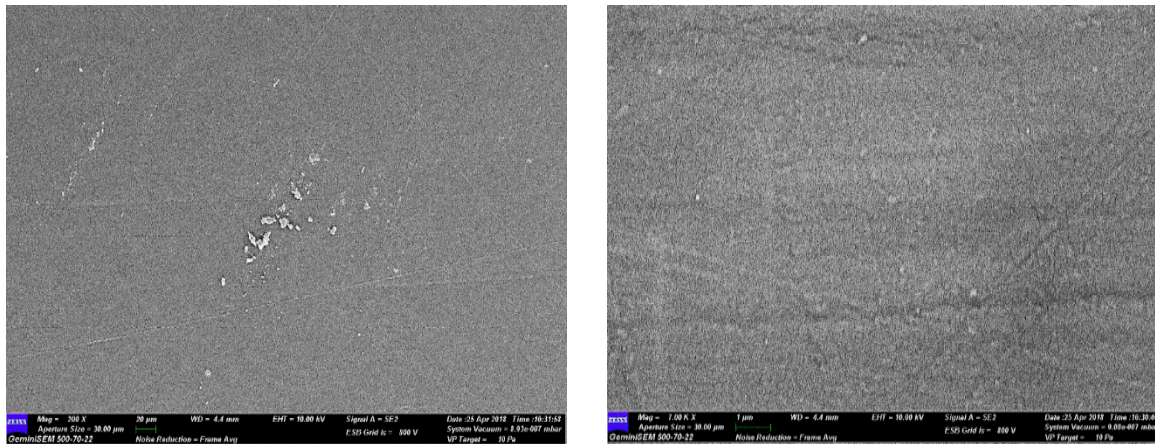
#### 334 b. Morphological analysis

335 The field emission scanning electron microscope micrograph in **Figure 6** shows the formation  
336 of a uniform polymer film contributed by the polymerization method applied. The



337 magnification used for this surface analysis ranged from 200 to 5000×. The polymerization  
 338 method can also avoid the failure of the reaction in PU polymerization. Furthermore, no trace  
 339 of separation was detected by FESEM. This has also been justified by the wavelengths obtained  
 340 by the FTIR spectra above.

341



342 **Figure 6.** The micrograph of polyurethane films was analyzed by FESEM at (a) 200× and (b)  
 343 5000× magnifications.

344

345 c. The crosslinking analysis

346 Soxhlet analysis was applied to determine the degree of crosslinking between the hard  
 347 segments and the soft segments in the polyurethane. The urethane group on the hard segment  
 348 along the polyurethane chain is polar (Cuve & Pascault 1991). Therefore, during the testing, it  
 349 was very difficult to dissolve in toluene, as the testing reagent. The degree of crosslinking is  
 350 determined by the percentage of the gel content. The analysis result obtained from the Soxhlet  
 351 testing indicated a 99.3% gel content. This is significant in getting a stable polymer at a higher  
 352 working temperature (Rogulska et al. 2007).

353

$$\text{Gel content (\%)} = \frac{(0.6 - 0.301) \text{ g}}{0.301 \text{ g}} \times 100\% = 99.33\%$$

354

355

356 d. The thermal analysis  
 357 Thermogravimetric analysis can be used to observe the material mass based on temperature  
 358 shift. It can also examine and estimate the thermal stability and materials properties such as the  
 359 alteration weight owing to absorption or desorption, decomposition, reduction, and oxidation.  
 360 The material composition of polymer is specified by analyzing the temperatures and the heights  
 361 of the individual mass steps (Alamawi et al. 2019). **Figure 7** shows the TGA and derivative  
 362 thermogravimetry (DTG) thermograms of polyurethane. The percentage weight loss (%) is  
 363 listed in **Table 2**. Generally, only a small amount of weight was observed. It is shown in **Figure**  
 364 **7** in the region of 45–180 °C. This is due to the presence of condensation on moisture and  
 365 solvent residues.

366  
 367 **Table 2** Weight loss percentage (*wt%*) and thermal degradation ( $T_d$ ) of polyurethane film

% Weight loss ( <i>wt%</i> ) and thermal degradation ( $T_d$ )					
$T_{max}$ , (°C)	$T_{d1}$ , 200–290 °C	$T_{d2}$ , 350–500 °C	$T_{d3}$ , 500–550 °C	Total of weight loss (%)	Residue after 550 °C (%)
240	8.04	39.29	34.37	81.7	18.3

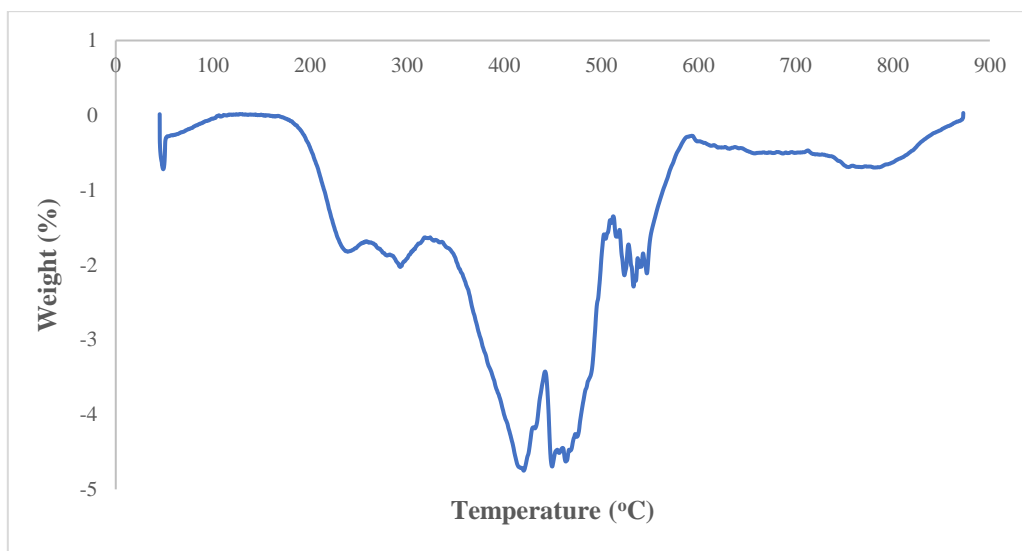
368  $T_{max}$ : The temperature of polyurethane started to degrade;  $T_{d1}$ : Thermal degradation first;  $T_{d2}$ : Thermal degradation second;  
 369  $T_{d3}$ : Thermal degradation third

370  
 371 The bio-based polyurethane is thermally stable up to 240 °C before it has undergone thermal  
 372 degradation (Agrawal et al. 2017). The first stage of thermal degradation ( $T_{d1}$ ) on polyurethane  
 373 films was shown in the region of 200–290 °C as shown in **Figure 7**. The  $T_{d1}$  is associated with  
 374 degradation of the hard segments of the urethane bond, forming alcohol or degradation of the  
 375 polyol chains and releasing of isocyanates (Berta et al. 2006), primary and secondary amines  
 376 as well as carbon dioxide (Corcuera et al. 2011; Pan & Webster 2012). Meanwhile, the second  
 377 thermal degradation stage ( $T_{d2}$ ) of polyurethane films experienced a weight loss of 39.29%.  
 378 This endotherm of  $T_{d2}$  is related to the dimerization of isocyanates to form carbodiimides and  
 379 release CO<sub>2</sub>. The formed carbodiimide reacts with alcohol to form urea. The third stage of

380 thermal degradation ( $T_{d3}$ ) is related to the degradation of urea (Berta et al. 2006) and the soft  
381 segment on polyurethane.

382

383 Generally, DSC analysis exhibited thermal transitions as well as the initial  
384 crystallization and melting temperatures of the polyurethane (Khairuddin et al. 2018). It serves  
385 to analyze changes in thermal behavior due to changes occurring in the chemical chain structure  
386 based on the  $T_g$  of the sample obtained from the DSC thermogram (**Figure 8**). DSC analysis  
387 on polyurethane film was performed in the temperature at the range 100 °C to 200 °C of using  
388 nitrogen gas as a blanket as proposed by Furtwengler et al. (2017). The glass transition  
389 temperature on polyurethane was above room temperature, at 78.1 °C indicated the state of  
390 glass on polyurethane. The presence of MDI contributes to the formation of hard segments in  
391 polyurethanes. Porcarelli et al. (2017) stated that possessing a low  $T_g$  may contribute to PU  
392 conductivity.



393

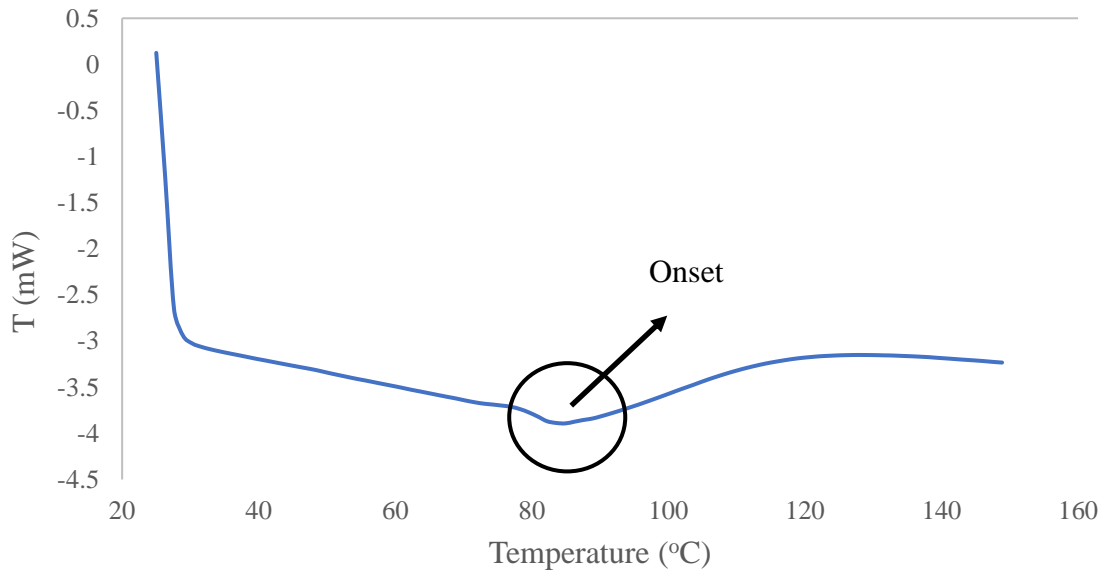
**Figure 7.** DTG thermogram of polyurethane film

394

395

396 During polymerization, this hard segment restricts the mobility of the polymer chain  
397 (Ren et al. 2013) owing to the steric effect on the benzene ring in the hard segment. The  
398 endothermic peak of acetone used as the solvent in this study was supposedly at 56 °C.

399 However, it was detected in the DSC thermogram nor the TGA thermogram, which indicates  
400 that acetone was removed from the polyurethane during the synthesis process, owing to its  
401 volatile nature. The presence of acetone in the synthesis was to lower the reaction kinetics.



402

**Figure 8.** DSC thermogram of polyurethane film

403

404

405

406 e. The solubility and mechanical properties of the polyurethane film

407 The chemical resistivity of a polymer will be the determinant in performing as a conductor.

408 Thus, its solubility in various solvents was determined by dissolving the polymer in selected

409 solvents such as hexane, benzene, acetone, THF, DMF, and DMSO. On the other hand, the

410 mechanical properties of polyurethane were determined based on the standard testing following

411 ASTM D638. The results from the polyurethane film solubility and tensile test are shown in

412 **Table 3.** Polyurethane films were insoluble with acetone, hexane, and benzene and are only

413 slightly soluble in THF, DMF, and DMSO solutions. While the tensile strength of a PU film

414 indicated how much elongation load the film was capable of withstanding the material before

415 breaking.

416

417 **Table 3** The solubility and mechanical properties of the polyurethane film

418

Parameters	Polyurethane film	
Solubility	Benzene	Insoluble
	Hexane	Insoluble
	Acetone	Insoluble
	THF	Less soluble
	DMF	Less soluble
	DMSO	Less soluble
Stress (MPa)	8.53	
Elongation percentage (%)	43.34	
Strain modulus (100) (MPa)	222.10	

419

420 The tensile stress, strain, and modulus of polyurethane film also indicated that polyurethane

421 has good mechanical properties that are capable of being a supporting substrate for the next

422 stage of the study. In the production of polyurethane, the properties of polyurethane are easily

423 influenced by the content of MDI and polyol used. The length of the chain and its flexibility

424 are contributed by the polyol which makes it elastic. High crosslinking content can also produce

425 hard and rigid polymers. MDI is a major component in the formation of hard segments in

426 polyurethane. It is this hard segment that determines the rigidity of the PU. Therefore, high

427 isocyanate content results in higher rigidity on PU (Petrovic et al. 2002). Thus, the polymer has

428 a higher resistance to deformation and more stress can be applied to the PU.

429

430 f. The conductivity of the polyurethane as a polymeric film on SPE

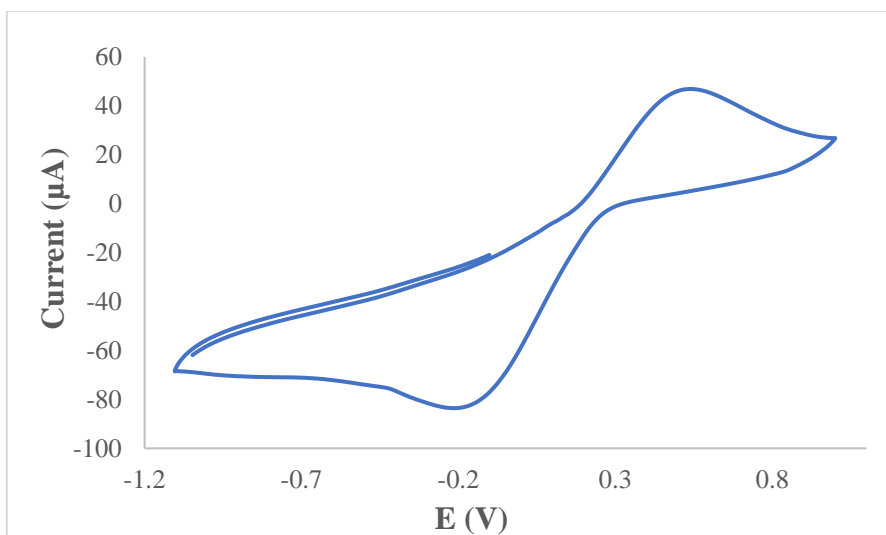
431 Polyurethane film was deposited onto the screen-printed electrode by casting method as shown

432 in **Figure 1**. After that, the modified electrode was analyzed using cyclic voltammetry and

433 differential pulse voltammetry in order to study the behavior of the modified electrode. The  
434 modified electrode was tested in a  $0.1 \text{ mmol}\cdot\text{L}^{-1}$  KCl solution containing  $5 \text{ mmol}\cdot\text{L}^{-1}$   
435 ( $\text{K}_3\text{Fe}(\text{CN})_6$ ). The use of potassium ferricyanide is intended to increase the sensitivity of the  
436 KCl solution. The conductivity of the modified electrode was studied. The electrode was  
437 analyzed by cyclic voltammetry method with a potential range of  $-1.00$  to  $+1.00$  with a scan  
438 rate of  $0.05 \text{ V}\cdot\text{s}^{-1}$ . The voltammograms at the electrode have shown a specific redox reaction.  
439 Furthermore, the conductivity of the modified electrode is lower due to the use of polyurethane.  
440 This occurs due to PU being a natural polymer produced from the polyol of palm kernel oil-  
441 based polyol. The electrochemical signal at the electrode is low if there is a decrease in  
442 electrochemical conductivity (El - Raheem et al. 2020). It can be concluded that polyurethane  
443 is a bio-polymer with a low current value. The current of the modified electrode was found at  
444  $5.3 \times 10^{-5} \text{ A}$  or  $53 \text{ }\mu\text{A}$ . Nevertheless, the current of PU in this study showed better results  
445 compared to Bahrami et al. (2019) that reported the current of PU as  $1.26 \times 10^{-6} \text{ A}$ , whereas Li  
446 et al. (2019) reported the PU current in their study was even very low, namely  $10^{-14} \text{ A}$ . The PU  
447 can obtain a current owing to the benzene ring in the hard segment (MDI) could exhibit the  
448 current by inducing electron delocalization along the polyurethane chain (Wong et al. 2014).  
449 The PU can also release a current caused by PEG. The application of PEG as polyol has been  
450 studied by Porcarelli et al. (2017), that reported that the current of PU based on PEG – polyol  
451 was  $9.2 \times 10^{-8} \text{ A}$ .

452 According to **Figure 9**, it can be concluded that the anodic peak present in the modified  
453 electrode was at  $+0.5 \text{ V}$ , it also represented the anodic peak of the SPE-PU. The first oxidation  
454 signal on both electrodes ranged from  $-0.2$  to  $+1.0 \text{ V}$ , which revealed a particular oxidative  
455 peak at a potential of  $+0.5 \text{ V}$ .

456

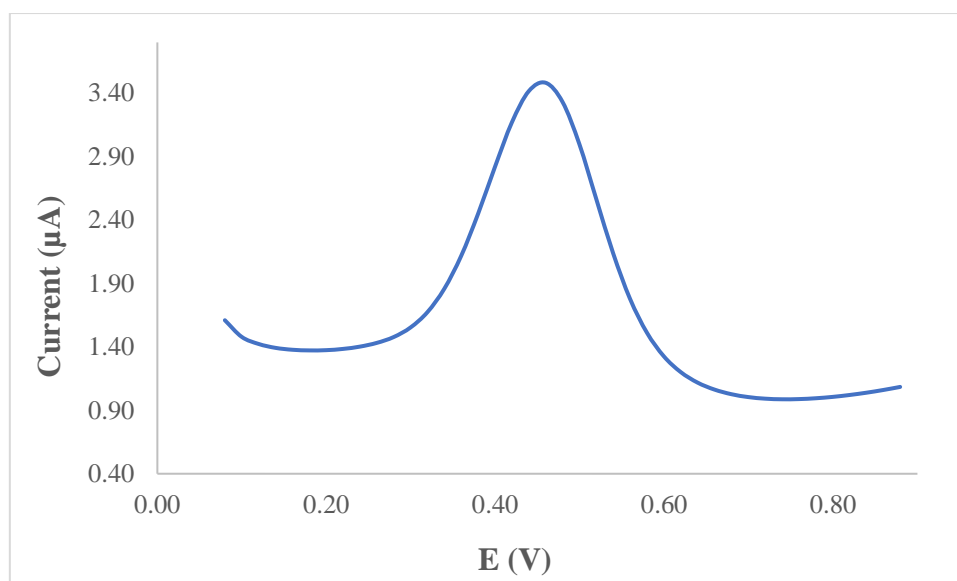


457  
 458 **Figure 9.** The voltammogram of SPE-PU modified electrode after analyzed using cyclic  
 459 voltammetry technique  
 460

461 **Figure 10** also presents the DPV voltammogram of the modified electrode. DPV is a  
 462 measurement based on the difference in potential pulses that produce an electric current.  
 463 Scanning the capability pulses to the working electrode will produce different currents. Optimal  
 464 peak currents will be produced to the reduction capacity of the redox material. The peak current  
 465 produced is proportional to the concentration of the redox substance and can be detected up to  
 466 a concentration below  $10^{-8}$  M. DPV was conducted to obtain the current value that is more  
 467 accurate than CV (Lee et al. 2018).

468 This study used a redox pair ( $K_3Fe(CN)_6$ ) as a test device (probe). The currents generated by  
 469 SPE-PU and proved by CV and DPV have shown conductivity on polyurethane films. This  
 470 suggests that polyurethane films can conduct electron transfer. The electrochemical area on the  
 471 modified electrode can be calculated using the formula from Randles-Sevcik (Butwong et al.  
 472 2019), where the electrochemical area for SPE-PU is considered to be A, using Equation 2:

473 **Current of SPE-PU,  $I_p = 2.65 \times 10^5 A C n^{3/2} \nu^{1/2} D^{1/2}$**  (2)



474  
475 **Figure 10.** The voltammogram of SPE – PU modified electrode after analyzed using  
476 differential pulse voltammetry technique

477

478 Where,  $n - 1$  is the amount of electron transfer involved, while  $C$  is the solvent concentration  
479 used ( $\text{mmol}\cdot\text{L}^{-1}$ ) and the value of  $D$  is the diffusion constant of  $5 \text{ mmol}\cdot\text{L}^{-1}$  at  $(\text{K}_3\text{Fe}(\text{CN})_6)$   
480 dissolved using  $0.1 \text{ mmol}\cdot\text{L}^{-1}$  KCl. The estimated surface area of the electrode (**Figure 1**) was  
481  $0.2 \text{ cm}^2$  where the length and width of the electrode used during the study was  $0.44 \text{ cm} \times 0.44$   
482  $\text{cm}$  while the surface area of the SPE-PU was  $0.25 \text{ cm}^2$  with the length and width of the  
483 electrode estimated at  $0.5 \text{ cm} \times 0.5 \text{ cm}$ , and causing the SPE-PU has a larger surface. The  
484 corresponding surface concentration ( $\tau$ ) ( $\text{mol}/\text{cm}^2$ ) is measured using Equation 3.

485

$$I_p = (n^2 F^2 / 4RT) A \tau v \quad (3)$$

486  $I_p$  is the peak current (A), while  $A$  is the surface area of the electrode ( $\text{cm}^2$ ), the value of  $v$  is  
487 the applied scan rate (mV/s) and  $F$  is the Faraday constant ( $96,584 \text{ C}/\text{mol}$ ),  $R$  is the constant  
488 ideal gas ( $8.314 \text{ J}/\text{mol K}$ ) and  $T$  is the temperature used during the experiment being conducted  
489 ( $298 \text{ K}$ ) (Koita et al. 2014). The application of PKOp to produce a conducting polymer will be  
490 a great prospect as this material can be employed in the analytical industry in order to modify  
491 electrodes for electrochemical purposes.



492 Furthermore, number of palm oils is abundant in Malaysia and Indonesia such as palm stearin  
493 and refined-bleached-deodorized (RBD) palm oil. They have several benefits such as being  
494 sustainable, cheap, and environmentally biodegradable. These palms are the potential to  
495 produce biomaterials that can be used to replace other polymers that are chemical-based (Tajao  
496 et al. 2021). Several studies have been reported the application of PU to produce elastic  
497 conductive fibres and films owing to it being highly elastic, scratch-resistant, and adhesive  
498 (Tadese et al. 2019), thus it is easy for PU to adhere to the screen-printed electrode to modify  
499 the electrode. PU is also being used as a composite material to make elastic conducting  
500 composite films (Khatoon & Ahmad 2017).

501

#### 502 **4. Conclusion**

503 Polyurethane film was prepared by pre-polymerization between palm kernel oil-based polyol  
504 (PKO-p) with MDI. The presence of PEG 400 as the chain extender formed freestanding  
505 flexible film. Acetone was used as the solvent to lower the reaction kinetics since the pre-  
506 polymerization was carried out at room temperature. The formation of urethane links (-  
507 NHC(O) backbone) after polymerization was confirmed by the absence of absorption bands at  
508  $2241\text{ cm}^{-1}$  associated with the  $\text{N}=\text{C}=\text{O}$  bond stretching, and the presence of N-H peak at  $3300\text{ cm}^{-1}$ ,  
509 carbonyl (C=O) at  $1710\text{ cm}^{-1}$ , carbamate (C-N) at  $1600\text{ cm}^{-1}$ , ether (C-O-C) at  $1065\text{ cm}^{-1}$ ,  
510 benzene ring (C=C) at  $1535\text{ cm}^{-1}$  in the bio-based polyurethane chain structure. Soxhlet  
511 analysis for the determination of crosslinking on polyurethane films has yielded a high  
512 percentage of 99.33%. This is contributed by the hard segments formed from the reaction  
513 between isocyanates and hydroxyl groups causing elongation of polymer chains. FESEM  
514 analysis exhibited an absence of phase separation and smooth surface. Meanwhile, the current  
515 of the modified electrode was found at  $5.2 \times 10^{-5}\text{ A}$ . This bio-based polyurethane film can be  
516 used as a conducting bio-polymer and it is very useful for other studies such as electrochemical

517 sensor purposes. Furthermore, advanced technologies are promising and the future of bio based  
518 polyol looks very bright.

519

## 520 **5. Acknowledgment**

521 The authors would like to thank Alma Ata University for the sponsorship given to the first  
522 author. We would like to also, thank The Department of Chemical Sciences, Universiti  
523 Kebangsaan Malaysia for the laboratory facilities and CRIM, UKM for the analysis  
524 infrastructure.

525

## 526 **6. Conflict of Interest**

527 The authors declare no conflict of interest.

528

## 529 **7. References**

530 Agrawal, A., Kaur, R., Walia, R. S. (2017). PU foam derived from renewable sources:

531 Perspective on properties enhancement: An overview. *European Polymer Journal*. **95**:  
532 255 – 274.

533 Akindoyo, J. O., Beg, M.D.H., Ghazali, S., Islam, M.R., Jeyaratnam, N. & Yuvaraj, A.R.

534 (2016). Polyurethane types, synthesis, and applications – a review. *RSC Advances*. **6**:  
535 114453 – 114482.

536 Alamawi, M. Y., Khairuddin, F. H., Yusoff, N. I. M., Badri, K., Ceylan, H. (2019).

537 Investigation on physical, thermal, and chemical properties of palm kernel oil polyobio-  
538 based binder as a replacement for bituminous binder. *Construction and Building*  
539 *Materials*. **204**: 122 – 131.

540 Alqarni, S. A., Hussein, M. A., Ganash, A. A. & Khan, A. (2020). Composite material-based  
541 conducting polymers for electrochemical sensor applications: a mini-review.  
542 *BioNanoScience*. **10**: 351 – 364.

543 Badan, A., Majka, T. M. (2017). The influence of vegetable – oil based polyols on physico –  
544 mechanical and thermal properties of polyurethane foams. *Proceedings*. 1 – 7.

545 Badri, K.H. (2012) Biobased polyurethane from palm kernel oil-based polyol. In Polyurethane;  
546 Zafar, F., Sharmin, E., Eds. InTechOpen: Rijeka, Croatia. pp. 447–470.

547 Badri, K.H., Ahmad, S.H. & Zakaria, S. 2000. Production of a high-functionality RBD palm  
548 kernel oil-based polyester polyol. *Journal of Applied Polymer Science*. **81**(2): 384 – 389.

549 Baig, N., Sajid, M. and Saleh, T. A. 2019. Recent trends in nanomaterial–modified electrodes  
550 for electroanalytical applications. *Trends in Analytical Chemistry*. **111**: 47 – 61.

551 Berta, M., Lindsay, C., Pans, G., & Camino, G. (2006). Effect of chemical structure on  
552 combustion and thermal behaviour of polyurethane elastomer layered silicate  
553 nanocomposites. *Polymer Degradation and Stability*. **91**: 1179-1191.

554 Borowicz, M., Sadowska, J. P., Lubczak, J. & Czuprynski, B. (2019). Biodegradable, flame–  
555 retardant, and bio-based rigid polyurethane/polyisocyanurate foams for thermal  
556 insulation application. *Polymers*. **11**: 1816 – 1839.

557 Butwong, N., Khajonklin, J., Thongbor, A. & Luong, J.H.T. (2019). Electrochemical sensing  
558 of histamine using a glassy carbon electrode modified with multiwalled carbon nanotubes  
559 decorated with Ag – Ag<sub>2</sub>O nanoparticles. *Microchimica Acta*. **186** (11): 1 – 10.

560 Chokkareddy, R., Thondavada, N., Kabane, B. & Redhi, G. G. (2020). A novel ionic liquid  
561 based electrochemical sensor for detection of pyrazinamide. *Journal of the Iranian*  
562 *Chemical Society*. **18**: 621 – 629.

563 Chokkareddy, R., Kanchi, S. & Inamuddin (2020). Simultaneous detection of ethambutol and  
564 pyrazinamide with IL@CoFe<sub>2</sub>O<sub>4</sub>NPs@MWCNTs fabricated glassy carbon electrode.  
565 *Scientific Reports*. **10**: 13563.

566 Clemitson, I. (2008). Castable Polyurethane Elastomers. Taylor & Francis Group, New York.  
567 doi:10.1201/9781420065770.

568 Corcuera, M.A., Rueda, L., Saralegui, A., Martin, M.D., Fernandez-d'Arlas, B., Mondragon,  
569 I. & Eceiza, A. (2011). Effect of diisocyanate structure on the properties and  
570 microstructure of polyurethanes based on polyols derived from renewable resources.  
571 *Journal of Applied Polymer Science*. **122**: 3677-3685.

572 Cuve, L. & Pascault, J.P. (1991). Synthesis and properties of polyurethanes based on  
573 polyolefine: Rigid polyurethanes and amorphous segmented polyurethanes prepared in  
574 polar solvents under homogeneous conditions. *Polymer*. **32** (2): 343- 352.

575 Degefu, H., Amare, M., Tessema, M. & Admassie, S. (2014). Lignin modified glassy carbon  
576 electrode for the electrochemical determination of histamine in human urine and wine  
577 samples. *Electrochimica Acta*. **121**: 307 – 314.

578 Dzulkipli, M. Z., Karim, J., Ahmad, A., Dzulkurnain, N. A., Su'ait, M S., Fujita, M. Y., Khoon,  
579 L. T. & Hassan, N. H. (2021). The influences of 1-butyl-3-methylimidazolium  
580 tetrafluoroborate on electrochemical, thermal and structural studies as ionic liquid gel  
581 polymer electrolyte. *Polymers*. **13** (8): 1277 – 1294.

582 El-Raheem, H.A., Hassan, R.Y.A., Khaled, R., Farghali, A. & El-Sherbiny, I.M. (2020).  
583 Polyurethane-doped platinum nanoparticles modified carbon paste electrode for the  
584 sensitive and selective voltammetric determination of free copper ions in biological  
585 samples. *Microchemical Journal*. **155**: 104765.

586 Fei, T., Li, Y., Liu, B. & Xia, C. (2019). Flexible polyurethane/boron nitride composites with  
587 enhanced thermal conductivity. *High Performance Polymers*. **32** (3): 1 – 10.

588 Furtwengler, P., Perrin R., Redl, A. & Averous, L. (2017). Synthesis and characterization of  
589 polyurethane foams derived of fully renewable polyesters polyols from sorbitol.  
590 *European Polymer Journal*. **97**: 319 – 327.

591 Ghosh, S., Ganguly, S., Remanan, S., Mondal, S., Jana, S., Maji, P. K., Singha, N., Das, N. C.  
592 (2018). Ultra-light weight, water durable and flexible highly electrical conductive  
593 polyurethane foam for superior electromagnetic interference shielding materials. *Journal*  
594 *of Materials Science: Materials in Electronics*. **29**: 10177 – 10189.

595 Guo, S., Zhang, C., Yang, M., Zhou, Y., Bi, C., Lv, Q. & Ma, N. (2020). A facile and sensitive  
596 electrochemical sensor for non – enzymatic glucose detection based on three –  
597 dimensional flexible polyurethane sponge decorated with nickel hydroxide. *Analytica*  
598 *Chimica Acta*. **1109**: 130 – 139.

599 Hamuzan, H.A. & Badri, K.H. (2016). The role of isocyanates in determining the viscoelastic  
600 properties of polyurethane. *AIP Conference Proceedings*. 1784, Issue 1.

601 Harmayani, E., Aprilia, V. & Marsono, Y. (2014). Characterization of glucomannan from  
602 *Amorphophallus oncophyllus* and its prebiotic activity in vivo. *Carbohydrate Polymers*.  
603 **112**: 475-79.

604 Herrington, R. & Hock, K. (1997). Flexible polyurethane foams. 2nd Edition. Dow Chemical  
605 Company. Midlan.

606 Inayatullah, A., Badrul, H.A., Munir, M.A. (2021). Fish analysis containing biogenic amines  
607 using gas chromatography flame ionization detector. *Science and Technology Indonesia*.  
608 **6** (1): 1-7.

609 Janpoung, P., Pattanauwat, P. & Potiyaraj, P. (2020). Improvement of electrical conductivity  
610 of polyurethane/polypyrrole blends by graphene. *Key Engineering Materials*. **831**: 122 –  
611 126.

612 Khairuddin, F.H., Yusof, N. I. M., Badri, K., Ceylan, H., Tawil, S. N. M. (2018). Thermal,  
613 chemical and imaging analysis of polyurethane/cecabase modified bitumen. *IOP Conf.*  
614 *Series: Materials Science and Engineering*. **512**: 012032.

615 Khatoon, H., Ahmad, S. (2017). A review on conducting polymer reinforced polyurethane  
616 composites. *Journal of Industrial and Engineering Chemistry*. **53**: 1 – 22.

617 Kilele, J. C., Chokkareddy, R., Rono, N. & Redhi, G. G. (2020). A novel electrochemical  
618 sensor for selective determination of theophylline in pharmaceutical formulations.  
619 *Journal of the Taiwan Institute of Chemical Engineers*. 111: 228-238.

620 Kilele, J. C., Chokkareddy, R. & Redhi, G. G. (2021). Ultra–sensitive electrochemical sensor  
621 for fenitrothion pesticide residues in fruit samples using IL@CoFe<sub>2</sub>ONPs@MWCNTs  
622 nanocomposite. *Microchemical Journal*. **164**: 106012.

623 Koita, D., Tzedakis, T., Kane, C., Diaw, M., Sock, O. & Lavedan, P. (2014). Study of the  
624 histamine electrochemical oxidation catalyzed by nickel sulfate. *Electroanalysis*. **26 (10)**:  
625 2224 – 2236.

626 Kotal, M., Srivastava, S.K. & Paramanik, B. (2011). Enhancements in conductivity and thermal  
627 stabilities of polyurethane/polypyrrole nanoblends. *The Journal of Physical Chemistry*  
628 *C*. **115 (5)**: 1496 – 1505.

629 Ladan, M., Basirun, W.J., Kazi, S.N., Rahman, F.A. (2017). Corrosion protection of AISI 1018  
630 steel using Co-doped TiO<sub>2</sub>/polypyrrole nanocomposites in 3.5% NaCl solution.  
631 *Materials Chemistry and Physics*. **192**: 361 – 373.

632 Lampman, G.M., Pavia, D.L., Kriz, G.S. & Vyvyan, J.R. (2010). Spectroscopy. 4th Edition.  
633 Brooks/Cole Cengage Learning, Belmont, USA.

634 Lee, K.J., Elgrishi, N., Kandemir, B. & Dempsey, J.L. 2018. Electrochemical and spectroscopic  
635 methods for evaluating molecular electrocatalysts. *Nature Reviews Chemistry*. **1(5)**: 1 -  
636 14.

637 Leykin, A., Shapovalov, L. & Figovsky, O. (2016). Non – isocyanate polyurethanes –  
638 Yesterday, today and tomorrow. *Alternative Energy and Ecology*. **191** (3 – 4): 95 – 108.

639 Li, H., Yuan, D., Li, P., He, C. (2019). High conductive and mechanical robust carbon  
640 nanotubes/waterborne polyurethane composite films for efficient electromagnetic  
641 interference shielding. *Composites Part A*. **121**: 411 – 417.

642 Nakthong, P., Kondo, T., Chailapakul, O., Siangproh, W. (2020). Development of an  
643 unmodified screen-printed electrode for nonenzymatic histamine detection. *Analytical*  
644 *Methods*. **12**: 5407 – 5414.

645 Mishra, K., Narayan, R., Raju, K.V.S.N. & Aminabhavi, T.M. (2012). Hyperbranched  
646 polyurethane (HBPU)-urea and HBPU-imide coatings: Effect of chain extender and  
647 NCO/OH ratio on their properties. *Progress in Organic Coatings*. **74**: 134 – 141.

648 Mohd Noor, M. A., Tuan Ismail, T. N. M., Ghazali, R. (2020). Bio-based content of oligomers  
649 derived from palm oil: Sample combustion and liquid scintillation counting technique.  
650 *Malaysia Journal of Analytical Science*. **24**: 906 – 917.

651 Munir, M. A., Badri, K. H., Heng, L. Y., Inayatullah, A., Nurinda, E., Estiningsih, D.,  
652 Fatmawati, A., Aprilia, V., Syafitri, N. (2022). The application of polyurethane-LiClO<sub>4</sub>  
653 to modify screen-printed electrodes analyzing histamine in mackerel using a  
654 voltammetric approach. *ACS Omega*. doi.org/10.1021/acsomega.1c06295.

655 Munir, M. A., Heng, L. Y., Sage, E. E., Mackeen, M. M. M., Badri, K. H. (2021). Histamine  
656 detection in mackerel (*Scomberomorus* Sp.) and its products derivatized with 9-  
657 fluorenilmethylchloroformate. *Pakistan Journal of Analytical and Environmental*  
658 *Chemistry*. **22** (2): 243-251.

659 Munir, M. A., Heng, L. Y., Badri, K. H. (2021). Polyurethane modified screen-printed  
660 electrode for the electrochemical detection of histamine in fish. *IOP Conference Series:*  
661 *Earth and Environmental Science*. **880**: 012032.

662 Munir, M.A., Mackeen, M.M.M., Heng, L.Y. Badri, K.H. (2021). Study of histamine detection  
663 using liquid chromatography and gas chromatography. *ASM Science Journal*. **16**: 1-9.

664 Mutsuhisa F., Ken, K. & Shohei, N. (2007). Microphase separated structure and mechanical  
665 properties of norbornane diisocyanate-based polyurethane. *Polymer*. **48** (4): 997 – 1004.

666 Mustapha, R., Rahmat, A. R., Abdul Majid, R., Mustapha, S. N. H. (2019). Vegetable oil-based  
667 epoxy resins and their composites with bio-based hardener: A short review. *Polymer-*  
668 *Plastic Technology and Materials*. **58**: 1311 – 1326.

669 Nohra, B., Candy, L., Blancos, J.F., Guerin, C., Raoul, Y. & Mouloungui, Z. (2013). From  
670 petrochemical polyurethanes to bio-based polyhydroxyurethanes. *Macromolecules*. **46**  
671 (10): 3771 – 3792.

672 Nurwanti, E., Uddin, M., Chang, J.S., Hadi, H., Abdul, S.S., Su, E.C.Y., Nursetyo, A.A.,  
673 Masud, J.H.B. & Bai, C.H. (2018). Roles of sedentary behaviors and unhealthy foods in  
674 increasing the obesity risk in adult men and women: A cross-sectional national study.  
675 *Nutrients*. **10** (6): 704-715.

676 Pan, T. & Yu, Q. (2016). Anti-corrosion methods and materials comprehensive evaluation of  
677 anti-corrosion capacity of electroactive polyaniline for steels. *Anti – Corrosion Methods*  
678 *and Materials*. **63**: 360 – 368.

679 Pan, X. & Webster, D.C. (2012). New biobased high functionality polyols and their use in  
680 polyurethane coatings. *ChemSusChem*. **5**: 419-429.

681 Petrovic, Z.S. (2008). Polyurethanes from vegetable oils. *Polymer Reviews*. **48** (1): 109 – 155.

682 Porcarelli, L., Manojkumar, K., Sardon, H., Llorente, O., Shaplov, A. S., Vijayakrishna, K.,  
683 Gerbaldi, C., Mecerreyes, D. (2017). Single ion conducting polymer electrolytes based  
684 on versatile polyurethanes. *Electrochimica Acta*. **241**: 526 – 534.



685 Priya, S. S., Karthika, M., Selvasekarapandian, S. & Manjuladevi, R. (2018). Preparation and  
686 characterization of polymer electrolyte based on biopolymer I-carrageenan with  
687 magnesium nitrate. *Solid State Ionics*. **327**: 136 – 149.

688 Ren, D. & Frazier, C.E. (2013). Structure–property behaviour of moisture-cure polyurethane  
689 wood adhesives: Influence of hard segment content. *Adhesion and Adhesives*. **45**: 118-  
690 124.

691 Rogulska, S.K., Kultys, A. & Podkoscielny, W. (2007). Studies on thermoplastic polyurethanes  
692 based on newdiphe – derivative diols. II. Synthesis and characterization of segmented  
693 polyurethanes from HDI and MDI. *European Polymer Journal*. **43**: 1402 – 1414.

694 Romaskevicius, T., Budriene, S., Pielichowski, K. & Pielichowski, J. (2006). Application of  
695 polyurethane-based materials for immobilization of enzymes and cells: a review.  
696 *Chemija*. **17**: 74 – 89.

697 Sengodu, P. & Deshmukh, A. D. (2015). Conducting polymers and their inorganic composites  
698 for advanced Li-ion battery electrolytes: a review. *RSC Advances*. **5**: 42109 – 42130.

699 Septevani, A. A., Evans, D. A. C., Chaleat, C., Martin, D. J., Annamalai, P. K. (2015). A  
700 systematic study substituting polyether polyol with palm kernel oil based polyester  
701 polyol in rigid polyurethane foam. *Industrial Crops and Products*. **66**: 16 – 26.

702 Su'ait, M. S., Ahmad, A., Badri, K. H., Mohamed, N. S., Rahman, M. Y. A., Ricardi, C. L. A.  
703 & Scardi, P. The potential of polyurethane bio-based solid polymer electrolyte for  
704 photoelectrochemical cell application. *International Journal of Hydrogen Energy*. **39** (6):  
705 3005 – 3017.

706 Tadesse, M. G., Mengistie, D. A., Chen, Y., Wang, L., Loghin, C., Nierstrasz, V. (2019).  
707 Electrically conductive highly elastic polyamide/lycra fabric treated with PEDOT: PSS  
708 and polyurethane. *Journal of Materials Science*. **54**: 9591 – 9602.

709 Tajau, R., R, Rosiah, Alias, M. S., Mudri, N. H., Halim, K. A. A., Harun, M. H., Isa, N. M.,  
710 Ismail, R. C., Faisal, S. M., Talib, M., Zin, M. R. M., Yusoff, I. I., Zaman, N. K., Illias,  
711 I. A. (2021). Emergence of polymeric material utilising sustainable radiation curable  
712 palm oil-based products for advanced technology applications. *Polymers*. **13**: 1865 –  
713 1886.

714 Tran, V.H., Kim, J.D., Kim, J.H., Kim, S.K., Lee, J.M. (2020). Influence of cellulose  
715 nanocrystal on the cryogenic mechanical behaviour and thermal conductivity of  
716 polyurethane composite. *Journal of Polymers and The Environment*. **28**: 1169 – 1179.

717 Viera, I.R.S., Costa, L.D.F.D.O., Miranda, G.D.S., Nardehhcia, S., Monteiro, M.S.D. S.D.B.,  
718 Junior, E.R. & Delpech, M.C. (2020). Waterborne poly (urethane – urea)s  
719 nanocomposites reinforced with clay, reduced graphene oxide and respective hybrids:  
720 Synthesis, stability and structural characterization. *Journal of Polymers and The  
721 Environment*. **28**: 74 – 90.

722 Wang, B., Wang, L., Li, X., Liu, Y., Zhang, Z., Hedrick, E., Safe, S., Qiu, J., Lu, G. & Wang,  
723 S. (2018). Template-free fabrication of vertically–aligned polymer nanowire array on the  
724 flat–end tip for quantifying the single living cancer cells and nanosurface interaction. a  
725 *Manufacturing Letters*. **16**: 27 – 31.

726 Wang, J., Xiao, L., Du, X., Wang, J. & Ma, H. (2017). Polypyrrole composites with carbon  
727 materials for supercapacitors. *Chemical Papers*. **71 (2)**: 293 – 316.

728 Wong, C.S. & Badri, K.H. (2012). Chemical analyses of palm kernel oil-based polyurethane  
729 prepolymer. *Materials Sciences and Applications*. **3**: 78 – 86.

730 Wong, C. S., Badri, K., Ataollahi, N., Law, K., Su’ait, M. S., Hassan, N. I. (2014). Synthesis  
731 of new bio–based solid polymer electrolyte polyurethane – LiClO<sub>4</sub> via prepolymerization  
732 method: Effect of NCO/OH ratio on their chemical, thermal properties and ionic  
733 conductivity. *World Academy of Science, Engineering and Technology, International*

734 *Journal of Chemical, Molecular, Nuclear, Materials and Metallurgical Engineering.* **8**:  
735 1243 – 1250.

736 Yong, Z., Bo, Z.M., Bo, W., Lin, J.Z. & Jun, N. (2009). Synthesis and properties of novel  
737 polyurethane acrylate containing 3-(2-Hydroxyethyl) isocyanurate segment. *Progress in*  
738 *Organic Coatings.* **67**: 264 – 268.

739 Zia, K. M., Anjum, S., Zuber, M., Mujahid, M. & Jamil, T. (2014). Synthesis and molecular  
740 characterization of chitosan based polyurethane elastomers using aromatic diisocyanate.  
741 *International of Journal of Biological Macromolecules.* **66**: 26 – 32.

[← BACK](#) [DASHBOARD / ARTICLE DETAILS](#)  Updated on 2022-03-29 Version 7.1 ▾

# Design and Synthesis of Conducting Polymer Bio-Based Polyurethane Produced from Palm Kernel Oil

PUBLISHED

ID 6815187

Muhammad Abdurrahman Munir <sup>SA CA</sup> <sup>1</sup>,  
Khairiah Haji Badri<sup>2</sup>, Lee Yook Heng<sup>2</sup>,  
Ahlam Inayatullah<sup>3</sup>, Hamid Alkhair Badrul<sup>3</sup>,  
Emelda Emelda<sup>4</sup>, Eliza Dwinta<sup>4</sup>,  
Nurul Kusumawardani<sup>4</sup>,  
Ari Susiana Wulandari<sup>4</sup>, Veriani Aprilia<sup>4</sup>,  
Rachmad Bagas Yahya Supriyono<sup>4</sup>  
[+ Show Affiliations](#)

## Article Type

Research Article

## Journal

International Journal of  
Polymer Science

Rydz Joanna

Submitted on 2021-06-14 (2 years ago)

[> Abstract](#)[∨ Author Declaration](#)**Conflict of interest:** *Not declared***Data availability statement:** All data experiments can be found in the manuscript.**Funding statement:** This research was funded by Universiti Kebangsaan Malaysia, through its internal grant number GGP-2019-021. The APC was funded by Faculty of Science and Technology, Universiti Kebangsaan Malaysia.[> Files](#) 2

